

UNIVERSITY OF ALBERTA

**Molecular and Functional Properties of Concentrative Nucleoside
Transport Proteins**

by

Shaun Kelly Loewen



A thesis submitted to the Faculty of Graduate Studies and Research in partial fulfillment of the
requirements for the degree of Doctor of Philosophy

Department of Physiology

Edmonton, Alberta
Fall 2002



National Library
of Canada

Acquisitions and
Bibliographic Services

395 Wellington Street
Ottawa ON K1A 0N4
Canada

Bibliothèque nationale
du Canada

Acquisitions et
services bibliographiques

395, rue Wellington
Ottawa ON K1A 0N4
Canada

Your file Votre référence

Our file Notre référence

The author has granted a non-exclusive licence allowing the National Library of Canada to reproduce, loan, distribute or sell copies of this thesis in microform, paper or electronic formats.

The author retains ownership of the copyright in this thesis. Neither the thesis nor substantial extracts from it may be printed or otherwise reproduced without the author's permission.

L'auteur a accordé une licence non exclusive permettant à la Bibliothèque nationale du Canada de reproduire, prêter, distribuer ou vendre des copies de cette thèse sous la forme de microfiche/film, de reproduction sur papier ou sur format électronique.

L'auteur conserve la propriété du droit d'auteur qui protège cette thèse. Ni la thèse ni des extraits substantiels de celle-ci ne doivent être imprimés ou autrement reproduits sans son autorisation.

0-612-81227-8

Canada

UNIVERSITY OF ALBERTA

LIBRARY RELEASE FORM

Name of Author: Shaun K. Loewen

Title of Thesis: Molecular and Functional Properties of Concentrative Nucleoside Transport Proteins

Degree: Doctor of Philosophy

Year this Degree Granted: 2002

Permission is hereby granted to the University of Alberta Library to reproduce single copies of this thesis and to lend or sell such copies for private, scholarly or scientific research purposes only.

The author reserves all other publication and other rights in association with the copyright in the thesis, and except as herein before provided, neither the thesis nor any substantial portion thereof may be printed or otherwise reproduced in any material form whatever without the author's prior written permission.



Shaun K. Loewen
37 Richards Crescent
Red Deer, Alberta
Canada
T4P 3B7

September 25, 2002

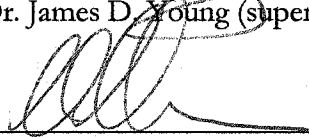
UNIVERSITY OF ALBERTA

FACULTY OF GRADUATE STUDIES AND RESEARCH

The undersigned certify that they have read, and recommend to the Faculty of Graduate Studies and Research for acceptance, a thesis entitled "Molecular and Functional Properties of Concentrative Nucleoside Transport Proteins" submitted by Shaun K. Loewen in partial fulfillment of the requirements for the degree of Doctor of Philosophy.



Dr. James D. Young (supervisor)



Dr. Chris I. Cheeseman



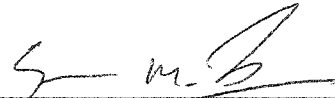
Dr. Joseph R. Casey



Dr. Carol E. Cass



Dr. Bernard D. Lemire



Dr. Simon M. Jarvis (external examiner)

May 30, 2002

ABSTRACT

The human concentrative (Na^+ -linked) plasma membrane transport proteins hCNT1 and hCNT2 are pyrimidine nucleoside-selective (system *cit*) and purine nucleoside-selective (system *cif*), respectively. Both have orthologs in other mammalian species and belong to a gene family (CNT) that has members in insects, nematodes, pathogenic yeast and bacteria. This thesis describes: (i) the cDNA cloning and *Xenopus* oocyte heterologous expression of new CNT family members in mammals (human (h) and mouse (m) CNT3), prevertebrates (*Eptatretus stouti* hCNT), and pathogenic yeast (*Candida albicans* CaCNT), (ii) structure/function studies of CNT proteins, and (iii) antiviral/antineoplastic nucleoside drug transport by a prokaryotic CNT, *Escherichia coli* H^+ /nucleoside symporter NupC.

When produced in *Xenopus* oocytes, hCNT3 and mCNT3 (691 and 703 residues, respectively) exhibited transport characteristics consistent with the missing mammalian *cib* transporter, mediating Na^+ -dependent (and H^+ - and Li^+ -dependent) fluxes of both pyrimidine and purine nucleosides. hCNT (683 residues) also showed Na^+ -dependent *cib*-type activity, but was H^+ -independent and had a lower apparent affinity for Na^+ ($K_{50} > 100$ mM) than mammalian CNT3 proteins (K_{50} 7-16 mM). hCNT3, mCNT3 and hCNT had 2:1 Na^+ :uridine coupling ratios. CaCNT (608 residues) exhibited H^+ -coupled, purine nucleoside-selective transport activity and is the first described cation-coupled nucleoside transporter in yeasts. Experiments with NupC represent the first successful expression of a bacterial transporter in *Xenopus* oocytes and establish the NupC-pGEM-HE/oocyte system as a useful tool for characterization of NupC-mediated transport of clinically relevant nucleoside therapeutic drugs.

Chimeric and site-directed mutagenesis studies between hCNT1/2 (650 and 658 residues, respectively) identified two pairs of adjacent residues in TM 7 (Ser³¹⁹/Gln³²⁰) and TM 8 (Ser³⁵³/Leu³⁵⁴) of hCNT1 involved in substrate specificity and/or cation coupling. Mutation of the two TM 7 residues to the corresponding residues in hCNT2 (Gly and Met, respectively) converted the transporter from *cit* to *cib*, while additional mutation of TM 8 residues to Thr and Val, respectively, changed the substrate selectivity from *cib* to *cif*. Mutations in TM 8 alone produced recombinant proteins with uridine-preferring transport characteristics and/or partially uncoupled transport properties. Chimeric studies using hCNT3 and hCNT in combination with hCNT1 identified regions in the C-terminal half of the protein involved in cation recognition.

ACKNOWLEDGEMENTS

There are a number of people without whom this thesis would not have been possible. I am indebted to my supervisor, Dr. James Young, for his encouragement, guidance, and inspiration throughout my project. I wish to thank "the ladies", Dr. Sylvia Yao, Amy Ng and Mabel Ritzel, for their infectious enthusiasm and well-rounded discussions in the coffee room. More specifically, I thank Dr. Sylvia Yao for teaching me the wonderful world of *Xenopus* oocytes, for providing the initial NupC cDNA construct, and for technical assistance with radioisotope flux assays. Amy Ng provided me with superb training in molecular biological techniques and assisted with the generation of hCNT1 mutant constructs and mCNT3 and hfCNT cDNAs. I am grateful to Mabel Ritzel for her expertise in molecular cloning without which I would have not been able to embark on this journey, and for technical assistance in the generation of hCNT3 cDNA and Northern blot analysis. I thank Professor Stephen Baldwin of the University of Leeds (UK) for assistance in the helical wheel modeling of the hCNT1 amino acid sequence. In addition, special thanks go out to Dr. Manickavasagam Sundaram for my initial training in the use of molecular biology to generate chimeric cDNA constructs. I am also grateful to Kyla Smith for her tireless collaborative work on CNT3 electrophysiology and for sharing an office space with me for all of those years. Thanks also to summer students Melissa Slugoski and Nadira Mohabir, whose efforts in preparing oocytes and assistance with transport assays are gratefully appreciated.

I am most grateful to Drs. Carol Cass, Christopher Cheeseman, Joseph Casey, Marek Duszyk and all of the members of their laboratories for their support and advice during my research. Thank you especially to Dr. Kathryn Graham, Delores Mowles and Pat Carpenter of the Cass laboratory for their work on HL-60 cells and TaqMan™ quantitative RT-PCR. Special thanks to Dr. Bernard Lemire for becoming a late addition to my PhD candidacy and examination committees. I also thank Drs. Xing-Zhen Chen and Edward Karpinski for teaching me oocyte electrophysiology. Also, I wish to thank the Alberta Heritage Foundation for Medical Research (AHFMR) for scholarship support. Last but not least, I would like to thank my family and Marce for their love and endless support.

TABLE OF CONTENTS

CHAPTER I: General Introduction.....	1
Preamble.....	2
Nucleoside Transport Proteins.....	3
Mammalian equilibrative nucleoside transporters (ENTs).....	5
Characteristics of mammalian equilibrative nucleoside transport processes.....	5
Functional and molecular properties of cloned mammalian ENTs.....	5
ENT1.....	5
ENT2.....	6
ENT3.....	8
ENT family members in other eukaryotes.....	9
<i>Toxoplasma gondii</i> TgAT.....	9
<i>Plasmodium falciparum</i> PfENT1.....	10
<i>Leishmania donovani</i> LdNT1.1 and LdNT1.2.....	11
<i>Leishmania donovani</i> LdNT2.....	11
<i>Trypanosoma brucei brucei</i> TbNT2-9.....	11
<i>Trypanosoma brucei brucei</i> TbAT1.....	13
<i>Caenorhabditis elegans</i> CeENT1.....	13
<i>Arabidopsis thaliana</i> AtENT1.....	14
<i>Saccharomyces cerevisiae</i> FUN26.....	14
Structure/function studies of ENT family members.....	15
Mammalian concentrative nucleoside transporters (CNTs).....	17
Characteristics of mammalian concentrative nucleoside transport processes.....	17
Functional and molecular properties of cloned mammalian CNTs.....	18
CNT1.....	18
CNT2.....	19
CNT3.....	20
CNT family members in prokaryotes and other eukaryotes.....	21
<i>Escherichia coli</i> NupC.....	21
<i>Caenorhabditis elegans</i> CeCNT3.....	21
Structure/function studies of CNT family members.....	22
Other nucleoside transport proteins.....	23
Bacteria.....	23
Nucleoside:H ⁺ symporter (NHS) family.....	23
Tsx channel-forming protein family.....	24
Yeast.....	25
Nucleoside uptake protein (NUP) family.....	25
FUI1 from the uracil/allantoin permease family.....	26
Mammals.....	26
OCT1 from the organic cation transporter (OCT) family.....	26
OAT1-4 from the organic anion transporter (OAT) family.....	27
Aims of the Present Studies.....	28
Bibliography.....	46

CHAPTER II: Identification of amino acid residues responsible for the pyrimidine and purine nucleoside specificities of human concentrative Na⁺ nucleoside cotransporters hCNT1 and hCNT2	64
Introduction.....	65
Materials and Methods.....	67
Nomenclature and construction of chimeric hCNT1 and hCNT2 transporters	67
Nomenclature and construction of site-specific mutated hCNT1 transporters	68
<i>In vitro</i> transcription and expression in <i>Xenopus</i> oocytes	68
Transport assays	68
Molecular modeling.....	69
Results and Discussion	70
hCNT1/hCNT2 chimeras	70
Identification of candidate residues for mutation in hCNT1	72
Characteristics of TM 7 mutants of hCNT1.....	73
Characteristics of TM 8 and TM 9 mutants of hCNT1	74
Combination mutants between TMs 7 and 8.....	75
Kinetic properties of M2/3/6/7, M2/3/6, and M6	76
Molecular modeling.....	77
Conclusions.....	79
Bibliography.....	91
CHAPTER III: Residue mutations in transmembrane helix 8 of human concentrative Na⁺-nucleoside cotransporter hCNT1 affect substrate selectivity and cation coupling	94
Introduction.....	95
Materials and Methods.....	97
Site-directed mutagenesis of hCNT1 and expression in <i>Xenopus</i> oocytes.....	97
Radioisotope flux studies.....	97
Measurements of hCNT1- and hCNT1/L354V-induced sodium currents.....	98
Results and Discussion	98
Expression of TM 8 hCNT1 mutants S353T, L354V, and S353T/L354V in <i>Xenopus</i> oocytes	99
Permeant specificity of TM 8 hCNT1 mutants S353T, L354V, and S353T/L354V.....	99
Kinetics of uridine transport by hCNT1 mutant S535T/L354V	100
Transport of uridine analogs by hCNT1 mutants S353T and S535T/L354V.....	101
Na ⁺ -dependence of hCNT1 mutants S353T, L354V, and S353T/L354V.....	101
Cation specificity and electrophysiology of hCNT1 mutant L354V.....	102
Kinetics of uridine transport by hCNT1 mutant L354V	103
Transport models and uncoupled substrate slippage.....	104
Conclusions.....	105

Bibliography.....	118
CHAPTER IV: Molecular identification and characterization of novel human and mouse concentrative Na⁺-nucleoside cotransporter proteins (hCNT3 and mCNT3) broadly selective for purine and pyrimidine nucleosides (system <i>cib</i>).	121
Introduction.....	122
Materials and Methods.....	124
Molecular cloning of hCNT3	124
Molecular cloning of mCNT3	126
Construction of chimeric hCNT3 and hCNT1 transporters.....	126
Expression of recombinant hCNT3 and mCNT3 in <i>Xenopus</i> oocytes ...	127
hCNT3 and mCNT3 radioisotope flux studies.....	127
Measurement of hCNT3-induced sodium and proton currents.....	128
Cation:Nucleoside Coupling Ratios	128
HL-60 cell culture and differentiation.....	129
HL-60 radioisotope flux studies.....	129
Tissue and cell distribution of hCNT3 mRNA.....	130
Quantitative real time RT-PCR.....	131
Chromosomal fluorescence <i>in situ</i> hybridization.....	131
Results and Discussion	132
Molecular identification of hCNT3 and mCNT3.....	132
hCNT3 and mCNT3 amino acid sequences.....	132
Functional expression and substrate specificity of recombinant hCNT3 and mCNT3.....	134
Kinetic properties and inhibitor sensitivity of recombinant hCNT3.....	135
hCNT3 Na ⁺ :nucleoside cotransport.....	136
pH- and lithium-dependence of recombinant hCNT3 and mCNT3	138
hCNT3-mediated transport of anticancer and antiviral nucleoside drugs	139
Characterization of hCNT3/hCNT1 Chimeras.....	140
Tissue and cell distribution.....	141
HL-60 cells (functional studies).....	142
HL-60 cells (TaqMan TM quantitative real time RT-PCR).....	143
Chromosomal localization of the hCNT3 gene.....	144
Conclusions.....	144
Bibliography.....	173
CHAPTER V: An ancient prevertebrate Na⁺-nucleoside cotransporter (hfcNT) from the Pacific hagfish (<i>Eptatretus stouti</i>)	178
Introduction.....	179
Materials and Methods.....	181
Molecular cloning of hfcNT	181
Other hagfish CNTs.....	182
Construction of chimeric hfcNT and hCNT1 transporters	182
<i>In vitro</i> transcription and expression in <i>Xenopus</i> oocytes	182
Radioisotope flux studies.....	183
Measurement of hfcNT-induced sodium currents.....	183

Results and Discussion	184
Molecular identification of hfcCNT	184
Other hagfish CNTs	186
Production of recombinant hfcCNT in <i>Xenopus</i> oocytes	186
Substrate selectivity and antiviral drug transport of recombinant hfcCNT	186
Kinetic properties	187
hfcCNT Na ⁺ :nucleoside cotransport	188
Characterization of hfcCNT/hCNT1 chimeras	190
Conclusions	191
Bibliography	211
CHAPTER VI: Transport of antiviral and antineoplastic nucleoside drug transport by recombinant <i>Escherichia coli</i> H⁺/nucleoside cotransporter (NupC) produced in <i>Xenopus laevis</i> oocytes	216
Introduction	217
Materials and Methods	218
Molecular cloning of NupC DNA	218
Functional production of recombinant NupC in <i>Xenopus</i> oocytes	219
NupC radioisotope flux studies	219
Results	220
Cloning of the <i>nupC</i> Gene	220
Functional production and cation-specificity of NupC in <i>Xenopus</i> oocytes	221
Substrate selectivity of recombinant NupC	221
Nucleoside drug transport by recombinant NupC	222
Kinetic properties	222
Discussion	223
Conclusions	226
Bibliography	234
CHAPTER VII: Functional characterization of a H⁺/nucleoside cotransporter (CaCNT) from <i>Candida albicans</i>, a fungal member of the concentrative nucleoside transporter (CNT) family of membrane proteins	238
Introduction	239
Materials and Methods	240
Molecular cloning of CaCNT	240
Functional production of CaCNT in <i>Xenopus</i> oocytes	241
CaCNT radioisotope flux studies	242
Measurements of CaCNT-induced H ⁺ currents	242
H ⁺ :nucleoside coupling ratios	243
Results and Discussion	243
<i>C. albicans</i> contains a mammalian/bacterial CNT homolog	244
Functional production of CaCNT in <i>Xenopus</i> oocytes	246
Permeant selectivity of recombinant CaCNT	247
Kinetic properties	247
Nucleoside drug transport by recombinant CaCNT	248

CaCNT H ⁺ :nucleoside cotransport	249
Conclusions.....	251
Bibliography.....	264
CHAPTER VIII: General Discussion	270
System <i>cib</i> belongs to the CNT family	272
Application of CaCNT in biochemical and biophysical studies of CNT proteins	274
Development of a single unified transport model for the CNT family	274
Helix Modeling of the CNT permeation pathway through mutagenesis studies.....	275
The role of CNT proteins in future therapeutic drug delivery and chemoprotective strategies	276
Bibliography.....	279

LIST OF TABLES

		<i>Page</i>
Table 1-1	Members of the Equilibrative Nucleoside Transporter (ENT) Family.....	29
Table 1-2	Concentrative Nucleoside Processes of Mammalian Cells.....	30
Table 1-3	Members of the Concentrative Nucleoside Transporter (CNT) Family ...	31
Table 1-4	Members of the Nucleoside:H ⁺ Family of Transporters.....	33
Table 1-5	Members of the Tsx Channel-forming Protein Family.....	34
Table 1-6	Members of the Nucleoside Uptake Protein (NUP) Family of Transporters.....	35
Table 1-7	Members of the Uracil/Allantoin Permease Family.....	36
Table 1-8	Members of the Organic Cation Transporter (OCT) Family.....	37
Table 1-9	Members of the Organic Anion Transporter (OAT) Family.....	38
Table 2-1	Nomenclature of hCNT1 Amino Acid Mutations.....	81
Table 2-2	Mediated Uptake of [¹⁴ C]-labeled Nucleosides by hCNT1 and hCNT1 Mutants.....	82
Table 2-3	Kinetic Properties of hCNT1 Mutants M2/3/6/7, M2/3/6, and M6.....	83
Table 3-1	Apparent K_m and K_{50} Values of hCNT1 and hCNT1 Mutants S353T/L354V and L354V.....	107
Table 3-2	Mediated Uptake of [¹⁴ C]-labeled Uridine and Pyrimidine Nucleoside Analogs by hCNT1, hCNT2 and Uridine-selective hCNT1 Mutants S353T and S353T/L354V.....	108
Table 4-1	Kinetic Properties of hCNT3.....	147
Table 5-1	Kinetic Properties of hfCNT.....	194
Table 6-1	Kinetic Parameters of Uridine, Adenosine, AZT, ddC, and Gemcitabine Influx Mediated by <i>E. coli</i> NupC and Mammalian CNT1 Transport Proteins.....	227
Table 7-1	Kinetic Parameters of CaCNT-mediated Nucleoside Influx.....	253

LIST OF FIGURES

		<i>Page</i>
Figure 1-1	Inhibitors of some ENT-mediated transport processes	39
Figure 1-2	Natural substrates transported by ENT and CNT transporters and by various members of other transporter families.....	40
Figure 1-3	Topographical model of hENT1.....	41
Figure 1-4	Phylogenetic tree of the ENT family.....	42
Figure 1-5	Transmembrane helix predictions for the ENT family of transporters.....	43
Figure 1-6	Topographical model of rCNT1.....	44
Figure 1-7	Phylogenetic tree of the CNT family.....	45
Figure 2-1	Topographical model of hCNT1 and hCNT2.....	84
Figure 2-2	Uptake of ¹⁴ C-labeled nucleosides by recombinant hCNT1, hCNT2, and chimeras C1122, C1112, C1221, and C1121 expressed in <i>Xenopus</i> oocytes	85
Figure 2-3	Nucleoside specificity of hCNT1, hCNT2, chimera C1121, and mutants M2/3, M2/3/6, M2/3/6/7, M2/3/6/8, and M4/5/6/7/8.....	86
Figure 2-4	Alignment of predicted amino acid sequences of h/rCNT1, h/rCNT2, and hCNT in TMs 7, 8, and 9.....	87
Figure 2-5	Kinetic properties of hCNT1 mutants M2/3/6/7, M2/3/6, and M6.....	88
Figure 2-6	Structural features of TMs in the CNT family and the proposed arrangement of TMs 7, 8 and 9 in hCNT1	89
Figure 3-1	Sequence alignment of h/rCNT1 and h/rCNT2 amino acid residues in putative TM 8.....	109
Figure 3-2	Nucleoside specificity of hCNT1, hCNT2, and hCNT1 mutants S353T, L354V, and S353T/L354V	111
Figure 3-3	Kinetic properties of hCNT1 mutants S353T/L354V and L354V	112
Figure 3-4	Chemical structures of selected pyrimidine nucleosides and nucleoside analogs	113
Figure 3-5	Na ⁺ -dependent and Na ⁺ -independent nucleoside transport activity of hCNT1 and hCNT1/L354V.....	114

Figure 3-6	Effects of pH and Li ⁺ replacement on hCNT1- and hCNT1/L354V-mediated uridine transport activity.....	115
Figure 3-7	Uridine-evoked currents in hCNT1- and hCNT1/L354V-producing oocytes.....	116
Figure 3-8	Ordered binding (AS) transport model with substrate slippage.....	117
Figure 4-1	hCNT3 and mCNT3 are members of the CNT family of nucleoside transporters.....	149
Figure 4-2	Topological model of hCNT3 and hCNT.....	150
Figure 4-3	Phylogenetic tree showing relationships between hCNT3 and mCNT3 and other eukaryotic and prokaryotic members of the CNT transporter family.....	152
Figure 4-4	Uptake of ¹⁴ C/ ³ H-labeled nucleosides and nucleobases by recombinant hCNT3 and mCNT3 expressed in <i>Xenopus</i> oocytes.....	153
Figure 4-5	Nucleoside selectivity of recombinant hCNT3, mCNT3, hCNT1, hCNT2 and hCNT.....	154
Figure 4-6	Kinetic properties of recombinant hCNT3.....	155
Figure 4-7	Recombinant hCNT3 is not inhibited by NBMPR, dipyridamole or dilazep.....	156
Figure 4-8	Sodium dependence of influx of uridine mediated by recombinant hCNT3 and mCNT3.....	157
Figure 4-9	Sodium currents induced by exposure of recombinant hCNT3 to nucleoside permeants.....	158
Figure 4-10	Stoichiometry of Na ⁺ /uridine and H ⁺ /uridine cotransport by recombinant hCNT3.....	159
Figure 4-11	pH dependence of recombinant hCNT3 and mCNT3.....	160
Figure 4-12	Effects of sodium, pH and lithium on the transport activities of oocytes expressing recombinant hCNT1, hCNT2, hCNT3, and mCNT3.....	161
Figure 4-13	Uptake of ³ H-labeled anticancer and antiviral nucleoside drugs by recombinant hCNT3 expressed in <i>Xenopus</i> oocytes.....	162
Figure 4-14	Representative nucleoside drug-induced currents in an hCNT3-producing <i>Xenopus</i> oocyte.....	163

Figure 4-15	Na ⁺ - and H ⁺ -dependence of radiolabeled ddC and uridine uptake by recombinant hCNT3 expressed in <i>Xenopus</i> oocytes.....	164
Figure 4-16	Topographical model of hCNT3 and hCNT1.....	165
Figure 4-17	Uptake of nucleosides by chimera hCNT3/1.....	166
Figure 4-18	Tissue distribution of hCNT3 mRNA.....	168
Figure 4-19	High stringency Northern analysis of mRNA from human tissues probed with ³² P-labeled hCNT3 cDNA.....	169
Figure 4-20	Time courses of ³ H-labeled uridine, thymidine and formycin B uptake by HL-60 cells.....	170
Figure 4-21	Non-quantitative RT-PCR and TaqMan TM quantitative RT-PCR of hCNT3 transcripts in HL-60 cells.....	172
Figure 5-1	hCNT is a member of the CNT family of nucleoside transporters.....	196
Figure 5-2	Phylogenetic tree showing relationships between hCNT and other functionally characterized members of the CNT transporter family.....	197
Figure 5-3	Time courses of uridine, thymidine and inosine uptake by recombinant hCNT produced in <i>Xenopus</i> oocytes.....	199
Figure 5-4	Uptake of nucleosides and anti-viral nucleoside drugs by hCNT.....	200
Figure 5-5	Kinetic properties of hCNT.....	202
Figure 5-6	Sodium currents induced by exposure of recombinant hCNT to nucleoside permeants.....	203
Figure 5-7	Sodium dependence of uridine, thymidine and inosine of influx by recombinant hCNT.....	205
Figure 5-8	Stoichiometry of Na ⁺ /uridine cotransport by recombinant hCNT.....	206
Figure 5-9	Topographical model of hCNT and hCNT1.....	207
Figure 5-10	Uptake of nucleosides and anti-viral nucleoside drugs by hCNT/hCNT1 chimera HF/H.....	208
Figure 5-11	Sodium-dependence of uridine, thymidine, and cytidine influx by hCNT/hCNT1 chimera HF/H.....	210
Figure 6-1	NupC is a member of the CNT family of nucleoside transport proteins...	229
Figure 6-2	Effect of external pH on NUPC- and rCNT1-mediated uridine influx.....	230

Figure 6-3	Substrate selectivity and drug transport by NupC.....	231
Figure 6-4	Kinetic properties of recombinant NupC	233
Figure 7-1	Alignment of the predicted amino acid sequences of CaCNT	255
Figure 7-2	Differences in deduced amino acid sequences of CaCNT and those derived from Contig6-1704 and Contig6-2474 (Stanford Genome Technology Center database)	256
Figure 7-3	Phylogenetic tree showing relationships between CaCNT and other functionally characterized members of the CNT transporter family.....	257
Figure 7-4	Time course of uridine uptake by recombinant CaCNT produced in <i>Xenopus</i> oocytes	258
Figure 7-5	Substrate selectivity and drug transport by CaCNT.....	259
Figure 7-6	Kinetic properties of CaCNT.....	260
Figure 7-7	Proton currents induced by exposure of recombinant CaCNT to nucleoside permeants.....	262
Figure 7-8	Stoichiometry of H ⁺ /uridine cotransport by recombinant CaCNT.....	263
Figure 8-1	Topologies of hCNT1, CaCNT and NupC.....	278

LIST OF ABBREVIATIONS, SYMBOLS, AND NOMENCLATURE

3TC	3'-thia-2',3'-dideoxycytidine (lamivudine)
5-FdUrd	5-fluoro-2'-deoxyuridine
5-FUrd	5-fluorouridine
AIDS	Acquired Immunodeficiency Syndrome
AtENT1-8	<i>Arabidopsis thaliana</i> ENT isoforms
AZT	3'-azido-3'-deoxythymidine
BAC library	Bacterial artificial chromosome library
BLAST	Basic Local Alignment Search Tool Algorithm
bp(s)	Nucleotide base pair(s)
Ca	<i>Candida albicans</i>
CaCo-2	Human colon carcinoma cell line
cDNA	Complementary DNA
Ce	<i>Caenorhabditis elegans</i>
CeENT1	<i>Caenorhabditis elegans</i> ENT isoform
<i>cib</i>	concentrative, insensitive to NBMPR inhibition, broadly selective
<i>cif</i>	concentrative, insensitive to NBMPR inhibition, formycin B is a permeant
<i>cit</i>	concentrative, insensitive to NBMPR inhibition, thymidine is a permeant
<i>cf</i>	<i>confer</i> (compare)
Cladribine	2-chloro-2'-deoxyadenosine
CNT	concentrative nucleoside transporter
CNT1	refers to a pyrimidine-nucleoside preferring CNT
CNT2	refers to a purine-nucleoside preferring CNT
CNT3	refers to a broadly selective CNT
<i>cs</i>	concentrative, sensitive to NBMPR inhibition
<i>csg</i>	concentrative, sensitive to NBMPR inhibition, guanosine is a permeant
Cytarabine	1-(β -D-arabinofuranosyl)cytosine, Ara-C
d4T	2',3'-didehydro 3'-deoxythymidine (stavudine)
DAL4	member of the uracil/allantoin transporter family that mediates allantoin
ddC	2',3'-dideoxycytidine
ddI	2',3'-dideoxyinosine
DHEA	dehydroepiandrosterone

DNA	deoxyribonucleic acid
<i>e.g.</i>	<i>exempli gratia</i> (for example)
<i>ei</i>	equilibrative, insensitive to NBMPR inhibition
EMBL	European Molecular Biology Laboratory database
ENT	equilibrative nucleoside transporter
ENT1	refers to an <i>es</i> -type transporter, with broad permeant selectivity for purine and pyrimidine nucleosides, sensitive to NBMPR inhibition
ENT2	refers to an <i>ei</i> -type transporter, with broad permeant selectivity for purine and pyrimidine nucleosides, insensitive to NBMPR inhibition
ENT3	refers to a novel mammalian member of the ENT family with unknown function
<i>es</i>	equilibrative, sensitive to NBMPR inhibition
EST	expressed sequence tag
FUI1	member of the uracil/allantoin transporter family that mediates uridine
FUN26	<i>Saccharomyces cerevisiae</i> ENT isoform
FUR4	member of the uracil/allantoin transporter family that mediates nucleobases
GAPDH	glyceraldehyde phosphate dehydrogenase
GCG	Genetics Computer Group
Gemcitabine	2',3'-difluorodeoxycytidine
GLUT	facilitative glucose transport proteins
h	Human
HEPES	4-(2-hydroxyethyl)-1-piperazineethanesulfonic acid
hf	Hagfish
HL-60	Myeloid cell line
<i>i.e.</i>	<i>id est</i> (that is)
I.M.A.G.E. Consortium	Integrated Molecular Analysis of Genomes and their Expression
IC ₅₀	Inhibitory concentration at which 50% of the activity is inhibited
kDa	kilodalton(s)
K _m	Permeant concentration at half-maximal unidirectional flux
LdNT1/2	<i>Leishmania donovani</i> nucleoside transport proteins
m	Mouse
MBM	Modified Barth's Medium
NBMPR	Nitrobenzylmercaptapurine ribonucleoside

NCBI	National Center for Biotechnology Information
ND	not determined
NHS	Nucleoside:H ⁺ Symporter family
NLM	National Library of Medicine
NMDG	N-methyl-D-glucamine
NT	Nucleoside transporters
NUP	Nucleoside Uptake Protein family
NupC	H ⁺ /nucleoside cotransporter from bacteria and member of the CNT family
NupG	H ⁺ /nucleoside cotransporter from bacteria and member of the NHS family
OAT	organic anion transporter
OCT	organic cation transporter
ORF	open reading frame
PAH	<i>p</i> -aminohippurate
pCMBS	<i>p</i> -chloromercuriphenylsulphonate
PCR	polymerase chain reaction
pfENT1	<i>Plasmodium falciparum</i> ENT1
PHDhtm	Helical transmembrane region prediction program
pk	Pig
r	Rat
rb	Rabbit
RNA	Ribonucleic acid
RPMI	Roswell Park Memorial Institute
RT-PCR	Reverse transcriptase polymerase chain reaction
SAAT1	sodium amino acid/(glucose) cotransporter (renamed SGLT3)
SDS	sodium dodecyl sulfate
S.E.	standard error
SGLT	Na ⁺ /glucose cotransporter family of transporters
SNST1	Na ⁺ /nucleoside co-transporter (renamed SGLT2)
SSS	Sodium/solute symporter family of transporters
TbAT1	<i>Trypanosoma brucei brucei</i> ENT isoform
TbNT2-9	<i>Trypanosoma brucei brucei</i> ENT isoforms
TgAT	Adenosine-preferring transporter from <i>Toxoplasma gondii</i>
TM	Transmembrane helix

TMHMM	Transmembrane helix prediction program
TMPred	Transmembrane helix prediction program
Tris	Tris-(hydroxymethyl) aminomethane
V_{\max}	Maximum transport rate
w/v	Weight per unit volume
XapB	H ⁺ /nucleoside cotransporter from bacteria and member of the NHS family

CHAPTER I:

General Introduction

Preamble

The movements of nucleosides across the lipid bilayer of cells are mediated and controlled by specific concentrative (Na^+ - and H^+ -dependent) and equilibrative transport mechanisms. At the time of my enrolment into the Department of Physiology graduate program at the University of Alberta in 1997, the first glimpses of the molecular properties of the proteins responsible for the cellular uptake of nucleosides across the plasma membrane of mammalian cells were beginning to take shape. Three years earlier in 1994, a cDNA encoding first mammalian concentrative Na^+ /nucleoside cotransporter, designated cNT_{rat} (and later rCNT1), was cloned from rat jejunum (Huang *et al.*, 1994) along with a related cDNA believed to encode an H^+ /nucleoside cotransporter (NupC) from *Escherichia coli* (Craig *et al.*, 1994). This was followed closely by the identification of a second mammalian CNT homolog from rat tissues, designated rCNT2 (Che *et al.*, 1995; Yao *et al.*, 1996a). In conjunction with my entry into laboratory research, the human orthologs of these Na^+ /nucleoside cotransporters were identified (hCNT1 and hCNT2) (Ritzel *et al.*, 1997; Wang *et al.*, 1997; Ritzel *et al.*, 1998), as well as the first equilibrative nucleoside transporters from rat (rENT1 and rENT2) and human (hENT1 and hENT2) tissues (Griffiths *et al.*, 1997a, 1997b; Yao *et al.*, 1997; Crawford *et al.*, 1998). Although the general functional properties of these first identified nucleoside transport proteins (with the exception of *E. coli* NupC) were established at the time of their initial cDNA cloning, very little was known about structure/function relationships or the diversity of functional activities exhibited by other CNT and ENT family members.

The studies described in *Chapters II-VII* of this thesis were carried out between 1997 and 2002 and had two related objectives. The first was to identify and characterize new members of the CNT protein family. The second was to undertake structure/function studies of CNT proteins. Initial studies focused on structure/function studies of hCNT1 and hCNT2 and the results of these experiments are described in *Chapters II* and *III*. This thesis also describes the identification, molecular cloning and functional characterization of human (hCNT3) and mouse (mCNT3) representatives of a third mammalian member of the CNT protein family. As described in *Chapter IV*, these proteins possess novel cation-coupling and nucleoside-selectivity properties that distinguish them functionally from mammalian CNT1 and CNT2. Two new CNT family members have also been identified and characterized from non-

mammalian species. One (hfCNT) is from an ancient marine prevertebrate, the Pacific hagfish (*Eptatretus stouti*) and is described in *Chapter V*. The other (CaCNT) is from pathogenic yeast (*Candida albicans*) and is described in *Chapter VII*. Both proteins provide unique perspectives on CNT molecular evolution. In addition, the functional characterization of *E. coli* NupC in *Xenopus laevis* (herein referred to as *Xenopus*) oocytes described in *Chapter VI* represents the first successful expression of a bacterial transport protein in *Xenopus* oocytes and establishes the utility of the NupC/oocyte system as a tool to further our understanding of the physiological and pharmacological roles of concentrative NTs in bacteria.

The remainder of this chapter describes current knowledge of the transporters (and their respective protein families) responsible for nucleoside uptake in mammalian and other cells, focusing on the studies that have led to our current understanding of their molecular properties and providing a background to the experiments described in subsequent chapters. The final chapter of this thesis (*Chapter VIII*) is a general discussion of the results obtained and the direction of future research.

Nucleoside Transport Proteins

Specialized plasma membrane nucleoside transporter (NT) proteins play key roles in many aspects of prokaryote and eukaryote physiology. NT-mediated nucleoside uptake is an essential component of the proliferative lifecycle of bacteria (Kubitschek, 1968; Kirchman *et al.*, 1982) and, in mammals and other eukaryotes, provides substrates for the salvage pathways required for synthesis of nucleotides in cells that lack *de novo* purine biosynthetic pathways (Griffith and Jarvis, 1996; Cheeseman *et al.*, 2000). These include protozoan parasites (Berens *et al.*, 1995) and, in mammals, bone marrow cells, enterocytes, and some brain cells (Murray, 1971). By regulating the concentration of adenosine available to cell-surface receptors, NTs in mammals also influence a wide variety of physiological processes including neurotransmission and cardiovascular activity (Shryock and Belardinelli, 1997). Adenosine, itself, is used clinically for the treatment of cardiac arrhythmias, while transport inhibitors such as dipyridamole and dilazep (Fig. 1-1) act as coronary vasodilators (Baldwin *et al.*, 1999). In addition to mediating transport of natural nucleosides (Fig. 1-2), NTs also provide the cellular uptake route for many

cytotoxic nucleoside derivatives used in the treatment of viral and neoplastic diseases (Mackey *et al.*, 1998; Young *et al.*, 2000).

Nucleosides are important precursors of nucleic acids and energy-rich cellular metabolites, and cells obtain nucleosides from breakdown of dietary and endogenous nucleotides (Griffith and Jarvis, 1996, Cheeseman *et al.*, 2000). The former are important nutrients and are absorbed as nucleosides by enterocytes of the intestinal mucosa. Many kinetically-distinct nucleoside transport processes have been identified in mammals. For example, mammalian cells possess both concentrative, sodium-linked and bi-directional, equilibrative nucleoside transport processes. Epithelia (*e.g.* intestine, kidney) and some nonpolarized cells (*e.g.* leukemic cells) coexpress both concentrative and equilibrative NTs, whereas other nonpolarized cells (*e.g.* erythrocytes) exhibit only equilibrative NT activity (Baldwin *et al.*, 1999). Over the past decade, the proteins responsible for many of these activities in mammals and other organisms have been identified by molecular cloning approaches. Most of those characterized thus far fall into one of eight integral membrane protein families. Four of these, the equilibrative nucleoside transporter (ENT) family, the concentrative nucleoside transporter (CNT) family, the organic cation transporter (OCT) family and the organic anion transporter (OAT) family have representatives that transport nucleosides in mammalian cells. The remaining four families, the nucleoside:H⁺ symporter (NHS) family, the Tsx channel-forming protein family, the nucleoside uptake protein (NUP) family, and the uracil/allantoin permease family, appear to be limited to prokaryotes and/or lower eukaryotes. In some instances, not all members of these protein families transport nucleosides or function primarily as nucleoside transporters (*e.g.* the OCT family, the OAT family and the uracil/allantoin permease family). For example, members of the uracil/allantoin family transport nucleosides (*i.e.* FUI1), nucleobases (*i.e.* FUR4), or allantoin (*i.e.* DAL4) (Wagner *et al.*, 1998; de Koning and Diallinas, 2000; Vickers *et al.*, 2000). As well, several ENTs are now known to transport nucleobases (Parker *et al.*, 2000; Sanchez *et al.*, 2002; Yao *et al.*, 2002). Functional diversity amongst ENTs also includes some which are concentrative rather than equilibrative (Sanchez *et al.*, 1999; Mohlmann *et al.*, 2001). The following sections of this chapter present an in depth review of the nucleoside transport literature, focusing on molecular aspects, and identifies several previously unreported cDNAs

gathered from database searches that underscores the extensive representation of these proteins throughout evolutionary history.

Mammalian Equilibrative Nucleoside Transporters (ENTs)

Characteristics of Mammalian Equilibrative Nucleoside Transport Processes – Equilibrative nucleoside transport processes are widely distributed in mammalian cells and tissues and exhibit the classic features of facilitated diffusion (Young and Jarvis, 1983; Paterson and Cass, 1986; Cass *et al.*, 1987; Plagemann *et al.*, 1988; Cabantchik, 1989; Gati and Paterson, 1989a; Paterson *et al.*, 1991). Their permeant selectivities are broad, transporting both purine and pyrimidine endogenous nucleosides as well as many structurally-related nucleoside analogs (Young and Jarvis, 1983; Paterson and Cass, 1986; Cass *et al.*, 1987; Plagemann *et al.*, 1988; Cabantchik, 1989; Gati and Paterson, 1989a; Paterson *et al.*, 1991). Two functionally distinct classes of equilibrative nucleoside transporters can be distinguished on the basis of their sensitivity to inhibition by NBMPR (Fig. 1-1), a specific inhibitor of nucleoside transport in human erythrocytes and many other cell types (Young and Jarvis, 1983; Paterson and Cass, 1986; Griffith and Jarvis, 1996; Cass *et al.*, 1999). Transport processes of the *es* (equilibrative sensitive) class are inhibited by low concentrations (< 1 nM) of NBMPR, whereas transport processes of the *ei* (equilibrative insensitive) class are relatively insensitive to the drug. Both *es* and *ei* transport processes, at least in humans, are potently inhibited by the vasodilator drugs dipyridamole, dilazep and drafazine (Fig. 1-1), although the level of inhibition varies between species and cell type. For example, the equilibrative transport processes in the rat are resistant to inhibition by these vasodilators (Griffith and Jarvis, 1996; Yao *et al.*, 1997), whereas the sensitivity of the mouse transport processes are intermediate (Hammond, 2000a).

Functional and Molecular Properties of Cloned Mammalian ENTs

ENT1 – The specificity of NBMPR for interaction with *es*-type processes allowed for identification and purification of the protein responsible for the archetypal *es*-type transport activity of human erythrocytes (Kwong *et al.*, 1988) that eventually led to cloning of the corresponding cDNA from human placenta in 1997 (Griffiths *et al.*, 1997a). Human (h) equilibrative nucleoside transporter 1 (designated hENT1) contains 456 amino acid residues and was the first identified example of a novel group of transporters that have since been

labeled collectively as the ENT protein family (Baldwin *et al.*, 1999; Cass *et al.*, 1999). The predicted membrane architecture of hENT1 suggests 11 transmembrane helices (TMs), with a cytoplasmic N-terminus, a central hydrophilic loop region, and an extracellular C-terminus (Fig. 1-3). Functional expression of hENT1 in *Xenopus* oocytes showed it to be a bona fide *es*-type transporter, with broad permeant selectivity for purine and pyrimidine nucleosides (Fig. 1-2) and sensitivity to inhibition by NBMPR, dipyridamole, dilazep, and draflazine (Griffiths *et al.*, 1997a, 1997b). hENT1 has an apparent affinity for natural nucleosides in the high micromolar range (the apparent K_m for uridine is $\sim 250 \mu\text{M}$) and transport was Na^+ -independent (Griffiths *et al.*, 1997a). Two additional orthologs of hENT1 from rat (r) and mouse (m), designated rENT1 and mENT1, have been cloned and characterized (Yao *et al.*, 1997; Kiss *et al.*, 2000). rENT1 (457 amino acid residues) and mENT1 (458 amino acid residues) are each 78% identical in sequence to hENT1 and have similar kinetic properties, except for the distinctive species differences with respect to inhibition by dipyridamole, dilazep and draflazine (human > mouse > rat). Several novel forms of ENT1 have been identified in mouse and possibly represent alternative splice variants or polymorphic forms of the transporter (Handa *et al.*, 2001; Kiss *et al.*, 2000), although no distinct physiological roles have been identified for these ENT1 variants. ENT1 proteins from human, rat, and mouse are believed to be ubiquitously distributed in most, possibly all, cell types, but are particularly abundant at the mRNA and protein levels in erythrocytes, placenta, liver, heart, lung, spleen, testis, kidney, colon and brain (Griffiths *et al.*, 1997a; Choi *et al.*, 2000).

In addition to mediating transport of natural substrates, hENT1 has the ability to transport antineoplastic nucleoside analog drugs used in cancer chemotherapy, including cladribine (2-chloro-2'-deoxyadenosine), cytarabine (1-(β -D-arabinofuranosyl)cytosine), Ara-C, and gemcitabine (2',3'-difluorodeoxycytidine) (Griffiths *et al.*, 1997a; Mackey *et al.*, 1998, 1999). In contrast, hENT1 does not transport the antiviral drug AZT (3'-azido-3'-deoxythymidine) and only weakly transports the antiviral drugs, ddC (2',3'-dideoxycytidine) and ddI (2',3'-dideoxyinosine) (Griffiths *et al.*, 1997a; Young *et al.*, 2000).

ENT2 – The molecular cloning and identification of a second cDNA encoding the human *ei*-type transporter by PCR amplification from a human placental cDNA library occurred shortly after the cloning of human ENT1 (Griffiths *et al.*, 1997b). A cDNA encoding

the same protein was cloned independently by functional complementation in a nucleoside transport-deficient leukemia cell line (Crawford *et al.*, 1998). The encoded protein, designated hENT2, contained 456 amino acid residues and was 50% identical in sequence to hENT1. When expressed in *Xenopus* oocytes, hENT2 exhibited functional properties consistent with *ei*-type transport activity, including the lack of sensitivity to inhibition by nanomolar concentrations of NBMPR, dipyridamole and other coronary vasodilators (Griffiths *et al.*, 1997; Ward *et al.*, 2000). hENT2, like hENT1, transports a broad range of purine and pyrimidine nucleosides, but appears to have significantly lower apparent affinities for most natural nucleosides compared to hENT1 (Griffiths *et al.*, 1997b; Crawford *et al.*, 1998; Ward *et al.*, 2000; Young *et al.*, 2000). Furthermore, hENT2 shows greater transport activity towards the antiviral nucleoside drugs AZT, ddC, and ddI, suggesting that the strict structural requirement for the sugar 3'-hydroxyl group in the case of hENT1-mediated (*es*-type) transport is less important for substrate binding and translocation of antiviral drugs by hENT2 (*ei*-type) (Gati *et al.*, 1984; Young *et al.*, 2000). This broader permeant profile of hENT2 also extends to the transport of nucleobases such as hypoxanthine, first indicated by inhibition of adenosine uptake by hypoxanthine the *ei*-type process of the human umbilical vein endothelial cell line ECV 304 (Osses *et al.*, 1996) and by hypoxanthine inhibition of recombinant hENT2-mediated uridine uptake in human CEM leukemia cells (Crawford *et al.*, 1998; Ward *et al.*, 2000). Direct uptake studies with radiolabeled hypoxanthine and other nucleobases in *Xenopus* oocytes subsequently confirmed nucleobases as hENT2 permeants (Young *et al.*, 2000; Yao *et al.*, 2002). Uptake of nucleosides and nucleobases is the first step of nucleotide synthesis in tissues such as bone marrow and intestinal epithelium that lack *de novo* pathways for purine biosynthesis (Murray, 1971; Young *et al.*, 2000). Nucleobase transport may, therefore, represent an important physiological function of ENT2 in human tissues not shared by hENT1.

Two additional orthologs of hENT2 from rat (r) and mouse (m), designated rENT2 and mENT2, have been cloned and characterized (Yao *et al.*, 1997; Kiss *et al.*, 2000). rENT2 (457 amino acid residues) and mENT2 (458 amino acid residues) are 89 and 88% identical in sequence, respectively, to hENT2 and ~ 50% identical to ENT1 proteins. Both have similar kinetic properties to hENT2, including characteristic *ei*-type activity marked by lack of

transport inhibition by NBMPR and relative insensitivity ($IC_{50} > 1 \mu\text{M}$) to inhibition by dipyrindamole and dilazep (Yao *et al.*, 1997; Kiss *et al.*, 2000). Investigations of ENT2 mRNA in rat and human tissues indicate that ENT2, like ENT1, is expressed in a wide range of tissues, including brain, heart, placenta, thymus, pancreas, prostate and kidney, but is particularly abundant in skeletal muscle (Griffiths *et al.*, 1997b; Crawford *et al.*, 1998).

ENT3 – The molecular cloning of ENT3 proteins from human and mouse is an example of the utility of *in silico* cloning approaches. Database searching using the BLAST algorithm to identify sequences with significant homology to known sequences has greatly accelerated the discovery of novel family members. In this case, ENT1 and ENT2 sequences were used to identify two previously unrecognized cDNA sequences that were homologous to, but differed from, published ENT1 and ENT2 sequences from human and mouse (Hyde *et al.*, 2001). A full-length cDNA clone from mouse kidney was obtained from the I.M.A.G.E. Consortium. The encoded protein, designated mENT3, was subsequently used as a search template to identify the full-length human CNT3 cDNA from the high throughput genome sequence GenBank™ database (Hyde *et al.*, 2001). A cDNA encoding the hENT3 protein was then obtained by PCR cloning from a placental cDNA library (Hyde *et al.*, 2001). Human and mouse ENT3 share 73% sequence identity and exhibit between 30-33% identity (42-48% sequence similarity) with ENT1 and ENT2 isoforms from human, rat, and mouse. There is no information presently available concerning ENT3 transport function, although its structural similarity to ENT1/2 proteins predicts transport of nucleosides and/or nucleobases. Functional expression of ENT3 proteins in *Xenopus* oocytes has so far been unsuccessful. Uniquely, however, these proteins possess a longer (51-residue) hydrophilic N-terminal region preceding TM1 than ENT1/2 and this region contains two pairs of conserved dileucine motifs. These motifs resemble targeting signals used to sort membrane proteins to the plasma membrane, endosomes and *trans*-Golgi network (Sandoval and Bakke, 1994). Furthermore, the glucose facilitators GLUT6 and GLUT8 possess similar membrane topologies to ENTs and normally target to intracellular compartments (Lisinski *et al.*, 2001). Mutation of N-terminal dileucine motifs in both GLUT6 and GLUT8 results in constitutive expression of both proteins to the plasma membrane (Lisinski *et al.*, 2001). It is therefore likely that ENT3 proteins reside not at the cell surface but in some intracellular compartment. Recruitment of

ENT3 to the plasma membrane may also be part of a hormone-mediated or dynamin-dependent regulatory process similar to insulin stimulation of GLUT4 cell surface expression and dynamin GTPase-dependent regulation of GLUT6 and GLUT8 (Holman and Sandoval, 2001; Lisinski *et al.*, 2001). Such possibilities might explain, at least in part, the variation in *es*- and *ei*-type activities identified in different populations of mammalian cells (Griffith and Jarvis, 1996).

ENT Family Members in Other Eukaryotes – The large array of on-line genomic sequence databases, combined with advanced BLAST searching techniques, has vastly expanded the number of ENT family members identified in other eukaryotes. Interestingly, database searches of complete and unfinished bacterial genome databases have yet to identify an ENT homolog in prokaryotes, indicating that the ENT ancestry is exclusive to eukaryotes or, perhaps, that ENTs were lost during prokaryote evolution. The current members of the family are listed in Table 1-1, and their phylogenetic relationships are presented in Fig. 1-4. The number of isoforms in different species seems to vary greatly, with just one family member in the yeast *Saccharomyces cerevisiae* (FUN26) and as many as eight and nine in the plant *Arabidopsis thaliana* (AtENT1-8) and the protozoan parasite *Trypanosoma brucei brucei* (TbAT1, TbNT2-9), respectively. Only a few of these ENT transporters, as described below, have been characterized functionally, including members from protozoa (*Toxoplasma gondii*, *Plasmodium falciparum*, *Leishmania donovani*, and *Trypanosoma brucei brucei*), nematodes (*Caenorhabditis elegans*), plants (*Arabidopsis thaliana*), and yeast (*Saccharomyces cerevisiae*). In general, there is considerable interest in protozoan ENT transporters, not only because protozoa are important parasites of man, but because many lack *de novo* purine biosynthetic pathways (Berens *et al.*, 1995) and therefore are completely dependent on purine salvage mechanisms for nucleotide synthesis. This makes protozoan ENTs an attractive drug target in antiparasite pharmacology.

***Toxoplasma gondii* TgAT** – An adenosine-preferring transporter in *Toxoplasma gondii* was identified by an insertional mutagenesis technique involving selection of mutants resistant to the cytotoxic adenosine analog adenine arabinosine (Chiang *et al.*, 1999). The resulting protein, designated TgAT, contains 462 amino acid residues and is 25-28% identical in sequence to human ENT1/2/3 proteins. Functionally, TgAT transports adenosine (apparent K_m of 114 μ M) but this activity can be inhibited competitively by other purine (but

not pyrimidine) nucleosides, hypoxanthine, and guanine. The transporter is sensitive to inhibition by dipyridamole (Chiang *et al.*, 1999). Mutation of the *TgAT* gene locus results in elimination of adenosine uptake in *T. gondii* tachyzoites, suggesting that TgAT is the sole adenosine transporter in *Toxoplasma gondii* (Chiang *et al.*, 1999).

***Plasmodium falciparum* PfENT1** – An equilibrative, broadly-selective NT has been identified and independently cloned by two groups using sequence information from the Malaria Genome Sequencing Project (Carter *et al.*, 2000a; Parker *et al.*, 2000). PfENT1 (also termed PfNT1) contains 422 amino acid residues and shares 20-26% sequence identity with human ENT1/2/3 proteins, and 22% identity with TgAT. When expressed in *Xenopus* oocytes, PfENT1 exhibited broad specificity for purine and pyrimidine nucleosides, but the two reports differ significantly with respect to the apparent affinity for adenosine (320 μM *vs.* 13 μM), the ability to transport nucleobases (only Parker *et al.* were able to demonstrate radiolabeled purine and pyrimidine nucleobase uptake), and sensitivity to classical mammalian ENT inhibitors (Parker *et al.* reported no transport inhibition by high concentrations (10 μM) of NBMPR and dipyridamole, whereas Carter *et al.* showed marked inhibition (~85%) of transporter-mediated [^3H]adenosine uptake by 10 μM dipyridamole). No explanation is available to account for these differences, although the sequences of the two proteins were not identical with a single amino acid difference at residue position 385 (Phe *vs.* Leu).

In general, PfENT1-mediated transport activity closely resembles that of the mammalian ENT2 isoform not only in transport of nucleosides and nucleobases but also in its ability to mediate influx of antiviral 3'-dideoxynucleoside drugs, including AZT, ddC and ddI (Parker *et al.*, 2000). With the Malaria Genome Sequencing Project nearing completion in summer of 2002 (Enserink and Pennisi, 2002), PfENT1 remains the sole identified route by which this parasite takes up essential nucleoside and nucleobases and, quite possibly, nucleoside- and nucleobase-derived therapeutic drugs. Western blot analysis using polyclonal antibodies specific for PfENT1 indicates that the transporter is localized predominantly, if not exclusively, to the parasite plasma membrane and not to the parasitophorous vacuolar or host erythrocyte membranes (Rager *et al.*, 2001).

***Leishmania donovani* LdNT1.1 and LdNT1.2** – Two nearly identical cDNAs, designated LdNT1.1 and LdNT1.2, were isolated by functional rescue of transport-deficient *L. donovani* mutants (Vasudevan *et al.*, 1998). LdNT1.1 and LdNT1.2 (each containing 491 amino acid residues) are 99% identical in sequence and differ at only six amino acid positions (Pro43Ser, Met107Ile, Thr160Ala, Ala489Glu, Thr490Arg and Tyr491His). They are not polymorphic forms of the same protein (such as may be the case for the reported forms of mENT1). Instead, LdNT1.1 and LdNT1.2 are encoded by tandemly-linked genes. When expressed in *Xenopus* oocytes, LdNT1.1 and LdNT1.2 mediated the uptake of adenosine and uridine with apparent K_m values of 0.17 and 0.66 μM (adenosine) and 5.6 and 40 μM (uridine), respectively. Nucleobase transport and uptake of other nucleosides were not measured.

***Leishmania donovani* LdNT2** – Another cDNA from *Leishmania donovani* that is related to, but differed from, LdNT1.1 and LdNT1.2, was identified by a similar functional rescue technique as described in the preceding section (Carter *et al.*, 2000b). The encoded protein, LdNT2 (499 residues), transported radiolabeled inosine and guanosine with reported apparent K_m values of 0.3 and 1.7 μM , respectively. Inhibition studies using 100-fold excess concentrations of naturally occurring nucleosides and nucleobases did not reveal other potential substrates of LdNT2, although poor, but significant, inhibition (12-35%) was observed by some nucleosides (xanthosine, uridine, and thymidine) and nucleobases (hypoxanthine, guanine, and xanthine), suggesting possible low affinity interactions with the transporter. LdNT2-mediated uptake of inosine was unaffected by micromolar concentrations of NBMPR.

***Trypanosoma brucei brucei* TbNT2-9** – Nucleoside transport processes have been well-characterized in *Trypanosoma brucei brucei*, the causative agent of African sleeping sickness in man (Carter and Fairlamb, 1993; de Koning *et al.*, 1998; de Koning and Jarvis, 1999). There are two major nucleoside transport processes identified in *Trypanosoma brucei* spp., P1 and P2, which differ in substrate specificity (P1 transports adenosine/inosine/guanosine whereas P2 transports adenosine/adenine), their affinities for adenosine (P1 exhibits higher apparent affinity for adenosine than P2), and their abilities to mediate transport of the antitrypanocidal drugs melarsoprol and pentamidine (P2, but not P1). Although P2 transports nucleobases in addition to adenosine, three additional nucleobase transport processes that accept

hypoxanthine have been described in *Trypanosoma brucei* spp. (designated H1-H3), which differ in their activities during the trypanosome lifecycle (H1 is found in the procyclic (insect-resident) form, whereas H2 and H3 are found in the bloodstream (mammalian parasitic) form and, in the case of H2 and H3, by their sensitivity to inhibition to guanosine, H3 being insensitive (de Koning and Jarvis, 1997a, 1997b). An additional nucleobase transport process selective for uracil, designated U1, has also been identified in the procyclic form (de Koning and Jarvis, 1998). Some of these transport processes for nucleosides (P1-type and P2-type) and nucleobases (H2-type and U1-type) have been shown to be driven by the proton motive force across the cell membrane (de Koning and Jarvis, 1997b, 1997c; de Koning *et al.*, 1998; de Koning and Jarvis, 1998).

An adenosine transporter corresponding with P1-type transport activity, designated TbNT2 (463 residues), was cloned by PCR amplification of genomic DNA using sequence information derived by searches of the non-redundant GenBank™ EST (expressed sequence tags) database with LdNT1.1 (Sanchez *et al.*, 1999). When expressed in *Xenopus* oocytes, TbNT2 showed high affinity for adenosine, guanosine and inosine (apparent $K_m \sim 1 \mu\text{M}$). TbNT2 was also sensitive to inhibition by proton-ionophores, suggesting that the transporter is a concentrative, proton-linked symporter (Sanchez *et al.*, 1999). TbNT2 appears to be expressed in bloodstream form parasites but not in trypanosomes of the procyclic form (Sanchez *et al.*, 1999). Since P1-like functional activity has been demonstrated in both lifecycle forms, P1-type transporters other than TbNT2 may exist (Carter and Fairlamb, 1993).

Recently, eight additional cDNAs have been identified from BLAST searches of the GenBank™/EMBL database (encoding TbNT2 isoforms TbNT2/927 and TbNT3-9), six of which (TbNT2/927 and TbNT3-7) have been cloned and functionally expressed in *Xenopus* oocytes (Sanchez *et al.*, 2002). Although nearly identical to TbNT2, the nomenclature TbNT2/927 was used to distinguish it from the closely related TbNT2-encoded gene that was originally cloned from a different *T. brucei* strain (EATRO 110 *vs.* TREU 927 for TbNT2/927), and which contains subtle differences in DNA and amino acid sequence (Sanchez *et al.*, 1999; Sanchez *et al.*, 2002). Together, these proteins share $\sim 20\text{-}25\%$ sequence identity with the human ENT1-3 proteins, and 81-96% identity with TbNT2. Their genes are clustered together on chromosome II, separated by $\sim 9\text{-kb}$ of intergenic sequence. In oocytes, only

TbNT2/927, TbNT5, TbNT6 and TbNT7 were functional, and exhibited high apparent affinity for adenosine, inosine and guanosine (P1-type activity) with K_m values $< 5 \mu\text{M}$. In addition, TbNT5, and to a lesser extent TbNT6 and TbNT7, also mediated the uptake of the nucleobase hypoxanthine. Unlike TbNT2, however, which was found only in the bloodstream form (Sanchez *et al.*, 1999), multiple forms of TbNT transporters are expressed both in the bloodstream (TbNT2/927, TbNT3-7) and procyclic stages (TbNT2/927 and TbNT5). There is therefore a complex network of purine uptake mechanisms involved in trypanosomal physiology.

***Trypanosoma brucei brucei* TbAT1** – A related, P2-type transporter, TbAT1, was cloned by transforming yeast cells defective in purine biosynthesis with a bloodstream form cDNA expression library, followed by growth selection in medium containing adenosine as the sole purine source (Maser *et al.*, 1999). TbAT1 is $\sim 30\%$ identical in sequence to human ENT1-3 and 27-32% identical to TbNT2-9. Functional expression of TbAT1 in *Saccharomyces cerevisiae* was shown to stimulate uptake of adenosine (apparent K_m $2.2 \mu\text{M}$) that was inhibited by adenine, but not by nucleosides (inosine, guanosine and uridine) or other nucleobases (hypoxanthine and uracil). TbAT1-mediated adenosine uptake was also inhibited by trypanocidal drugs, including melaminophenyl arsenicals, but not by diamidines, consistent with P2-type functional activity. A variant of TbAT1 (TbAT1') isolated from a drug-resistant clone of *T. brucei brucei* differed at 10 nucleotide positions, resulting in 6 amino acid substitutions (Leu71Val, Leu380Pro, Ala178Thr, Gly181Glu, Asp239Gly and Asn286Ser). Yeasts carrying the TbAT1' gene were unable to transport adenosine and remained insensitive to the melaminophenyl arsenical, melarsen oxide. Mutational inactivation of transport function may not however be the sole mechanism of trypanocidal drug-resistance, since in 65 different *T. brucei* spp. isolates collected from patients with melarsoprol treatment failures, only 38 contained mutations in their TbAT1 gene (Matovu *et al.*, 2001). A recent *T. brucei brucei* study has suggested that cellular uptake of pentamidine is mediated by P2 and at least one other additional transporter (de Koning and Jarvis, 2001).

***Caenorhabditis elegans* CeENT1** – Homology searches of the *Caenorhabditis elegans* GenBank™ database identified 6 putative ENT-like proteins (Table 1-1), designated CeENT1-6 (formerly ZK809.4, K09A9.3, K02E11.1, C47A4.2, F16H11.3 and F36H2.2). A

cDNA for CeENT1 was generated by PCR cloning approaches using template DNA from a cDNA clone (yk77f11) obtained from a *C. elegans* (Bristol N2 strain) hermaphrodite embryo cDNA library (Young *et al.*, 2000). When produced in *Xenopus* oocytes, CeENT1 mediated uptake of purine and pyrimidine nucleosides, including adenosine (apparent K_m 0.55 mM) and uridine (apparent K_m 0.67 mM), but was unable to transport the nucleobase hypoxanthine. Fluxes were Na^+ - and H^+ -independent. Furthermore, the antiviral nucleoside analogs AZT, ddI and ddC were good substrates for the nematode transporter, with apparent K_m values (0.50, 0.84 and 1.39 mM, respectively) similar to those for antiviral drug transport by hENT2 (Young *et al.*, 2000). CeENT1-mediated influx of uridine was relatively insensitive to inhibition by NBMPR and the vasoactive drugs dilazep and draflazine (IC_{50} values $> 1 \mu\text{M}$), properties that also resemble those of mammalian *ei*-type (ENT2) transporters. However, in marked contrast to hENT2, CeENT1 was inhibited by dipyrindamole with an IC_{50} of 165 nM.

***Arabidopsis thaliana* AtENT1** – cDNA for an *Arabidopsis* ENT was cloned by two independent groups using (i) RT-PCR, and (ii) adenosine growth selection in yeast defective in purine biosynthesis (Li and Wang, 2000; Mohlmann *et al.*, 2001). The encoded protein, AtENT1 (or ENT1,*At*), contained 428 amino acid residues and was $\sim 30\%$ identical in sequence to human ENT1-3. The properties of AtENT1 expressed in yeast included high affinity for adenosine (apparent K_m 3.6 μM) and insensitivity to inhibition by NBMPR, dipyrindamole, and dilazep (Mohlmann *et al.*, 2001). [^3H]Adenosine transport was inhibited by unlabeled adenosine, inosine, cytidine, and guanosine with IC_{50} values between 4-28 μM , demonstrating broad permeant selectivity for pyrimidine and purine nucleosides. AtENT1 was also sensitive to inhibition by proton-ionophores, suggesting that the transporter is a concentrative, proton-linked symporter. A 10-fold excess concentration of uridine failed to inhibit adenosine influx, indicating either a low-affinity of the transporter for uridine or, perhaps, an inability of AtENT1 to transport uridine. Similarly, purine and pyrimidine nucleobases did not inhibit AtENT1-mediated adenosine uptake.

***Saccharomyces cerevisiae* FUN26** – A cDNA encoding FUN26 was isolated by PCR cloning from yeast chromosomal DNA using sequence information derived the GenBank™ database (Vickers *et al.*, 2000). FUN26 contains 517 amino acid residues and showed limited but significant sequence homology (18-20% identity) to human ENT1-3.

Expression of the FUN26 cDNA failed to confer uridine transport capability in transport-deficient yeast and was therefore also tested in *Xenopus* oocytes, which exhibited low-level FUN26-mediated transport of pyrimidine and purine nucleosides, but not nucleobases. Uridine influx by FUN26 was also independent of pH and insensitive to inhibition by NBMPR, dilazep and dipyridamole. The lack of transport activity in FUN26-expressing yeast was investigated by tagging the transporter with the c-Myc immunopeptide (producing FUN26myc). Yeast membrane fractions prepared by sucrose density centrifugation were then analyzed for the presence of recombinant FUN26myc by immunoblotting. The results of these experiments suggested that FUN26 resides primarily in the membrane fractions of intracellular compartments, possibly in late endosomal/vacuolar membranes demonstrating, for the first time, an ENT protein with potential intracellular nucleoside transport function.

Structure/Function Studies of ENT Family Members – Hydrophathy analyses of mammalian ENTs predict a common membrane topology 11 TMs with a cytoplasmic N-terminal, one or more putative *N*-linked glycosylation sites in the extracellular loop between TMs 1 and 2, a large central hydrophilic loop, and a short extracellular C-terminus (Fig. 1-5). This model has now been verified by a number of supporting biochemical and molecular biology studies. For example, site-directed mutagenesis combined with oocyte expression and endoglycosidase digestion identified Asn⁴⁸ as the single site of glycosylation in hENT1, confirming the large loop between TMs 1 and 2 as extracellular (Sundaram *et al.*, 2001a). The aglyco hENT1 mutant (Asn48Gln) then served as the template to introduce artificial *N*-linked glycosylation sites at the amino and carboxyl termini, in the central hydrophilic loop between TMs 6 and 7, and in three of the four putative extracellular loops (between TMs 3 and 4, TMs 7 and 8, and TMs 9 and 10). Immunoblot analysis of the engineered hENT1 constructs in the presence and absence of endoglycosidase digestion demonstrated glycosylation of each of the exofacial loops and the C-terminus, validating the predicted topology illustrated in Fig. 1-3. No glycosylation was observed at *N*-linked glycosylation sites introduced in the central cytosolic loop or at the N-terminus. Predictive algorithms suggest that an hENT1-like membrane architecture with 11 TMs is common to all known ENT family members (Sundaram *et al.*, 2001a).

The topology of hENT1 has been used as a structural guide to help identify the regional and molecular determinants of substrate (and inhibitor) binding. Because ENTs, like other transport proteins, shuttle substrates across the plasma membrane, it is likely that residues within transmembrane regions are responsible for the recognition of substrates and their subsequent translocation. It is therefore not surprising that a majority of conserved residues in $\geq 50\%$ of ENTs listed in Table 1-1 reside in predicted transmembrane helices. As outlined earlier in this chapter, mammalian ENTs possess functional properties that differ in their sensitivities to inhibitors and in their transport capabilities for nucleobases and antiviral 3'-dideoxynucleoside drugs. Several studies have successfully exploited these functional differences to identify regions of the protein directly (or indirectly) involved in inhibitor recognition and substrate specificity. For example, chimeric constructs between coronary vasodilator drug-sensitive hENT1 and its drug-insensitive rat homolog, rENT1, identified a region within TMs 3-6 (corresponding to residues 100-231 of hENT1) that conferred inhibitor sensitivity to dilazep, dipyridamole, and draflazine (Sundaram *et al.*, 1998). Likewise, chimeric constructs engineered between NBMPR-sensitive rENT1 and NBMPR-insensitive rENT2 revealed two contiguous regions within TMs 3-6 (corresponding to residues 100-171 of hENT1) and TMs 5-6 (corresponding to residues 172-231 of hENT1) that were responsible for *es*- and *ei*-type NBMPR sensitivity (Sundaram *et al.*, 2001b), and in the case of TMs 5-6, nucleobase transport activity (Yao *et al.*, 2002). Since both coronary vasodilators and NBMPR function as exofacial competitive inhibitors of nucleoside transport by the *es*-type transporter hENT1 (Jarvis *et al.*, 1982; Jarvis and Young, 1982, 1987; Gati and Paterson, 1989b), it is likely that these transmembrane helices contribute, at least in part, to the exofacial substrate-binding site of the transporter.

Other evidence has been gathered that points to specific residues involved in substrate/inhibitor binding. A novel technique using random mutagenesis of an expression plasmid containing hENT1 cDNA combined with phenotypic complementation in yeast isolated a mutant variant of hENT1 with reduced dilazep and dipyridamole (but not NBMPR) sensitivity (Visser *et al.*, 2002). Sequencing of the rescued mutated construct revealed a single point mutation (Met33Ile) that corresponded to conserved residues in human, mouse, and rat ENT1/2 proteins (Met in hENT1/mENT1 and Ile in rENT1 and hENT2/mENT2/rENT2).

When produced in *Xenopus* oocytes, hENT1/Met33Ile exhibited a dipyrindamole sensitivity ($IC_{50} \sim 3.6 \mu\text{M}$) intermediate between that of hENT1 (dipyrindamole $IC_{50} \sim 0.3 \mu\text{M}$) and dipyrindamole-resistant rENT1 (Visser *et al.*, 2002), in agreement with the earlier chimeric studies (Sundaram *et al.*, 1998) which identified the TM 3-6 region as the major site of interaction with dilazep and dipyrindamole, but which also implicated TMs 1-2 (corresponding to residues 1-99 of hENT1) as having a minor, secondary role in transport inhibition by these compounds (Sundaram *et al.*, 1998).

In another study, site-directed mutagenesis of a unique rENT2 cysteine residue (Cys¹⁴⁰ → Ser) in the predicted exofacial half of TM 4 removed the substrate-protectable inhibition of rENT2-mediated transport by pCMBS (p-cholormercuribenzenesulphonate) (Yao *et al.*, 2001). Similarly, mutagenesis of Gly¹⁵⁴ in TM 5 of hENT1 to the corresponding residue in hENT2 (serine) rendered the transporter insensitive to inhibition by NBMPR (Hyde *et al.*, 2001). Two naturally occurring mutations, Gly183Asp and Cys337Tyr (corresponding to residue positions 184 and 296 in hENT1 TMs 5 and 7, respectively), identified between wildtype LdNT1.1 and drug-resistant clonal mutants of *Leishmania donovani* have been implicated in lower overall transport function (Gly183Asp and Cys337Tyr) and altered substrate selectivity (Gly183Asp) (Vasudevan *et al.*, 2001). Interestingly, independent mutagenesis studies suggest that the human ENT1 equivalent of one of these residues (Gly¹⁸⁴) may be important for proper targeting of the transporter to the plasma membrane, while a second highly conserved Gly residue in TM 5 (Gly¹⁷⁹) may have minor contributing roles to overall transport function and NBMPR sensitivity (SenGupta *et al.*, 2002). Taken together, the residue positions so far identified with the largest impact on inhibitor sensitivity and/or substrate transport are clustered within TMs 3-6 (Fig. 1-3), implicating this region as a major part of the permeant translocation channel, with secondary contributions from the adjacent TMs 1-2 and TM 7.

Mammalian Concentrative Nucleoside Transporters (CNTs)

Characteristics of Mammalian Concentrative Nucleoside Transport Processes – Concentrative nucleoside transport processes have been demonstrated in a variety of cell types and tissues, including intestine (Bronk and Hastewell, 1989; Jarvis, 1989; Roden *et al.*, 1991), kidney (Le Hir and Dubach, 1985a, 1985b; Lee *et al.*, 1988, 1990; Williams *et al.*, 1989; Franco *et*

et al., 1990; Le Hir, 1990; Williams and Jarvis, 1991; Gutierrez *et al.*, 1992; Gutierrez and Giacomini, 1993; Brett *et al.*, 1993), liver (Holstege *et al.*, 1991; Moseley *et al.*, 1991; Che *et al.*, 1992) and choroid plexus (Spector and Huntoon, 1984; Wu *et al.*, 1992), in other regions of the brain (Johnston and Geiger, 1989, 1990), and in splenocytes (Baer and Moorji, 1990; Baer *et al.*, 1992), macrophages (Plagemann and Woffendin, 1989; Plagemann and Aran, 1990; Plagemann *et al.*, 1990; Plagemann, 1991) and leukemic cells (Crawford *et al.*, 1990a, 1990b). Three major (*cit*, *cif*, and *cib*) and two minor (*cs* and *csg*) subclasses are presently recognized on the basis of permeant selectivity and sensitivity to inhibition by NBMPR (Table 1-2) (Griffith and Jarvis, 1996; Cheeseman *et al.*, 2000). Systems *cit*, *cif* and *cib* are NBMPR-insensitive and otherwise selective for pyrimidine nucleosides, purine nucleosides, or both, respectively. All three transport uridine and adenosine. Furthermore, a Na⁺/nucleoside coupling ratio of 2:1 has been reported for system *cib* in choroid plexus and microglia (Wu *et al.*, 1992; Hong *et al.*, 2000), whereas coupling ratios of 1:1 have been described for various *cit* and *cif* transport activities in different mammalian cells and tissues (Cass, 1995). In contrast, the permeant preferences for the minor concentrative NT processes in mammalian cells have not been well defined: the *csg* process (Flanagan and Meckling-Gill, 1997) accepts guanosine, while the *cs* process (Belt *et al.*, 1993) accepts adenosine analogs as permeants. Unlike the *cit*-, *cif*- and *cib*-type processes, both *cs* and *csg* are inhibited by nanomolar concentrations of NBMPR (Paterson *et al.*, 1993; Flanagan and Meckling-Gill, 1997).

Functional and Molecular Properties of Cloned Mammalian CNTs

CNT1 – Expression screening of a cDNA library prepared from size-selected poly(A)⁺-selected RNA in *Xenopus* oocytes identified a cDNA from rat jejunal epithelium responsible for the *cit*-type, Na⁺-dependent nucleoside transport activity (Huang *et al.*, 1994). Rat (r) concentrative nucleoside transporter 1 (designated rCNT1) contained 648 amino acid residues and was the first example of a novel group of transport proteins that have since been labeled collectively as the CNT family (Baldwin *et al.*, 1999; Cass *et al.*, 1999). The predicted membrane architecture of rCNT1 contains 13 TMs, with a cytoplasmic N-terminus and an exofacial glycosylated tail at the C-terminus (Fig. 1-6) (Hamilton *et al.*, 2000). Functional expression in *Xenopus* oocytes showed rCNT1 to have *cit*-type characteristics, with a permeant selectivity for adenosine and pyrimidine nucleosides that was not susceptible to inhibition by

NBMPR (Huang *et al.*, 1994). rCNT1, in contrast to mammalian ENT proteins, had relatively high affinity for physiological nucleosides (the apparent K_m for uridine was $\sim 30\text{-}40\ \mu\text{M}$). Transport was Na^+ -dependent with a K_{50} value for Na^+ activation of 9.5 mM, and a calculated Hill coefficient of 1.12 (± 0.10), consistent with 1:1 Na^+ :nucleoside cotransport activity (Huang *et al.*, 1994; Yao *et al.*, 1996a). rCNT1 also mediates transport of the antiviral nucleoside drugs, AZT and ddC, although with lower affinity ($K_m \sim 0.5\ \text{mM}$) (Yao *et al.*, 1996b). Two additional orthologs of rCNT1 from human (h) and pig (pk), designated hCNT1 and pkCNT1, have been cloned and functionally characterized in *Xenopus* oocytes (Ritzel *et al.*, 1997; Pajor, 1998). hCNT1 (650 amino acid residues) and pkCNT1 (648 amino acid residues) are 83 and 84% identical in sequence to rCNT1, respectively, and have similar functional properties, including the ability to transport antiviral (AZT, ddC) and anticancer (gemcitabine) nucleoside analog drugs (Ritzel *et al.*, 1997; Pajor, 1998; Mackey *et al.* 1998, 1999). CNT1 transcripts have been demonstrated in brain, liver, kidney, uterus, lung, and small intestine (Anderson *et al.*, 1996; Pennycooke *et al.*, 2001).

CNT2 – Following the identification of rCNT1, *Xenopus* oocyte expression selection of a rat liver cDNA library identified a cDNA encoding a second mammalian CNT isoform, this time with *cif*-type transport characteristics (Che *et al.*, 1995). A cDNA encoding a nearly identical protein with two polymorphic differences in predicted amino acid sequence at position 419 (Gly *versus* Ala) and position 522 (Val *versus* Ile) was also isolated independently from rat jejunum (Yao *et al.*, 1996a). This second rat CNT isoform, designated rCNT2, contained 659 amino acid residues and was 66% identical in sequence to rCNT1. When produced in *Xenopus* oocytes, rCNT2 exhibited Na^+ -dependent transport of purine nucleosides and uridine (Che *et al.*, 1995; Yao *et al.*, 1996a). Unlike rCNT1, which exhibits low level adenosine transport activity, rCNT2 efficiently transported adenosine and uridine with similar apparent K_m and V_{\max} values (Yao *et al.*, 1996a). Three additional orthologs of rCNT2 from human (h), rabbit (rb), and mouse (m), designated hCNT2, rbCNT2, and mCNT2, have been cloned and functionally characterized in *Xenopus* oocytes (Wang *et al.*, 1997; Ritzel *et al.*, 1998; Gerstin *et al.*, 2000; Patel *et al.*, 2000). These proteins contain 658-660 residues, are 81-93% identical in sequence to rCNT2, and $\sim 70\%$ identical in sequence to mammalian CNT1 proteins. Substrate inhibition and radiolabeled nucleoside uptake assays indicate that CNT2

proteins from human, rabbit, and mouse have a transport specificity for purine nucleoside and uridine that, in the case of hCNT2, also includes the ability to transport antiviral (ddI) and antineoplastic (5-fluorouridine and 5-fluoro-2'-deoxyuridine) nucleoside analog drugs (Yao *et al.*, 1998; Lang *et al.*, 2001). Investigations of CNT2 mRNA in human, rat and rabbit tissues indicates that CNT2, unlike CNT1, may be expressed in a wider range of tissues, including kidney, liver, small intestine, brain, lung, prostate, cervix, colon, stomach, rectum, heart and epididymis (Anderson *et al.*, 1996; Gerstin *et al.*, 2000; Leung *et al.*, 2001; Pennycooke *et al.*, 2001).

CNT3 – There is strong evidence that system *cib* functional activity exists in small intestine, choroid plexus, microglia, and in human colon carcinoma (CaCo-2) and myeloid (HL-60) cells (Lee *et al.*, 1991; Wu *et al.*, 1992; Huang *et al.*, 1993; Lee *et al.*, 1994; Wu *et al.*, 1994; Washington *et al.*, 1995; Redlak *et al.*, 1996; Waclawski and Sinko, 1996; Hong *et al.*, 2000). Although a rabbit protein, SNST1, from the sodium/solute symporter (SSS) family (formerly the Na⁺/glucose cotransporter (SGLT) family) was reported in 1992 to possess low-level *cib*-type transport activity in oocytes (Pajor and Wright, 1992), this protein is now recognized as a rabbit ortholog of human SGLT2 and has been reclassified as a rbSGLT2, although glucose transport activity has not been demonstrated for the recombinant protein (Turk and Wright, 1997; Wright, 2001). Reported uridine fluxes for SNST1 (rbSGLT2) expressed in *Xenopus* oocytes were only marginally higher than background, suggesting that nucleosides are not physiological substrates for this transporter. Other proteins in the SSS family have also been renamed, including a pig protein first called SAAT1 because it displayed low-level amino acid transport activity, then pSGLT2 because of apparent low-affinity glucose uptake, and now pSGLT3 after it was finally shown to be a high-affinity, Na⁺-dependent glucose (but not galactose) symporter (Wright, 2001).

From these and other considerations, we hypothesized that the protein responsible for *cib* activity in mammalian cells might be a member of the CNT protein family. I have been part of a consolidated group effort to clone and characterize a potential *cib*-type protein revealed by homology searches of genomic and EST sequence databases. Results from these studies, which describe human and mouse CNT3 proteins with *cib*-type functional activities, are presented in *Chapter IV*.

CNT Family Members in Prokaryotes and Other Eukaryotes – As of April 2002, over 60 members of the CNT family have been identified in bacteria, insects, nematodes, yeast, prevertebrates, and mammals. The current members of the family are listed in Table 1-3, and their phylogenetic relationships are presented in Fig. 1-7. Similar to members of the ENT family, the number of isoforms present in different species seems to vary, with just one in the yeast *Candida albicans* (CaCNT), for instance, and as many as six or seven, respectively, in bacteria *Bacillus cereus* (BcORF1-6) and *Bacillus anthracis* (BaORF1-7). However, other than the research described in this thesis (*Chapters V-VII*), only two CNT proteins from organisms other than mammals have been cloned (NupC from *Escherichia coli* and CeCNT3 from *Caenorhabditis elegans*), and only one of these (*C. elegans* CeCNT3) has been characterized in any detail.

***Escherichia coli* NupC** – A cDNA was isolated by functional rescue of nucleoside transport-deficient *E. coli* and selection for growth in medium containing cytidine as the sole carbon source (Craig *et al.*, 1994). The encoded protein, designated NupC, contained 400 amino acid residues and was ~ 25% identical in sequence to human CNT1/2. NupC is believed to transport nucleosides. This premise, based on growth studies in cytidine-containing media and restored sensitivity of transport-deficient *E. coli* to 5'-azacytidine cytotoxicity, has never been functionally demonstrated for the recombinant protein and its kinetic parameters, nucleoside selectivity, and cation dependence have not been established (Craig *et al.*, 1994). *E. coli* also possesses two NupC homologs (YeiJ and YeiM) of undetermined function. *Chapter VI* of this thesis describes the cloning and functional characterization of NupC in *Xenopus* oocytes.

***Caenorhabditis elegans* CeCNT3** – *C. elegans* CeCNT3 (formerly F27E11.2) was cloned by a nested PCR technique using sequence information gathered from the F27E11.2 genomic locus (GenBank™ accession AF016413) and *C. elegans* total RNA as the PCR template (Xiao *et al.*, 2001). When produced in *Xenopus* oocytes, CeCNT3 transported physiological pyrimidine and purine nucleosides, except for cytidine, and was H⁺-dependent and Na⁺-independent. Inosine and thymidine apparent K_m values were 15 and 11 μ M, respectively. Although not truly broadly selective, CeCNT3 was designated “CNT3” in anticipation that it would prove to be an ortholog of mammalian *cib* (Xiao *et al.*, 2001). The

nomenclature “CeCNT3” also implies the presence of CNT1 and CNT2 equivalents in *C. elegans*. However, with the *C. elegans* genome now fully sequenced (*C. elegans* Sequencing Consortium, 1998), only one other CNT-like sequence (F27E11.1) has been identified. This second *C. elegans* CNT was also cloned by Xiao *et al.* (2001), but showed poor transport activity when expressed in *Xenopus* oocytes and was not characterized further. Amino acid sequence identity between CeCNT3 and mammalian CNT3 (and CNT1/2) is ~ 30%.

Structure/Function Studies of CNT Family Members – Sequence analyses of mammalian and other eukaryotic CNTs using multiple predictive algorithms (Hamilton *et al.*, 2001) predict a unified topological model with 13 TMs (one less than previous models (Huang *et al.*, 1994)), a cytoplasmic N-terminus, and an exofacial, glycosylated C-terminus (Fig. 1-6). This model is supported by a number of biochemical and molecular biology studies. For example, site-directed mutagenesis combined with oocyte expression and endoglycosidase digestion have identified Asn⁶⁰⁵ and Asn⁶⁴³ as the sites of glycosylation in rCNT1, confirming the exofacial location of the C-terminal tail (Hamilton *et al.*, 2001). As also predicted by the model, artificial N-linked glycosylation sites introduced into aglyco rCNT1 (Asn605Thr/Asn643Thr) at the N-terminus and the predicted cytoplasmic loop between TMs 4 and 5 were not glycosylated (Hamilton *et al.*, 2001). Similarly, polyclonal antibodies raised against residues 46-67 of the N-terminal tail, unlike those raised against residues 505-524 of the exofacial loop between TMs 11-12, were immunoreactive only in saponin-permeabilized membranes (Hamilton *et al.*, 2001). Unlike eukaryotic CNTs, *E. coli* NupC possesses only 10 putative TMs, TMs 1-10 of NupC corresponding to TMs 4-13 of the eukaryotic proteins (Hamilton *et al.*, 2001).

When I started my graduate studies in the summer of 1997, very little was known about the regional and molecular determinants of CNT transporter function. As described in *Chapter II*, I used chimeric and site-directed mutagenesis studies to identify two pairs of residues in TMs 7 and 8 of hCNT1 (Ser³¹⁹/Gln³²⁰ and Ser³⁵³/Leu³⁵⁴) that, when converted to the corresponding residues in hCNT2 (Gly/Met and Thr/Val), changed the specificity of the transporter from *cit* to *cif* (Loewen *et al.*, 1999). Residue mutations in TM 7 (Ser319Gly and Ser319Gln/Gln320Met) resulted in an intermediate *cib*-type phenotype (*Chapter II*), whereas mutations in TM 8 (Leu354Val, Ser353Thr, and Ser353Thr/Leu354Val) reduced pyrimidine

nucleoside transportability (*Chapters II and III*) and/or affected Na⁺-coupling and uridine analog recognition (*Chapter III*). A similar approach has been utilized with CNT1 and CNT2 orthologs from rat, which identified TMs 7-8 and Ser³¹⁸ (the rat equivalent of Ser³¹⁹ from hCNT1) as corresponding determinants of nucleoside specificity in the rat proteins (Wang and Giacomini, 1997, 1999). In *C. elegans*, a double mutation (Thr327Ser/Val328Leu) in TM 8 of CeCNT3 at amino acid positions equivalent to hCNT1 TM 8 residues 353 and 354 led to low functional activity, while mutagenesis of another TM 8 residue (Tyr332Phe) preserved the overall transport profile of wild-type CeCNT3, but increased the apparent K_m values for thymidine and inosine from 11 and 15 μ M, respectively, to 32 and 103 μ M, respectively (Xiao *et al.*, 2001).

Other Nucleoside Transport Proteins

Over the past decade, successes in molecular cloning have identified the transport proteins responsible for each of the major nucleoside transport processes (systems *cit*, *cif*, *cib*, *es* and *ei*) in mammalian cells. These transporters belong the CNT and ENT protein families: CNTs are found in both prokaryotes and eukaryotes, whereas ENTs occur only in eukaryotes. The molecular identities of the proteins responsible for the two remaining minor nucleoside processes defined by functional studies in mammalian cells (systems *es* and *csg*) remain to be identified. Besides CNTs and ENTs, there are five other protein families with representative members from bacteria, yeast, and mammals that are also able to mediate transport of nucleosides, and in some cases, nucleoside analog drugs, across cell membranes.

Bacteria

Nucleoside:H⁺ Symporter (NHS) Family – The inner membrane of bacteria contains specific transport proteins that allow selective uptake for nucleosides by H⁺-linked mechanisms (Hammer-Jespersen, 1983; Munch-Petersen and Mygrind, 1983). Two major high-affinity nucleoside transport processes, designated systems NupC and NupG, have been well-characterized in *Escherichia coli* (Munch-Petersen *et al.*, 1975; Mygrind and Munch-Petersen, 1979). Systems NupC and NupG are capable of transporting a broad selection of nucleosides and deoxynucleosides, but can be distinguished by the poor ability of system NupC to transport guanosine and deoxyguanosine and by differential sensitivity of the two transporters

to showdomycin (Komatsu and Tanaka, 1972). The transporter responsible for system NupC activity in *E. coli*, called NupC, as discussed earlier, is a member of the CNT protein family (Craig *et al.*, 1994; Huang *et al.*, 1994). Identified by restriction mapping and complementation studies in nucleoside transport-deficient *E. coli*, the *E. coli* NupG protein contains 418 amino acid residues and has a predicted membrane architecture of 12 TMs (Westh Hansen *et al.*, 1987). NupG is not related in sequence to either the ENT or CNT protein families and was the first representative of a separate transporter family (now called the nucleoside:H⁺ symporter (NHS) family). Bacteria expressing recombinant NupG were able to transport radiolabeled cytidine and guanosine, consistent with the broadly-selective NupG transport processes in native bacterial cells (Westh Hansen *et al.*, 1987). H⁺-dependence has not been demonstrated for the recombinant protein, but transport appears to be concentrative.

A homolog of NupG, designated XapB, was subsequently identified in *E. coli* during isolation of genes involved in xanthosine catabolism (Seeger *et al.*, 1995). XapB, shares 65% sequence identity with NupG. Previously considered to be xanthosine-specific (Seeger *et al.*, 1995), XapB has subsequently been shown to possess a similar permeant selectivity (plus xanthosine) to NupC (Norholm and Dandanell, 2001). The recently established close proximity of the *xapB* and *nupC* genes on the *E. coli* chromosome (54.34' and 54.13', respectively) and their similar inability to transport guanosine suggest that earlier NupC studies may have grouped both activities as a single transport system (Karp *et al.*, 2002). *E. coli* also possesses one other NupG homolog (YegT) of undetermined function. A current list of known and putative members of the nucleoside:H⁺ symporter family is provided in Table 1-4.

Tsx Channel-Forming Protein Family – The outer membrane of *E. coli* serves as a permeability barrier against toxic compounds and functions as a molecular filter for hydrophilic substances. The first evidence for a nucleoside transport mechanism separate from NupC and NupG came from studies of mutant strains of *E. coli* that identified a single gene responsible for thymidine uptake at submicromolar extracellular concentrations (< 1 μ M) that dramatically reduced, but did not eliminate, subsequent intracellular thymidine incorporation into DNA (Hantke, 1976; McKeown *et al.*, 1976). The protein responsible for this phenotype, designated Tsx after the gene of the same name, localized to the *E. coli* outer membrane and contained 272 amino acid residues with 14 predicted membrane-associated

segments arranged in a porin-type β -barrel membrane topology (Bremer *et al.*, 1990; Nieweg and Bremer, 1997). Reconstitution of purified Tsx into artificial membranes proved its function as a channel-forming protein with broad transport selectivity for pyrimidine and purine nucleosides as well as the antibiotic albicidin, a potent inhibitor of prokaryotic DNA replication (Maier *et al.*, 1988; Birch *et al.*, 1990; Fsihi *et al.*, 1993). Tsx is structurally unrelated to the CNT and ENT protein families and appears to be found only in gram-negative bacteria. A current list of known and putative members of the Tsx channel-forming protein family is provided in Table 1-5.

Yeast

Nucleoside Uptake Protein (NUP) Family – Unlike *Saccharomyces cerevisiae*, which appears to lack the capacity to transport purine nucleosides, yeasts like *Candida albicans* are able to mediate transport of both pyrimidine and purine nucleosides (Horák, 1997). A novel *C. albicans* cDNA was isolated by functional rescue of nucleoside transport-deficient yeast and selection for growth in medium containing adenosine as the sole carbon source (Detke, 1998). The encoded protein, designated NUP, contained 406 amino acid residues and a signal peptide sequence in the N-terminus, suggesting a membrane localization of the protein. Although no membrane topology for NUP has been published, submission of the NUP sequence to the Tmpred online server (Prediction of Transmembrane Regions and Orientation; Hoffman and Stoffel, 1993) suggests that NUP has 5-7 putative TMs. When produced in yeast, NUP was able to mediate influx of radiolabeled adenosine that was inhibited competitively by the presence of excess unlabeled adenosine and guanosine but not uridine, thymidine, and cytidine, suggesting that NUP is a purine nucleoside-selective transporter (Detke, 1998). Transport activity was also partially inhibited (> 70%) by micromolar concentrations of NBMPR and dipyrindamole. NUP, however, is not related to either the ENT or CNT protein families. It has also not been tested for Na^+ - or H^+ -dependence. *Chapter VII* in this thesis describes the cloning and functional characterization of a second purine nucleoside-selective NT in *C. albicans* (CaCNT), which exhibits H^+ -linked, concentrative transport activity and is a member of the CNT family. A current list of known and putative members of the nucleoside uptake protein (NUP) family is provided in Table 1-6.

FUI1 from the Uracil/Allantoin Permease Family – Gene disruption experiments identified an *S. cerevisiae* chromosome II open reading frame (YBL042, now FUI1) as a putative uridine permease (Wagner *et al.*, 1998). The encoded protein was ~ 70% identical in sequence to *S. cerevisiae* FUR4 (uracil permease) and DAL4 (allantoin permease). FUI1 contains 639 amino acid residues, has a predicted membrane architecture of 10 TMs, and is not related to either CNTs or ENTs. Production of recombinant FUI1 in *fui1*-disrupted *S. cerevisiae* showed restoration of radiolabeled uridine uptake (K_m 22 μ M) that was unaffected by, or only partly inhibited by high concentrations (1 mM) of a variety of ribo- and deoxyribonucleosides or nucleobases, confirming that FUI1 was indeed a uridine-specific transporter (Vickers *et al.*, 2000). FUI1 has not been tested for Na⁺- or H⁺-dependence. A current list of known and putative members of the uracil/allantoin permease family is provided in Table 1-7.

Mammals

OCT1 from the Organic Cation Transporter (OCT) Family – The organic cation transporter (OCT) family in mammalian cells includes four potential-sensitive (OCT1, OCT2, OCT3 and OCT4) and three H⁺-driven (OCT1N, OCT2N, and OCT3N) membrane transport proteins responsible for transport of a diverse group of bioactive amines (acetylcholine, choline, dopamine, epinephrine norepinephrine, guanidine, N¹-methylnicotinamide, thiamine, carnitine), therapeutic drugs (cimetidine, amiloride, mepiperphenidol, morphine, quinine, tetraethylammonium, verapamil, methoprim), and xenobiotics (paraquat) (Rennick, 1981; Zhang *et al.*, 1998; Nishiwaki *et al.*, 1998). In general, OCTs (551-593 residues) contain 12 putative TMs with a large extracellular, hydrophobic loop between TMs 1 and 2 containing conserved N-linked glycosylation sites, a large intracellular loop between TMs 6 and 7, and relatively short intracellular N- and C-terminal tails (Koepsell, 1998). Several studies have implicated an organic cation carrier system in the renal secretion of 2'-deoxyadenosine, 2'-deoxytubercidin and 5-fluoro-2'-deoxyuridine by mouse kidney (Kuttesch *et al.*, 1982; Nelson *et al.*, 1983; Enigbokan *et al.*, 1994) and involving a process that was sensitive to inhibition by dipyrindamole, NBMPR and classical organic cation secretory system substrates such as tetraethylammonium, choline and N¹-methylnicotinamide (Nelson *et al.*, 1988; Bendayan, 1997). Expressed in *Xenopus* oocytes, rOCT1 was found to mediate efflux of radiolabeled 2'-deoxytubercidin (Nelson *et al.*, 1995). Transport of nucleosides and

nucleoside analog drugs is a feature not shared by other known members of the OCT family (Chen and Nelson, 2000), although a novel uptake system in microglia separate from currently known organic cation transport processes has been implicated in the cellular uptake of AZT by a process inhibited by organic cations verapamil, mepiperphenidol, quinidine, cimetidine, and N¹-methylnicotinamide (Hong *et al.*, 2001). AZT is not a substrate of organic cation transporters expressed in kidney (Griffiths *et al.*, 1991). Table 1-8 lists the currently known members of the organic cation transporter (OCT) family in mammals.

OAT1-4 from the Organic Anion Transporter (OAT) Family – The organic anion transporter (OAT) family in mammalian cells includes four isoforms (OAT1, OAT2, OAT3 and OAT4) responsible for membrane transport and renal elimination of a diverse group of organic anions (*p*-aminohippurate, dicarboxylates, cyclic nucleotides, prostaglandin E, urate, salicylate, acetylsalicylate, cimetidine, estrone sulphate and dehydroepiandrosterone sulfate) (Sekine *et al.*, 2000). Although unrelated to OCTs, OATs (535-568 residues) also contain 12 putative TMs with a large extracellular hydrophilic loop between TMs 1 and 2 containing conserved N-linked glycosylation sites, a large intracellular loop between TMs 6 and 7, and intracellular N- and C-terminal tails (Sekine *et al.*, 2000). The first evidence for the involvement of organic anion transport systems in nucleoside drug transport was demonstrated in rat renal membrane vesicles, where transport of [³H]*p*-aminohippurate transport, a classic organic anion transporter substrate, was inhibited by micromolar concentrations of AZT (Griffiths *et al.*, 1991). Similarly, AZT transport across the blood-brain barrier is inhibited by probenecid, a potent organic anion transport inhibitor (Masereeuw *et al.*, 1994; Gibbs and Thomas, 2002), while AZT and ddI inhibit active transport of [³H]benzylpenicillin, a prototypic organic anion, in choroid plexus (Takasawa *et al.*, 1997). Direct evidence of involvement of OATs in nucleoside drug transport came with rOAT1-expression studies in *Xenopus* oocytes, which demonstrated mediated transport of radiolabeled AZT, ddC, ddI, lamivudine (3TC), stavudine (d4T), and trifluridine as well as the nucleobase analog, acyclovir (Wada *et al.*, 2000). For AZT, the apparent K_m value was 68 μ M (Wada *et al.*, 2000), which is lower than exhibited by mammalian ENT and CNT proteins. In a recent study, stable transfectants of human OAT1, OAT2, OAT3 and OAT4 in mouse kidney cells mediated transport of AZT with K_m values between 26 and 152 μ M, suggesting that all four

OAT isoforms contribute to the transport of antiviral nucleoside analog drugs (Takeda *et al.*, 2002). Table 1-9 lists the currently known members of the organic anion transporter (OAT) family in mammals.

Aims of the Present Studies

Over the last 35 years, nucleoside transport systems have been studied in a variety of human and other mammalian cells and tissues. A number of distinct processes were resolved on the basis of substrate selectivity, kinetic properties, inhibitor susceptibility, and ionic requirements. It is only recently, however, that the membrane proteins responsible for these functional activities have begun to be identified. In humans and other mammals, nucleoside transport is mediated predominantly by members of two previously unrecognized protein families (CNT and ENT).

The aims of my research were: (i) to identify and characterize new members of the CNT protein family, and (ii) to undertake structure/function studies of CNT proteins. Specific research objectives were: (i) to exploit the substrate selectivity differences between hCNT1 and hCNT2 using chimeric and site-directed mutagenesis approaches to identify the regional and molecular determinants of CNT1/2 nucleoside specificity (*Chapter II*), (ii) to characterize the effects of mutations in TM 8 of hCNT1 in continuation from *Chapter II* that resulted in novel uridine-selective transport characteristics and changes in cation-coupling (*Chapter III*), (iii) to identify and functionally characterize in *Xenopus* oocytes the cDNA encoding mammalian *cib*-type activity observed in earlier functional studies, which was hypothesized to be a member of the CNT family (*Chapter IV*), (iii) to isolate and functionally characterize in *Xenopus* oocytes two cDNAs (hfCNT and CaCNT) encoding CNT family members from non-mammalian sources (*Eptatretus stouti* and *Candida albicans*, respectively) that possess novel functional activities (*Chapters V* and *VII*), and (iv) to characterize the anticancer and antiviral nucleoside drug transport properties of the putative H⁺/nucleoside symporter from *E. coli* (NupC) in *Xenopus* oocytes (*Chapter VI*). Chimeric studies using hCNT3 and hfCNT in combination with hCNT1 (as described in *Chapters IV* and *V*, respectively) identified regions of the protein involved in cation recognition.

Table 1-1 Members of the Equilibrative Nucleoside Transporter (ENT) Family.

Transporter	Species	Residues	GenBank™ accession	Permeant selectivity ^a	References
hENT1	<i>Homo sapiens</i>	456	AAC51103	nucleosides	Griffiths <i>et al.</i> , 1997a
rENT1	<i>Rattus norvegicus</i>	457	AAB88049	nucleosides	Yao <i>et al.</i> , 1997
mENT1.1	<i>Mus musculus</i>	460	AAF76429	nucleosides	Choi <i>et al.</i> , 2000
hENT2	<i>H. sapiens</i>	456	AAC39526	nucleosides, nucleobases	Griffiths <i>et al.</i> , 1997b
rENT2	<i>R. norvegicus</i>	456	AAB88050	nucleosides, nucleobases	Yao <i>et al.</i> , 1997
mENT2	<i>M. musculus</i>	456	AAF76431	ND	Kiss <i>et al.</i> , 2000
rbENT2	<i>Oryctolagus cuniculus</i>	456	AAK11605	ND	
rbENT2A	<i>O. cuniculus</i>	415	AAK11606	ND	
hENT3	<i>H. sapiens</i>	475	AAK00958	ND	
mENT3	<i>M. musculus</i>	474	AAK00957	ND	
DmENT1	<i>Drosophila melanogaster</i>	458	AAF52405	ND	
DmENT2	<i>D. melanogaster</i>	476	AAF51506	ND	
CeENT1	<i>Caenorhabditis elegans</i>	445	CAA92642	nucleosides	Young <i>et al.</i> , 2000
CeENT2	<i>C. elegans</i>	450	CAB01882	ND	
CeENT3	<i>C. elegans</i>	729	CAB01223	ND	
CeENT4	<i>C. elegans</i>	451	CAB62793	ND	
CeENT5	<i>C. elegans</i>	434	AAA98003	ND	
CeCNT6	<i>C. elegans</i>	384	CAB03075	ND	
AtENT1/ ENT1, <i>At</i>	<i>Arabidopsis thaliana</i>	428	AAC18807 AAF26446	nucleosides except uridine	Li and Wang, 2000 Mohlmann <i>et al.</i> , 2001
AtENT2	<i>A. thaliana</i>	417	AAF04424	ND	
AtENT3	<i>A. thaliana</i>	418	CAB81054	ND	
AtENT4	<i>A. thaliana</i>	418	CAB81055	ND	
AtENT5	<i>A. thaliana</i>	419	CAB81056	ND	
AtENT6	<i>A. thaliana</i>	418	CAB81053	ND	
AtENT7	<i>A. thaliana</i>	417	AAD25545	ND	
AtENT8	<i>A. thaliana</i>	389	AAG10625	ND	
TbAT1	<i>Trypanosoma brucei brucei</i>	463	AAD45278	adenosine, adenine	Maser <i>et al.</i> , 1999
TeAT1	<i>Trypanosoma equiperdum</i>	463	CAC41330	ND	
TbNT2	<i>T. brucei brucei</i>	463	AAF04490	adenosine, inosine, guanosine	Sanchez <i>et al.</i> , 1999
TbNT2/927	<i>T. brucei brucei</i>	462	pending	adenosine, inosine	Sanchez <i>et al.</i> , 2002
TbNT3	<i>T. brucei brucei</i>	464	pending	ND	
TbNT4	<i>T. brucei brucei</i>	462	pending	ND	
TbNT5	<i>T. brucei brucei</i>	463	pending	adenosine, inosine	Sanchez <i>et al.</i> , 2002
TbNT6	<i>T. brucei brucei</i>	462	pending	adenosine, inosine, hypoxanthine	Sanchez <i>et al.</i> , 2002
TbNT7	<i>T. brucei brucei</i>	467	pending	adenosine, inosine, hypoxanthine	Sanchez <i>et al.</i> , 2002
TbNT8	<i>T. brucei brucei</i>	ND	pending	ND	
TbNT9	<i>T. brucei brucei</i>	ND	pending	ND	
LdNT1.1/ LdNT1.2	<i>Leishmania donovani</i>	491	AAC32597 AAC32315	adenosine, pyrimidine nucleosides	Vasudevan <i>et al.</i> , 1998
LmaNT1	<i>L. mexicana amazonensis</i>	491	AAL87658	ND	
LdNT2	<i>L. donovani</i>	499	AAF74264	inosine, guanosine	Carter <i>et al.</i> , 2000b
LmaNT2	<i>L. mexicana amazonensis</i>	499	AAL87659	ND	
L2464.04	<i>L. major</i>	501	CAB96736	ND	
CfNT1	<i>Crithidia fasciculata</i>	497	AAG22610	ND	
CfNT2	<i>C. fasciculata</i>	502	AAG22611	ND	
TgAT	<i>Toxoplasma gondii</i>	462	AAF03247	adenosine	Chiang <i>et al.</i> , 1999
PfENT1/ PfNT1	<i>Plasmodium falciparum</i>	422	AAF67613 AAG09713	nucleosides, nucleobases	Carter <i>et al.</i> , 2000a Parker <i>et al.</i> , 2000
EhENT1	<i>Entamoeba histolytica</i>	396	S49592	ND	
FUN26	<i>Saccharomyces cerevisiae</i>	517	AAC04935	nucleosides	Vickers <i>et al.</i> , 2000

^a, purine and pyrimidine nucleosides/nucleobases unless indicated; ND, not determined

Table 1-2 Concentrative Nucleoside Processes of Mammalian Cells.

Process name	Permeant selectivity	Transporter Protein	Inhibitor Sensitivity^a	References
System <i>ct</i>	Pyrimidine nucleosides, adenosine	CNT1	No	Huang <i>et al.</i> , 1994 Ritzel <i>et al.</i> , 1997
System <i>cf</i>	Purine nucleosides, uridine	CNT2	No	Che <i>et al.</i> , 1995 Yao <i>et al.</i> , 1996a
System <i>cb</i>	Purine and pyrimidine nucleosides	CNT3	No	Ritzel <i>et al.</i> , 2001
System <i>cs</i>	2'-chloro-2'-deoxyadenosine Formycin B	ND	Yes	Belt <i>et al.</i> , 1993
System <i>cg</i>	guanosine	ND	Yes	Flanagan and Meckling-Gill, 1997

^a, sensitivity to inhibition by NBMPR; ND, not determined

Table 1-3 Members of the Concentrative Nucleoside Transporter (CNT) Family.

Transporter	Species	Residues	GenBank™ accession	Permeant selectivity ^a	References
hCNT1a	<i>Homo sapiens</i>	650	AAB53837	adenosine, pyrimidine nucleosides	Ritzel <i>et al.</i> , 1997
hCNT1b		649	AAB53838		
hCNT1c		649	AAB53839		
rCNT1	<i>Rattus norvegicus</i>	648	AAB03626	adenosine, pyrimidine nucleosides	Yao <i>et al.</i> , 1996a
pkCNT1	<i>Sus scrofa</i>	647	AAC17947	adenosine, pyrimidine nucleosides	
hCNT2	<i>H. sapiens</i>	658	AAB88539	uridine, purine nucleosides	Ritzel <i>et al.</i> , 1998
rCNT2	<i>R. norvegicus</i>	659	AAD00159	uridine, purine nucleosides	Yao <i>et al.</i> , 1996a
mCNT2	<i>M. musculus</i>	660	AAC28858	uridine, purine nucleosides	Patel <i>et al.</i> , 2000
rbCNT2	<i>Oryctolagus cuniculus</i>	658	AAF80451	uridine, purine nucleosides	Gerstin <i>et al.</i> , 2000
hCNT3	<i>H. sapiens</i>	691	AAG22551	nucleosides	Ritzel <i>et al.</i> , 2001 Chapter IV
rCNT3	<i>R. norvegicus</i>	705	NM_080908	nucleosides (unpublished data)	Yao <i>et al.</i> , 2002
mCNT3	<i>M. musculus</i>	703	AAG22552	nucleosides	Ritzel <i>et al.</i> , 2001 Chapter IV
hFCNT	<i>Eptatretus stouti</i>	683	AAD52151	nucleosides	Yao <i>et al.</i> , 2002 Chapter V
CaCNT	<i>Candida albicans</i>	608 ^b	pending	uridine, purine nucleosides	Chapter VII
AfCNT	<i>Aspergillus fumigatus</i>	598 ^b	pending	ND	
F27E11.1	<i>Caenorhabditis elegans</i>	568	AAB65255	ND	Xiao <i>et al.</i> , 2001
CeCNT3	<i>C. elegans</i>	575	AAB65256	nucleosides except cytidine	Xiao <i>et al.</i> , 2001
CG8083	<i>Drosophila melanogaster</i>	603	AAF58997	ND	Adams <i>et al.</i> , 2000
CG11778	<i>D. melanogaster</i>	528	AAF58996	ND	Adams <i>et al.</i> , 2000
NupC	<i>Escherichia coli</i>	400	AAC75452	nucleosides except guanosine	Craig <i>et al.</i> , 1994 Chapter VI
YejJ	<i>E. coli</i>	418	AAC75222	ND	Blattner <i>et al.</i> , 1997
YeiM	<i>E. coli</i>	416	AAC75225	ND	Blattner <i>et al.</i> , 1997
SAV0645	<i>Staphylococcus aureus</i>	409	BAB56807	ND	Kuroda <i>et al.</i> , 2001
SAV0313	<i>S. aureus</i>	406	BAB56475	ND	Kuroda <i>et al.</i> , 2001
SAV0521	<i>S. aureus</i>	404	BAB56683	ND	Kuroda <i>et al.</i> , 2001
CPE1284	<i>Clostridium perfringens</i>	393	BAB80990	ND	Shimizu <i>et al.</i> , 2002
CPE2496	<i>C. perfringens</i>	408	BAB82202	ND	Shimizu <i>et al.</i> , 2002
NupC	<i>Bacillus subtilis</i>	393	CAA57663	ND	Saxild <i>et al.</i> , 1996
YxjA	<i>B. subtilis</i>	397	BAA11702	ND	Kunst <i>et al.</i> , 1997
YutK	<i>B. subtilis</i>	404	CAB15208	ND	Kunst <i>et al.</i> , 1997
NupC	<i>Yersinia pestis</i>	394	CAC92227	ND	Parkhill <i>et al.</i> , 2001a
YPO0435	<i>Y. pestis</i>	423	CAC89293	ND	Parkhill <i>et al.</i> , 2001a
VC1953	<i>Vibrio cholerae</i>	405	AAF95101	ND	Heidelberg <i>et al.</i> , 2000
VC2352	<i>V. cholerae</i>	418	AAF95495	ND	Heidelberg <i>et al.</i> , 2000
VCA0179	<i>V. cholerae</i>	402	AAF96092	ND	Heidelberg <i>et al.</i> , 2000
NupC	<i>Salmonella typhimurium</i>	400	CAD07647	ND	Parkhill <i>et al.</i> , 2001b
CC2089	<i>Caulobacter crescentus</i>	426	AAK24060	ND	Neirman <i>et al.</i> , 2001
M18_1932	<i>Streptococcus pyogenes</i>	400	AAL98430	ND	Smoot <i>et al.</i> ,
HP1180	<i>Helicobacter pylori</i>	418	AAD08224	ND	Tomb <i>et al.</i> , 1997
HI0519	<i>Haemophilus influenzae</i>	417	AAC22177	ND	Fleischmann <i>et al.</i> , 1995
BH1446	<i>Bacillus halodurans</i>	406	BAB05165	ND	Takami <i>et al.</i> , 2000
PM1292	<i>Pasteurella multocida</i>	420	AAK03376	ND	May <i>et al.</i> , 2001
ALL0378	<i>Nostoc spp.</i>	402	BAB72336	ND	Kaneko <i>et al.</i> , 2001

(continued on following page)

^a, purine and pyrimidine nucleosides unless indicated; ^b, prediction of coding sequence from unfinished genome sequence databases; ND, not determined

Table 1-3 Members of the Concentrative Nucleoside Transporter (CNT) family (*continued*).

Transporter	Species	Residues	GenBank™ accession	Permeant selectivity ^a	References
CBORF01	<i>Clostridium botulinum</i>	407 ^b	pending	ND	
YeORF01	<i>Yersinia enterocolitica</i>	423 ^b	pending	ND	
YeORF02	<i>Y. enterocolitica</i>	394 ^b	pending	ND	
SpORF01	<i>Shewanella putrefuscians</i>	432 ^b	pending	ND	
SpORF02	<i>S. putrefuscians</i>	422 ^b	pending	ND	
SpORF03	<i>S. putrefuscians</i>	423 ^b	pending	ND	
SpORF04	<i>S. putrefuscians</i>	401 ^b	pending	ND	
HdORF01	<i>Haemophilus ducreyi</i>	422 ^b	pending	ND	
SeORF01	<i>Staphylococcus epidermidis</i>	422 ^b	pending	ND	
BaORF01	<i>Bacillus anthracis</i>	392 ^b	pending	ND	
BaORF02	<i>B. anthracis</i>	392 ^b	pending	ND	
BaORF03	<i>B. anthracis</i>	393 ^b	pending	ND	
BaORF04	<i>B. anthracis</i>	398 ^b	pending	ND	
BaORF05	<i>B. anthracis</i>	391 ^b	pending	ND	
BaORF06	<i>B. anthracis</i>	400 ^b	pending	ND	
BaORF07	<i>B. anthracis</i>	396 ^b	pending	ND	
BcORF01	<i>Bacillus cereus</i>	392 ^b	pending	ND	
BcORF02	<i>B. cereus</i>	393 ^b	pending	ND	
BcORF03	<i>B. cereus</i>	393 ^b	pending	ND	
BcORF04	<i>B. cereus</i>	398 ^b	pending	ND	
BcORF05	<i>B. cereus</i>	397 ^b	pending	ND	
BcORF06	<i>B. cereus</i>	403 ^b	pending	ND	

^a, purine and pyrimidine nucleosides unless indicated; ^b, prediction of coding sequence from unfinished genome sequence databases; ND, not determined

Table 1-4 Members of the Nucleoside:H⁺ Family of Transporters.

Transporter	Species	Residues	GenBank™ accession	Permeant selectivity	References
NupG	<i>Escherichia coli</i>	418	CAA29541	nucleosides ^a	Westh Hansen <i>et al.</i> , 1987
XapB	<i>E. coli</i>	418	CAA52048	nucleosides ^a	Seeger <i>et al.</i> , 1995
YegT	<i>E. coli</i>	425	BAA15967	ND	Itoh <i>et al.</i> , 1996
DhnA	<i>E. coli</i>	374	AAB18249	ND	
STY3268	<i>Salmonella typhimurium</i>	418	CAD02938	ND	Parkhill <i>et al.</i> , 2001b
STY2657	<i>S. typhimurium</i>	418	CAD07653	ND	Parkhill <i>et al.</i> , 2001b
STY2371	<i>S. typhimurium</i>	423	CAD02521	ND	Parkhill <i>et al.</i> , 2001b
CC1628	<i>Caulobacter crescentus</i>	413	AAK23606	ND	Nierman <i>et al.</i> , 2001
MalA	<i>Geobacillus stearothermophilus</i>	394	AAA71980	maltose	Stover <i>et al.</i> , 2000
ECU11_1880	<i>Encephalitozoon cuniculi</i>	495	CAD26098	ND	Katinka <i>et al.</i> , 2001

^a, purine and pyrimidine nucleosides; ND, not determined

Table 1-5 Members of the Tsx Channel-forming Protein Family.

Porin	Species	Residues	GenBank™ accession	Function	References
Tsx	<i>Escherichia coli</i>	294	AAA24701	nucleoside ^a facilitator	Bremer <i>et al.</i> , 1990
Tsx	<i>Klebsiella pneumoniae</i>	294	CAA81397	nucleoside ^a facilitator	Nieweg and Bremer, 1997
Tsx	<i>Enterobacter aerogenes</i>	294	CAA81396	nucleoside ^a facilitator	Nieweg and Bremer, 1997
Tsx	<i>Salmonella typhimurium</i>	287	CAD08869	nucleoside ^a facilitator	Nieweg and Bremer, 1997
OmpK	<i>Vibrio parahaemolyticus</i>	263	BAA09613	ND	Inoue <i>et al.</i> , 1995
OmpK	<i>Vibrio cholerae</i>	296	AAF95449	ND	Heidelberg <i>et al.</i> , 2000

^a, purine and pyrimidine nucleosides; ND, not determined

Table 1-6 Members of the Nucleoside Uptake Protein (NUP) family of transporters.

Transporter	Species	Residues	GenBank™ accession	Permeant selectivity ^a	References
NUP	<i>Candida albicans</i>	406	AAG38103	purine nucleosides	Detke, 1998
SPCC285.05	<i>Schizosaccharomyces pombe</i>	348	CAA20844	ND	
RSc0798	<i>Ralstonia solanacearum</i>	381	CAD14500	ND	
RSc0799	<i>R. solanacearum</i>	346	CAD14501	ND	
BMEI0469	<i>Brucella melitensis</i>	345	AAL51650	ND	DeVecchio <i>et al.</i> , 2002
CC0187	<i>Caulobacter crescentus</i>	347	NP_419006	ND	Neirman <i>et al.</i> , 2001

ND, not determined

Table 1-7 Members of the Uracil/Allantoin Permease Family.

Transporter	Species	Residues	GenBank™ accession	Permeant selectivity	References
FUI1	<i>Saccharomyces cerevisiae</i>	639	CAA84862	uridine	De Wergifosse <i>et al.</i> , 1994 Wagner <i>et al.</i> , 1998 Vickers <i>et al.</i> , 2000
DAL4	<i>S. cerevisiae</i>	635	CAA78826	allantoin	Yoo <i>et al.</i> , 1992
FUR4	<i>S. cerevisiae</i>	633	CAA53678	uracil	Smits <i>et al.</i> , 1994
YOR071C	<i>S. cerevisiae</i>	598	Q08485	ND	Valens <i>et al.</i> , 1997
THI7	<i>S. cerevisiae</i>	598	BAA09504	thiamine	Enjo <i>et al.</i> , 1997
YOR192C	<i>S. cerevisiae</i>	599	Q08579	ND	
NCS1	<i>Schizosaccharomyces pombe</i>	581	CAB16258	uracil	
FUR4	<i>S. pombe</i>	589	AAB88050	uracil	de Montigny <i>et al.</i> , 1998
SPAC29- B12.14c	<i>S. pombe</i>	581	AB16258	ND	
SPBC1683.05	<i>S. pombe</i>	559	CAB91167	ND	
YbbW	<i>Escherichia coli</i>	437	AAC73613	ND	Blattner <i>et al.</i> , 1997
YwoE	<i>Bacillus subtilis</i>	490	P94575	ND	Presecan <i>et al.</i> , 1997
SSO2042	<i>Sulfolobus solfataricus</i>	492	AAK42228	ND	She <i>et al.</i> , 2001
SSO1905	<i>S. solfataricus</i>	488	AAK42097	ND	She <i>et al.</i> , 2001
ST1564	<i>Sulfolobus tokodaii</i>	523	BAB66639	ND	Kawarabayasi <i>et al.</i> , 2001
BMEI0155	<i>Brucella melitensis</i>	409	AAL51337	ND	DelVecchio <i>et al.</i> , 2002
SCBAC17- A6.33c	<i>Streptomyces coelicolor</i>	495	CAC44678	ND	Redenbach <i>et al.</i> , 1996
SC1A6.06	<i>S. coelicolor</i>	522	CAA18904	ND	Redenbach <i>et al.</i> , 1996
HyuP	<i>Arthrobacter aurescens</i>	478	AAG02128	ND	Wiese <i>et al.</i> , 2000
MLR0604	<i>Mesorhizobium loti</i>	485	BAB48161	ND	Kaneko <i>et al.</i> , 2000
SMc00922	<i>Sinorhizobium meliloti</i>	485	CAC45355	ND	Capela <i>et al.</i> , 2001
PA0443	<i>Pseudomonas aeruginosa</i>	496	AAG03832	ND	Stover <i>et al.</i> , 2000
PA0476	<i>P. aeruginosa</i>	575	AAG03865	ND	Stover <i>et al.</i> , 2000
YPO1083	<i>Yersinia pestis</i>	494	CAC89926	ND	Parkhill <i>et al.</i> , 2001a
ALLB	<i>Salmonella typhimurium</i>	453	CAD05007	ND	Parkhill <i>et al.</i> , 2001b
ALLP	<i>Salmonella typhimurium</i>	437	AAL19476	ND	McClelland <i>et al.</i> , 2001
CC2347	<i>Caulobacter crescentus</i>	488	AAK24318	ND	Nierman <i>et al.</i> , 2001
RSc1233	<i>Ralstonia solanacearum</i>	502	CAD14935	ND	
F12E4_350	<i>Arabidopsis thaliana</i>	599	CAB83318	ND	

ND, not determined

Table 1-8 Members of the Organic Cation Transporter (OCT) Family.

Transporter	Species	Residues	GenBank™ accession	Driving Force	References
hOCTN1	<i>Homo sapiens</i>	551	BAA23356	Na ⁺ - and H ⁺ -linked	Tamai <i>et al.</i> , 1997
rOCTN1	<i>Rattus norvegicus</i>	553	AAD46922	Na ⁺ - and H ⁺ -linked	Wua <i>et al.</i> , 2000
mOCTN1	<i>Mus musculus</i>	553	BAA36626	Na ⁺ - and H ⁺ -linked	Tamai <i>et al.</i> , 2000
hOCTN2	<i>H. sapiens</i>	557	AAC24828	Na ⁺ - and H ⁺ -linked	Wu <i>et al.</i> , 1998
rOCTN2	<i>R. norvegicus</i>	557	AAD54059	Na ⁺ - and H ⁺ -linked	Wu <i>et al.</i> , 1999
mOCTN2	<i>M. musculus</i>	557	AAD54060	Na ⁺ - and H ⁺ -linked	Wu <i>et al.</i> , 1999
pOCT2	<i>Sus scrofa</i>	554	CAA70567	Na ⁺ - and H ⁺ -linked	Grundemann <i>et al.</i> , 1997
mOCTN3	<i>M. musculus</i>	564	BAA78343	H ⁺ -linked	Tamai <i>et al.</i> , 2000
rOCT1/ rOCT1A	<i>R. norvegicus</i>	556 430	CAA55411 AAB67702	Electrogenic ND	Grundemann <i>et al.</i> , 1994 Zhang <i>et al.</i> , 1997a
hOCT1	<i>H. sapiens</i>	554	AAB67703	Electrogenic	Zhang <i>et al.</i> , 1997b
mOCT1	<i>M. musculus</i>	556	AAB19097	Electrogenic	Schweifer and Barlow, 1996
rbOCT1	<i>Oryctolagus cuniculus</i>	554	AAC23661	Electrogenic	Terashita <i>et al.</i> , 1998
rOCT2	<i>R. norvegicus</i>	593	BAA11754	Electrogenic	Okuda <i>et al.</i> , 1996
hOCT2	<i>H. sapiens</i>	555	CAA66978	Electrogenic	Gorboulev <i>et al.</i> , 1997
mOCT2	<i>M. musculus</i>	553	CAA06827	Electrogenic	Mooslehner and Allen, 1999
hOCT3	<i>H. sapiens</i>	551	BAA76350	Electrogenic	Nishiwaki <i>et al.</i> , 1998
rOCT3	<i>R. norvegicus</i>	551	AAC40150	Electrogenic/ H ⁺ -linked	Kekuda <i>et al.</i> , 1998
mOCT3	<i>M. musculus</i>	551	AAD20978	ND	Verhaagh <i>et al.</i> , 1999
hOCT4	<i>H. sapiens</i>	594	BAA76351	Electrogenic	Nishiwaki <i>et al.</i> , 1998

ND, not determined

Table 1-9 Members of the Organic Anion Transporter (OAT) family.

Transporter	Species	Residues	GenBank™ accession	Permeant selectivity	References
hOAT1/ hOAT1-1	<i>Homo sapiens</i>	550 563	AAD19356 BAA75072	PAH, dicarboxylates, cyclic nucleotides, prostaglandin E, urate, μ -lactam antibiotics, acyclovir, ganciclovir, AZT	Race <i>et al.</i> , 1999 Hosoyamada <i>et al.</i> , 1999
rOAT1	<i>Rattus norvegicus</i>	551	AAC18772	same as above	Sekine <i>et al.</i> , 1997
rbOAT1	<i>Oryctolagus cuniculus</i>	551	CAB62587	ND	
mOAT1	<i>Mus musculus</i>	545	AAC53112	ND	
hOAT2	<i>H. sapiens</i>	548	AAD37091	tetracycline, prostaglandins, AZT	Takeda <i>et al.</i> , 2002
rOAT2	<i>R. norvegicus</i>	535	AAA57157	PAH, salicylate, acetylsalicylate, dicarboxylates, prostaglandin E	Simonson <i>et al.</i> , 1994
mOAT2	<i>Mus musculus</i>	540	AAH13474	ND	
hOAT3	<i>H. sapiens</i>	568	AAD19357	PAH, cimetidine, esterone sulfate, valacyclovir, AZT	Race <i>et al.</i> , 1999
rOAT3	<i>R. norvegicus</i>	536	BAA82552	same as above	Kusuhara <i>et al.</i> , 1999
mOAT3	<i>Mus musculus</i>	537	AAC61265	ND	Heaney <i>et al.</i> , 1998
hOAT4	<i>H. sapiens</i>	550	BAA95316	Estrone sulfate, DHEA sulfate AZT	Cha <i>et al.</i> , 2000

PAH, *p*-aminohippurate; DHEA, dehydroepiandrosterone; AZT, 3'-azido-3'-deoxythymidine; ND, not determined

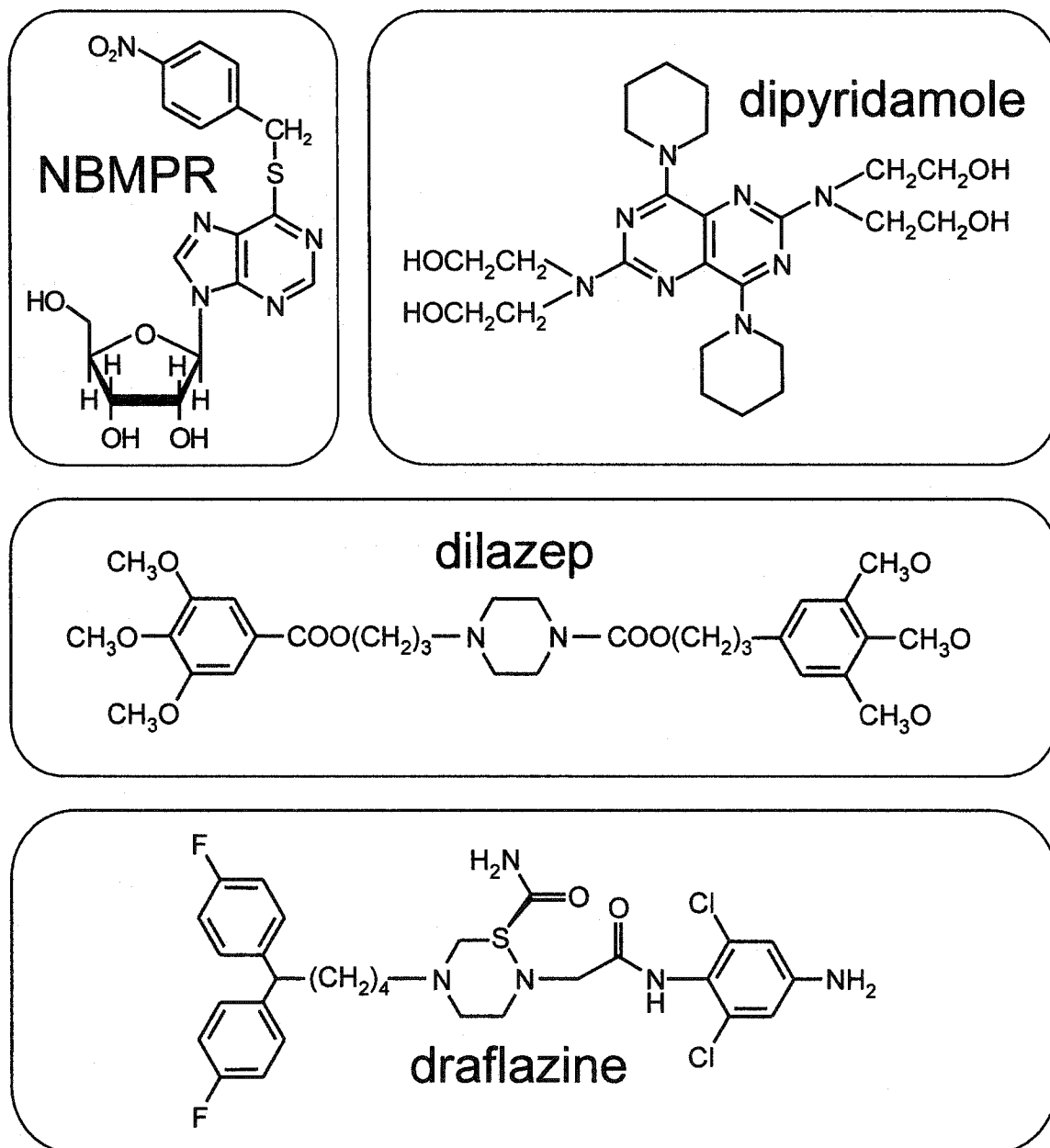


Figure 1-1. Inhibitors of some ENT-mediated transport processes. The chemical structures of NBMPR, dipyridamole, dilazep and draflazine are presented.

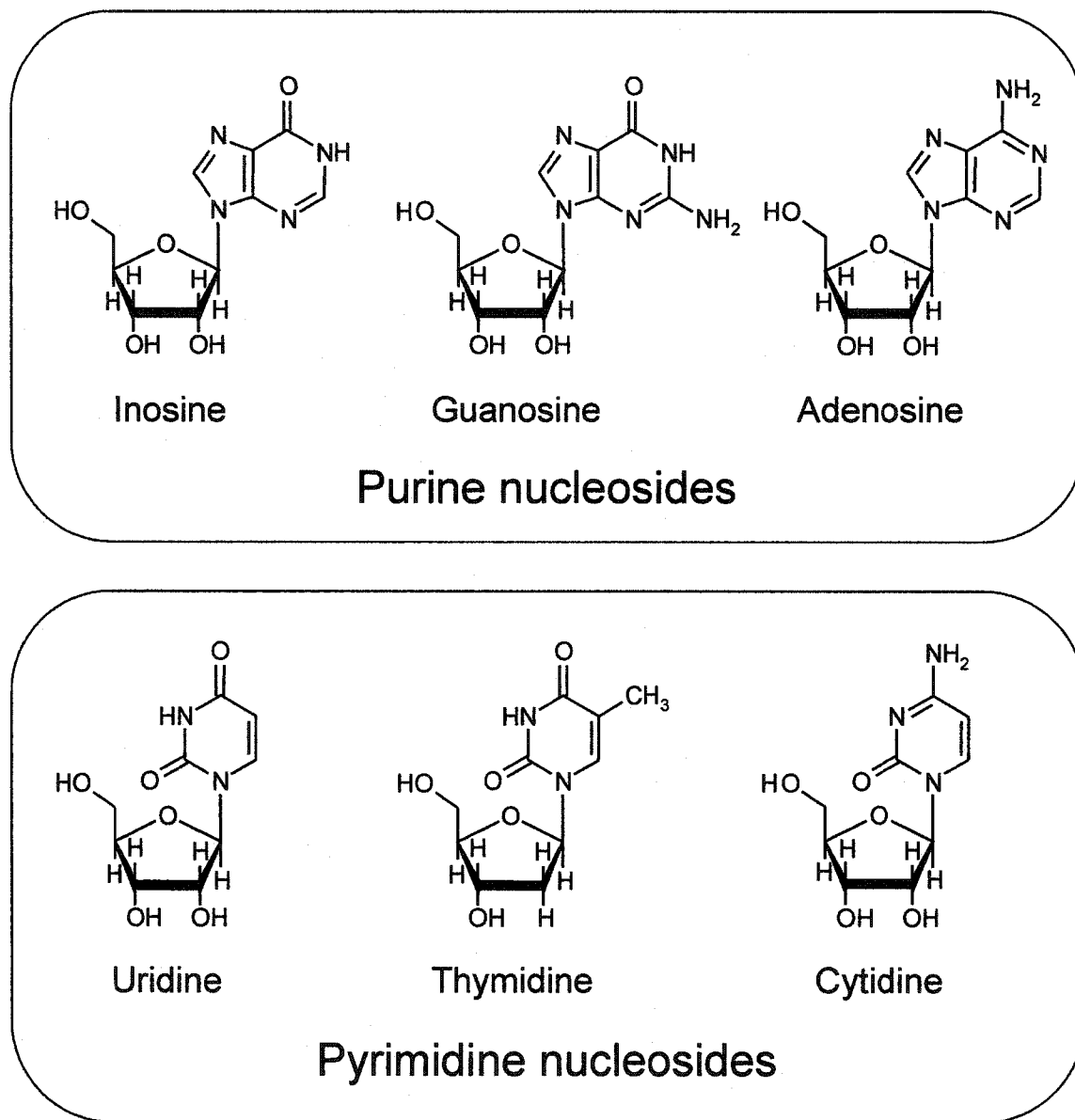


Figure 1-2. Natural substrates transported by ENT and CNT transporters and by various members of other transporter families. The chemical structures of physiological purine and pyrimidine nucleosides are presented.

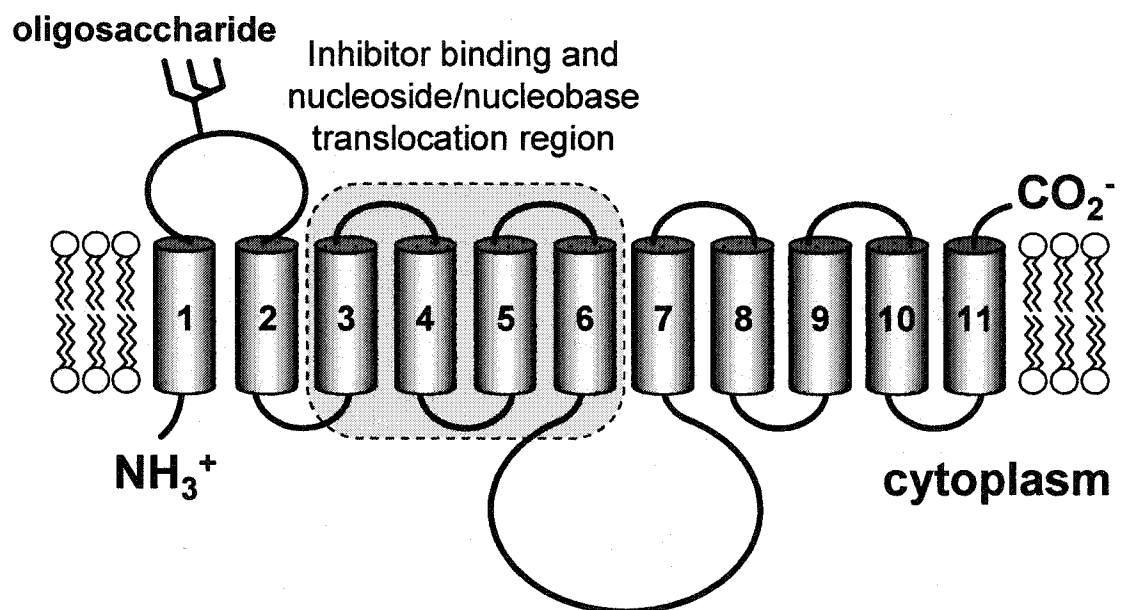


Figure 1-3. Topographical model of hENT1. Potential membrane-spanning α -helices are *numbered* and the site of *N*-glycosylation indicated. The *shaded box* shows the region implicated in the recognition of inhibitor drugs, nucleosides and nucleobases.

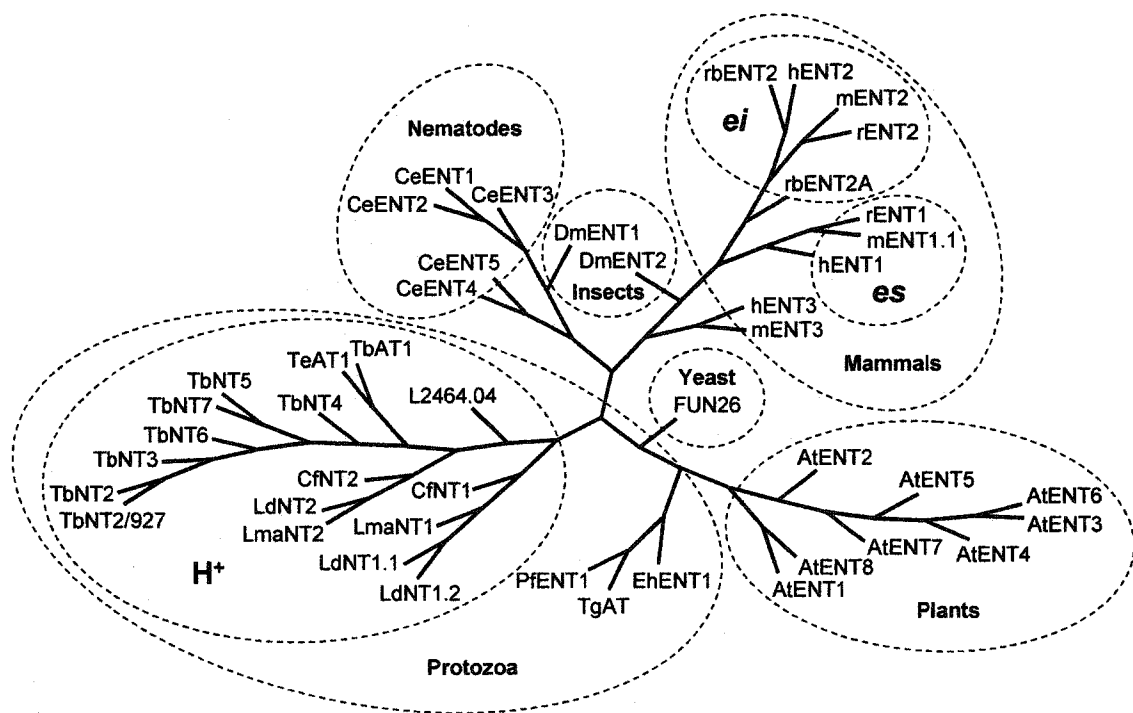


Figure 1-4. Phylogenetic tree of the ENT family. Accession numbers for each transporter sequence are given in *Table 1-1*. Genetic distances were estimated using the program Prodist (Categories model) and the phylogeny was estimated from the resultant distance matrix using the program Kitsch, both programs forming part of the PHYLIP package, version 3.5c (Felsenstein, 1989). Mammalian transporters of known substrate selectivity have been grouped into NBMPR-sensitive (*es*) and NBMPR-insensitive (*ei*) classes. Protozoan transporters known or predicted by homology to be proton symporters are also grouped (H^+).

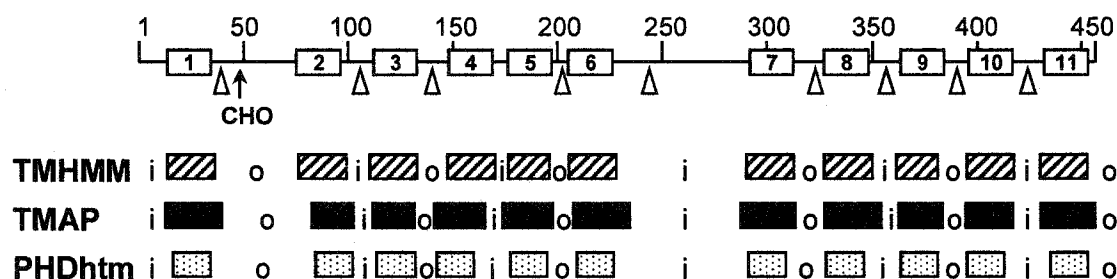


Figure 1-5. Transmembrane helix predictions for the ENT family of transporters. Computer predictions of membrane topology (Rost et al., 1996; Persson and Argos, 1997; Sonnhammer *et al.*, 1998) were performed on 34 mammalian, insect, nematode, protozoan, fungal and plant members of the ENT protein family. The *solid line* represents the sequence of hENT1, with the location of the natural glycosylation site indicated by an *arrow*. The locations of the eleven segments previously predicted from hydrophathic analysis to be transmembrane helices (Sundaram *et al.*, 2001b) are shown as the open, numbered boxes along the sequence, while the approximate locations of insertions and deletions in the aligned sequences of the ENT family are shown by triangles. The locations of transmembrane helices predicted using the TMHMM algorithm are shown beneath the representation of hENT1 as *cross-hatched rectangles*. The results of analyses of the aligned sequences by the TMAP and PHDhtm methods are illustrated as *black* and *dotted* rectangles, respectively. Segments predicted by the three algorithms to be intracellular or extracellular are indicated by 'i' and 'o', respectively. Adapted from Sundaram *et al.*, 2001a.

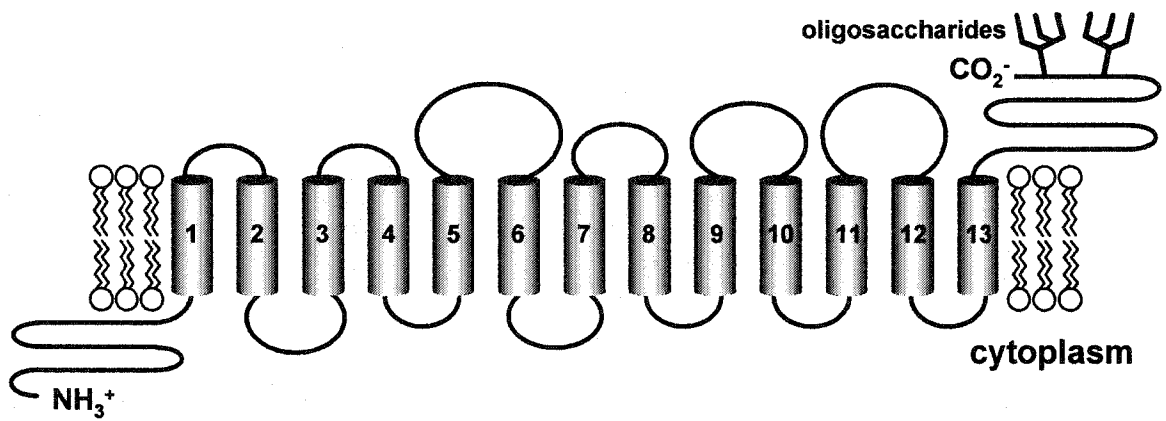


Figure 1-6. Topographical model of rCNT1. Potential membrane-spanning α -helices are *numbered* and the site of *N*-glycosylation is indicated.

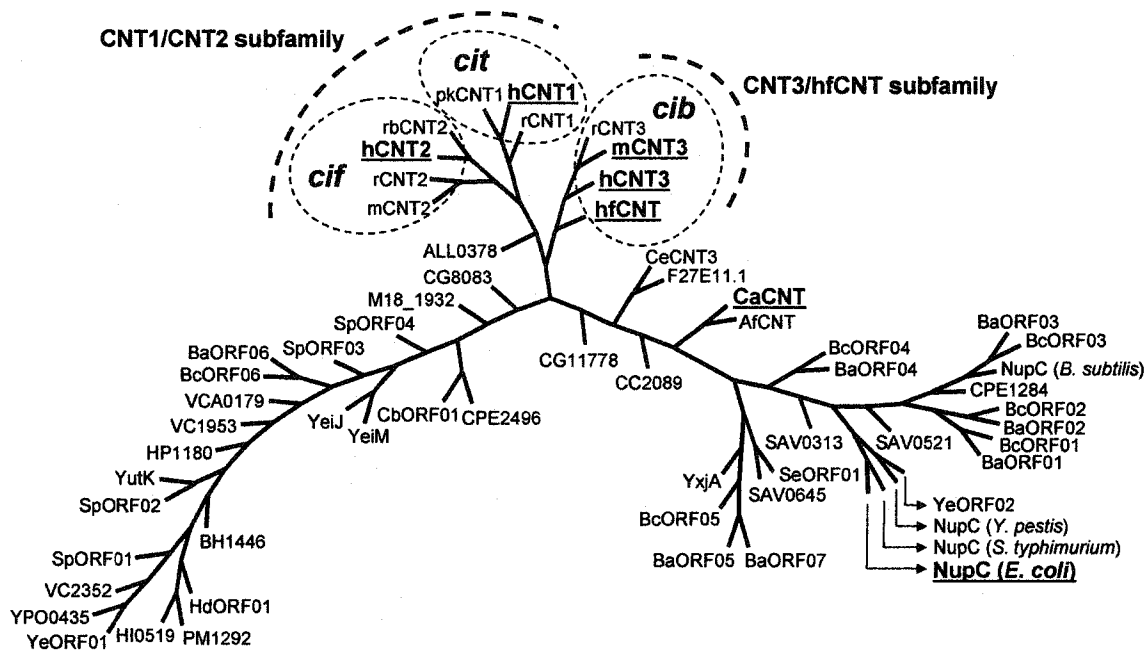


Figure 1-7. Phylogenetic tree of the CNT family. Accession numbers for each transporter sequence are given in *Table 1-3*. Genetic distances were estimated using the program Prodist (Categories model) and the phylogeny was estimated from the resultant distance matrix using the program Kitsch, both programs forming part of the PHYLIP package, version 2.5c (Felsenstein, 1989). Mammalian transporters of known nucleoside selectivity have been grouped into *cit*, *cif*, and *cib* classes. Transporters pertaining to the chapters of this thesis are underlined and indicated by **bold font**.

Bibliography

- Adams MD, Celniker SE, Holt RA, Evans CA, Gocayne JD, Amanatides PG, et al.** (2000) The genome sequence of *Drosophila melanogaster*. *Science* 287: 2185-2195.
- Anderson CM, Xiong W, Young JD, Cass CE, and Parkinson FE** (1996) Demonstration of the existence of mRNAs encoding N1/cif and N2/cit sodium/nucleoside cotransporters in rat brain. *Brain Res Mol Brain Res* 42: 358-361.
- Baer HP, and Moorji A** (1990) Sodium-dependent and inhibitor-insensitive uptake of adenosine by mouse peritoneal exudate cells. *Biochim Biophys Acta* 1026: 241-247.
- Baer HP, Moorji A, Ogbunude PO, and Serignese V** (1992) Sodium-dependent nucleoside transport in mouse lymphocytes, human monocytes, and hamster macrophages and peritoneal exudate cells. *Can J Physiol Pharmacol* 70: 29-35.
- Baldwin SA, Mackey JR, Cass CE, and Young JD** (1999) Nucleoside transporters: molecular biology and implications for therapeutic development. *Mol Med Today* 5: 216-224.
- Belt JA, Marina NM, Phelps DA, and Crawford CR** (1993) Nucleoside transport in normal and neoplastic cells. *Adv Enzyme Regul* 33: 235-252.
- Bendayan R** (1997) Interaction of dipyridamole, a nucleoside transport inhibitor, with the renal transport of organic cations by LLCPK1 cells. *Can J Physiol Pharmacol* 75: 52-56.
- Berens RL, Krug EC, and Marr JJ** (1995) Purine and pyrimidine metabolism. In *Biochemistry of Parasitic Organisms and Its Molecular Foundations*. (Marr JJ and Muller M, eds.) pp. 89-117, Academic Press, London.
- Birch RG, Pemberton JM, and Basnayake WV** (1990) Stable albicidin resistance in *Escherichia coli* involves an altered outer-membrane nucleoside uptake system. *J Gen Microbiol* 136: 51-58.
- Blattner FR, Plunkett G III, Bloch CA, Perna NT, Burland V, Riley M, et al.** (1997) The complete genome sequence of *Escherichia coli* K-12. *Science* 277: 1453-1474.
- Bremer E, Middendorf A, Martinussen J, and Valentin-Hansen P** (1990) Analysis of the *tsx* gene, which encodes a nucleoside-specific channel-forming protein (Tsx) in the outer membrane of *Escherichia coli*. *Gene* 96: 59-65.
- Brett CM, Washington CB, Ott RJ, Gutierrez MM, and Giacomini KM** (1993) Interaction of nucleoside analogues with the sodium-nucleoside transport system in brush border membrane vesicles from human kidney. *Pharm Res* 10: 423-426.
- Bronk JR, and Hastewell JG** (1989) The specificity of pyrimidine nucleoside transport and metabolism by rat jejunum in vitro. *J Physiol* 408: 405-411.

- C. elegans Sequencing Consortium** (1998) Genome sequence of the nematode *C. elegans*: a platform for investigating biology. *Science* 282: 2012-2018.
- Cabantchik ZI** (1989) Nucleoside transport across red cell membranes. *Methods Enzymol* 230: 13-40.
- Capela D, Barloy-Hubler F, Gouzy J, Bothe G, Ampe F, Batut J, et al.** (2001) From the Cover: Analysis of the chromosome sequence of the legume symbiont *Sinorhizobium meliloti* strain 1021. *Proc Natl Acad Sci USA* 98: 9877-9882.
- Carter NS, and Fairlamb AH** (1993) Arsenical-resistant trypanosomes lack an unusual adenosine transporter. *Nature* 361: 173-176.
- Carter NS, Ben Mamoun C, Liu W, Silva EO, Landfear SM, Goldberg DE, and Ullman B** (2000a) Isolation and functional characterization of the PfNT1 nucleoside transporter gene from *Plasmodium falciparum*. *J Biol Chem* 275: 10683-10691.
- Carter NS, Drew ME, Sanchez M, Vasudevan G, Landfear SM, and Ullman B** (2000b) Cloning of a novel inosine-guanosine transporter gene from *Leishmania donovani* by functional rescue of a transport-deficient mutant. *J Biol Chem* 275: 20935-20941.
- Cass CE, Belt JA, and Paterson ARP** (1987) Adenosine transport in cultured cells. *Prog Clin Biol Res* 230: 13-40.
- Cass CE** (1995) Nucleoside transport. In *Drug Transport in Antimicrobial and Anticancer Chemotherapy*. (Georgopapadakou NH, ed) pp. 404-451, Marcel Dekker, New York.
- Cha SH, Sekine T, Kusuhara H, Yu E, Kim JY, Kim DK, Sugiyama Y, Kanai Y, and Endou H** (2000) Molecular cloning and characterization of multispecific organic anion transporter 4 expressed in the placenta. *J Biol Chem* 275: 4507-4512.
- Che M, Nishida T, Gatmaitan Z, Arias IM** (1992) A nucleoside transporter is functionally linked to ectonucleotidases in rat liver canalicular membrane. *J Biol Chem* 267: 9684-9688.
- Che M, Ortiz DF, and Arias IM** (1995) Primary structure and functional expression of a cDNA encoding the bile canalicular, purine-specific Na⁺-nucleoside cotransporters. *J Biol Chem* 270: 13596-13599.
- Cheeseman CI, Mackey JR, Cass CE, Baldwin SA, and Young JD** (2000) Molecular mechanism of nucleoside and nucleoside drug transport. In *Gastrointestinal Transport*. (Barrett KE and Donowitz M, eds.) pp. 330-379, Academic Press, San Diego.
- Chen R, and Nelson JA** (2000) Role of organic cation transporters in the renal secretion of nucleosides. *Biochem Pharmacol* 60: 215-219.
- Chiang CW, Carter N, Sullivan WJ Jr, Donald RG, Roos DS, Naguib FN, el Kouni MH, Ullman B, and Wilson CM** (1999) The adenosine transporter of *Toxoplasma gondii*. Identification by insertional mutagenesis, cloning, and recombinant expression. *J Biol Chem* 274: 35255-35261.

- Choi DS, Handa M, Young H, Gordon AS, Diamond I, and Messing RO** (2000) Genomic organization and expression of the mouse equilibrative, nitrobenzylthioinosine-sensitive nucleoside transporter 1 (ENT1) gene. *Biochem Biophys Res Commun* 277: 200-208.
- Craig JE, Zhang Y, and Gallagher MP** (1994) Cloning of the *nupC* gene of *Escherichia coli* encoding a nucleoside transport system, and identification of an adjacent insertion element, IS 186. *Mol Microbiol* 11: 1159-1168.
- Crawford CR, Ng CY, and Belt JA** (1990a) Isolation and characterization of an L1210 cell line retaining the sodium-dependent carrier *cif* as its sole nucleoside transport activity. *J Biol Chem* 265: 13730-13734.
- Crawford CR, Ng CY, Noel LD, and Belt JA** (1990b) Nucleoside transport in L1210 murine leukemia cells. Evidence for three transporters. *J Biol Chem* 265: 9732-9736.
- Crawford CR, Patel DH, Naeve C, and Belt JA** (1998) Cloning of a human equilibrative, nitrobenzylmercaptapurine riboside (NBMPR)-insensitive nucleoside transporter *ei* by functional expression in a transport-deficient cell line. *J Biol Chem* 273: 5288-5293.
- de Koning H, and Diallinas G** (2000) Nucleobase transporters (review). *Mol Membr Biol* 17: 75-94.
- de Koning HP, and Jarvis SM** (1997a) Purine nucleobase transport in bloodstream forms of *Trypanosoma brucei brucei*. *Biochem Soc Tran* 25: 476S.
- de Koning HP, and Jarvis SM** (1997b) Purine nucleobase transport in bloodstream forms of *Trypanosoma brucei* is mediated by two novel transporters. *Mol Biochem Parasitol* 89: 245-258.
- de Koning HP, and Jarvis SM** (1997c) Hypoxanthine uptake through a purine-selective nucleobase transporter in *Trypanosoma brucei brucei* procyclic cells is driven by protonmotive force. *Eur J Biochem* 1997 247: 1102-1110.
- de Koning HP, Watson CJ, and Jarvis SM** (1998) Characterization of a nucleoside/proton symporter in procyclic *Trypanosoma brucei brucei*. *J Biol Chem* 273: 9486-9494.
- de Koning HP, and Jarvis SM** (1998) A highly selective, high-affinity transporter for uracil in *Trypanosoma brucei brucei*: evidence for proton-dependent transport. *Biochem Cell Biol* 76: 853-858.
- de Koning HP, and Jarvis SM** (1999) Adenosine transporters in bloodstream forms of *Trypanosoma brucei brucei*: substrate recognition motifs and affinity for trypanocidal drugs. *Mol Pharmacol* 56: 1162-1170.
- de Koning HP, and Jarvis SM** (2001) Uptake of pentamidine in *Trypanosoma brucei brucei* is mediated by the P2 adenosine transporter and at least one novel, unrelated transporter. *Acta Trop* 80: 245-250.
- de Montigny J, Straub ML, Wagner R, Bach ML, and Chevallier MR** (1998) The uracil permease of *Schizosaccharomyces pombe*: a representative of a family of 10 transmembrane helix transporter proteins of yeasts. *Yeast* 14: 1051-1059.

- de Wergifosse P, Jacques B, Jonniaux JL, Purnelle B, Skala J, and Goffeau A** (1994) The sequence of a 22.4 kb DNA fragment from the left arm of yeast chromosome II reveals homologues to bacterial proline synthetase and murine alpha-adaptin, as well as a new permease and a DNA-binding protein. *Yeast* 10: 1489-1496.
- DeVecchio VG, Kapatral V, Redkar RJ, Patra G, Mujer C, Los T, et al.** (2002) The genome sequence of the facultative intracellular pathogen *Brucella melitensis*. *Proc Natl Acad Sci USA* 99: 443-448.
- Detke S** (1998) Cloning of the *Candida albicans* nucleoside transporter by complementation of nucleoside transport-deficient *Saccharomyces*. *Yeast* 14: 1257-1265.
- Enigbokan MA, Preston J, Hubbard C, and Thompson JO** (1994) Characterization of and the influence of calcium channel blockers on the renal excretion of pyrimidine anticancer agents. *Res Commun Chem Pathol Pharmacol* 83: 270-278.
- Enjo F, Nosaka K, Ogata M, Iwashima A, and Nishimura H** (1997) Isolation and characterization of a thiamin transport gene, THI10, from *Saccharomyces cerevisiae*. *J Biol Chem* 272: 19165-19170.
- Enserink M, and Pennisi E** (2002) Infectious diseases. Researchers crack malaria genome. *Science* 295: 1207.
- Felsenstein J** (1989) Phylip-Phylogeny inference package (version 3.2). *Cladistics* 5: 164-166.
- Flanagan SA, and Meckling-Gill KA** (1997) Characterization of a novel Na⁺-dependent, guanosine-specific, nitrobenzylthioinosine-sensitive transporter in acute promyelocytic leukemia cells. *J Biol Chem* 272: 18026-18032.
- Fleischmann RD, Adams MD, White O, Clayton RA, Kirkness EF, Kerlavage AR, et al.** (1995) Whole-genome random sequencing and assembly of *Haemophilus influenzae* Rd. *Science* 269: 496-512.
- Franco R, Centelles JJ, and Kinne RK** (1990) Further characterization of adenosine transport in renal brush-border membranes. *Biochim Biophys Acta* 1024: 241-248.
- Fsihi H, Kottwitz B, and Bremer E** (1993) Single amino acid substitutions affecting the substrate specificity of the *Escherichia coli* K-12 nucleoside-specific Tsx channel. *J Biol Chem* 268: 17495-17503.
- Gati WP, Misra HK, Knaus EE, and Weibe LI** (1984) Structural modifications at the 2'- and 3'-positions of some pyrimidine nucleosides as determinants of their interaction with the mouse erythrocyte nucleoside transporter. *Biochem Pharmacol* 33: 3325-3331.
- Gati WP, and Paterson ARP** (1989a) Nucleoside transport. In *Red Blood Cell Membranes*. (Arge P and Parker JC, eds.) pp. 635-661, Marcel Dekker, New York.
- Gati WP, and Paterson ARP** (1989b) Interaction of [³H]dilatsep at nucleoside transporter-associated binding sites on S49 mouse lymphoma cells. *Mol Pharmacol* 36: 134-141.

- Gerstin KM, Dresser MJ, Wang J, and Giacomini KM** (2000) Molecular cloning of a Na⁺-dependent nucleoside transporter from rabbit intestine. *Pharm Res* 17: 906-910.
- Gibbs JE, and Thomas SA** (2002) The distribution of the anti-HIV drug, 2'3'-dideoxycytidine (ddC), across the blood-brain and blood-cerebrospinal fluid barriers and the influence of organic anion transport inhibitors. *Neurochem* 80: 392-404.
- Gorboulev V, Ulzheimer JC, Akhoundova A, Ulzheimer-Teuber I, Karbach U, Quester S, Baumann C, Lang F, Busch AE, and Koepsell H** (1997) Cloning and characterization of two human polyspecific organic cation transporters. *DNA Cell Biol* 16: 871-881.
- Griffiths DA, Hall SD, and Sokol PP** (1991) Interaction of 3'-azido-3'-deoxythymidine with organic ion transport in rat renal basolateral membrane vesicles. *J Pharmacol Exp Ther* 257: 149-155.
- Griffith DA and Jarvis SM** (1996) Nucleoside and nucleobase transport systems of mammalian cells. *Biochim Biophys Acta Rev Biombr* 1286: 153-181.
- Griffiths M, Beaumont N, Yao SYM, Sundaram M, Bouman CE, Davies A, Kwong FYP, Coe IR, Cass CE, Young JD, and Baldwin SA** (1997a) Cloning of a human nucleoside transporter implicated in the cellular uptake of adenosine and chemotherapeutic drugs. *Nat Med* 3: 89-93.
- Griffiths M, Yao SYM, Abidi F, Phillips SEV, Cass CE, Young JD, and Baldwin SA** (1997b) Molecular cloning and characterization of a nitrobenzylthioinosine-insensitive (*ei*) equilibrative nucleoside transporter from human placenta. *Biochem J* 328: 739-743.
- Grundemann D, Gorboulev V, Gambaryan S, Veyhl M, and Koepsell H** (1994) Drug excretion mediated by a new prototype of polyspecific transporter. *Nature* 372: 549-552.
- Grundemann D, Babin-Ebell J, Martel F, Ording N, Schmidt A, and Schomig E** (1997) Primary structure and functional expression of the apical organic cation transporter from kidney epithelial LLC-PK1 cells *J Biol Chem* 272: 10408-10413.
- Gutierrez MM, Brett CM, Ott RJ, Hui AC, and Giacomini KM** (1992) Nucleoside transport in brush border membrane vesicles from human kidney. *Biochim Biophys Acta* 1105: 1-9.
- Gutierrez MM, and Giacomini KM** (1993) Substrate selectivity, potential sensitivity and stoichiometry of Na⁺-nucleoside transport in brush border membrane vesicles from human kidney. *Biochim Biophys Acta* 1149: 202-208.
- Hamilton SR, Yao SYM, Ingram JC, Hadden DA, Ritzel MWL, Gallagher MP, Henderson PJ, Cass CE, Young JD, and Baldwin SA** (2001) Subcellular distribution and membrane topology of the mammalian concentrative Na⁺-nucleoside cotransporter rCNT1. *J Biol Chem* 276: 27981-27988.
- Hammer-Jespersen K** (1983) Nucleoside catabolism. In *Metabolism of Nucleoside and Nucleobases in Microorganisms*. (Munch-Petersen A, ed.), pp. 203-238, Academic Press, London.

- Hammond JR** (2000) Interaction of a series of draflazine analogues with equilibrative nucleoside transporters: species differences and transporter subtype selectivity. *Naunyn Schmiedebergs Arch Pharmacol* 361: 373-382.
- Handa M, Choi DS, Caldeiro RM, Messing RO, Gordon AS, and Diamond I** (2001) Cloning of a novel isoform of the mouse NBMPR-sensitive equilibrative nucleoside transporter (ENT1) lacking a putative phosphorylation site. *Gene* 262: 301-307.
- Hantke K** (1976) Phage T6--colicin K receptor and nucleoside transport in *Escherichia coli*. *FEBS Lett* 70: 109-112.
- Heaney C, Shalev H, Elbedour K, Carmi R, Staack JB, Sheffield VC, and Beier DR** (1998) Human autosomal recessive osteopetrosis maps to 11q13, a position predicted by comparative mapping of the murine osteosclerosis (oc) mutation. *Hum Mol Genet* 7: 1407-1410.
- Heidelberg JF, Eisen JA, Nelson WC, Clayton RA, Gwinn ML, Dodson RJ, et al.** (2000) DNA sequence of both chromosomes of the cholera pathogen *Vibrio cholerae*. *Nature* 406: 477-483.
- Hofmann K, and Stoffel W** (1993) TMbase - A database of membrane spanning proteins segments. *Biol Chem Hoppe-Seyler* 374: 166.
- Holman GD, and Sandoval IV** (2001) Moving the insulin-regulated glucose transporter GLUT4 into and out of storage. *Trends Cell Biol* 11: 173-179.
- Holstege A, Gengenbacher HM, Jehle L, and Hoppmann J** (1991) Facilitated diffusion and sodium-dependent transport of purine and pyrimidine nucleosides in rat liver. *Hepatology* 14: 373-380.
- Hong M, Schlichter L, and Bendayan R** (2000) A Na⁺-dependent nucleoside transporter in microglia. *J Pharmacol Exp Ther* 292: 366-374.
- Hong M, Schlichter L, and Bendayan R** (2001) A novel zidovudine uptake system in microglia. *J Pharmacol Exp Ther* 296: 141-149.
- Horak J** (1997) Yeast Nutrient Transporters. *Biochim Biophys Acta* 1331: 41-79.
- Hosoyamada M, Sekine T, Kanai Y, and Endou H** (1999) Molecular cloning and functional expression of a multispecific organic anion transporter from human kidney. *Am J Physiol* 276: 122-128.
- Huang QQ, Harvey CM, Paterson AR, Cass CE, and Young JD** (1993) Functional expression of Na⁺-dependent nucleoside transport systems of rat intestine in isolated oocytes of *Xenopus laevis*. Demonstration that rat jejunum expresses the purine-selective system N1 (*cif*) and a second, novel system N3 having broad specificity for purine and pyrimidine nucleosides. *J Biol Chem* 268: 20613-20619.

- Huang QQ, Yao SYM, Ritzel MWL, Paterson ARP, Cass CE, and Young JD** (1994) Cloning and functional expression of a complementary DNA encoding a mammalian nucleoside transport protein. *J Biol Chem* 269: 17757-17760.
- Hyde RJ, Cass CE, Young JD, and Baldwin SA** (2001) The ENT family of eukaryote nucleoside and nucleobase transporters: recent advances in the investigation of structure/function relationships and the identification of novel isoforms. *Mol Membr Biol* 18: 53-63.
- Inoue T, Matsuzaki S, and Tanaka S** (1995) Cloning and sequence analysis of *Vibrio parahaemolyticus* ompK gene encoding a 26-kDa outer membrane protein, OmpK, that serves as receptor for a broad-host-range vibriophage, KVP40. *FEMS Microbiol Lett* 134: 245-249.
- Itoh T, Aiba H, Baba T, Fujita K, Hayashi K, Inada T, et al.** (1996) A 460-kb DNA sequence of the *Escherichia coli* K-12 genome corresponding to the 40.1-50.0 min region on the linkage map. *DNA Res* 3: 379-392.
- Jarvis SM, McBride D, and Young JD** (1982) Erythrocyte nucleoside transport: asymmetrical binding of nitrobenzylthioinosine to nucleoside permeation sites. *J Physiol* 324: 31-46.
- Jarvis SM, and Young JD** (1982) Nucleoside translocation in sheep reticulocytes and fetal erythrocytes: a proposed model for the nucleoside transporter. *J Physiol* 324: 47-66.
- Jarvis SM, and Young JD** (1987) Photoaffinity labelling of nucleoside transporter polypeptides. *Pharmacol Ther* 32: 339-359.
- Jarvis SM** (1989) Characterization of sodium-dependent nucleoside transport in rabbit intestinal brush-border membrane vesicles. *Biochim Biophys Acta* 979: 132-138.
- Johnston ME, and Geiger JD** (1989) Sodium-dependent uptake of nucleosides by dissociated brain cells from the rat. *J Neurochem* 52: 75-81.
- Johnston ME, and Geiger JD** (1990) Adenosine transport systems on dissociated brain cells from mouse, guinea-pig, and rat. *Neurochem Res* 15: 911-915.
- Kaneko T, Nakamura Y, Sato S, Asamizu E, Kato T, Sasamoto S, et al.** (2000) Complete genome structure of the nitrogen-fixing symbiotic bacterium *Mesorhizobium loti*. *DNA Res* 7: 331-338.
- Kaneko T, Nakamura Y, Wolk CP, Kuritz T, Sasamoto S, Watanabe A, et al.** (2001) Complete genomic sequence of the filamentous nitrogen-fixing cyanobacterium *Anabaena* sp. strain PCC 7120. *DNA Res* 8: 205-213.
- Karp PD, Riley M, Saier M, Paulsen IT, Paley S, and Pellegrini-Toole A** (2002) The EcoCyc Database. *Nucleic Acids Res* 30: 56-58.
- Katinka MD, Duprat S, Cornillot E, Metenier G, Thomarat F, Prensier G, et al.** (2001) Genome sequence and gene compaction of the eukaryote parasite *Encephalitozoon cuniculi*. *Nature* 414: 450-453.

- Kawarabayasi Y, Hino Y, Horikawa H, Jin-no K, Takahashi M, Sekine M, et al.** (2001) Complete genome sequence of an aerobic thermoacidophilic crenarchaeon, *Sulfolobus tokodaii* strain 7. *DNA Res* 8: 123-140.
- Kekuda R, Prasad PD, Wu X, Wang H, Fei YJ, Leibach FH, and Ganapathy V** (1998) Cloning and functional characterization of a potential-sensitive, polyspecific organic cation transporter (OCT3) most abundantly expressed in placenta. *J Biol Chem* 273: 15971-15979.
- Kirchman D, Ducklow H, and Mitchell R** (1982) Estimates of bacterial growth from changes in uptake rates and biomass. *Appl Environ Microbiol* 44: 1296-1307.
- Kiss A, Farah K, Kim J, Garriock RJ, Drysdale TA, and Hammond JR** (2000) Molecular cloning and functional characterization of inhibitor-sensitive (mENT1) and inhibitor-resistant (mENT2) equilibrative nucleoside transporters from mouse brain. *Biochem J* 352: 363-372.
- Koepsell H** (1988) Organic cation transporters in intestine, kidney, liver, and brain. *Annu Rev Physiol* 60: 243-266.
- Komatsu Y, and Tanaka K** (1972) A showdomycin-resistant mutant of *Escherichia coli* K-12 with altered nucleoside transport character. *Biochim Biophys Acta* 288: 390-403.
- Kubitschek HE** (1968) Constancy of uptake during the cell cycle in *Escherichia coli*. *Biophys J* 8: 1401-1412.
- Kunst F, Ogasawara N, Moszer I, Albertini AM, Alloni G, Azevedo V, et al.** (1997) The complete genome sequence of the gram-positive bacterium *Bacillus subtilis*. *Nature* 390: 249-256.
- Kuroda M, Ohta T, Uchiyama I, Baba T, Yuzawa H, Kobayashi I, et al.** (2001) Whole genome sequencing of methicillin-resistant *Staphylococcus aureus*. *Lancet* 357: 1225-1240.
- Kusuhara H, Sekine T, Utsunomiya-Tate N, Tsuda M, Kojima R, Cha SH, Sugiyama Y, Kanai Y, and Endou H** (1999) Molecular cloning and characterization of a new multispecific organic anion transporter from rat brain. *J Biol Chem* 274: 13675-13680.
- Kuttesch JF Jr, Robins MJ, and Nelson JA** (1982) Renal transport of 2'-deoxytubercidin in mice. *Biochem Pharmacol* 31: 3387-3394.
- Kwong FY, Davies A, Tse CM, Young JD, Henderson PJ, and Baldwin SA** (1988) Purification of the human erythrocyte nucleoside transporter by immunoaffinity chromatography. *Biochem J* 255: 243-249.
- Lang TT, Selner M, Young JD, and Cass CE** (2001) Acquisition of human concentrative nucleoside transporter 2 (hCNT2) activity by gene transfer confers sensitivity to fluoropyrimidine nucleosides in drug-resistant leukemia cells. *Mol Pharmacol* 60: 1143-1152.
- Lee CW, Cheeseman CI, and Jarvis SM** (1988) Na⁺- and K⁺-dependent uridine transport in rat renal brush-border membrane vesicles. *Biochim Biophys Acta* 942: 139-149.

- Lee CW, Cheeseman CI, and Jarvis SM** (1990) Transport characteristics of renal brush border Na⁺- and K⁺-dependent uridine carriers. *Am J Physiol* 258: F1203-F1210.
- Lee CW, Sokoloski JA, Sartorelli AC, and Handschumacher RE** (1991) Induction of the differentiation of HL-60 cells by phorbol 12-myristate 13-acetate activates a Na⁺-dependent uridine-transport system. Involvement of protein kinase C. *Biochem J* 274: 85-90.
- Lee CW, Sokoloski JA, Sartorelli AC, and Handschumacher RE** (1994) Differentiation of HL-60 cells by dimethylsulfoxide activates a Na⁺-dependent nucleoside transport system. *In Vivo* 8: 795-801.
- Le Hir M, and Dubach UC** (1985a) Concentrative transport of purine nucleosides in brush border vesicles of the rat kidney. *Eur J Clin Invest* 15: 121-127.
- Le Hir M, and Dubach UC** (1985b) Uphill transport of pyrimidine nucleosides in renal brush border vesicles. *Pflugers Arch* 404: 238-243.
- Le Hir M** (1990) Evidence for separate carriers for purine nucleosides and for pyrimidine nucleosides in the renal brush border membrane. *Ren Physiol Biochem* 13: 154-161.
- Leung GP, Ward JL, Wong PY, and Tse CM** (2001) Characterization of nucleoside transport systems in cultured rat epididymal epithelium. *Am J Physiol Cell Physiol* 280: C1076-C1082.
- Li J, and Wang D** (2000) Cloning and *in vitro* expression of the cDNA encoding a putative nucleoside transporter from *Arabidopsis thaliana*. *Plant Sci* 157: 23-32.
- Lisinski I, Schurmann A, Joost HG, Cushman SW, and Al-Hasani H** (2001) Targeting of GLUT6 (formerly GLUT9) and GLUT8 in rat adipose cells. *Biochem J* 358: 517-522.
- Loewen SK, Ng AML, Yao SYM, Cass CE, Baldwin SA and Young JD** (1999) Identification of amino acid residues responsible for the pyrimidine and purine nucleoside specificities of human concentrative Na⁺ nucleoside cotransporters hCNT1 and hCNT2. *J Biol Chem* 274: 24475-24484.
- Lopez-Nieto CE, You G, Bush KT, Barros EJ, Beier DR, and Nigam SK** (1997) Molecular cloning and characterization of NKT, a gene product related to the organic cation transporter family that is almost exclusively expressed in the kidney. *J Biol Chem* 272: 6471-6478.
- Mackey JR, Baldwin SA, Young JD, and Cass CE** (1998) Nucleoside transport and its significance for anticancer drug resistance. *Drug Resistance Updates* 1: 310-324.
- Mackey JR, Yao SYM, Smith KM, Karpinski E, Baldwin SA, Cass CE, and Young JD** (1999) Gemcitabine transport in *Xenopus* oocytes expressing recombinant plasma membrane mammalian nucleoside transporters. *J Natl Cancer Inst* 91: 1876-1881.
- Maier C, Bremer E, Schmid A, and Benz R** (1988) Pore-forming activity of the Tsx protein from the outer membrane of *Escherichia coli*. Demonstration of a nucleoside-specific binding site. *J Biol Chem* 263: 2493-2499.

- Maser P, Sutterlin C, Kralli A, and Kaminsky R** (1999) A nucleoside transporter from *Trypanosoma brucei* involved in drug resistance *Science* 285: 242-244.
- Masereeuw R, Jaehde U, Langemeijer MW, de Boer AG, and Breimer DD** (1994) *In vitro* and *in vivo* transport of zidovudine (AZT) across the blood-brain barrier and the effect of transport inhibitors. *Pharm Res* 11: 324-330.
- Matovu E, Geiser F, Schneider V, Maser P, Enyaru JC, Kaminsky R, Gallati S, and Seebeck T** (2001) Genetic variants of the TbAT1 adenosine transporter from African trypanosomes in relapse infections following melarsoprol therapy. *Mol Biochem Parasitol* 117: 73-81.
- May BJ, Zhang Q, Li LL, Paustian ML, Whittam TS and Kapur V** (2001) Complete genomic sequence of *Pasteurella multocida*, Pm70. *Proc Natl Acad Sci USA* 98: 3460-3465.
- McClelland M, Sanderson KE, Spieth J, Clifton SW, Latreille P, Courtney L, et al.** (2001) Complete genome sequence of *Salmonella enterica* serovar typhimurium LT2. *Nature* 413: 852-856.
- McKeown M, Kahn M, and Hanawalt P** (1976) Thymidine uptake and utilization in *Escherichia coli*: a new gene controlling nucleoside transport. *J Bacteriol* 126: 814-822.
- Mohlmann T, Mezher Z, Schwerdtfeger G, and Neuhaus HE** (2001) Characterisation of a concentrative type of adenosine transporter from *Arabidopsis thaliana* (ENT1,At). *FEBS Lett* 509: 370-374.
- Mooslehner KA, and Allen ND** (1999) Cloning of the mouse organic cation transporter 2 gene, Slc22a2, from an enhancer-trap transgene integration locus. *Mamm Genome* 10: 218-224.
- Moseley RH, Jarose S, and Permod P** (1991) Adenosine transport in rat liver plasma membrane vesicles. *Am J Physiol* 261: G716-G722.
- Munch-Petersen A, Mygrind B, Nicolaisen A, and Pihl NJ** (1979) Nucleoside transport in cells and membrane vesicles from *Escherichia coli* K12. *J Biol Chem* 254: 3730-3737.
- Munch-Petersen A, and Mygrind B** (1983) Transport of nucleic acid precursors. In *Metabolism of Nucleotides, Nucleosides, Nucleobases in Microorganisms*. (Munch-Petersen A, ed), pp. 259-305, Academic Press, London.
- Murray AW** (1971) The biological significance of purine salvage. *Annu Rev Biochem* 40: 811-826.
- Mygrind B, and Munch-Petersen A** (1975) Transport of pyrimidine nucleosides in cells of *Escherichia coli* K12. *Eur J Biochem* 59: 365-372.
- Nelson JA, Kuttesch JR Jr, and Herbert BH** (1983) Renal secretion of purine nucleosides and their analogs in mice. *Biochem Pharmacol* 32: 2323-2327.
- Nelson JA, Vidale E, and Enigbokan M** (1988) Renal transepithelial transport of nucleosides. *Drug Metab Dispos* 16: 789-792.

- Nelson JA, Dutt A, Allen LH, and Wright DA** (1995) Functional expression of the renal organic cation transporter and P-glycoprotein in *Xenopus laevis* oocytes. *Cancer Chemother Pharmacol* 37: 187-189.
- Nierman WC, Feldblyum TV, Laub MT, Paulsen IT, Nelson KE, Eisen J, et al.** (2001) Complete genome sequence of *Caulobacter crescentus*. *Proc Natl Acad Sci USA* 98: 4136-4141.
- Nieweg A, and Bremer E** (1997) The nucleoside-specific Tsx channel from the outer membrane of *Salmonella typhimurium*, *Klebsiella pneumoniae* and *Enterobacter aerogenes*: functional characterization and DNA sequence analysis of the *tsx* genes. *Microbiology* 143: 603-615.
- Nishiwaki T, Daigo Y, Tamari M, Fujii Y, and Nakamura Y** (1998) Molecular cloning, mapping, and characterization of two novel human genes, ORCTL3 and ORCTL4, bearing homology to organic-cation transporters. *Cytogenet Cell Genet* 83: 251-255.
- Norholm MH, and Dandanell G** (2001) Specificity and topology of the *Escherichia coli* xanthosine permease, a representative of the NHS subfamily of the major facilitator superfamily. *J Bacteriol* 183: 4900-4904.
- Okuda M, Saito H, Urakami Y, Takano M, and Inui K** (1996) cDNA cloning and functional expression of a novel rat kidney organic cation transporter, OCT2. *Biochem Biophys Res Commun* 224: 500-507.
- Osses N, Pearson JD, Yudilevich DL, and Jarvis SM** (1996) Hypoxanthine enters human vascular endothelial cells (ECV 304) via the nitrobenzylthioinosine-insensitive equilibrative nucleoside transporter. *Biochem J* 317: 843-848.
- Pajor AM, and Wright EM** (1992) Cloning and functional expression of a mammalian Na⁺/nucleoside cotransporter. A member of the SGLT family. *J Biol Chem* 267: 3557-3560.
- Pajor AM** (1998) Sequence of a pyrimidine-selective Na⁺/nucleoside cotransporter from pig kidney, pkCNT1. *Biochim Biophys Acta* 1415: 266-269.
- Parkhill J, Wren BW, Thomson NR, Titball RW, Holden MTG, Prentice MB, et al.** (2001a) Genome sequence of *Yersinia pestis*, the causative agent of plague. *Nature* 413: 523-527.
- Parkhill J, Dougan G, James KD, Thomson NR, Pickard D, Wain J, et al.** (2001b) Complete genome sequence of a multiple drug resistant *Salmonella enterica* serovar Typhi CT18. *Nature* 413: 848-852.
- Parker MD, Hyde RJ, Yao SY, McRobert L, Cass CE, Young JD, McConkey GA, and Baldwin SA** (2000) Identification of a nucleoside/nucleobase transporter from *Plasmodium falciparum*, a novel target for anti-malarial chemotherapy. *Biochem J* 349: 67-75.
- Patel DH, Crawford CR, Naeve CW, and Belt JA** (2000) Cloning, genomic organization and chromosomal localization of the gene encoding the murine sodium-dependent, purine-selective, concentrative nucleoside transporter (CNT2). *Gene* 242: 51-58.

- Paterson ARP, and Cass CE** (1986) Transport of nucleoside drugs in animal cells. In *Membrane Transport of Antineoplastic Agents*. (Goldman ID, ed.) pp. 309-329, Pergamon Press, Oxford.
- Paterson ARP, Clanachan AS, Craik JD, Gati WP, Jakobs JS, and Cass CE** (1991) Plasma membrane transport of nucleosides, nucleobases and nucleotides: an overview. In *Role of Adenosine and Adenine Nucleotides in Biological Systems*. (Imai S. and Nakazawa M, eds.) pp. 133-148, Elsevier Science, New York.
- Pennycooke M, Chaudary N, Shuralyova I, Zhang Y, and Coe IR** (2001) Differential expression of human nucleoside transporters in normal and tumor tissue. *Biochem Biophys Res Commun* 280: 951-959.
- Persson B, and Argos P** (1997) Prediction of membrane protein topology utilizing multiple sequence alignments. *J Protein Chem* 16: 453-457.
- Plagemann PGW, Wohlheuter RM, and Woffendin C** (1988) Nucleoside and nucleobase transport in animal cells *Biochim Biophys Acta* 947: 405-443.
- Plagemann PG, and Woffendin C** (1989) Na⁺-dependent and -independent transport of uridine and its phosphorylation in mouse spleen cells. *Biochim Biophys Acta* 981: 315-325.
- Plagemann PG, and Aran JM** (1990) Na⁺-dependent, active nucleoside transport in mouse spleen lymphocytes, leukemia cells, fibroblasts and macrophages, but not in equivalent human or pig cells; dipyridamole enhances nucleoside salvage by cells with both active and facilitated transport. *Biochim Biophys Acta* 1025: 32-42.
- Plagemann PG, Aran JM, and Woffendin C** (1990) Na⁺-dependent, active and Na⁺-independent, facilitated transport of formycin B in mouse spleen lymphocytes. *Biochim Biophys Acta* 1022: 93-102.
- Plagemann PG** (1991) Na⁺-dependent, concentrative nucleoside transport in rat macrophages. Specificity for natural nucleosides and nucleoside analogs, including dideoxynucleosides, and comparison of nucleoside transport in rat, mouse and human macrophages. *Biochem Pharmacol* 42: 247-252.
- Presecan E, Moszer I, Boursier L, Cruz Ramos HC, de la Fuente V, Hullo MF, Lelong C, Schleich S, Sekowska A, Song BH, Villani G, Kunst F, Danchin A, Glaser P.** (1997) The *Bacillus subtilis* genome from *gerBC* (311 degrees) to *licR* (334 degrees). *Microbiology* 143: 3313-3328.
- Race JE, Grassl SM, Williams WJ and Holtzman EJ** (1999) Molecular cloning and characterization of two novel human renal organic anion transporters (hOAT1 and hOAT3). *Biochem Biophys Res Commun* 255: 508-514.
- Rager N, Mamoun CB, Carter NS, Goldberg DE, and Ullman B** (2001) Localization of the *Plasmodium falciparum* PfNT1 nucleoside transporter to the parasite plasma membrane. *J Biol Chem* 276: 41095-41099.

- Redenbach M, Kieser HM, Denapaite D, Eichner A, Cullum J, Kinashi H, and Hopwood DA** (1996) A set of ordered cosmids and a detailed genetic and physical map for the 8 Mb *Streptomyces coelicolor* A3(2) chromosome. *Mol Microbiol* 21: 77-96.
- Redlak MJ, Zehner ZE, and Betcher SL** (1996) Expression of rabbit ileal N3 Na⁺/nucleoside cotransport activity in *Xenopus laevis* oocytes. *Biochem Biophys Res Commun* 225: 106-111.
- Rennick BR** (1981) Renal tubule transport of organic cations. *Am J Physiol* 240: F83-F89.
- Ritzel MWL, Yao SYM, Huang MY, Elliot JF, Cass CE, and Young JD** (1997) Molecular cloning and functional expression of cDNAs encoding a human Na⁺-nucleoside cotransporters (hCNT1). *Am J Physiol* 272: C707-C714.
- Ritzel MWL, Yao SYM, Ng AML, Mackey JR, Cass CE, and Young JD** (1998) Molecular cloning, functional expression and chromosomal localization of a cDNA encoding a human Na⁺ nucleoside cotransporters (hCNT2) selective for purine nucleosides and uridine. *Mol Membr Biol* 15: 203-211.
- Roden M, Paterson AR, and Turnheim K** (1991) Sodium-dependent nucleoside transport in rabbit intestinal epithelium. *Gastroenterology* 100: 1553-1162.
- Rost B, Fariselli P, and Casadio R** (1996) Topology prediction for helical transmembrane proteins at 86% accuracy. *Prot Sci* 5: 1704-1718.
- Sanchez MA, Ullman B, Landfear SM, and Carter NS** (1999) Cloning and functional expression of a gene encoding a P1 type nucleoside transporter from *Trypanosoma brucei*. *J Biol Chem* 274: 30244-30249.
- Sanchez MA, Tryon R, Green J, Boor I, and Landfear SM** (2002) Six related nucleoside/nucleobase transporters from *Trypanosoma brucei* exhibit distinct biochemical function. *J Biol Chem* [epub ahead of print].
- Sandoval IV, and Bakke O** (1994) Targeting of membrane proteins to endosomes and lysosomes. *Trends Cell Biol* 4: 292-297.
- Saxild HH, Andersen LN, and Hammer K** (1996) Dra-nupC-pdp operon of *Bacillus subtilis*: nucleotide sequence, induction by deoxyribonucleosides, and transcriptional regulation by the deoR-encoded DeoR repressor protein. *J Bacteriol* 178: 424-434.
- Schweifer N, and Barlow DP** (1996) The *Lx1* gene maps to mouse chromosome 17 and codes for a protein that is homologous to glucose and polyspecific transmembrane transporters. *Mamm Genome* 7: 735-740.
- Seeger C, Poulsen C, and Dandanell G** (1995) Identification and characterization of genes (*xapA*, *xapB*, and *xapR*) involved in xanthosine catabolism in *Escherichia coli*. *J Bacteriol* 177: 5506-5516.
- Sekine T, Watanabe N, Hosoyamada M, Kanai Y, and Endou H** (1997) Expression cloning and characterization of a novel multispecific organic anion transporter. *J Biol Chem* 272: 18526-18529.

- Sekine T, Cha SH, and Endou H** (2000) The multispecific organic cation transporter (OAT) family. *Pfluegers Arch* 89: 337-344.
- SenGupta DJ, Lum PY, Lai Y, Shubochkina E, Bakken AH, Schneider G, and Unadkat JD** (2002) A single glycine mutation in the equilibrative nucleoside transporter gene, hENT1, alters nucleoside transport activity and sensitivity to nitrobenzylthioinosine. *Biochemistry* 41: 1512-1519.
- She Q, Singh RK, Confalonieri F, Zivanovic Y, Allard G, Aways MJ, et al.** (2001) The complete genome of the crenarchaeon *Sulfolobus solfataricus* P2. *Proc Natl Acad Sci USA* 98: 7835-7840.
- Simonson GD, Vincent AC, Roberg KJ, Huang Y, and Iwanij V** (1994) Molecular cloning and characterization of a novel liver-specific transport protein *J Cell Sci* 107: 1065-1072.
- Smits PHM, de Hann M, Maat C and Grivell LA** (1994) The complete sequence of a 33 kb fragment on the right arm of chromosome II from *Saccharomyces cerevisiae* reveals 16 open reading frames, five previously identified genes and a homologue of the SCO1 gene. *Yeast* 10: 75-80.
- Smoot JC, Barbian KD, Van Gompel JJ, Smoot LM, Chaussee MS, Sylva GL, et al.** (2002) Genome sequence and comparative microarray analysis of serotype M18 group A *Streptococcus* strains associated with acute rheumatic fever outbreaks. *Proc Natl Acad Sci USA* 99: 4668-4673.
- Sonnhammer ELL, von Heijne G, and Krogh A** (1998) A hidden Markov model for predicting transmembrane helices in protein sequences. In *Proceedings of the Sixth International Conference on Intelligent Systems for Molecular Biology* (Glasgow J, Littlejohn T, Major F, Lathrop R, Sankoff D, and Sensen C, eds.) pp. 175-182, AAAI Press, Menlo Park, CA.
- Sundaram M, Yao SYM, Ng AML, Griffiths M, Cass CE, Baldwin SA, and Young JD** (1998) Chimeric constructs between human and rat equilibrative nucleoside transporters (hENT1 and rENT1) reveal hENT1 structural domains interacting with coronary vasoactive drugs. *J Biol Chem* 273: 21519-21525.
- Sundaram M, Yao SYM, Ingram JC, Berry ZA, Abidi F, Cass CE, Baldwin SA, and Young JD** (2001a) Topology of a human equilibrative, nitrobenzylthioinosine (NBMPR)-sensitive nucleoside transporter (hENT1) implicated in the cellular uptake of adenosine and anti-cancer drugs. *J Biol Chem* 276: 45270-45275.
- Sundaram M, Yao SY, Ng AM, Cass CE, Baldwin SA, and Young JD** (2001b) Equilibrative nucleoside transporters: mapping regions of interaction for the substrate analogue nitrobenzylthioinosine (NBMPR) using rat chimeric proteins. *Biochemistry* 40: 8146-8151.
- Shimizu T, Ohtani K, Hirakawa H, Ohshima K, Yamashita A, Shiba T, Ogasawara N, Hattori M, Kuhara S, and Hayashi H** (2002) Complete genome sequence of *Clostridium perfringens*, an anaerobic flesh-eater. *Proc Natl Acad Sci USA* 99: 996-1001.
- Shryock JC, and Belardinelli L** (1997) Adenosine and adenosine receptors in the cardiovascular system: biochemistry, physiology and pharmacology. *Am J Cardiol* 79: 2-10.

- Spector R, and Huntoon S** (1984) Specificity and sodium dependence of the active nucleoside transport system in choroid plexus. *J Neurochem* 42: 1048-1052.
- Stover CK, Pham XQ, Erwin AL, Mizoguchi SD, Warrenner P, Hickey MJ, et al.** (2000) Complete genome sequence of *Pseudomonas aeruginosa* PA01, an opportunistic pathogen. *Nature* 406: 959-964.
- Takami H, Nakasone K, Takaki Y, Maeno G, Sasaki R, Masui N, Fuji F, Hiramata C, Nakamura Y, Ogasawara N, Kuhara S, and Horikoshi K** (2000) Complete genome sequence of the alkaliphilic bacterium *Bacillus halodurans* and genomic sequence comparison with *Bacillus subtilis*. *Nucleic Acids Res* 28: 4317-4331.
- Takasawa K, Suzuki H, and Sugiyama Y** (1997) Transport properties of 3'-azido-3'-deoxythymidine and 2',3'-dideoxyinosine in the rat choroid plexus. *Biopharm Drug Dispos* 18: 611-622.
- Takeda M, Khamdang S, Narikawa S, Kimura H, Kobayashi Y, Yamamoto T, Cha SH, Sekine T, and Endou H** (2002) Human organic anion transporters and human organic cation transporters mediate renal antiviral transport. *J Pharmacol Exp Ther* 300: 918-924.
- Tamai I, Yabuuchi H, Nezu J, Sai Y, Oku A, Shimane M, and Tsuji A** (1997) Cloning and characterization of a novel human pH-dependent organic cation transporter, OCTN1 *FEBS Lett* 419: 107-111.
- Tamai I, Ohashi R, Nezu JI, Sai Y, Kobayashi D, Oku A, Shimane M, and Tsuji A** (2000) Molecular and functional characterization of organic cation/carnitine transporter family in mice. *J Biol Chem* 275: 40064-40072.
- Terashita S, Dresser MJ, Zhang L, Gray AT, Yost SC, and Giacomini KM** (1998) Molecular cloning and functional expression of a rabbit renal organic cation transporter. *Biochim Biophys Acta* 1369: 1-6.
- Tomb J-F, White O, Kerlavage AR, Clayton RA, Sutton GG, Fleischmann RD, et al.** (1997) The complete genome sequence of the gastric pathogen *Helicobacter pylori*. *Nature* 388: 539-547.
- Turk E, and Wright EM** (1997) Membrane topology motifs in the SGLT cotransporter family. *J Membr Biol* 159: 1-20.
- Valens M, Bohn C, Daignan-Fornier B, Dang VD and Bolotin-Fukuhara M** (1997) The sequence of a 54.7 kb fragment of yeast chromosome XV reveals the presence of two tRNAs and 24 new open reading frames. *Yeast* 13: 379-390.
- Vasudevan G, Carter NS, Drew ME, Beverley SM, Sanchez MA, Seyfang A, Ullman B, and Landfear SM** (1998) Cloning of *Leishmania* nucleoside transporter genes by rescue of a transport-deficient mutant. *Proc Natl Acad Sci U S A* 95: 9873-9878.
- Vasudevan G, Ullman B, and Landfear SM** (2001) Point mutations in a nucleoside transporter gene from *Leishmania donovani* confer drug resistance and alter substrate selectivity. *Proc Natl Acad Sci U S A* 98: 6092-6097.

- Verhaagh S, Schweifer N, Barlow DP, and Zwart R** (1999) Cloning of the mouse and human solute carrier 22a3 (Slc22a3/SLC22A3) identifies a conserved cluster of three organic cation transporters on mouse chromosome 17 and human 6q26-q27. *Genomics* 55: 209-218.
- Vickers MF, Yao SYM, Baldwin SA, Young JD, and Cass CE** (2000) Nucleoside transporter proteins of *Saccharomyces cerevisiae*. Demonstration of a transporter (FUI1) with high uridine selectivity in plasma membranes and a transporter (FUN26) with broad nucleoside selectivity in intracellular membranes. *J Biol Chem* 275: 25931-25938.
- Visser F, Vickers MF, Ng AM, Baldwin SA, Young JD, and Cass CE** (2002) Mutation of residue 33 of human equilibrative nucleoside transporters 1 and 2 alters sensitivity to inhibition of transport by dilazep and dipyrindamole. *J Biol Chem* 277: 395-401.
- Waclawski AP, and Sinko PJ** (1996) Oral absorption of anti-acquired immune deficiency syndrome nucleoside analogues. 2. Carrier-mediated intestinal transport of stavudine in rat and rabbit preparations. *J Pharm Sci* 85: 478-485.
- Wada S, Tsuda M, Sekine T, Cha SH, Kimura M, Kanai Y, and Endou H** (2000) Rat multispecific organic anion transporter 1 (rOAT1) transports zidovudine, acyclovir, and other antiviral nucleoside analogs. *J Pharmacol Exp Ther* 294: 844-849.
- Wagner R, de Montigny J, de Wergifosse P, Souciet JL, and Potier S** (1998) The ORF YBL042 of *Saccharomyces cerevisiae* encodes a uridine permease. *FEMS Microbiol Lett* 159: 69-75.
- Wang J, and Giacomini KM** (1997) Molecular determinants of substrate selectivity in Na⁺-dependent nucleoside transporters. *J Biol Chem* 272: 28845-28848.
- Wang J, Su SF, Dresser MJ, Schaner ME, Washington CB, and Giacomini KM** (1997) Na⁺-dependent purine nucleoside transporter from human kidney: cloning and functional characterization. *Am J Physiol* 273: F1058-F1065.
- Wang J, and Giacomini KM** (1999) Serine 318 is essential for the pyrimidine selectivity of the N2 Na⁺-nucleoside transporter. *J Biol Chem* 274: 2298-2302.
- Ward JL, Sherali A, Mo ZP, and Tse CM** (2000) Kinetic and pharmacological properties of cloned human equilibrative nucleoside transporters, ENT1 and ENT2, stably expressed in nucleoside transporter-deficient PK15 cells. ENT2 exhibits a low affinity for guanosine and cytidine but a high affinity for inosine. *J Biol Chem* 275: 8375-8381.
- Washington CB, Brett CM, Wu X, and Giacomini KM** (1995) The effect of N-ethylmaleimide on the Na⁺-dependent nucleoside transporter (N3) in rabbit choroid plexus. *J Pharmacol Exp Ther* 274: 110-114.
- Westh Hansen SE, Jensen N, Munch-Petersen A** (1987) Studies on the sequence and structure of the *Escherichia coli* K-12 *nupG* gene, encoding a nucleoside-transport system. *Eur J Biochem* 168: 385-391.

- Wiese A, Pietzsch M, Syldatk C, Mattes R, and Altenbuchner J** (2000) Hydantoin racemase from *Arthrobacter aureescens* DSM 3747: heterologous expression, purification and characterization. *J Biotechnol* 80: 217-230.
- Williams TC, Doherty AJ, Griffith DA, and Jarvis SM** (1989) Characterization of sodium-dependent and sodium-independent nucleoside transport systems in rabbit brush-border and basolateral plasma-membrane vesicles from the renal outer cortex. *Biochem J* 264: 223-231.
- Williams TC, and Jarvis SM** (1991) Multiple sodium-dependent nucleoside transport systems in bovine renal brush-border membrane vesicles. *Biochem J* 274: 27-33.
- Wright EM** (2001) Renal Na⁺-glucose cotransporters. *Am J Physiol Renal Physiol* 280: F10-F18.
- Wu X, Yuan G, Brett CM, Hui AC, and Giacomini KM** (1992) Sodium-dependent nucleoside transport in choroid plexus from rabbit. Evidence for a single transporter for purine and pyrimidine nucleosides. *J Biol Chem* 267: 8813-8818.
- Wu X, Gutierrez MM, and Giacomini KM** (1994) Further characterization of the sodium-dependent nucleoside transporter (N3) in choroid plexus from rabbit. *Biochim Biophys Acta* 1191: 190-196.
- Wu X, Prasad PD, Leibach FH, and Ganapathy V** (1998) cDNA sequence, transport function, and genomic organization of human OCTN2, a new member of the organic cation transporter family. *Biochem Biophys Res Commun* 246: 589-595.
- Wu X, Huang W, Prasad PD, Seth P, Rajan DP, Leibach FH, Chen J, Conway SJ, and Ganapathy V** (1999) Functional characteristics and tissue distribution pattern of organic cation transporter 2 (OCTN2), an organic Cation/Carnitine transporter. *J Pharmacol Exp Ther* 290: 1482-1492.
- Wua X, Georgeb RL, Huanga W, Wang H, Conwayc SJ, Leibacha FH, and Ganapathya V** (2000) Structural and functional characteristics and tissue distribution pattern of rat OCTN1, an organic cation transporter, cloned from placenta. *Biochim Biophys Acta* 1466: 315-327.
- Xiao G, Wang J, Tangen T, and Giacomini KM** (2001) A novel proton-dependent nucleoside transporter, CeCNT3, from *Caenorhabditis elegans*. *Mol Pharmacol* 59:339-348
- Yao SYM, Ng AML, Ritzel MWL, Gati WP, Cass CE, and Young JD** (1996a) Transport of adenosine by recombinant purine- and pyrimidine-selective sodium/nucleoside cotransporters from rat jejunum expressed in *Xenopus laevis* oocytes. *Mol Pharmacol* 50: 1529-1535.
- Yao SYM, Cass CE, and Young JD** (1996b) Transport of the antiviral nucleoside analogs 3'-azido-3'-deoxythymidine and 2',3'-dideoxycytidine by a recombinant nucleoside transporter (rCNT) expressed in *Xenopus laevis* oocytes. *Mol Pharmacol* 50: 388-393.
- Yao SYM, Ng AML, Muzyka WR, Griffiths M, Cass CE, Baldwin SA, and Young JD** (1997) Molecular cloning and functional characterization of nitrobenzylthioinosine (NBMPR)-sensitive (*es*) and NBMPR-insensitive (*ez*) equilibrative nucleoside transporter proteins (rENT1 and rENT2) from rat tissues. *J Biol Chem* 272: 28423-28430.

- Yao SYM, Sundaram M, Chomey EG, Cass CE, Baldwin SA, and Young JD** (2001) Identification of Cys140 in helix 4 as an exofacial cysteine residue within the substrate-translocation channel of rat equilibrative nitrobenzylthioinosine (NBMPR)-insensitive nucleoside transporter rENT2. *Biochem J* 353: 387-393.
- Yao SYM, Ng, AML, Sundaram M, Cass CE, Baldwin SA, and Young JD** (2002) Functional and molecular characterization of nucleobase transport by recombinant human and rat ENT1 and ENT2 equilibrative nucleoside transport proteins: chimeric constructs reveal a role for the ENT2 helix 5-6 region in nucleobase translocation. *J Biol Chem* (in press).
- Yoo HS, Cunningham TS, and Cooper TG** (1992) The allantoin and uracil permease gene sequences of *Saccharomyces cerevisiae* are nearly identical. *Yeast* 8: 997-1006.
- Young JD and Jarvis SM** (1983) Nucleoside transport in animal cells. *Biosci Reports* 3: 309-322.
- Young JD, Cheeseman CI, Mackey JR, Cass CE, and Baldwin SA** (2000) Molecular mechanisms of nucleoside and nucleoside drug transport. In *Gastrointestinal Transport*. (Barrett KE and Donowitz M, eds.) pp. 329-378, San Diego, CA, Academic Press.
- Zhang L, Dresser MJ, Chun JK, Babbitt PC, and Giacomini KM** (1997a) Cloning and functional characterization of a rat renal organic cation transporter isoform (rOCT1A). *J Biol Chem* 272: 16548-16554.
- Zhang L, Dresser MJ, Gray AT, Yost SC, Terashita S, and Giacomini KM** (1997b) Cloning and functional expression of a human liver organic cation transporter. *Mol Pharmacol* 51: 913-921.
- Zhang L, Brett CM, Giacomini KM.** (1998) Role of organic cation transporters in drug absorption and elimination. *Annu Rev Pharmacol Toxicol* 38: 431-460.

CHAPTER II:*

Identification of amino acid residues responsible for the pyrimidine and purine nucleoside specificities of human concentrative Na⁺ nucleoside cotransporters hCNT1 and hCNT2.**

* *A version of this chapter has been published.*

Loewen SK, Ng AML, Yao SYM, Cass CE, Baldwin SA, and Young JD (1999) *J Biol Chem* 274: 24475-24484.

** In this chapter, all of the work is my own. Dr. Stephen Baldwin from the University of Leeds assisted with the helical wheel analysis.

Introduction

Specialized nucleoside transporter (NT) proteins are required for uptake or release of purine and pyrimidine nucleosides from cells (Baldwin *et al.*, 1999; Cass *et al.*, 1999). Most nucleosides, including those with antineoplastic and/or antiviral activity (Handschumacher and Cheng, 1993; Groothuis and Levy, 1997), are hydrophilic, and transportability across plasma membranes is a critical determinant of metabolism and, in the case of nucleoside drugs, pharmacologic actions (Mackey *et al.*, 1998a). NTs also regulate adenosine concentrations in the vicinity of its cell surface receptors and have profound effects on neurotransmission, vascular tone and other processes (Fredholm, 1997; Shryock and Belardinelli, 1997). In human and other mammalian cells, seven nucleoside transport processes that differ in their cation dependence, permeant selectivities and inhibitor sensitivities have been observed. The major (*cit*, *cif*) and minor (*cib*, *cs*, *cs*) concentrative NTs are inwardly-directed Na⁺-dependent processes and have been demonstrated functionally in specialized epithelia such as intestine, kidney, liver and choroid plexus, in other regions of the brain, and in splenocytes, macrophages and leukemic cells (Baldwin *et al.*, 1999; Cass *et al.*, 1999). Concentrative NT transcripts have also been found in heart, skeletal muscle, placenta, pancreas and lung. The equilibrative (bidirectional) transport processes (*es*, *et*) have generally lower substrate affinities and occur in most, possibly all, cell types (Baldwin *et al.*, 1999; Cass *et al.*, 1999). Epithelia (*e.g.* intestine, kidney) and some nonpolarized cells (*e.g.* leukemic cells) therefore coexpress both concentrative and equilibrative NTs, whereas other nonpolarized cells (*e.g.* erythrocytes) exhibit only equilibrative NT (Baldwin *et al.*, 1999; Cass *et al.*, 1999).

Molecular cloning studies have isolated cDNAs encoding the human and rat proteins responsible for each of the major NT processes (*cit*, *cif*, *es*, *et*) operative in mammalian cells (Huang *et al.*, 1994; Che *et al.*, 1995; Yao *et al.*, 1996a; Griffiths *et al.*, 1997a, 1997b; Ritzel *et al.*, 1997; Wang *et al.*, 1997; Yao *et al.*, 1997, Crawford *et al.*, 1998; Ritzel *et al.*, 1998). These proteins comprise two previously unrecognized families of integral membrane proteins (CNT and ENT) with quite different predicted architectural designs (Baldwin *et al.*, 1999; Cass *et al.*, 1999). The relationships of these NT proteins to the processes defined by functional studies are: CNT1 (*cit*), CNT2 (*cif*), ENT1 (*es*), and ENT2 (*et*). While the NT proteins responsible for the minor mammalian concentrative processes (*cib*, *cs*, *cs*) remain to be identified, we have cloned a cDNA

encoding a CNT protein with *cib*-like transport activity from the ancient marine vertebrate the Pacific hagfish (*Eptatretus stouti*, as described in *Chapter V*). The CNT family also includes the *Escherichia coli* proton/nucleoside co-transporter NupC (Craig *et al.*, 1994; and as described in *Chapter VI*).

Human and rat CNT1 (650 and 684 residues, 71 kDA), designated hCNT1 and rCNT1, respectively, are 83% identical in amino acid sequence (Huang *et al.*, 1994; Ritzel *et al.*, 1997), and contain 13 putative TMs (one less than predicted in earlier models (Huang *et al.*, 1994)) with an exofacial glycosylated tail at the carboxyl-terminus (Hamilton *et al.*, 2001). hCNT2 (658 residues) (Wang *et al.*, 1997, Ritzel *et al.*, 1998) is 83% identical to rCNT2 (659 residues) (Che *et al.*, 1995; Yao *et al.*, 1996a) and 72% identical to hCNT1 (Ritzel *et al.*, 1997). Recombinant hCNT1 and rCNT1 produced in oocytes mediate saturable Na⁺-dependent transport of uridine (apparent K_m 40 μ M), with a Na⁺/uridine coupling stoichiometry of 1:1. Transport is inhibited by pyrimidine nucleosides (thymidine, cytidine) and adenosine, but not by guanosine or inosine (Huang *et al.*, 1994; Ritzel *et al.*, 1997). Adenosine is transported by rCNT1 with a similar K_m (25 μ M) as uridine, but with a substantially reduced V_{max} (Yao *et al.*, 1996a). The nucleoside specificity of hCNT2 and rCNT2 is complementary to that of h/rCNT1, showing a preference for adenosine, other purine nucleosides and uridine (Yao *et al.*, 1996a, Ritzel *et al.*, 1998). Although hCNT2 has a higher K_m (40 μ M) for uridine than adenosine (8 μ M), V_{max} values for the two nucleosides are similar. Thus, "purine nucleoside selective" CNT2 shows a greater tolerance for uridine as a permeant than does "pyrimidine nucleoside selective" CNT1 for adenosine. The difference in substrate specificity between CNT1 and CNT2 is reflected in their capabilities to transport different pyrimidine and purine antiviral and anticancer nucleoside drugs. For example, h/rCNT1 transport AZT and ddC, but not ddI, while hCNT2 transports only ddI (Huang *et al.*, 1994; Yao *et al.*, 1996b; Ritzel *et al.*, 1997). Gemcitabine, an anticancer cytidine analog, is a good hCNT1 permeant, but is not transported by hCNT2 (Mackey *et al.*, 1998b, 1999).

Chimeric studies between the CNT1 and CNT2 proteins of rat have identified TMs 7 and 8 as potential determinants of substrate selectivity (Wang and Giacomini, 1997). When a point mutation (Ser318Gly) was introduced into TM 7 of rat CNT1, it was converted from being pyrimidine nucleoside selective into an apparently broad specificity transporter (Wang and

Giacomini, 1999). In this chapter, I present a comprehensive and independent study of the structural features responsible for the substrate specificities of the human CNT1 and CNT2 proteins, focusing not only on TM 7 but also TM 8 and combinations thereof. I have used information derived from chimeric constructs between hCNT1 and hCNT2, sequence comparisons between mammalian CNTs and the hagfish *cib* transporter (hfCNT) (which is broadly selective for both pyrimidine and purine nucleosides), and site-directed mutagenesis to identify two sets of adjacent residues in TMs 7 and 8 (including the human counterpart of rCNT1 Ser³¹⁸) that when converted to the corresponding residues in hCNT2, dramatically alter the substrate selectivity of hCNT1. Mutation of the two adjacent residues in TM 7 alone convert hCNT1 into a protein with *cib*-like activity, while the concurrent mutation of two adjacent residues in TM 8 convert the latter protein with *cib*-type characteristics into one with purine nucleoside selective, *cif*-like characteristics. Mutations in TM 8 of hCNT1 alone produced a novel uridine-selective transport phenotype. Molecular modeling studies have identified possible roles for each of the four identified hCNT1 residues.

Materials and Methods

Nomenclature and Construction of Chimeric hCNT1 and hCNT2 Transporters – Chimeras between hCNT1 and hCNT2 were created using the three junction points (*Arrows A, B, and C*) illustrated in Fig. 2-1. A four-character numerical nomenclature was chosen to represent each chimera. The numbers of 1's and 2's in the name indicates the approximate percentage of each wild-type cDNA in a particular construct, where '1' represents the DNA and encoded amino acid sequence of hCNT1 and '2' denotes that of hCNT2. For instance, C2211 is a 50:50 chimeric transporter whose amino-terminal half is hCNT2 and whose carboxyl-terminal half is hCNT1; C2221 is a 75:25 chimeric transporter whose amino-terminal three-quarters is hCNT2 and whose carboxyl-terminal one-quarter is hCNT1.

hCNT1 and hCNT2 cDNAs (GenBankTM accession numbers AF036109 and HSU62968) used to construct the chimeras were cloned in this laboratory as described previously (Ritzel *et al.*, 1997, 1998) into the pBluescript II KS⁺ (Stratagene) vector. All chimeras were produced in two steps by the overlap extension PCR method (Horton *et al.*, 1989) using high-fidelity

Pyrococcus furiosus DNA polymerase. All chimeras were sequenced in both directions to ensure that the correct splice sites had been introduced.

Nomenclature and Construction of Site-specific Mutated hCNT1 Transporters – Sequence comparisons between the TM 7-9 regions of h/rCNT1 (*cit*), hCNT (*cib*), and h/rCNT2 (*cif*) were used to identify residue differences between the *cit*, *cib* and *cif* transport proteins (Fig. 2-4). The nine residues of hCNT1 selected for mutagenesis are shown by arrows: three in TM 7, five in TM 8, and one in TM 9. In each case the residue in hCNT1 was converted to the corresponding residue at that position in hCNT2 and are designated M1-M9 (Table 2-1). For example, mutant M1 has the single substitution Ser311Ala, while M1/2/3 is a combination mutant with three substitutions in TM 7 corresponding to Ser311Ala, Ser319Gly, and Gln320Met. All hCNT1 point mutations were produced in two steps by a modified overlap extension PCR method (Ho *et al.*, 1989). All constructs were sequenced in both directions to confirm that the correct mutations had been introduced. The final combination mutant M2/3/6/7 was sequenced in its entirety to ensure that no additional mutations had been introduced.

In Vitro Transcription and Expression in *Xenopus* Oocytes – Plasmid DNAs were linearized with *NotI* and transcribed with T3 polymerase using the mMACHINE™ (Ambion) transcription system. Defolliculated stage VI *Xenopus* oocytes (Ritzel *et al.*, 1997) were microinjected with 20 nl of water or 20 nl of water containing capped RNA transcript (20 ng) and incubated in modified Barth's medium (changed daily) at 18 °C for 72 h prior to the assay of transport activity.

Transport Assays – Transport assays were performed as described previously (Huang *et al.*, 1994; Ritzel *et al.*, 1997) on groups of 12 oocytes at 20°C using [¹⁴C]-labeled nucleosides (Moravek Biochemicals or Amersham Pharmacia Biotech) (1 µCi/ml) in 200 µl of transport buffer containing either 100 mM NaCl or 100 mM choline chloride and 2 mM KCl, 1 mM CaCl₂, 1 mM MgCl₂, and 10 mM HEPES, pH 7.5. Except where otherwise indicated, nucleoside uptake was determined at a concentration of 20 µM using an incubation period of 30 min (Huang *et al.*, 1994). Each experiment was performed at least twice on different batches of cells and included hCNT1 and hCNT2 as controls to eliminate transport variability

between batches of oocytes. The flux values shown are means \pm S.E. of 10-12 oocytes from one representative experiment. Significant differences in mean flux values were determined by Student's t-test ($P = 0.05$).

Molecular Modeling – Predictions of the possible orientations of putative TMs 7, 8 and 9 in hCNT1 and its homologs, with respect both to the lipid bilayer and to other helices, were made by analysis of the patterns of residue substitution in these regions of the aligned sequences of the following 18 members of the CNT transporter family: rCNT1 (rat CNT1, GenBank™ accession U10279); hCNT1 (human CNT1, GenBank™ accession U62968); pkCNT1 (pig kidney CNT1, GenBank™ accession AF009673); rCNT2 (rat CNT2, GenBank™ accession U25055); mCNT2 (mouse CNT2, GenBank™ accession AF079853); hCNT2 (human CNT2, GenBank™ accession AF036109); hfCNT (hagfish *cib* transporter, GenBank™ accession AF132298); F27E11.1 (*Caenorhabditis elegans*, GenBank™ accession AF016413); F27E11.2 (*Caenorhabditis elegans*, GenBank™ accession AF016413); YEIM_HAEIN (*Haemophilus influenzae*, Swissprot accession P44742); NUPC_HELPY (*Helicobacter pylori*, GenBank™ accession AE000623); YEIM_ECOLI (*Escherichia coli*, Swissprot accession P33024); YEIJ_ECOLI (*Escherichia coli*, Swissprot accession P33021); YXJA_BACSU (*Bacillus subtilis*, Swissprot accession P42312); NUPC_ECOLI (*Escherichia coli*, Swissprot accession P33031); NUPC_BACSU (*Bacillus subtilis*, Swissprot accession P39141); NUPC_STREP (*Streptococcus pyogenes*, open reading frame present in contig188 from the *S. pyogenes* genome sequencing project, Oklahoma University); YUTK_BACSU (*Bacillus subtilis*, GenBank™ accession Z99120).

The patterns of residue substitution in the aligned sequences were investigated by the graphical method of Baldwin (Baldwin, 1993). Two approaches were used to predict the location of buried and lipid-accessible residues: the identification of TM positions able to accommodate polar residues and the identification of positions of restricted variability. Residues at these locations would be predicted to be buried within the bundle of TMs, either forming helix-helix contacts or lining the substrate translocation pathway. Conversely, positions of high variability, and where polar residues are never found, might be predicted to be exposed to the hydrophobic core of the lipid bilayer. Polar residues which would not be expected to be in contact with the lipid acyl chains were defined as charged residues and those

capable of forming more than one hydrogen bond. Because of their potential involvement in substrate recognition, serine and threonine were included in the category of polar residues, although their side-chains can hydrogen bond to the main chain of an α -helix and so can be on its lipid-facing surface. Non-polar residues, which could be in contact with the lipid acyl chains, were defined as those normally classed as hydrophobic, but also including tyrosine, which has been found on the lipid-facing surface of TMs in other membrane proteins including bacteriorhodopsin (Baldwin, 1993).

Results and Discussion

hCNT1 (650 residues) and hCNT2 (658 residues) belong to different CNT sub-families and exhibit strongest residue similarity within TMs of the carboxyl-terminal halves of the proteins (Fig. 2-1). Functionally, hCNT1 and hCNT2 display *cit*- and *cif*-type Na⁺-dependent nucleoside transport activities (Ritzel *et al.*, 1997, 1998). Therefore, while both hCNT1 and hCNT2 transport uridine, they are otherwise selective for pyrimidine (hCNT1) and purine (hCNT2) nucleosides (except for modest transport of adenosine by hCNT1). Below, we describe a series of chimeric and site-directed mutagenesis experiments aimed at identifying hCNT1/2 domains and amino acid residues responsible for the marked differences in permeant selectivity between the two transporters.

hCNT1/hCNT2 Chimeras – Splice sites between hCNT1 and hCNT2 were engineered at the beginning or end of putative extramembranous domains as predicted by the topology model in Fig. 2-1, thereby minimizing disruption of native TMs and loops. To further increase the probability of obtaining functional hCNT1/2 chimeras, we concealed splice sites within regions of identical amino acid sequence in the two proteins. These splice sites divided the proteins into four unequal quarters ranging from 85 to 261 residues, each containing 2-4 TMs (Fig. 2-1).

RNA transcripts for each chimeric cDNA were synthesized by *in vitro* transcription and microinjected into *Xenopus* oocytes, which were then assayed for (i) functionality (using uridine as a universal hCNT1/2 permeant), and (ii) substrate selectivity (using thymidine and inosine as diagnostic hCNT1 and hCNT2 permeants, respectively). Shown in Fig. 2-2 is a representative transport experiment for the two wild-type transporters hCNT1 and hCNT2

and for chimeras C2211, C2221, C1221, and C1121 (where '1' is hCNT1 and '2' is hCNT2). The first in the series, C2211, was a 50:50 chimera incorporating the amino-terminal half (TMs 1-6) of hCNT2 and the carboxyl-terminal half (TMs 7-13) of hCNT1. Functionally, C2211 exhibited pyrimidine nucleoside selective characteristics similar to hCNT1 (marked thymidine uptake, low inosine transport), indicating that the regions conferring substrate selectivity were located largely within the carboxyl-terminal half of the transporter. The second chimera, C2221, increased the hCNT2 portion of the transporter by 3 TMs, leaving the 4 remaining TMs at the carboxyl-terminus as hCNT1. This 75:25 hCNT2/hCNT1 construct displayed inosine and thymidine transport characteristics similar to hCNT2, implicating residues 303-387 (incorporating TMs 7-9) as the determinant of substrate specificity. The hCNT2-like transport profile of chimera C1221 (incorporating the middle 5 TMs of hCNT2 (TMs 5-9) into hCNT1) was consistent with this conclusion. Chimera C1121 (incorporating only residues 303-387 of hCNT2 into hCNT1) directly confirmed involvement of the TM 7-9 region by also exhibiting hCNT2-like transport properties.

While these studies implicated TMs 7-9 as the primary region responsible for substrate specificity, the finding that chimeras C2221, C1221 and C1121 showed modestly increased uptake of thymidine relative to wild-type hCNT2 (Fig. 2-2) suggested secondary involvement of other regions of the protein. Similarly, Fig. 2-2 shows that chimera C2211 exhibited significantly increased uptake of inosine relative to wild-type hCNT1. The chimeras transported uridine to similar extents as hCNT1 and hCNT2, suggesting that the native conformations were retained in all constructs.

Complementary reciprocal chimeras were also prepared (C1122, C1112, C2112 and C2212). C1122 displayed low uridine transport but maintained purine nucleoside-selectivity with an ~ 5-fold increase in inosine uptake compared to water-injected oocytes (2.0 ± 0.6 pmol/oocyte.30 min⁻¹ versus 0.42 ± 0.04 pmol/oocyte.30 min⁻¹) and no detectable thymidine transport. The other chimeras were non-functional, perhaps because of altered helical packing or improper plasma membrane targeting. A structural feature shared by these chimeras (and by low-activity C1122) was the presence of hCNT2 sequence at the carboxyl-terminus.

As shown in Fig. 2-3, the *cif*-like transport characteristics of chimera C1121 was confirmed by testing the transportability of a panel of six physiological purine and pyrimidine nucleosides (adenosine, uridine, inosine, thymidine, guanosine and cytidine). Fluxes were similar in profile and magnitude to those exhibited by wild-type hCNT2 (adenosine, uridine, inosine, guanosine >> thymidine, cytidine). Furthermore, uridine uptake was strongly Na⁺-dependent, providing additional evidence that the native conformation of the transporter had been retained.

Identification of Candidate Residues for Mutation in hCNT1 – Our analysis of hCNT1/hCNT2 chimeras located an 85-residue segment in the C-terminal half of hCNT1 (residues 303-387) that when substituted by corresponding hCNT2 sequence resulted in a purine nucleoside selective transporter. hCNT1 and hCNT2 are 80% identical and 85% similar within this region. When aligned with rCNT1 and rCNT2, which are functionally similar to their human counterparts, there is 98% identity between hCNT1 and rCNT1, and 92% identity between hCNT2 and rCNT2 in this 85-residue domain. With so few sequence differences between the CNT1 and CNT2 subfamilies, it seemed likely that introduction of point mutations into hCNT1 would identify individual residues contributing to hCNT1/2 substrate specificity. These amino acids would be expected to be located within transmembrane helices.

Comparison of sequences of h/rCNT1 and h/rCNT2 in TMs 7, 8, and 9 (Fig. 2-4) identified nine residues that were conserved in CNT1 and CNT2 transporter subtypes, respectively, but differed between the subtypes and might therefore contribute to permeant selectivity (Table 2-1). Some were common to h/rCNT1 and hCNT, a native broad specificity *cif*-type transporter (*i.e.* transports both pyrimidine and purine nucleosides), which we have identified from the Pacific hagfish (Fig. 2-4; as described in *Chapter V*). Others were common to hCNT and h/rCNT2. In subsequent experiments, these nine residues in hCNT1 were mutated singly and in combination to the corresponding residues in hCNT2 (Table 2-1). Three of the mutations were in TM 7 (M1-3), five were in TM 8 (M4-8), and one was in TM 9 (M9). Each mutant protein was assayed for uridine, inosine and thymidine transport activity. Representative transport data for each of the hCNT1 mutants investigated in our study are presented in Table 2-2. The results (described below) are presented as expressed fluxes corrected for endogenous uptake in control water-injected oocytes.

Characteristics of TM 7 Mutants of hCNT1 – Simultaneous mutation of the three candidate residues in TM 7 of hCNT1 into the corresponding residues of hCNT2 (mutant M1/2/3) altered the substrate selectivity of hCNT1 from being pyrimidine nucleoside selective to non-selective (broad specificity), allowing uptake of inosine in addition to thymidine and uridine. Mediated uptake of inosine was similar to that of chimera C1121 (Fig. 2-2 & Table 2-2), suggesting that TM 7 is largely responsible for allowing transport of purine nucleoside substrates. Similarly, introduction of TM 7 from rCNT2 into rCNT1 produced a chimeric transporter with inosine transport capability (Wang and Giacomini, 1997). To explore which of the three mutated residues in hCNT1 contributed this change, we systematically changed each residue separately to create mutants M1, M2, and M3. The single mutations at positions 311 (mutant M1) and 320 (mutant M3) had no apparent effect on transport, whereas the Ser to Gly shift at position 319 of hCNT1 (mutant M2) allowed for marked inosine uptake. Ratios of inosine:thymidine and inosine:uridine uptake for this mutant were, however, consistently lower than those for mutant M1/2/3. This would suggest that although mutant M2 allowed transport of inosine, other residues also contributed to the higher inosine flux evident with mutant M1/2/3.

The combination TM 7 mutants M1/2, M2/3, and M1/3 were therefore constructed and tested for inosine, thymidine, and uridine transport (Table 2-2). Mutant M1/2 exhibited a transport profile similar to mutant M2, suggesting that the substitution of Ala for Ser at position 311 did not contribute to inosine transportability. In contrast, substitution of glutamine by methionine at position 320 in TM 7 in combination with the change of Ser to Gly at position 319 (mutant M2/3) resulted in a transport profile resembling that of mutant M1/2/3. Mutant M1/3 showed little apparent uptake of inosine, confirming that the Ser319Gly mutation is required for purine nucleoside transport. Mutation of the corresponding residue in CNT1 of rat (Ser³¹⁸) also produced an increase in inosine transport activity (Wang and Giacomini, 1999). The ratio of inosine:thymidine uptake was enhanced by additional mutation of rCNT1 Gln³¹⁹ (the rat equivalent of hCNT1 Gln³²⁰), but resulted in a combination rCNT1 mutant (Ser318Gly/Gln319Met) with low overall transport activity (Wang and Giacomini, 1999). Compared to rCNT1Ser318Gly, rCNT1

Ser318Gly/Gln319Met exhibited a decreased apparent K_m for inosine influx and an increased K_m for thymidine (Wang and Giacomini, 1999).

To test whether the hCNT1 mutant M2/3 was truly a broad specificity transporter, oocytes producing the recombinant protein were assayed using the full panel of purine and pyrimidine nucleosides. As shown in Fig. 2-3, all nucleosides were transported. As well, the Na^+ -dependence of uridine uptake was maintained. Identification of M2 (Ser319Gly) in the phenotype change between *cit* and *cib* is consistent with the sequence comparisons in Fig. 2-4 between h/rCNT1, h/rCNT2 and hCNT. The latter protein exhibits a very similar transport profile to mutant M2/3 when produced in oocytes, and also has a glycine residue at this position (Fig. 2-4).

Characterization of TM 8 and TM 9 Mutants of hCNT1 – Mutations in TM 7 did not modify uptake of thymidine (Table 2-2). Substitutions in TM 8 or 9 (Table 2-1) were therefore predicted to result in changes in pyrimidine nucleoside selectivity. Simultaneous mutation of the five candidate residues in TM 8 of hCNT1 into the corresponding residues in hCNT2 (mutant M4/5/6/7/8) led to a substantial decrease in thymidine transport, while leaving uridine uptake unaffected. A reduction in thymidine uptake has also been reported for introduction of TM 8 of rCNT2 into rCNT1, but was associated with very low uridine transport activity (Wang and Giacomini, 1997). As shown in Fig. 2-3, the loss of thymidine transportability extended also to cytidine, creating a recombinant protein with a unique uridine-selective transport profile. Interestingly, the M4/5/6/7/8 combination mutant exhibited a modest increase in inosine transport (Fig. 2-3 & Table 2-2), suggesting that TM 7 is not exclusively responsible for purine nucleoside selectivity. Mutation of hCNT1 Ala³⁷⁰, the only candidate residue in TM 9 (Fig. 2-4 & Table 2-1), did not alter uridine, inosine or thymidine transport, either alone (mutant M9) or in combination with M2/3 (mutant M2/3/9) (Table 2-2) and was not investigated further. TM9 residues are also potentially excluded by chimeric studies between rCNT1 and rCNT2, where incorporation of TMs 7-8 of rCNT2 into rCNT1 was sufficient to change the transporter from *cit* to *cif* (Wang and Giacomini, 1997). Unlike hCNT1 C1121 (Fig. 2-2), the rat chimera was only partly Na^+ -dependent (Wang and Giacomini, 1997).

Two strategies were employed to identify individual residues or combinations of residues in TM 8 that might contribute to the specificity profile of mutant M4/5/6/7/8. First, two double mutants were constructed. One (M6/8) was suggested by the sequence alignment between h/CNT1, h/rCNT2 and hCNT in Fig. 2-4 which identified only two residues in TM8 (Ser³⁵³ and Tyr³⁵⁸) that were common to h/CNT1 and hCNT, but different in h/rCNT2 (and might therefore be involved in loss of thymidine/cytidine transportability). The other (M6/7) was suggested by the two adjacent residues (Ser³⁵³ and Leu³⁵⁴) in TM 8 that were different between h/rCNT1 and h/rCNT2 (Fig. 2-4). Like Ser³¹⁹ and Gln³²⁰ in TM 7, one of the residues was conserved between h/rCNT1 and hCNT, and the other between hCNT and h/rCNT2. Second, each of the five candidate residues was mutated individually to generate mutants M4-9.

As shown in Table 2-2, both of the double mutants (M6/7 and M6/8) exhibited thymidine uptake comparable to M4/5/6/7/8. Of the single residue substitutions, only M6 (Ser353Thr) exhibited reduced thymidine uptake, and the measured flux was comparable to that of M6/7, M6/8 and M4/5/6/7/8. Uridine uptake by mutants M6/7, M6/8 and M6 was consistently lower than either M4/5/6/7/8 or hCNT1 in repeated experiments, but substantially higher than reported for the TM8 chimera of rCNT1/2 (Wang and Giacomini, 1997).

Combination Mutants between TM 7 and 8 – We next combined mutations M2/3 and M6 to generate the composite TM7/8 mutant M2/3/6. This recombinant protein, when screened for uridine, inosine and thymidine transport (Table 2-2), exhibited properties similar to chimera C1121 (uridine, inosine >> thymidine). However, when assayed with the full panel of physiological nucleosides, it was discovered that mutant M2/3/6 exhibited relatively low transport of adenosine compared to mutant M2/3, chimera C1121 and hCNT2 (Fig. 2-3). We therefore tested the combination mutants M2/3/6/7 and M2/3/6/8 (Table 2-2 & Fig. 2-3). Whereas mutant M2/3/6/8 was indistinguishable from M2/3/6, mutant M2/3/6/7 showed a marked increase in adenosine transport, while maintaining the other *cif*-like characteristics of mutant M2/3/6. Uridine uptake by mutants M2/3/6/7 and M2/3/6 was confirmed to be Na⁺-dependent and was similar in magnitude to that of wild-type hCNT1 and hCNT2.

Kinetic Properties of M2/3/6/7, M2/3/6 and M6 – Fig. 2-5 shows representative concentration dependence curves for initial rates of transport (3-min flux) of uridine, thymidine, inosine and adenosine by the combination mutants M2/3/6/7 and M2/3/6. Calculated kinetic parameters (apparent K_m and V_{max}) from these influx data are presented in Table 2-3. M2/3/6/7-mediated transport of uridine was saturable and conformed to Michaelis-Menten kinetics with an apparent K_m value (29 μM) in the range reported previously for hCNT1, rCNT1 and hCNT2 (37-45 μM) (Huang *et al.*, 1994; Ritzel *et al.*, 1997, 1998). Inosine and adenosine influx were both CNT2-like, with V_{max} values similar to uridine and apparent K_m values of 20 and 18 μM , respectively (*cf* 15 μM for inosine transport by rCNT2 and 8 μM for adenosine transport by hCNT2) (Ritzel *et al.*, 1998, Wang and Giacomini, 1997). In contrast, h/rCNT1 also mediate high-affinity transport of adenosine, but with a very much reduced V_{max} relative to uridine (resulting from a low rate of conversion of the CNT1/adenosine complex from outward-facing to inward-facing conformations) (Yao *et al.*, 1996a). Mutant M2/3/6/7 retained some thymidine transport activity (see also Table 2-2), but both the apparent affinity and maximum velocity were reduced relative to those of the other three permeants. The ratio $V_{max}:K_m$ was 0.3 for thymidine compared to 7.5, 6.5 and 11.3 for adenosine, uridine and inosine, respectively, a difference of \sim 20-fold (Table 2-3). Human and rat CNT1 transport thymidine and uridine to similar extents (Huang *et al.*, 1994; Ritzel *et al.*, 1997), with a reported apparent K_m of 5 μM for rCNT1 (*cf* 170 μM for M2/3/6/7 in Table 2-3), while wild-type rCNT2 has been reported to mediate low fluxes of thymidine (Che *et al.*, 1995). Therefore, mutant M2/3/6/7 showed hCNT2 (*cif*)-type transport characteristics for all four permeants.

Mutant M2/3/6 exhibited very similar kinetics to M2/3/6/7, except for a reduced V_{max} of adenosine influx. In agreement with the 20 μM adenosine uptake data shown in Fig. 2-3, $V_{max}:K_m$ ratios for M2/3/6/7 and M2/3/6 were, respectively, 7.5 and 2.5, a difference of 3.1-fold. In contrast, corresponding ratios for uridine transport by the two mutants were similar (6.5 and 7.9, respectively). Thus, the M7 mutation increased the maximum velocity of adenosine transport while having no effect on adenosine apparent affinity or the kinetics of other permeants.

Mutant M6 was characterized using a 10-min flux because of its relatively low transport activity and, consistent with the results presented in Table 2-2, exhibited a reduced $V_{\max}:K_m$ ratio for thymidine (0.8) relative to uridine (2.8). The apparent K_m for thymidine influx was 48 μM , compared with 160 μM for mutant M2/3/6 and 167 μM for mutant M2/3/6/7, suggesting an interaction of mutations in the two TMs.

Molecular Modeling – Examination of the aligned sequences of putative TMs 7, 8 and 9 in the CNT family of transporters revealed the presence of a number of positions where residue variability was very restricted. Conservation of these characteristic residues suggests that they are involved either in maintaining the structure of the transporters or in the binding of nucleoside substrates, these being features of the family members that are held in common. They are thus likely either to face the putative substrate translocation channel or another helix. The positions of the conserved residues are fairly symmetrically distributed around the circumference of TMs 7, 8 and 9, although TM 8 shows a slightly more asymmetric distribution (Fig. 2-6A). The distributions of positions that can accommodate polar residues in one or more of the transporters, or at which no polar residue is found, are likewise fairly symmetrical for TM 9. In contrast, TMs 7 and 8 exhibit a more amphipathic character, with predominantly polar residues clustered on one face of the helix and predominantly hydrophobic residues clustered on the other. These distributions of conserved residues, and the existence of conserved residues in the apolar faces of the TMs, suggest that all three TMs are largely sequestered from contact with membrane lipids, presumably by interactions with other transmembrane segments of the protein. The nature of these TMs can be contrasted with, for example, TM 4 which has a much more asymmetric distribution of both conserved and polar residues, and which is likely to occupy a position in the transporter structure that is much more exposed to the membrane lipids (Fig. 2-6A).

Because the loops connecting putative TMs 7, 8 and 9 in the transporter are predicted to be very short (5 and 13 residues), it is likely that these three putative helices are adjacent in the tertiary structure of the protein. The pattern of conserved polar residues within the helices, together with the results of site-directed mutagenesis, allow a model to be proposed for their arrangement in the transporter structure, which is shown in Fig. 2-6B. Although tentative, this model aids interpretation of the experimental results and more importantly may be used to

make predictions that can be tested by future site-directed mutagenesis experiments. Hydrophilic portions of the surfaces of TMs 7, 8 and 9 are proposed to contribute to the substrate translocation-channel or binding site. In the case of TM 7, this surface would include the highly conserved residues Glu³⁰⁸, Asn³¹⁵ and Glu³²², (present in 100%, 61% and 94% of the CNT family members, respectively), one or more of which might form hydrogen bonds with the nucleoside substrate. Ser³¹⁹, located close to Glu³⁰⁸ on this surface, would likewise be located in the substrate translocation channel. However, the fact that changing this residue in mutant M2 to glycine (which is found at this position in 78% of the other family members) allows hCNT1 to transport inosine, suggests that it sterically hinders transport of the purine nucleoside in the wild-type molecule rather than contributing to substrate binding. Similarly Ser³¹¹, mutation of which to alanine in mutant M1 had no effect on transport activity, is located near the hydrophobic surface of TM 7 and presumably plays no part in substrate binding. Potentiation of the effect of the M2 mutation by simultaneous mutation of Gln³²⁰ to methionine (mutant M2/3) may reflect an alteration of helix packing resulting from the predicted location of this residue at the interface with an adjacent helix, suggested to be TM 8 in the model shown in Fig. 2-6B.

A similar alteration of helix packing may account for the effect of mutating Leu³⁵⁴ in TM 8 to valine on the ability of the combination mutant M2/3/6 to transport adenosine. The lack of effect of mutating Val³⁴¹ to Ala, and of Tyr³⁴⁷ or Tyr³⁵⁸ to phenylalanine (mutants M4 and M8, respectively), probably reflects the location of these residues on the surface of TM 8 distant from the substrate channel and other channel-forming helices. In contrast, Ser³⁵³ is predicted to lie on the surface of TM 8 that faces the translocation channel. The reduction in thymidine uptake activity produced by mutation of this residue in hCNT1 to threonine (M6 mutation) suggests that it might be directly involved in substrate recognition via hydrogen bonding, a suggestion strengthened by the observation that this position is occupied by either a serine or a threonine residue in all members of the CNT family except for the putative transporter of *Helicobacter pylori*, where a proline residue is found.

Mutation of Ala³⁷⁰ in TM 9 to serine (M9 mutation) was without effect on the transport activity of hCNT1, and so it is not possible to conclude whether or not this helix contributes to the substrate translocation channel. However, it does bear a number of highly-conserved

hydrophilic residues that might contribute to solute recognition, in particular at position 372 which is occupied by a serine residue in 83% of the CNT family members. Because of the conservation of these residues, and the fact that TM 9 is likely to be adjacent to TM 8 in the transporter tertiary structure, it has therefore been included as a channel lining helix in the model shown in Fig. 2-6B, oriented such that Ser³⁷² faces the channel and Ala³⁷⁰ is located on the helix surface at greatest distance from the channel. This proposed involvement of TM 9 in the translocation channel should be readily testable by site-directed mutation of Ser³⁷² and the adjacent residue Ser³⁸³.

Conclusions – hCNT1 and hCNT2 have *cit* and *cif* transport activity for pyrimidine and purine nucleosides, respectively. We have identified four residues (Ser³¹⁹, Gln³²⁰, Ser³⁵³, and Leu³⁵⁴) in the TM 7-9 region of hCNT1 that, when mutated together to the corresponding residues in hCNT2, converted hCNT1 (*cit*) into a transporter with *cif* functional characteristics. An intermediate broad specificity *cib*-like transport activity was produced by mutation of the two TM 7 residues alone: mutation of Ser³¹⁹ to Gly allowed for transport purine nucleosides and this was augmented by mutation of Gln³²⁰ to Met. Mutation of Ser³⁵³ in TM 8 to Thr converted the *cib*-like transport of the TM 7 double mutant into one with *cif*-like characteristics, but with relatively low adenosine transport activity. Mutation of Leu³⁵⁴ to Val increased the adenosine transport capability of the TM 7/8 triple mutant, producing a full *cif* transport phenotype. On its own, mutation of Ser³⁵³ converted hCNT1 into a transporter with novel uridine-selective transport properties.

A *cib*-type transport activity has been described in human colon and myeloid cell lines (Belt *et al.*, 1993; Lee *et al.*, 1992), in rabbit choroid plexus (Wu *et al.*, 1992) and in *Xenopus* oocytes injected with rat jejunal mRNA (Huang *et al.*, 1993). A candidate *cib*-type transporter SNST1 that is related to the Na⁺-dependent glucose transporter SGLT1 was identified in 1992 in rabbit kidney (Pajor and Wright, 1992). There is no sequence similarity between SNST1 and either the CNT or ENT protein families. Although recombinant SNST1, when produced in oocytes, stimulates low levels of Na⁺-dependent uptake of uridine that is inhibited by pyrimidine and purine nucleosides (*i.e.* *cib*-type pattern), its function remains unclear because (i) the rate of uridine transport in oocytes is only two-fold above endogenous (background) levels, whereas a > 500-fold stimulation is observed with h/rCNT1 (Huang *et al.*, 1994; Ritzel *et al.*,

1997), and (ii) *cib*-type transport activity has not been observed in the tissues (kidney, heart) in which SNST1 message was reported (Conant and Jarvis, 1994; Griffith and Jarvis, 1996). From the experiments reported here and our cDNA cloning of a broad specificity CNT for hagfish (hfCNT), it is likely that mammalian *cib* is a member of the CNT protein family.

Information from the aligned sequences of TMs 7-9 in CNT family members produced a model for their possible arrangement in the transporter structure, in which Ser³¹⁹ lies within the substrate translocation channel and sterically hinders purine nucleoside transport in wild-type hCNT1. Mutation of the other residue in TM 7, Gln³²⁰, which is predicted to interface with an adjacent helix, may potentiate purine nucleoside transportability through an alteration in helix packing. Altered helix packing may also account for the augmentation of adenosine transport caused by mutation of Leu³⁵⁴, since this residue is also predicted to be located on a surface of TM 8 distant from the substrate channel. In contrast, the other TM 8 residue Ser³⁵³ is predicted to face the translocation channel and may directly participate in substrate recognition via hydrogen bonding.

Table 2-1 – Nomenclature of hCNT1 Amino Acid Mutations

Designation	hCNT1 Mutation	Region
M1	Ser311Ala	TM 7
M2	Ser319Gly	TM 7
M3	Gln320Met	TM 7
M4	Val341Ala	TM 8
M5	Tyr347Phe	TM 8
M6	Ser353Thr	TM 8
M7	Leu354Val	TM 8
M8	Tyr358Phe	TM 8
M9	Ala370Ser	TM 9

Table 2-2 – Mediated Uptake of [¹⁴C]-labeled Nucleosides by hCNT1 and hCNT1 Mutants

Transporter		Nucleoside Uptake (pmol/oocyte.30 min ⁻¹) ^a		
		Uridine	Thymidine	Inosine
Wild-type	hCNT1	20.9 ± 3.6	16.3 ± 3.3	0.09 ± 0.06
	hCNT2	20.9 ± 2.6	0.04 ± 0.02	15.8 ± 1.3
TM 7	M-1/2/3	31.7 ± 5.3	25.7 ± 3.1	21.4 ± 4.1
	M-1	28.4 ± 3.6	26.9 ± 2.5	0.09 ± 0.04
	M-2	28.2 ± 3.3	23.6 ± 2.0	8.91 ± 1.50
	M-3	28.8 ± 4.0	22.5 ± 2.0	0.21 ± 0.05
	M-1/2	27.3 ± 3.2	26.9 ± 2.1	7.27 ± 1.38
	M-2/3	29.3 ± 2.7	18.5 ± 2.3	19.3 ± 1.5
	M-1/3	20.2 ± 2.1	26.9 ± 2.5	0.96 ± 0.11
TM 8	M-4/5/6/7/8	19.7 ± 2.2	2.54 ± 0.14	3.20 ± 0.28
	M-6/7	7.58 ± 0.45	2.33 ± 0.31	0.34 ± 0.04
	M-6/8	8.24 ± 0.80	2.86 ± 0.47	0.29 ± 0.02
	M-4	22.6 ± 3.1	17.5 ± 2.2	0.11 ± 0.04
	M-5	30.9 ± 4.9	17.8 ± 3.0	0.08 ± 0.05
	M-6	12.2 ± 2.2	3.47 ± 0.65	0.16 ± 0.04
	M-7	26.6 ± 3.3	14.8 ± 1.7	0.07 ± 0.03
	M-8	24.0 ± 2.8	18.0 ± 2.0	0.08 ± 0.05
TM 9	M-9	32.1 ± 5.1	22.2 ± 4.1	0.10 ± 0.04
TM 7/ TM 8	M-2/3/6	27.8 ± 2.1	1.18 ± 0.34	20.5 ± 2.6
	M-2/3/8	29.7 ± 3.1	19.5 ± 1.8	18.5 ± 2.0
	M-2/3/6/7	21.6 ± 3.1	1.46 ± 0.19	19.5 ± 2.7
	M-2/3/6/8	23.9 ± 3.6	1.88 ± 0.38	15.2 ± 3.5
TM 7/ TM 9	M-2/3/9	28.2 ± 2.1	22.0 ± 2.6	17.0 ± 1.8

^a, 20 μM nucleoside flux, 20°C.

Table 2-3 – Kinetic Properties of hCNT1 Mutants M2/3/6/7, M2/3/6, and M6

Transporter	Substrate	Apparent K_m^a	V_{max}^{ab}	$V_{max}:K_m$ ($\times 10^2$) ^b
		μM	$pmol/oocyte.min^{-1}$	
M2/3/6/7	Adenosine	18 \pm 1	1.3 \pm 0.01	7.51
	Uridine	29 \pm 1	1.9 \pm 0.01	6.48
	Inosine	20 \pm 1	2.3 \pm 0.1	11.3
	Thymidine	167 \pm 4	0.6 \pm 0.04	0.33
M2/3/6	Adenosine	16 \pm 2	0.4 \pm 0.01	2.48
	Uridine	33 \pm 3	2.6 \pm 0.2	7.93
	Inosine	34 \pm 4	1.9 \pm 0.1	5.67
	Thymidine	160 \pm 2	0.6 \pm 0.09	0.38
M6	Uridine	23 \pm 3	0.6 \pm 0.01	2.82
	Thymidine	48 \pm 6	0.4 \pm 0.01	0.75
M6/7	Uridine	16 \pm 1	1.0 \pm 0.02	6.06
M2	Adenosine	17 \pm 2	1.9 \pm 0.1	11.2
	Uridine	45 \pm 2	7.0 \pm 0.1	15.7
	Inosine	64 \pm 6	1.9 \pm 0.1	3.05
	Thymidine	44 \pm 4	5.6 \pm 0.2	12.7
M2/3	Adenosine	20 \pm 1	1.5 \pm 0.03	7.42
	Uridine	41 \pm 4	5.2 \pm 0.1	12.7
	Inosine	36 \pm 3	4.5 \pm 0.1	12.7
	Thymidine	89 \pm 5	6.4 \pm 0.1	7.15

^a, from Fig. 2-5; ^b, calculated per min.

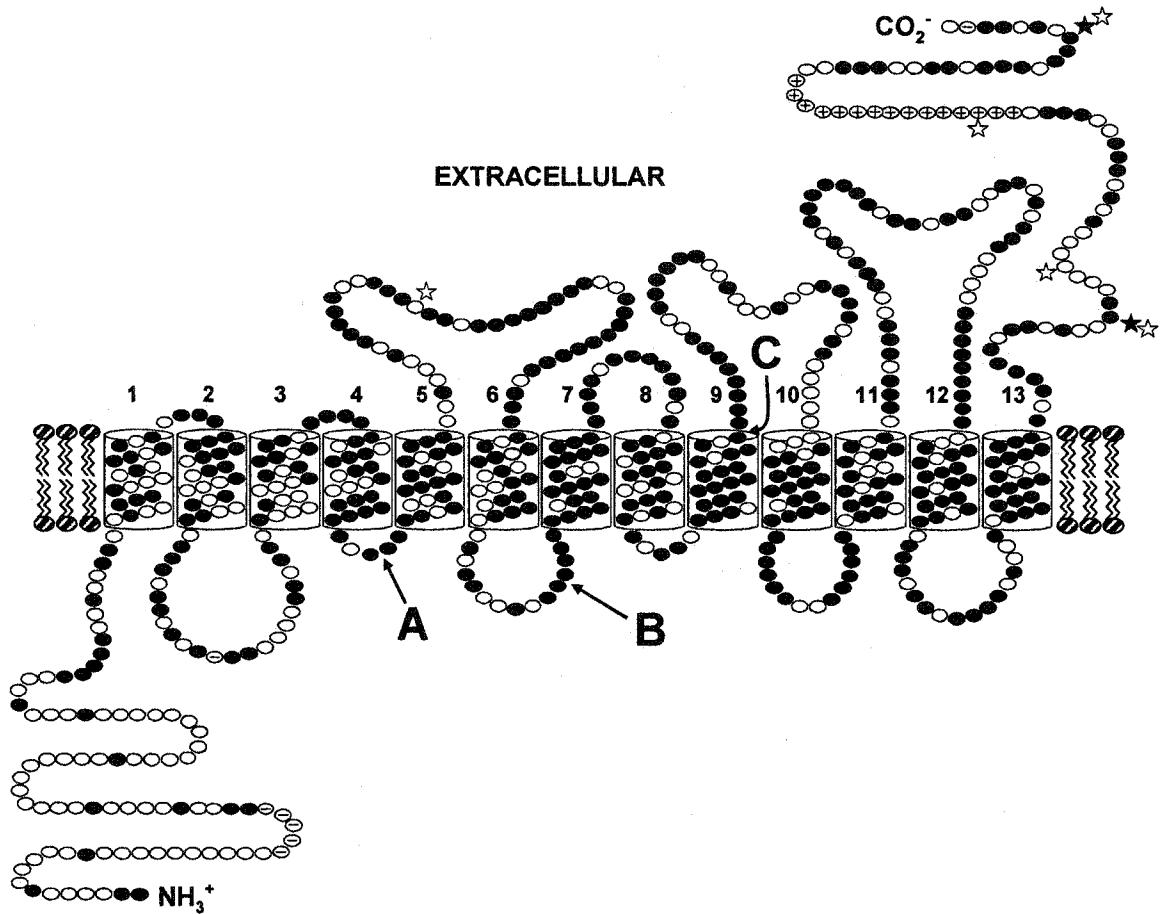


Figure 2-1. Topographical model of hCNT1 and hCNT2. Potential membrane-spanning α -helices (Hamilton *et al.*, 2001) are *numbered*, and putative glycosylation sites in hCNT1 and hCNT2 are indicated by *solid* and *open stars*, respectively. Residues identical in the two proteins are shown as *solid circles*. Residues corresponding to insertions in the sequence of hCNT1 or hCNT2 are indicated by circles containing “+” and “-” signs, respectively. *Arrows A, B, and C* represent splice sites used for the construction of chimeras.

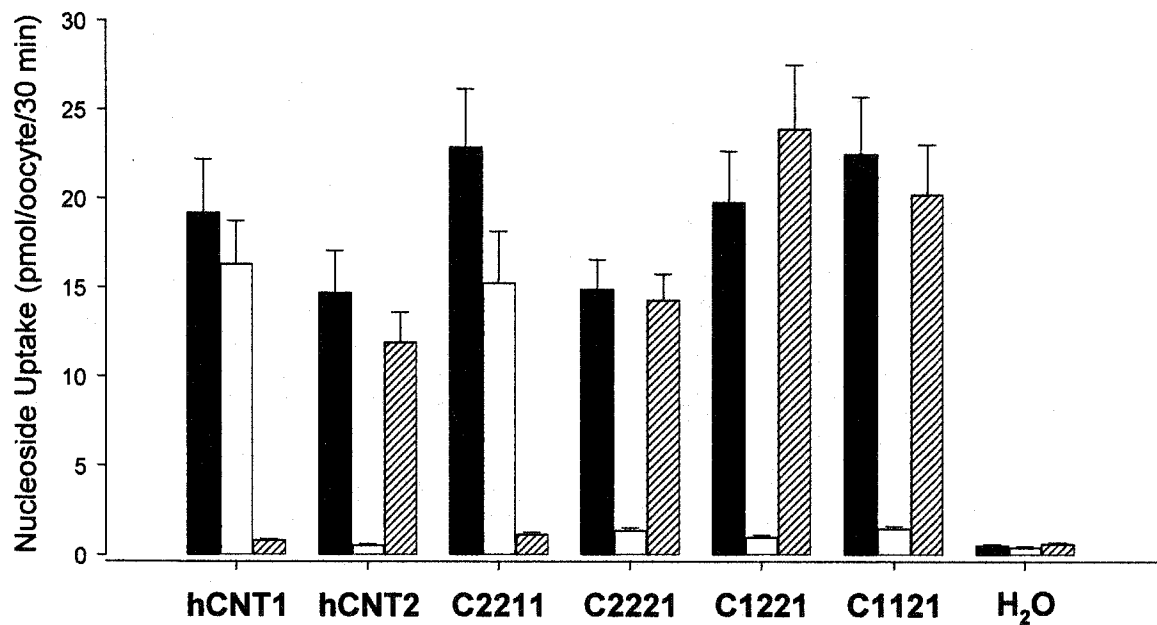


Figure 2-2. Uptake of ¹⁴C-labeled nucleosides by recombinant hCNT1, hCNT2, and chimeras C1122, C1112, C1221, and C1121 expressed in *Xenopus* oocytes. Uptake of uridine (*solid bars*), thymidine (*open bars*), and inosine (*hatched bars*) (20 μM, 20°C, 30 min) in oocytes injected with RNA transcript or water alone was measured in transport buffer containing NaCl.

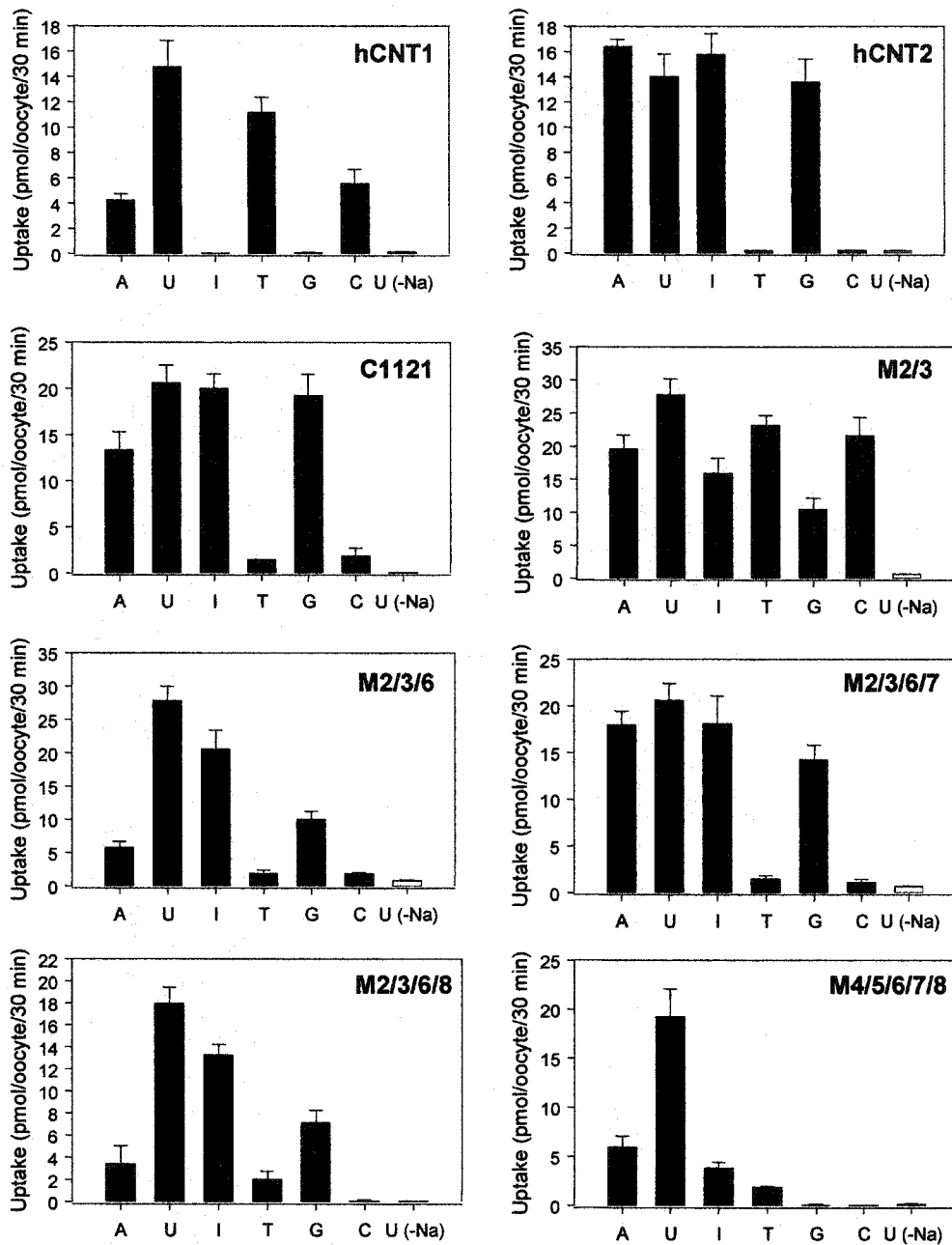


Figure 2-3. Nucleoside specificity of hCNT1, hCNT2, chimera C1121, and mutants M2/3, M2/3/6, M2/3/6/7, M2/3/6/8, and M4/5/6/7/8. Transporter-mediated nucleoside uptake (A, adenosine; U, uridine, I, inosine; T, thymidine, G, guanosine; C, cytidine) (20 μ M, 20°C, 30 min) was measured in transport buffer containing 100 mM NaCl (*black bars*) or 100 mM choline chloride (*open bars*). Mediated transport was calculated as uptake in RNA-injected oocytes minus uptake in oocytes injected with water alone.

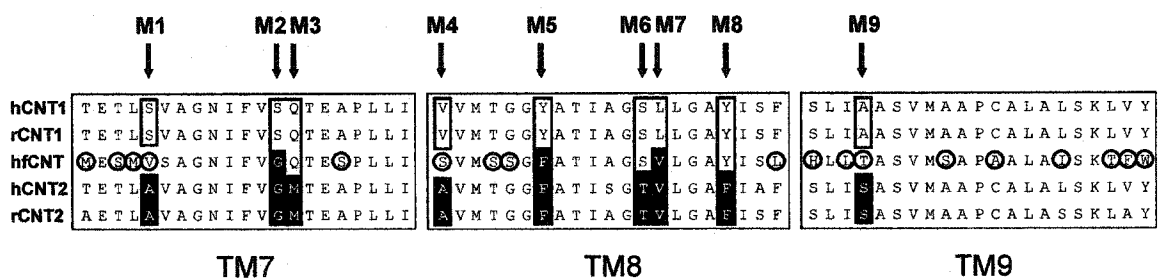


Figure 2-4. Alignment of predicted amino acid sequences of h/rCNT1, h/rCNT2, and hfCNT in TMs 7, 8, and 9. Positions of conserved residues that differ between hCNT1/rCNT1 (Huang *et al.*, 1994; Ritzel *et al.*, 1997) and hCNT2/rCNT2 (Wang *et al.*, 1997; Ritzel *et al.*, 1998) and selected for mutation in hCNT1 are indicated by *arrows* (M1-M9). At each of these positions, amino acids in h/rCNT1 and h/rCNT2 in common with hfCNT3 are shown as *open boxes* and *solid boxes*, respectively. *Circles* indicate amino acids in hfCNT that differ from conserved residues in either h/rCNT1 or h/rCNT2.

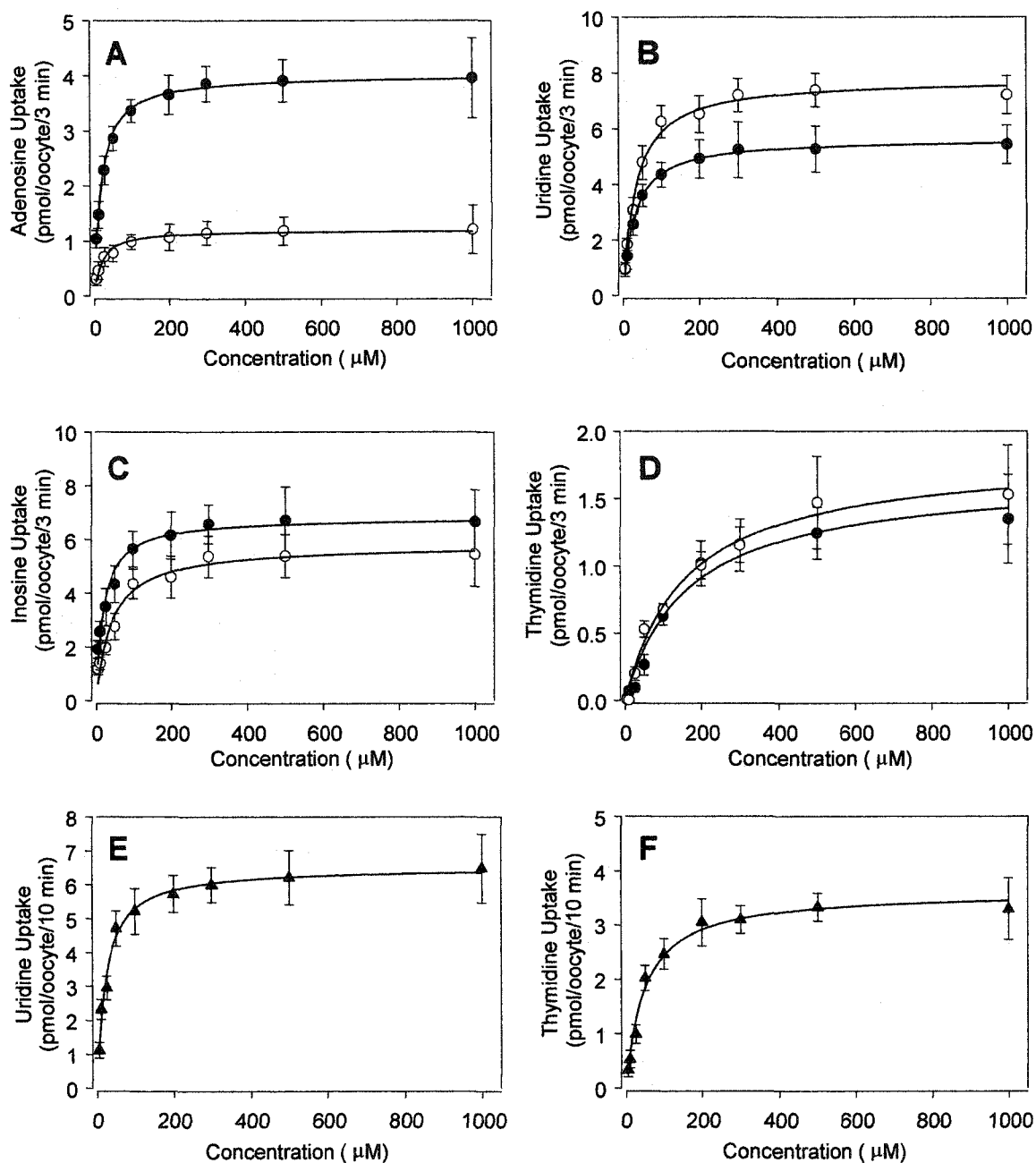
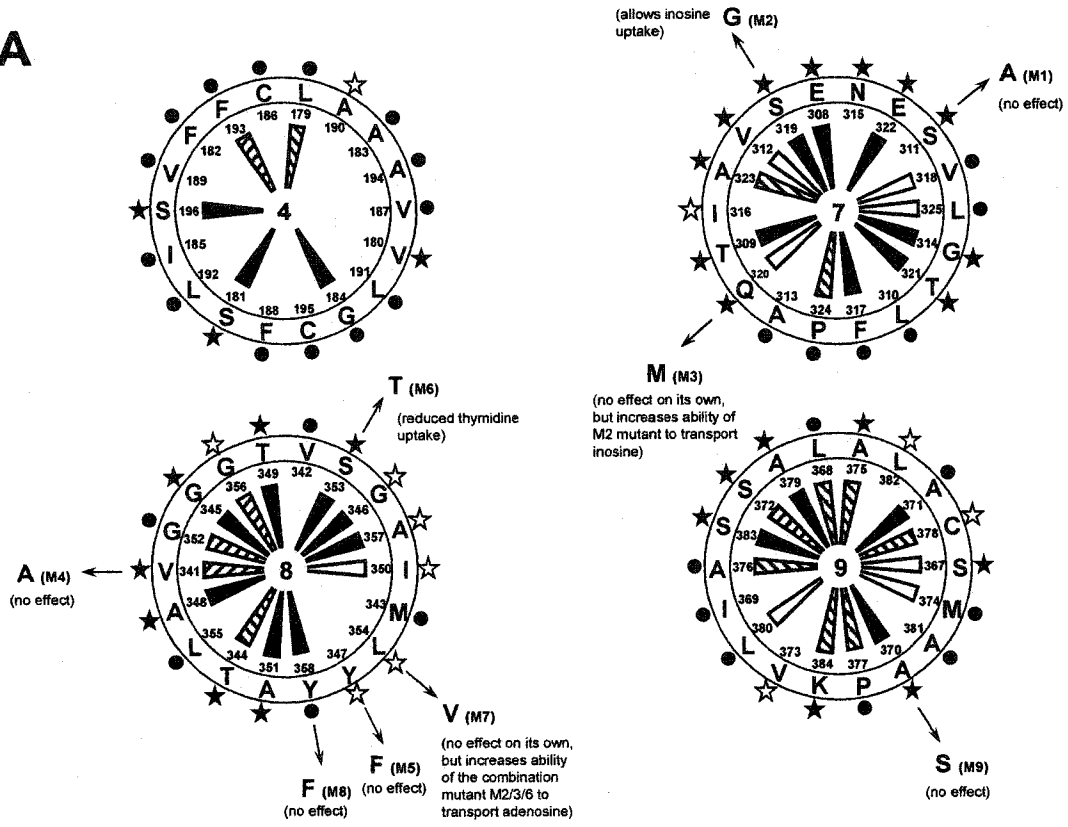
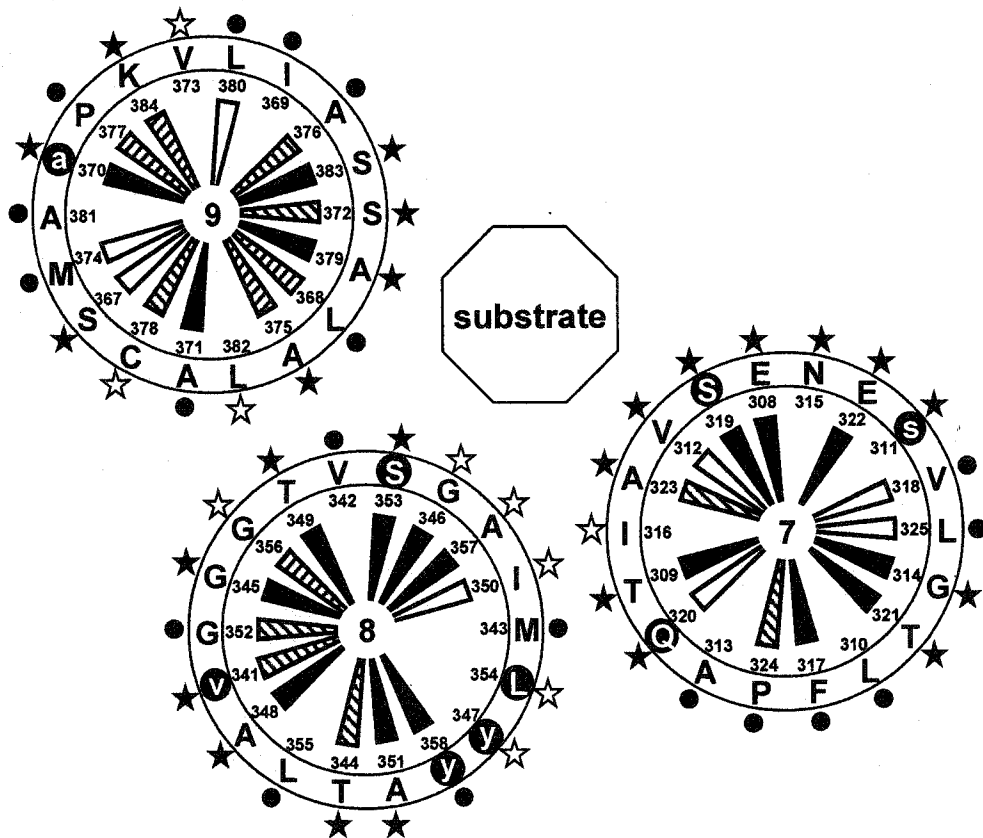


Figure 2-5. Kinetic properties of hCNT1 mutants M2/3/6/7, M2/3/6, and M6. Initial rates of transporter-mediated nucleoside uptake were measured in NaCl transport buffer at 20°C (3 min flux for M2/3/6/7 and M2/3/6, 10 min flux for M6). Mediated transport was calculated as the difference in uptake between RNA-injected oocytes and control oocytes injected with water alone. All of the fluxes were performed on the same batch of oocytes. A - D, M2/3/6/7 (solid circles) and M2/3/6 (open circles); E and F, M6 (triangles). Kinetic parameters calculated from these curves are presented in Table 2-3.

Figure 2-6. Structural features of TMs in the CNT family and the proposed arrangement of TMs 7, 8 and 9 in hCNT1. *A*, Helical wheel plots for TMs 4, 7, 8 and 9 of the CNT family of nucleoside transporters, viewed from the extracellular side of the membrane, indicating the degree of residue conservation and the locations of positions accommodating polar residues or where only non-polar residues are found. The residue identities and sequence positions shown are those of hCNT1. The distribution of residue types is indicated by *symbols* on the periphery of the plots: (●) a position that is always occupied by a non-polar residue, (☆) a position occupied by a polar residue in < 15% of the sequences and (★) a position occupied by a polar residue in > 15% of the aligned sequences. The extent of residue variability at each position is indicated by the nature of the central spokes: *solid spokes* indicate the presence of the same residue or members of a closely-related group of residue types (E/Q/D/N; R/K; Y/F/W; A/G/C/S/T/P) in ≥ 85% of the aligned sequences; *hatched spokes* indicate the same type of residue conservation in 75 - 85 % of the sequences; *open spokes* indicate the same type of residue conservation in 65 - 75 % of the sequences, or the presence of members of a less closely-related pair of residue types (*e.g.* Ile and Leu) in ≥ 85% of the sequences. The nature and effects of mutations M1 to M8 are also indicated. *B*, Putative arrangement of TMs 7, 8 and 9 in hCNT1 surrounding a substrate translocation pathway. The symbols used are the same as those in *A*. Residues mutated in the present study are indicated in *white letters on a black background*: those that affected the transport activity of the protein are in *capital letters*, those which were without effect are shown in *lower case*.

A**B**

Bibliography

- Baldwin, JM** (1993) The probable arrangement of the helices in G protein-coupled receptors. *EMBO J* 12: 1693-1703.
- Baldwin SA, Mackey JR, Cass CE, and Young JD** (1999) Nucleoside transporters: molecular biology and implications for therapeutic development. *Mol Med Today* 5: 216-224.
- Belt JA, Marina NM, Phelps DA, and Crawford CR** (1993) Nucleoside transport in normal and neoplastic cells. *Adv Enzyme Regul* 33: 235-252.
- Cass CE, Young JD, Baldwin SA, Cabrita MA, Graham KA, Griffiths M, Jennings LL, Mackey JR, Ng AML, Ritzel MWL, Vickers MF, and Yao SYM** (1999) Nucleoside transporters of mammalian cells. *Pharm Biotechnol* 12: 313-352.
- Che M, Ortiz DF, and Arias IM** (1995) Primary structure and functional expression of a cDNA encoding the bile canalicular, purine-specific Na⁺-nucleoside cotransporters. *J Biol Chem* 270: 13596-13599.
- Conant AR and Jarvis SM** (1994) Nucleoside influx and efflux in guinea-pig ventricular myocytes. Inhibition by analogues of lidoflazine. *Biochem Pharmacol* 48: 873-880.
- Craig JE, Zhang Y, and Gallagher MP** (1994) Cloning of the *nupC* gene of *Escherichia coli* encoding a nucleoside transport system, and identification of an adjacent insertion element, IS 186. *Mol Microbiol* 11: 1159-1168.
- Crawford CR, Patel DH, Naeve C, and Belt JA** (1998) Cloning of a human equilibrative, nitrobenzylmercaptapurine riboside (NBMPR)-insensitive nucleoside transporter *ei* by functional expression in a transport-deficient cell line. *J Biol Chem* 273: 5288-5293.
- Fredholm BB** (1997) Adenosine and neuroprotection. *Int Rev Neurobiol* 40 :259-80.
- Griffith DA and Jarvis SM** (1996) Nucleoside and nucleobase transport systems of mammalian cells. *Biochim Biophys Acta Rev Biombr* 1286: 153-181.
- Griffiths M, Beaumont N, Yao SYM, Sundaram, M, Bouman CE, Davies A, Kwong FYP, Coe IR, Cass CE, Young JD, and Baldwin SA** (1997a) Cloning of a human nucleoside transporter implicated in the cellular uptake of adenosine and chemotherapeutic drugs. *Nat Med* 3: 89-93.
- Griffiths M, Yao SYM, Abidi F, Phillips SEV, Cass CE, Young JD, and Baldwin SA** (1997b) Molecular cloning and characterization of a nitrobenzylthioinosine-insensitive (*ei*) equilibrative nucleoside transporter from human placenta. *Biochem J* 328: 739-743.
- Groothuis DR and Levy RM** (1997) The entry of antiviral and antiretroviral drugs into the central nervous system. *J Neurovirol* 3: 387-400.

- Hamilton SR, Yao SYM, Gallagher MP, Henderson PJF, Cass CE, Young JD, and Baldwin SA** (2001) Subcellular distribution and membrane topology of the mammalian concentrative Na⁺-nucleoside cotransporters rCNT1. *J Biol Chem* 276: 27981-27988.
- Handschumacher RE and Cheng CY** (1993) In *Cancer Metabolism* (E Holland, E Frei, RC Bast, DW Kufe, DL Morton and RR Weichselbaum, eds.) pp. 712-732, Lea & Febiger, Philadelphia.
- Ho SN, Hunt HD, Horton RM, Pullen JK, and Pease LR** (1989) Site-directed mutagenesis by overlap extension using the polymerase chain reaction. *Gene (Amst)* 77: 51-59.
- Horton RM, Hunt HD, Ho SN, Pullen JK, and Pease LR** (1989) Engineering hybrid genes without the use of restriction enzymes: gene splicing by overlap extension. *Gene (Amst)* 77: 61-68.
- Huang QQ, Harvey CM, Paterson ARP, Cass CE, and Young JD** (1993) Functional expression of Na⁺-dependent nucleoside transport systems of rat intestine in isolated oocytes of *Xenopus laevis*. Demonstration that rat jejunum expresses the purine-selective system N1 (*cif*) and a second, novel system N3 having broad specificity for purine and pyrimidine nucleosides. *J Biol Chem* 268: 20613-20619.
- Huang QQ, Yao SYM, Ritzel MWL, Paterson ARP, Cass CE, and Young JD** (1994) Cloning and functional expression of a complementary DNA encoding a mammalian nucleoside transport protein. *J Biol Chem* 269: 17757-17760.
- Lee CW, Sokoloski JA, Sartorelli AC, and Handschumacher RE** (1991) Induction of the differentiation of HL-60 cells by phorbol 12-myristate 13-acetate activates a Na⁺-dependent uridine-transport system. Involvement of protein kinase C. *Biochem J* 274: 85-90.
- Mackey JR, Baldwin SA, Young JD, and Cass CE** (1998a) Nucleoside transport and its significance for anticancer drug resistance. *Drug Resistance Updates* 1: 310-324.
- Mackey JR, Mani RS, Selner M, Molwes D, Young JD, Belt JA, Crawford CR, and Cass CE** (1998b) Functional nucleoside transporters are required for gemcitabine influx and manifestation of toxicity in cancer cell lines. *Cancer Res* 58: 4349-4357.
- Mackey JR, Yao SYM, Smith KM, Karpinski E, Baldwin SA, Cass CE, and Young JD** (1999) Gemcitabine transport in *Xenopus* oocytes expressing recombinant plasma membrane mammalian nucleoside transporters. *J Natl. Cancer Inst USA* 91: 1876-81.
- Pajor AM and Wright EM** (1992) Cloning and functional expression of a mammalian Na⁺-nucleoside cotransporters. A member of the SGLT family. *J Biol Chem* 267: 3557-3560.
- Ritzel MWL, Yao SYM, Huang MY, Elliot JF, Cass CE, and Young JD** (1997) Molecular cloning and functional expression of cDNAs encoding a human Na⁺-nucleoside cotransporters (hCNT1). *Am J Physiol* 272: C707-C714.
- Ritzel MWL, Yao SYM, Ng AML, Mackey JR, Cass CE, and Young JD** (1998) Molecular cloning, functional expression and chromosomal localization of a cDNA encoding a human Na⁺ nucleoside cotransporters (hCNT2) selective for purine nucleosides and uridine. *Mol Membr Biol* 15: 203-211.

- Shryock JC and Belardinelli L** (1997) Adenosine and adenosine receptors in the cardiovascular system: biochemistry, physiology and pharmacology. *Am J Cardiol* 79: 2-10.
- Wang J, Su SF, Dresser MJ, Schaner ME, Washington CB, and Giacomini KM** (1997) Na⁺-dependent purine nucleoside transporter from human kidney: cloning and functional characterization. *Am J Physiol* 273: F1058-F1065.
- Wang J and Giacomini KM** (1997) Molecular determinants of substrate selectivity in Na⁺-dependent nucleoside transporters. *J Biol Chem* 272: 28845-28848.
- Wang J and Giacomini KM** (1999) Serine 318 is essential for the pyrimidine selectivity of the N2 Na⁺-nucleoside transporter. *J Biol Chem* 274: 2298-2302.
- Wu X, Yuan G, Brett CM, Hui AC, and Giacomini, KM** (1992) Sodium-dependent nucleoside transport in choroid plexus from rabbit. Evidence for a single transporter for purine and pyrimidine nucleosides. *J Biol Chem* 267: 8813-8818.
- Yao SYM, Ng AML, Ritzel MWL, Gati WP, Cass CE, and Young JD** (1996a) Transport of adenosine by recombinant purine- and pyrimidine-selective sodium/nucleoside cotransporters from rat jejunum expressed in *Xenopus laevis* oocytes. *Mol Pharmacol* 50: 1529-1535.
- Yao SYM, Cass CE, and Young JD** (1996b) Transport of the antiviral nucleoside analogs 3'-azido-3'-deoxythymidine and 2',3'-dideoxycytidine by a recombinant nucleoside transporter (rCNT) expressed in *Xenopus laevis* oocytes. *Mol Pharmacol* 50: 388-393.
- Yao SYM, Ng AML, Muzyka WR, Griffiths M, Cass CE, Baldwin SA, and Young JD** (1997) Molecular cloning and functional characterization of nitrobenzylthioinosine (NBMPR)-sensitive (*es*) and NBMPR-insensitive (*ei*) equilibrative nucleoside transporter proteins (rENT1 and rENT2) from rat tissues. *J Biol Chem* 272: 28423-28430.

*CHAPTER III:**

Residue Mutations in Transmembrane Helix 8 of Human
Concentrative Na⁺-Nucleoside Cotransporter hCNT1 affect Permeant
Selectivity and Cation Coupling.**

* *A version of this chapter has been submitted for publication.*

Loewen SK, Ng AML, Smith KM, Yao SYM, Karpinski E, Cass CE, Baldwin SA, and Young JD (2002) *J Biol Chem* (submitted).

** Except for the electrophysiological recording of the TM 8 mutant M7 (Fig. 3-7), all of the experiments of this chapter presented in this chapter are my own work.

Introduction

Most natural and synthetic nucleosides are hydrophilic and require specialized nucleoside transporter (NT) proteins for passage across the plasma membrane (Griffith and Jarvis, 1996; Baldwin *et al.*, 1999; Cheeseman *et al.*, 2000). NT-mediated transport is therefore a critical determinant of intracellular nucleoside metabolism and the pharmacological actions of antineoplastic and antiviral nucleoside drugs (Mackey *et al.*, 1998; Cheeseman *et al.*, 2000). By regulating adenosine concentrations in the vicinity of cell-surface purinoreceptors, NTs profoundly affect neurotransmission, vascular tone and other processes (Shryock and Belardinelli, 1997; Dunwiddie and Masino, 2001). Five major nucleoside transport processes that differ in their cation dependence, permeant selectivities and inhibitor sensitivities have been observed in human and other mammalian tissues (Griffith and Jarvis, 1996; Baldwin *et al.*, 1999). Three are concentrative (Na^+ -dependent) (systems *cit*, *cif*, and *cib*) and two are equilibrative (Na^+ -independent) (systems *es* and *ei*). The former are found primarily in specialized epithelia such as intestine, kidney, liver, choroids plexus, and in leukemic cells, while the latter are ubiquitously distributed in most, possibly all, cell types (Griffith and Jarvis, 1996; Baldwin *et al.*, 1999; Cheeseman *et al.*, 2000). System *cit* exhibits permeant selectivity for pyrimidine nucleosides whereas system *cif* is selective for purine nucleosides. Both transport adenosine and uridine. Systems *cib*, *es*, and *ei* are broadly selective for both pyrimidine and purine nucleosides. The *ei* system also transports nucleobases (Yao *et al.*, 2002a).

These transport activities are brought about by members of the CNT (concentrative, Na^+ -dependent) and ENT (equilibrative, Na^+ -independent) integral membrane protein families. Three CNT and three ENT isoforms have been identified in human and rodent cells (Huang *et al.*, 1994; Che *et al.*, 1995; Yao *et al.*, 1996; Griffiths *et al.*, 1997a, 1997b; Ritzel *et al.*, 1997; Wang *et al.*, 1997; Yao *et al.*, 1997; Crawford *et al.*, 1998; Ritzel *et al.*, 1998, 2001; Hyde *et al.*, 2001). Their relationships to the processes defined by functional studies are: CNT1 (*cit*), CNT2 (*cif*), CNT3 (*cib*), ENT1 (*es*), and ENT2 (*ei*). The transport properties of ENT3 are presently uncharacterized. The two protein families are unrelated and have different membrane architectures (Hamilton *et al.*, 2001; Sundaram *et al.*, 2001), mammalian CNTs having 13 putative transmembrane helices (TMs) with an intracellular amino-terminus and an exofacial glycosylated tail at the carboxyl-terminus (Hamilton *et al.*, 2001). NupC, a CNT family

member from *Escherichia coli*, has a similar membrane topology to mammalian CNTs, but lacks TMs 1-3.

Human (h) CNT1 contains 650 amino acid residues and is 83% identical in sequence to rat (r) CNT1 (648 residues) (Huang et al., 1994; Ritzel *et al.*, 1997). hCNT2 (658 residues) is 83% identical to rCNT2 (659 residues) and 72% identical to hCNT1 (Che *et al.*, 1995; Yao *et al.*, 1996; Ritzel *et al.*, 1997; Wang *et al.*, 1997). hCNT3 (691 residues) is 78% identical to rCNT3 and mouse (m) CNT3 (both 703 residues), ~ 50% identical to h/rCNT1 and h/rCNT2 (Ritzel *et al.*, 2001), and 57% identical (77% identical within TMs 4-13) to a CNT3 ortholog, hfCNT, from an ancient marine pre-vertebrate, the Pacific hagfish (*Eptatretus stouti*). Like its mammalian counterparts, hfCNT mediates *cib*-type transport characteristics, but shows markedly lower apparent affinity for Na⁺ (Yao *et al.*, 2002b). CNTs are unrelated to SNST1 (now SGLT2), a previous candidate *cib*-type nucleoside transport protein from rabbit kidney (Pajor and Wright, 1992).

The generally accepted model for secondary active transport depends on alternating access of bound substrate and driving cation to external and internal sides of the membrane (Mitchell, 1990; Krupka, 1993). TMs serve as the transport conduit, and protein conformational changes expose the substrate and cation binding site(s) to alternate sides of the membrane. Multiple alignments of CNT family members reveal strong sequence homologies within the carboxyl-terminal half of the proteins, particularly within TMs. Previously, we used hCNT1/2 chimeric constructs and site-directed mutagenesis in combination with heterologous expression in *Xenopus* oocytes to identify two pairs of residues in TMs 7 and 8 of hCNT1 (Ser³¹⁹/Gln³²⁰ and Ser³⁵³/Leu³⁵⁴) that, when converted to the corresponding residues in hCNT2 (Gly/Met and Thr/Val), changed the permeant selectivity of the transporter from *cit* to *cif* (Loewen *et al.*, 1999). Mutation of Ser³¹⁹ TM 7 to Gly allowed for uptake of purine nucleosides, producing an intermediate *cib*-type phenotype. Concurrent mutation of the adjacent TM 7 residue Gln³²⁰ to Met, which had no effect on its own, augmented this transport. The additional mutation of Ser³⁵³ in TM 8 to Thr converted hCNT1/S319G/Q320M from broad selectivity (*cib*) to *cif*, but with relatively low adenosine transport activity. Substitution of the adjacent TM 8 residue Leu³⁵⁴ to Val enhanced the adenosine transport capability of the hCNT1/S319G/Q320M/S353T, producing a full *cif*-type phenotype. Here, we have extended

these two-helix mutagenesis studies by providing a detailed transport characterization of the hCNT1 S353T and L354V TM 8 substitutions (corresponding to mutations M6 and M7, respectively, in *Chapter II*) independent of those engineered in TM 7.

Materials and Methods

Site-directed Mutagenesis of hCNT1 and Expression in *Xenopus* Oocytes – hCNT1 mutants hCNT1/S353T, hCNT1/L354V and hCNT1/S353T/L354V were engineered as previously described (Loewen *et al.*, 1999). Constructs were sequenced in their entirety in both directions to confirm that the correct mutation had been introduced. Plasmid DNAs were linearized with *NotI* and transcribed with T3 polymerase using the mMACHINE mMACHINE™ (Ambion) transcription system. Defolliculated stage VI *Xenopus* oocytes (Ritzel *et al.*, 1997) were microinjected with 20 nl of water or 20 nl of water containing capped RNA transcript (20 ng) and incubated in modified Barth's medium (changed daily) at 18 °C for 72 h prior to the assay of transport activity.

Radioisotope Flux Studies – Transport assays were performed as described previously (Ritzel *et al.*, 1996, 2001) on groups of 12 oocytes at 20 °C using ¹⁴C-labeled nucleosides or ¹⁴C- or ³H-labeled nucleoside analogs (Moravek Biochemicals or Amersham Pharmacia Biotech) (1 and 2 µCi/ml for ¹⁴C-labeled and ³H-labeled compounds, respectively) in 200 µl of transport medium containing either 100 mM NaCl, 100 mM choline chloride or 100 mM LiCl and 2 mM KCl, 1 mM CaCl₂, 1 mM MgCl₂, and 10 mM HEPES. Except where otherwise indicated, the medium pH was 7.5, and nucleoside uptake was determined at a concentration of 20 µM using an incubation period of 30 min. Experiments replacing NaCl with equimolar choline chloride included a 10 min pre-incubation period and several washes with choline-containing transport buffer prior to addition of radiolabeled substrate to ensure complete removal of extracellular Na⁺. At the end of the incubation period, extracellular label was removed by six rapid washes in ice-cold transport medium, and individual oocytes were dissolved in 5% (w/v) SDS for quantitation of cell-associated radioactivity by liquid scintillation counting (LS 6000 IC, Beckman). Each experiment was performed at least twice on different batches of cells and included wild-type hCNT1 and hCNT2 as controls to eliminate transport variability between different batches of oocytes. The flux values shown are means ± S.E. of 10-12 oocytes from

one representative experiment. Significant differences in mean flux values were determined by Student's t-test ($P = 0.05$). Kinetic (K_m , K_{50} , Hill coefficient) parameters (\pm S.E.) were calculated using ENZFITTER software (Elsevier-Biosoft, Cambridge, UK).

Measurements of hCNT1- and hCNT1/L354V-Induced Sodium Currents – Membrane currents were measured at room temperature using the whole-cell, two-electrode voltage clamp technique (CA-1B oocyte clamp, Dagan Corp.). The microelectrodes were filled with 3 M KCl and had resistances that ranged from 0.5 to 1.5 M Ω . The CA-1B was interfaced to a dedicated computer via a Digidata 1200B A/D converter and controlled by Axoscope software (Axon Instruments). Current signals were filtered at 20 Hz (four-pole Bessel filter) at a sampling interval of 50 ms. For data presentation, the signals were further filtered at 0.5 Hz by use of pCLAMP software (Axon Instruments). Following microelectrode penetration, resting membrane potential was measured over a 15 min period prior to the start of the experiment. Oocytes exhibiting an unstable membrane potential or a potential less than -30 mV were discarded. Individual oocytes with good resting membrane potentials were clamped at -50 mV and current measurements were sampled in NaCl or choline chloride transport media of the same composition used in the radioisotope transport assays. During the course of data collection, the transport medium perfusing the oocyte was changed to one containing 100 μ M uridine for approximately 60 s and then immediately washed and exchanged with fresh medium lacking the nucleoside substrate.

Results and Discussion

The sequence alignment in Fig. 3-1 of the 21 amino acids in putative TM 8 of human and rat CNT1 (*cit*) and CNT2 (*cif*) identifies 5 amino acid residues that are conserved within the h/rCNT1 and h/rCNT2 subtypes, but that differ between the CNT1/2 isoforms. Two of these form an adjacent pair of residues (Ser/Leu in hCNT1 and Thr/Val in hCNT2) studied in earlier site-directed mutagenesis experiments (Loewen *et al.*, 1999). In these previous studies, residues Ser³⁵³ and Leu³⁵⁴ of hCNT1 were mutated to the corresponding residues of hCNT2 in combination with the parallel mutation of a similar pair of isoform-specific adjacent residues (Ser³¹⁹ and Gln³²⁰) in TM 7. Initial mutation of the two TM 7 residues to the corresponding amino acids in hCNT2 (Gly and Met, respectively) converted the permeant selectivity from *cit*

to *cib*, since the mutant (hCNT1/S319G/Q320M) transported both pyrimidine and purine nucleosides. Additional mutation of Ser³⁵³ in TM 8 to Thr changed the permeant selectivity of hCNT1/S319G/Q320M from *cib* to *cif*, producing a transporter with selectivity for purine nucleosides and uridine, but with relatively low transport activity for adenosine. Substitution of the adjacent TM 8 residue Leu³⁵⁴ to Val enhanced the adenosine transport capability of the hCNT1/S319G/Q320M/S353T, producing a full *cif*-type phenotype.

From these results, it was anticipated that mutation of the two TM 8 residues against a wild-type hCNT1 background might also lead to changes in permeant selectivity. In the present study, I therefore considered the effects of mutating the two hCNT1 TM 8 residues independent of those in TM 7. Helix modeling of hCNT1 has placed one of these residues (Ser³⁵³) within the putative permeant translocation channel, whereas the other (Leu³⁵⁴) is predicted to interface with an adjacent TM (Loewen *et al.*, 1999). The first part of this paper describes experiments undertaken to investigate the effects of mutating the two TM 8 residues on hCNT1 permeant selectivity. The second describes investigations of the unexpected observation that mutation of the TM 8 residues also led to changes in cation coupling.

Expression of TM 8 hCNT1 Mutants S353T, L354V, and S353T/L354V in *Xenopus* oocytes – RNA transcripts for hCNT1/S353T, hCNT1/L354V, hCNT1/S353T/L354V and wild-type hCNT1 and hCNT2 were synthesized *in vitro* and produced as recombinant proteins in *Xenopus laevis* oocytes to permit assay of their transport activities. Fig. 3-2 shows representative mediated fluxes of uridine measured concentration of 20 μ M (30 min flux at 20°C), where mediated uptake is defined as uptake in RNA transcript-injected oocytes minus uptake in control water-injected oocytes. Each of the three hCNT1 mutant constructs gave good functional activity similar to wild-type hCNT1 and hCNT2. In subsequent experiments, uridine uptake was used as an internal control in each experiment to compare: (i) overall transport function between mutated and wildtype transporters, and (ii) transport activity for other permeants relative to that of uridine.

Permeant Specificity of TM 8 hCNT1 Mutants S353T, L354V, and S353T/L354V – Also presented in Fig. 3-2 are representative mediated fluxes of a panel of other pyrimidine and purine nucleosides (adenosine, thymidine, inosine, guanosine, and cytidine) measured

under the same conditions and in the same batch of oocytes as uridine. The results showed that substitution of hCNT1 Ser³⁵³ by Thr (mutant hCNT1/S353T) significantly reduced thymidine and cytidine fluxes compared to wild-type hCNT1. Thymidine:uridine and cytidine:uridine transport ratios were 0.37 and 0.11, respectively, for hCNT1/S353T, compared to 0.88 and 0.60, respectively, for hCNT1. Adenosine transport was virtually eliminated. Substitution of hCNT1 Leu³⁵⁴ by Val (mutant hCNT1/L354V) did not affect substrate selectivity on its own but, in combination with S353T (hCNT1/S353T/L354V), further reduced thymidine and cytidine transportability, dramatically altering hCNT1 permeant selectivity to produce a transporter that appeared to be uridine-specific. hCNT1/S353T/L354V is the first reported CNT, engineered or otherwise, that is selective for a single physiological nucleoside permeant. The molecular identity of an apparently guanosine-preferring *csf*-type concentrative NT from acute promyelocytic leukemia cells is presently unknown (Flanagan and Meckling-Gill, 1997).

Kinetics of Uridine Transport by hCNT1 Mutant S353T/L354V – Fig. 3-3A compares representative concentration dependence curves for uridine uptake by wild-type hCNT1 and the uridine-selective mutant hCNT1/S353T/L354V measured in the same batch of oocytes. The experiment was performed in NaCl transport medium using a 5-min uptake interval to measure initial rates of transport (influx) (Loewen *et al.*, 1999). Apparent K_m values calculated from the data are presented in Table 3-1. Transport by hCNT1/S353T/L354V was saturable and conformed to simple Michaelis-Menten kinetics with an apparent K_m value of 16 μM that was one-third that of wild-type hCNT1 (48 μM). In addition to being selective for uridine, therefore, hCNT1/S353T/L354V had a higher apparent affinity for uridine than wild-type hCNT1. V_{\max} values from Fig 3-3A for hCNT1/S353T/L354V and wild-type hCNT1 were 4.8 ± 0.2 and 8.5 ± 0.5 pmol/oocyte.5min⁻¹, respectively, giving $V_{\max}:K_m$ ratios (a measure of transporter efficiency) of 0.18 and 0.30, respectively. Although the V_{\max} values and $V_{\max}:K_m$ ratios of the two transporters are not strictly comparable because of possible differences in cell-surface abundance of the recombinant transporters, the results clearly indicated that hCNT1/S353T/L354V functioned normally as a uridine transporter. Selectivity differences between wild-type hCNT1 and hCNT1 mutants S353T and S353T/L354V were therefore

most likely the result of alterations within the nucleoside binding pocket that compromised interactions with other CNT1 permeants.

Transport of Uridine Analogs by hCNT1 Mutants S353T and S535T/L354V – To explore further the substrate specificity of the TM 8 hCNT1 mutants, we compared the ability of hCNT1, hCNT2, hCNT1/S353T and hCNT1/S535T/L354V to transport three radiolabeled uridine nucleoside analogs (5-fluorouridine (5-FUrd), 5-fluoro-2'-deoxyuridine (5-FdUrd), and zebularine). The structures of these synthetic nucleosides in relation to uridine, thymidine, and cytidine are shown in Fig. 3-4. Representative transport data for these compounds are presented in Table 3-2. The results demonstrated that the narrowed substrate selectivities of hCNT1/S353T and hCNT1/S535T/L354V extended to these uridine analogs. Wild-type hCNT1 was more tolerant of deviations in chemical composition, allowing higher fluxes of 5-FUrd, 5-FdUrd and zebularine than either of the two hCNT1 mutants. Wild-type hCNT2, in contrast, exhibited transport activities similar to hCNT1/S353T and hCNT1/S535T/L354V.

For 5-FUrd and 5-FdUrd, the structural basis for weak transport by hCNT1/S353T and hCNT1/S535T/L354V was most likely the presence of a bulky electronegative fluorine atom at the 5-position (R_2 in Fig. 3-4) of the pyrimidine ring (*versus* H in uridine). The presence of a methyl group at this position in thymidine may also explain why its transport was also affected. Similarly, the structural feature common to zebularine and cytidine (which were also poorly transported by the hCNT1 mutants (Table 3-2)) is the absence of the uridine keto group at the 4-position of the pyrimidine ring (R_1 in Fig. 3-4). This keto group, which has the potential to hydrogen bond to an adjacent amino acid side chain, was not essential for transport by wild-type hCNT1 since cytidine and zebularine are normally good hCNT1 permeants (Fig. 3-2 and Table 3-2). Together, these data suggest that mutation of Ser³⁵³ and Leu³⁵⁴ led to changes in the hCNT1 binding pocket in the vicinity of positions occupied by substrate groups R_1 and R_2 .

Na⁺-dependence of hCNT1 Mutants S353T, L354V, and S353T/L354V – When Na⁺ in the transport medium was replaced by choline⁺, wild-type hCNT1 and hCNT2 exhibited the expected large reduction in uridine transport activity, consistent with the function of both proteins as Na⁺/nucleoside symporters (Ritzel *et al.*, 1997, 1998) (Fig. 3-2). The small (< 5%)

residual component of uptake seen in Na⁺-free conditions, defined previously as “slippage” (uncoupled transport of uridine) (Huang *et al.*, 1995), was similar in magnitude to that found in earlier studies (Huang *et al.*, 1994; Ritzel *et al.*, 1997, 1998). Similarly, uridine uptake by mutant hCNT1/S353T was > 95% Na⁺-dependent. In marked contrast, mutant hCNT1/L354V exhibited an unexpectedly large uptake of uridine in the absence of Na⁺ (31% of the control flux in NaCl medium). A smaller, but still elevated Na⁺-independent flux was also seen with the combination mutant hCNT1/S353T/L354V. As shown in Fig. 3-5, hCNT1/L354V also exhibited elevated Na⁺-independent transport of thymidine and cytidine (and, to a lesser extent, adenosine), indicating that the phenomenon was not restricted to uridine. Uridine, however, showed the largest transport activity in Na⁺-free medium and was used as permeant for further characterization of the uncoupled transport exhibited by the hCNT1/L353V mutant.

Cation Specificity and Electrophysiology of hCNT1 Mutant L354V – Under the rigorously Na⁺-free conditions used in our experiments (see *Materials and Methods*), there are two explanations for the large Na⁺-independent uptake of nucleosides mediated by hCNT1/L343V: (i) the mutant protein coupled transport to another cation present in the medium, possibly H⁺, or (ii) the mutant protein was partially uncoupled, allowing elevated slippage whereby the permeant was translocated without a requirement for Na⁺. The experiments shown in Figs. 3-6 & 3-7 tested these possibilities.

Consistent with the data in Figs. 3-2 & 3-5, transport of uridine by hCNT1/L354V in Na⁺-free choline chloride medium at pH 5.5, 7.5, and 8.5 (Fig. 3-6A) was substantially higher than that of wild-type hCNT1 under the same conditions, and did not show signs of pH-dependence, even though the difference between pH 5.5 to 8.5 represented a 1000-fold increase in H⁺ concentration. There was also no evidence of any pH-dependence for the wild-type transporter, suggesting that neither protein can substitute H⁺ for Na⁺. We also tested Na⁺ replacement with Li⁺ (Fig. 3-6B). Li⁺ is an intermediate-sized cation larger than H⁺ but smaller than Na⁺, and could substitute for Na⁺ in a number of secondary active transport systems. Transport of uridine by wild-type hCNT1 in LiCl medium was not significantly different from the residual uptake seen in choline chloride medium, demonstrating discrimination between Na⁺ and Li⁺ as the coupling cation. Transport of uridine by hCNT1/L354V was also similar

in Li^+ - and choline⁺-containing media, suggesting that the mutant protein retained the cation specificity of the wild-type transporter.

Representative whole-cell current recordings of hCNT1- and hCNT1/L354V-mediated uridine uptake using the two-electrode, voltage clamp method are shown in Fig. 3-7. In Na^+ -containing transport medium, hCNT1- and hCNT1/L354V-producing oocytes both exhibited a uridine-evoked inward current that ranged between 23-30 nA in repeated trials with different oocytes. No uridine-evoked current was observed in control water-injected oocytes or in hCNT1-producing oocytes perfused with choline chloride transport medium, confirming that the measured current represented electrogenic transporter-mediated Na^+ /uridine cotransport across the cell plasma membrane. Similarly, there was no detectable uridine-evoked current in hCNT1/L354V-producing oocytes in choline chloride transport medium, thereby excluding the possibility that hCNT1/L354V coupled transport of uridine to a cation other than Na^+ and suggesting that hCNT1/L354V-mediated transport of uridine in Na^+ -free conditions was routed through a Na^+ -uncoupled transport pathway.

Kinetics of Uridine Transport by hCNT1 Mutant L354V – The concentration-dependence of uridine transport by hCNT1/L354V was investigated in parallel with the previously discussed studies of hCNT1/S354T/L354V (Fig. 3-3A), we also investigated the concentration-dependence of uridine transport by hCNT1/L354V. The experiment presented in Fig. 3-3B was performed in choline chloride transport medium to study behaviour of the protein under Na^+ -free conditions. Because of the lower fluxes seen in choline chloride transport medium (Fig. 3-2), a 10-min uptake interval was used to measure initial rates of transport. The control was a parallel analysis of the concentration dependence of uridine uptake by wild-type hCNT1, also in choline chloride transport medium. Under these conditions, hCNT1 transport of uridine was slow and nonsaturable, with an apparent K_m value > 1 mM compared to 48 μM in the presence of Na^+ (Fig. 3-3A), a result consistent with previous findings for hCNT1 (Ritzel *et al.*, 1997) and rCNT1 (Huang *et al.*, 1994). Mutant hCNT1/L354V showed a high apparent affinity for uridine under identical Na^+ -free conditions. The measured apparent K_m value of 47 μM was similar to wild-type hCNT1 in the presence of Na^+ . No current was associated with this transport (Fig. 3-7). Therefore, in the absence of Na^+ , hCNT1/L354V functioned as a high-affinity equilibrative NT.

When the concentration dependence of the hCNT1/L354V mutant was measured in NaCl transport medium, an apparent K_m value that was lower than that of wild type hCNT1 was obtained (28 *versus* 48 μM , respectively) (Table 3-1). Despite this, hCNT1/L354V retained a high apparent affinity for Na^+ -activation. This is illustrated in Figs. 3-3C & D, which compared Na^+ -activation curves for wild-type hCNT1 and mutant hCNT1/L354V measured at a uridine concentration of 20 μM uridine (5-min flux). For hCNT1, the relationship between uridine influx and Na^+ concentration was hyperbolic, with a Hill coefficient of 1.1 ± 0.1 (Fig. 3-6C). This suggested a Na^+ /nucleoside coupling stoichiometry of 1:1 and is consistent with previous results for both hCNT1 (Ritzel *et al.*, 1997) and rCNT1 (Yao *et al.*, 1996). Similarly, hCNT1/L354V also exhibited a hyperbolic Na^+ -activation curve, but with a non-zero intercept, reflecting its uridine transport capability under Na^+ -free conditions (Fig. 3-3D). Both proteins showed high apparent affinities for Na^+ , with apparent K_{50} values for Na^+ -activation of 8.7 and 4.3 mM for hCNT1 and hCNT1/L354V, respectively (Table 3-1).

Transport Models and Uncoupled Substrate Slippage – Solute coupling in secondary active transport systems has been suggested to occur *via* a common ordered binding mechanism, where the driving solute (activator), typically Na^+ or H^+ , binds to the transport protein first followed closely by binding of the driven solute (substrate), such as a nucleoside (Yamato, 1992). An ordered transport model of this design is favored over alternate binding mechanisms because of its efficient handling of substrate at low concentration (Yamato, 1992). Several Na^+ -dependent and H^+ -dependent transporters have been identified with ordered binding mechanisms of this type, including Na^+ /glucose, Na^+ /iodide, and H^+ /oligopeptide symporters from mammals (Panayotova-Heiermann *et al.*, 1995; Mackenzie *et al.*, 1996; Eskandari *et al.*, 1997), the *Leishmania* H^+ /myo-inositol symporter (Klamo *et al.*, 1996), and *E. coli* H^+ /lactose permease (Yamato and Anraku, 1989). In depth electrophysiological studies in *Xenopus* oocytes suggest a similar ordered (and not random) binding mechanism for hCNT1 (unpublished observation), a model also consistent with previous transport studies of system *cit* in bovine kidney vesicles (Williams and Jarvis, 1991). Our present results for the effects of the L354V mutation on hCNT1 Na^+ -dependence are consistent with a refinement of the ordered binding mechanism that also incorporates uncoupled pathways of solute leak and substrate slippage (Krupka, 1994). Developed by Krupka, this modified ordered binding model of

transport alleviates the stringent carrier states of earlier models that assumed perfectly solute-coupled cotransport and instead allows for the flexibility of mobile, uncoupled carrier states. A simplified version of Krupka's kinetic model, incorporating full or partial nucleoside slippage is presented for hCNT1 in Fig. 3-8.

Because the transporter can accept two different solutes, Na^+ (A) and the nucleoside (S), it is proposed to exist in two inwardly-facing or outwardly-facing conformational states: one with one binding site (T_i' or T_o') and one with two binding sites (T_i'' or T_o''). Normally, the equilibrium between the two outwardly-facing carrier states overwhelmingly favors the T_o' form and requires the addition of Na^+ to "unlock" or open the second site ($T_o'A \leftrightarrow T_o''A$), thereby promoting active transport. Both $T_o''S$ and $T_o''AS$ are considered mobile. However, were the equilibrium between the two empty carrier forms ($T_o' \leftrightarrow T_o''$) to be shifted in favour of that with two binding sites (T_o''), nucleosides would have an increased ability to bind to the transporter through a slippage pathway without the requirement of Na^+ . In the presence of Na^+ , both pathways would occur simultaneously, whereas in the absence of Na^+ , only the slippage pathway would be present.

The simplest explanation of the L354V mutation in hCNT1 is that the equilibrium between T_o' and T_o'' is shifted towards T_o'' . In the Krupka model, the apparent affinity (K_m) of S is determined by the ratio $[T_o']/[T_o'']$ (Krupka, 1994). The model therefore explains why the apparent K_m for uridine transport by wild-type hCNT1 is lower in the presence of Na^+ than in the absence of Na^+ (Figs. 3-3A & B), why hCNT1/L354V exhibits a high apparent affinity for uridine, even in the absence of Na^+ , and why there is a further increase in apparent affinity of hCNT1/L354V for uridine in the presence of Na^+ . The Krupka model also has utility in interpreting mutagenesis studies of other secondary active transporters (Krupka, 1994).

Conclusions – Mutation of two adjacent residues (Ser³⁵³ and Leu³⁵⁴) in TM 8 of hCNT1 to the corresponding residues in hCNT2 (Thr and Val, respectively) produced novel transporters with uridine-selective transport characteristics (hCNT1/S353T and hCNT1/S353T/L354V) and/or partially uncoupled permeant fluxes (hCNT1/S353T/L354V and hCNT1/L354V). Helix modeling of CNTs suggests that TM 8, in addition to TMs 7 and 9, forms part of the permeant translocation channel, where hCNT1 Ser³⁵³ (Thr³⁴⁷ in hCNT2) is

predicted to face inwardly into the channel pore while Leu³⁵⁴ (Val³⁴⁸ in hCNT2) is most likely involved in helix-helix packing (Loewen *et al.*, 1999). Ser and Thr both contain a side-chain hydroxyl group but differ in their relative side-chain length (Thr has an additional CH₃ group). This small structural difference in residue 347 of hCNT1 is sufficient to alter the nucleoside binding pocket and induce the observed change in substrate specificity. The ability of the residue 348 mutation (Leu to Val) to augment the permeant selectivity change caused by the mutation of residue 347 produced a transporter that was essentially uridine-specific and is most likely mediated by altered helix-helix packing (Loewen *et al.*, 1999). Whether Ser³⁵³ in wild-type hCNT1 or Thr³⁴⁷ in hCNT1/S353T and hCNT1/S353T/L354V forms hydrogen bonds with the nucleoside substrate remains to be determined. All CNTs so far characterized transport uridine, even if the transporter is otherwise purine nucleoside-selective. The present mutagenesis studies of hCNT1 emphasize the role of uridine as a “universal” CNT permeant. Mechanistically, this may be related, at least in part, to uridine being the smallest of the physiological nucleosides. Binding forces involved in CNT/permeant interactions are likely to include a similar combination of hydrogen bonds and π - π interactions documented for trypanosomal ENT nucleoside transport proteins (de Koning and Jarvis, 1999).

On its own, mutation of Leu³⁵⁴ produced a partially uncoupled transporter that functioned as a high-affinity equilibrative NT under Na⁺-free conditions. This phenotype, most likely also mediated by altered helix-helix packing, validates an ordered AS binding model of Na⁺/nucleoside co-transport incorporating a pathway for Na⁺-uncoupled substrate slippage. The model, which has wide applicability to other native (and mutated) secondary active transport proteins (Krupka, 1994), attributes the effects of the L354V mutation to a shift in equilibrium between two outward-facing carrier states, one of which binds Na⁺ (A) only, and the other which has binding sites for both Na⁺ (A) and nucleoside (S). Additional hCNT1 mutations within or adjacent to the translocation channel may serve to restore Na⁺-coupling, since the hCNT1 TM 7 and TM 8 combination mutant S319G/Q320M/S353T/L354V is strictly Na⁺-dependent (Loewen *et al.*, 1999).

Table 3-1 – Apparent K_m and K_{50} Values of hCNT1 and hCNT1 Mutants S353T/L354V and L354V

Transporter	Apparent K_m (μM)	Apparent K_{50} (mM)
hCNT1	48 ± 6^a	8.7 ± 0.9^a
hCNT1/S353T/L354V	16 ± 1^a	—
hCNT1/L354V	28 ± 3 47 ± 7^{ab}	4.3 ± 0.9^a

^a, from Fig. 3-3; ^b, in transport medium containing 100 mM choline chloride.

Table 3-2 – Mediated Uptake of [¹⁴C]-labeled Uridine and Pyrimidine Nucleoside Analogs by hCNT1, hCNT2 and Uridine-selective hCNT1 Mutants S353T and S353T/L354V

Substrate ^a	Nucleoside Uptake (pmol/oocyte.30 min ⁻¹) ^b			
	hCNT1	hCNT2	S353T	S353T/L354V
Uridine	20.7 ± 3.9	17.6 ± 1.4	13.1 ± 1.8	15.3 ± 1.7
5-FUrd	18.5 ± 2.9	13.6 ± 1.5	9.92 ± 0.98	9.58 ± 1.70
5-FdUrd	19.2 ± 2.4	11.0 ± 1.4	8.12 ± 1.01	4.53 ± 1.02
Zebularine	19.1 ± 2.1	3.71 ± 0.57	5.55 ± 0.46	2.51 ± 0.47

^a, The structures of 5-FU (5-flourouridine), 5-FdU (5-flouro-2'-deoxyuridine) and zebularine are given in Fig. 3-4; ^b, 20 μM nucleoside flux, 20 °C.

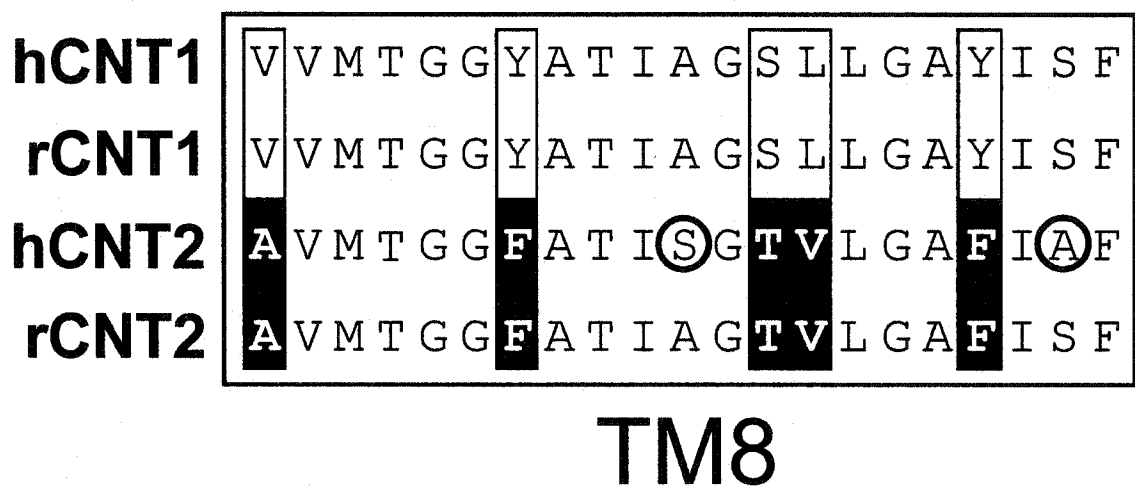
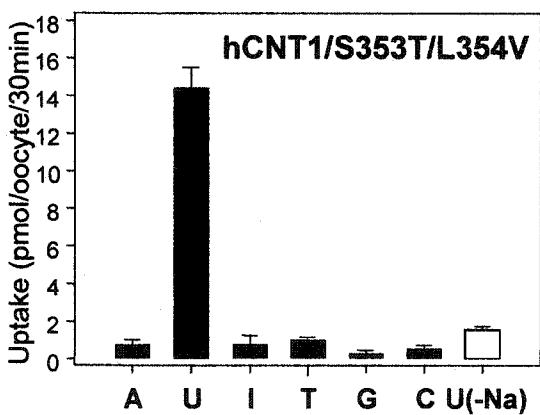
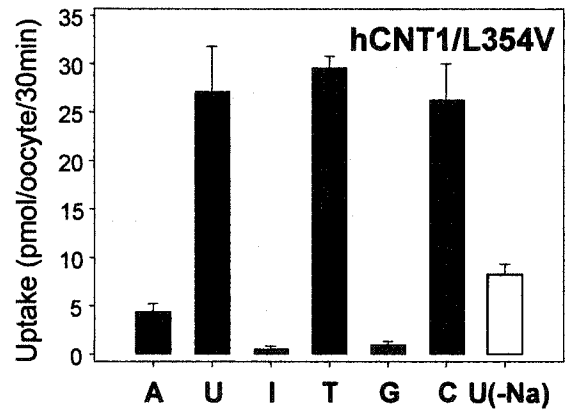
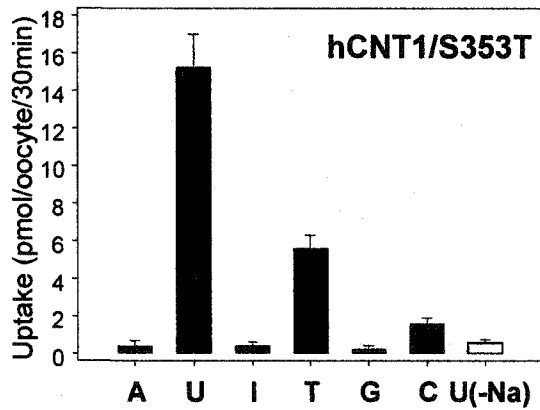
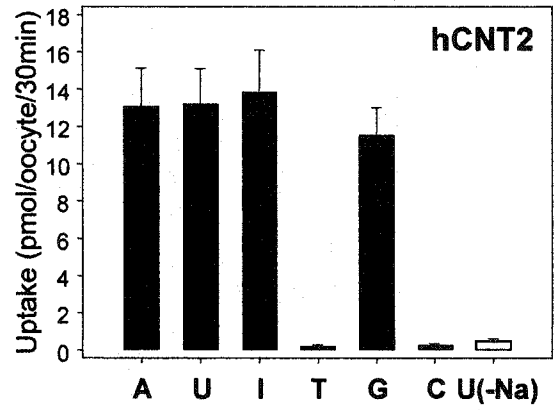
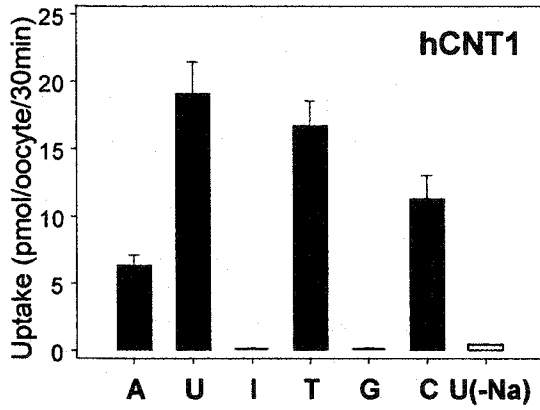


Figure 3-1. Sequence alignment of h/rCNT1 and h/rCNT2 amino acid residues in putative TM 8. The positions of conserved residues that differ between h/rCNT1 and h/rCNT2 are shown as *open* and *solid boxes*, respectively. *Circles* indicate residues unique to hCNT2.

Figure 3-2. Nucleoside specificity of hCNT1, hCNT2, and hCNT1 mutants S353T, L354V, and S353T/L354V. *Xenopus* oocytes were injected with either 20 nl of water alone or 20 nl of water containing 10 ng of RNA transcripts encoding hCNT1, hCNT2, hCNT1/S353T, hCNT1/L354V or hCNT/S353T/L354V. Uptake of a panel of physiological nucleosides (*A*, adenosine; *U*, uridine; *I*, inosine; *T*, thymidine; *G*, guanosine; *C*, cytidine) (20 μ M, 20 °C, 30 min flux) were measured in transport media containing 100 mM NaCl (*black bars*) or 100 mM choline chloride (*open bars*). Data are presented as mediated transport, calculated as uptake in RNA-injected oocytes minus uptake in oocytes injected with water alone. Each value represents the mean \pm S.E. of 10-12 oocytes.



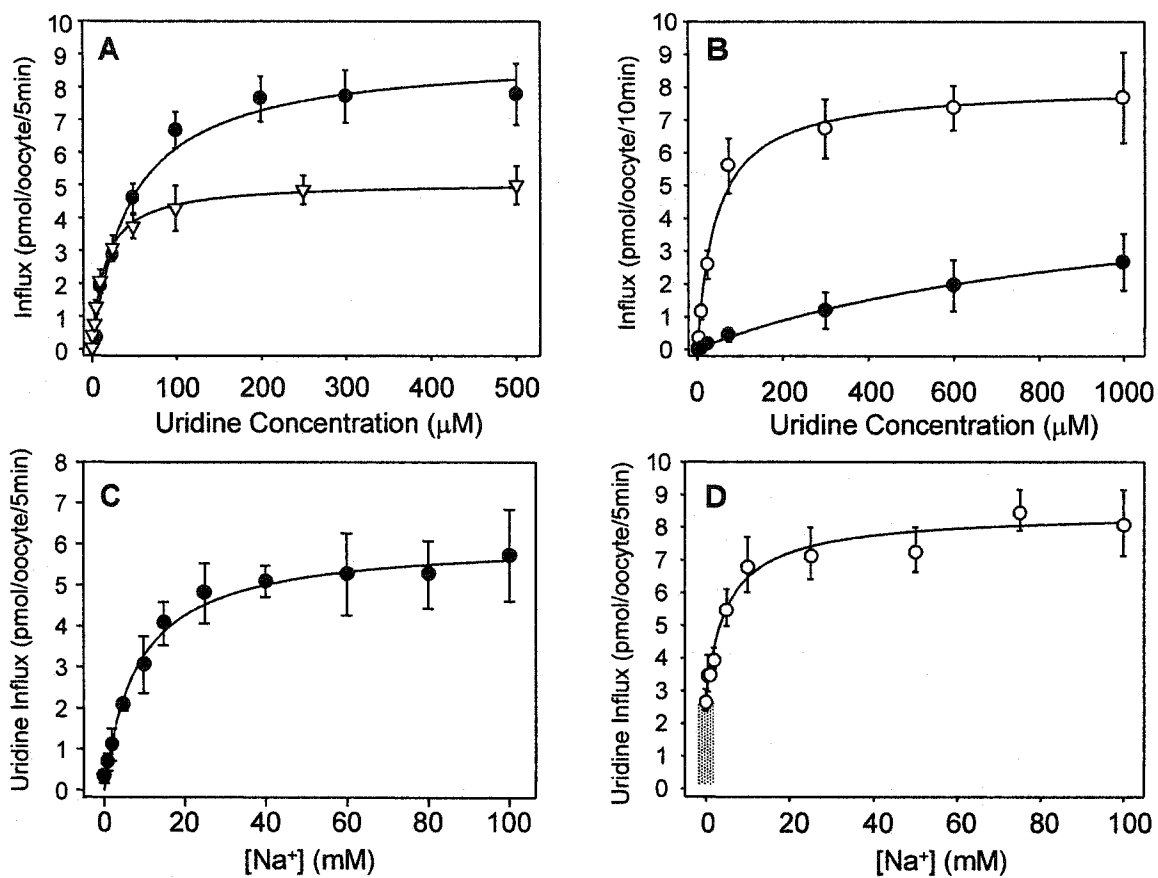


Figure 3-3. Kinetic properties of hCNT1 mutants S353T/L354V and L354V. *A*, initial rates of uridine uptake by hCNT1 (*solid circles*) and hCNT1/S353T/L354V (*open triangles*) measured in NaCl transport medium (20°C, 5 min flux). *B*, initial rates of uridine uptake by hCNT1 (*solid circles*) and hCNT1/L354V (*open circles*) measured in choline chloride transport medium (20°C, 10 min flux). *C* and *D*, initial rates of 20 μM uridine uptake (20°C, 5 min flux) by hCNT1 (*solid circles*) and hCNT1/L354V (*open circles*) measured as a function of transport medium Na⁺ concentration, using choline⁺ as isosmotic Na⁺ substitute. Data are presented as mediated transport, calculated as uptake in RNA-injected oocytes minus uptake in water-injected oocytes. Each value represents the mean ± S.E. of 10-12 oocytes.

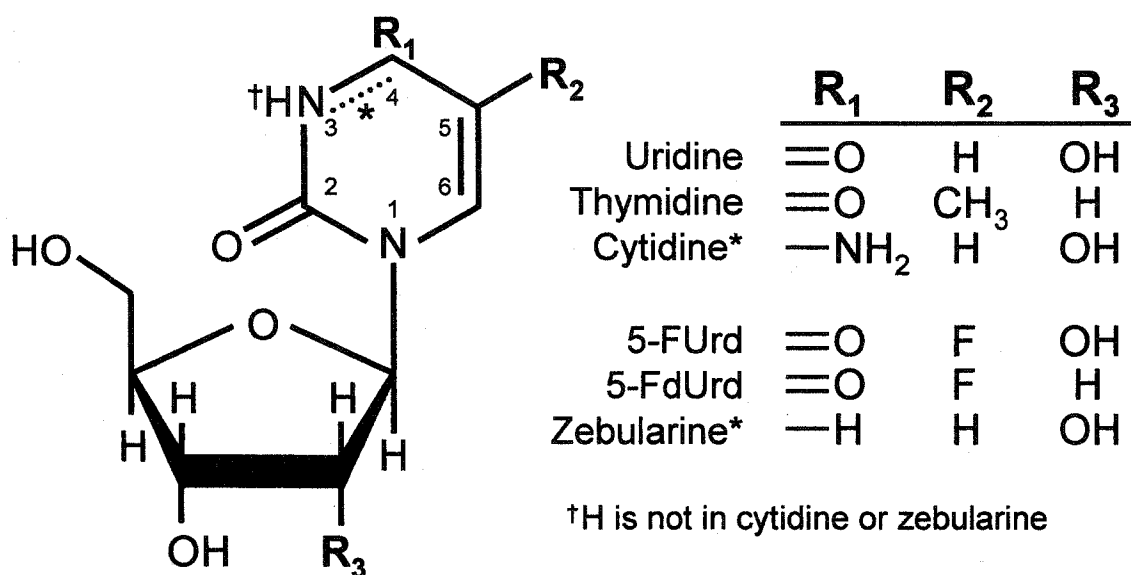


Figure 3-4. Chemical structures of selected pyrimidine nucleosides and nucleoside analogs. A common pyrimidine nucleoside chemical structure is shown. Structural variations between pyrimidine nucleosides (uridine, thymidine, cytidine) and pyrimidine nucleoside analogs (5-fluorouridine (5-FUrd), 5-fluoro-2'-deoxyuridine (5-FdUrd), zebularine) are represented by three R groups, where R_1 , R_2 , and R_3 are defined in the adjacent table. The double bond denoted by the *asterisk* is present only in cytidine and zebularine.

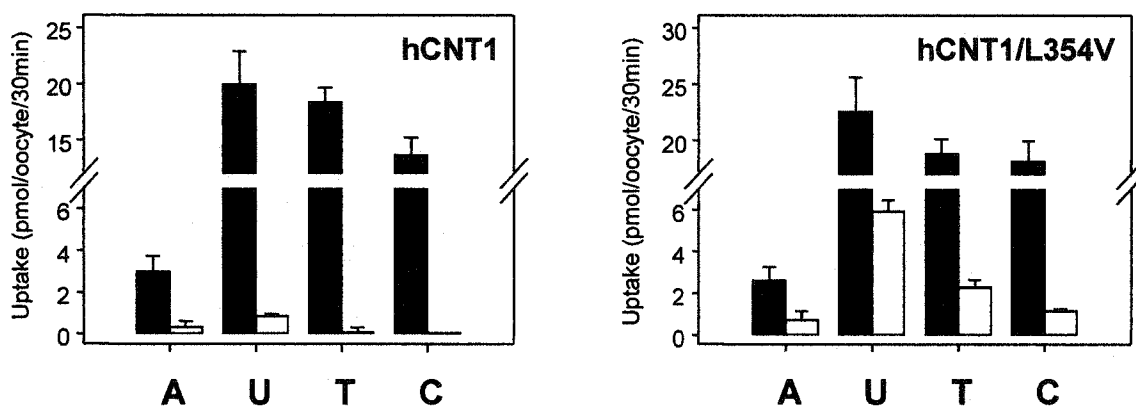


Figure 3-5. Na^+ -dependent and Na^+ -independent nucleoside transport activity of hCNT1 and hCNT1/L354V. Uptake of physiological nucleosides (*A*, adenosine; *U*, uridine; *T*, thymidine; *C*, cytidine) ($20 \mu\text{M}$, 20°C , 30 min flux) in oocytes injected with hCNT1 or hCNT1/L354V RNA transcript or water alone was measured in transport media containing NaCl (*solid bars*) or choline chloride (*open bars*). Data are presented as mediated transport, calculated as uptake in RNA-injected oocytes minus uptake in water-injected oocytes. Each value represents the mean \pm S.E. of 10-12 oocytes.

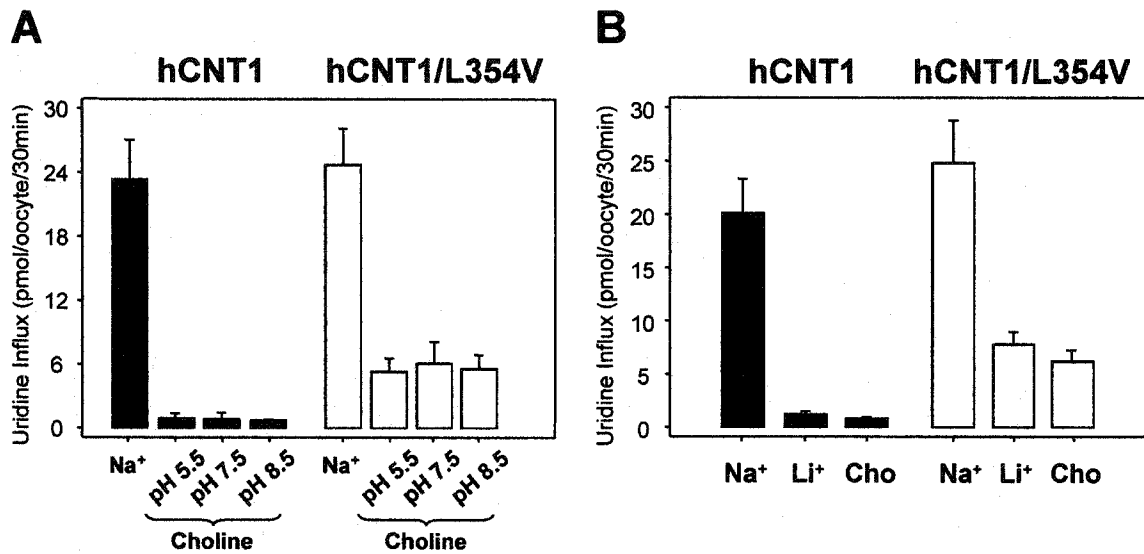


Figure 3-6. Effects of pH and Li⁺ replacement on hCNT1- and hCNT1/L354V-mediated uridine transport activity. *A*, uptake of uridine by hCNT1 (*solid bars*) and hCNT1/L354V (*open bars*) measured in NaCl transport medium (pH 7.5) or in choline chloride transport medium at pH 5.5, 7.5, or 8.5 (20 μ M, 20°C, 30 min flux). *B*, uptake of uridine by hCNT1 (*solid bars*) and hCNT1/L354V (*open bars*) measured at pH 7.5 in transport media containing 100 mM NaCl, LiCl, or choline chloride (20 μ M, 20°C, 30 min flux). Data are presented as mediated transport, calculated as uptake in RNA-injected oocytes minus uptake in water-injected oocytes. Each value represents the mean \pm S.E. of 10-12 oocytes.

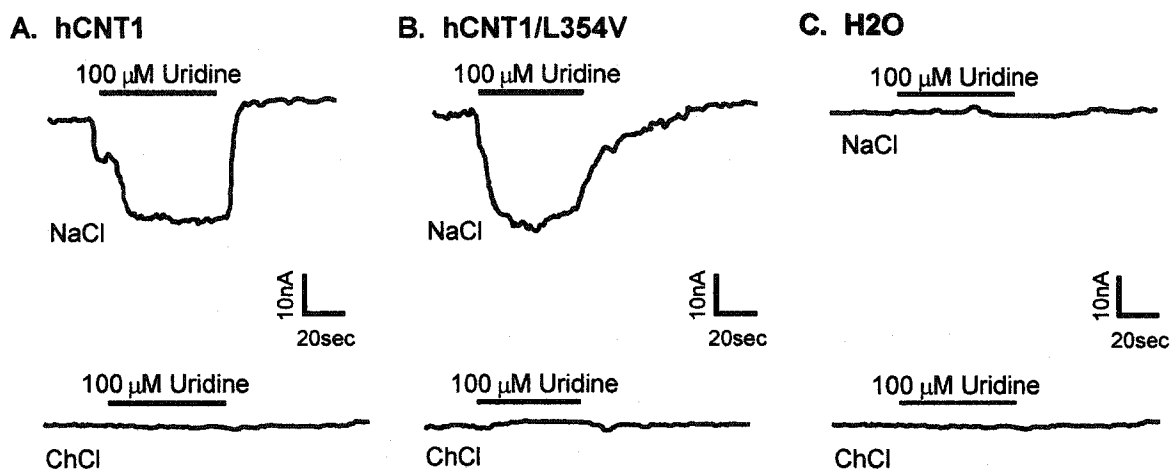


Figure 3-7. Uridine-evoked currents in hCNT1- and hCNT1/L354V-producing oocytes. *Upper traces* show uridine-evoked currents in NaCl transport medium at 20°C by representative oocytes producing hCNT1 or hCNT1/L354V in comparison with a control water-injected oocyte. *Lower traces* show corresponding traces for the same oocytes perfused with choline chloride transport medium. *Bars* indicate the duration of exposure to uridine (100 μ M).

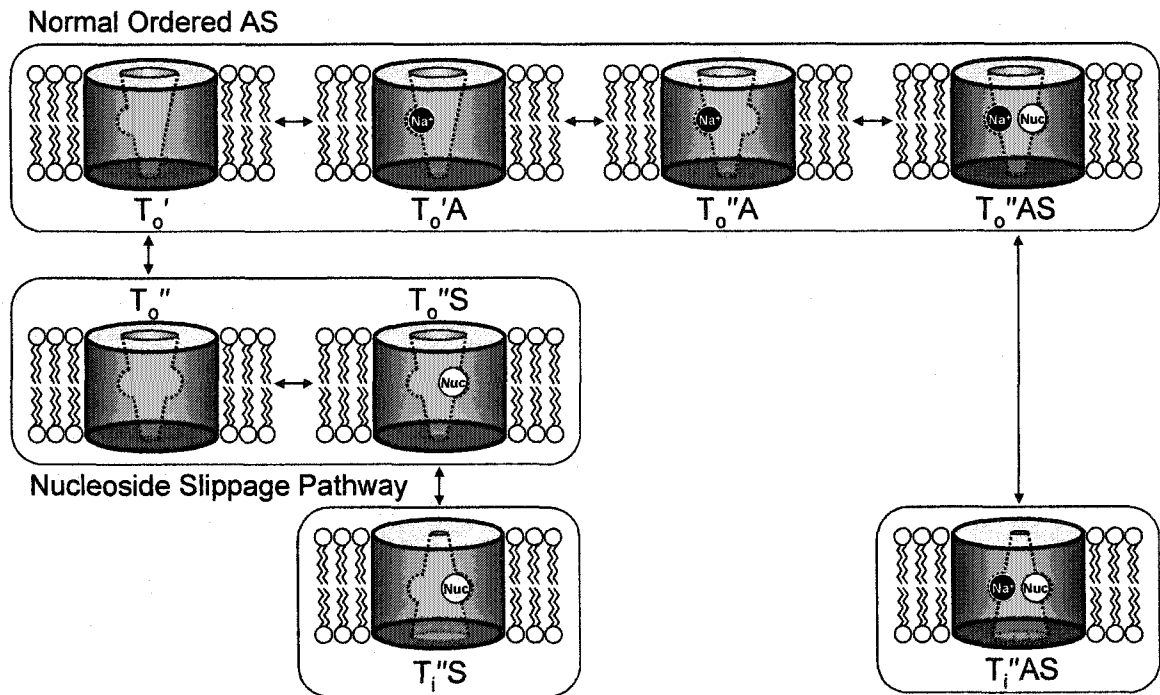


Figure 3-8. Ordered binding (AS) transport model with substrate slippage. Selected carrier states are depicted for an ordered transport model incorporating secondary uncoupled transport pathways based on a theoretical kinetic model developed by Krupka (Krupka, 1993). Nomenclature for the carrier states is as follows: T_i' and T_o' , inwardly- and outwardly-facing conformations of the transporter, respectively, with a single binding site; T_i'' and T_o'' , inwardly- and outwardly-facing conformations of the transporter, respectively, with two binding sites; A, Na^+ (activator); S, nucleoside (substrate).

Bibliography

- Baldwin SA, Mackey JR, Cass CE, and Young JD** (1999) Nucleoside transporters: molecular biology and implications for therapeutic development. *Mol Med Today* 5: 216-224.
- Che M, Ortiz DF, and Arias IM** (1995) Primary structure and functional expression of a cDNA encoding the bile canalicular, purine-specific Na⁺-nucleoside cotransporters. *J Biol Chem* 270: 13596-13599.
- Cheeseman CI, Mackey JR, Cass CE, Baldwin SA, and Young JD** (2000) Molecular mechanism of nucleoside and nucleoside drug transport. In *Gastrointestinal Transport*. (Barrett KE and Donowitz M, eds.) pp. 330-379, Academic Press, San Diego.
- Crawford CR, Patel DH, Naeve C, and Belt JA** (1998) Cloning of a human equilibrative, nitrobenzylmercaptapurine riboside (NBMPR)-insensitive nucleoside transporter *ei* by functional expression in a transport-deficient cell line. *J Biol Chem* 273: 5288-5293.
- de Koning HP, and Jarvis SM** (1999) Adenosine transporters in bloodstream forms of *Trypanosoma brucei brucei*: substrate recognition motifs and affinity for trypanocidal drugs. *Mol Pharmacol* 56: 1162-1170.
- Dunwiddie TV, and Masino SA** (2001) The role and regulation of adenosine in the central nervous system. *Annu Rev Neurosci* 24: 31-55.
- Eskandari S, Loo DD, Dai G, Levy O, Wright EM, and Carrasco N** (1997) Thyroid Na⁺/I⁻ symporter. Mechanism, stoichiometry, and specificity. *J Biol Chem* 272: 27230-27238.
- Flanagan SA, and Meckling-Gill KA** (1997) Characterization of a novel Na⁺-dependent, guanosine-specific, nitrobenzylthioinosine-sensitive transporter in acute promyelocytic leukemia cells. *J Biol Chem* 272: 18026-18032.
- Griffith DA and Jarvis SM** (1996) Nucleoside and nucleobase transport systems of mammalian cells. *Biochim Biophys Acta Rev Biombr* 1286: 153-181.
- Griffiths M, Beaumont N, Yao SYM, Sundaram M, Bouman CE, Davies A, Kwong FYP, Coe IR, Cass CE, Young JD, and Baldwin SA** (1997a) Cloning of a human nucleoside transporter implicated in the cellular uptake of adenosine and chemotherapeutic drugs. *Nat Med* 3: 89-93.
- Griffiths M, Yao SYM, Abidi F, Phillips SEV, Cass CE, Young JD, and Baldwin SA** (1997b) Molecular cloning and characterization of a nitrobenzylthioinosine-insensitive (*ei*) equilibrative nucleoside transporter from human placenta. *Biochem J* 328: 739-743.
- Hamilton SR, Yao SYM, Ingram JC, Hadden DA, Ritzel MWL, Gallagher MP, Henderson PJ, Cass CE, Young JD, and Baldwin SA** (2001) Subcellular distribution and membrane topology of the mammalian concentrative Na⁺-nucleoside cotransporter rCNT1. *J Biol Chem* 276: 27981-27988.

- Huang QQ, Yao SYM, Ritzel MWL, Paterson ARP, Cass CE, and Young JD** (1994) Cloning and functional expression of a complementary DNA encoding a mammalian nucleoside transport protein. *J Biol Chem* 269: 17757-17760.
- Hyde RJ, Cass CE, Young JD, and Baldwin SA** (2001) The ENT family of eukaryote nucleoside and nucleobase transporters: recent advances in the investigation of structure/function relationships and the identification of novel isoforms. *Mol Membr Biol* 18: 53-63.
- Klamo EM, Drew ME, Landfear SM, and Kavanaugh MP** (1996) Kinetics and stoichiometry of a proton/myo-inositol cotransporters. *J Biol Chem* 271: 14937-14943.
- Krupka RM** (1993) Coupling mechanisms in active transport. *Biochim Biophys Acta* 1183: 105-113.
- Krupka RM** (1994) Interpreting the effects of site-directed mutagenesis on active transport systems. *Biochim Biophys Acta* 1193: 165-178.
- Loewen SK, Ng AML, Yao SYM, Cass CE, Baldwin SA and Young JD** (1999) Identification of amino acid residues responsible for the pyrimidine and purine nucleoside specificities of human concentrative Na⁺ nucleoside cotransporters hCNT1 and hCNT2. *J Biol Chem* 274: 24475-24484.
- Mackenzie B, Loo DD, Fei Y, Liu WJ, Ganapathy V, Leibach FH, and Wright EM** (1996) Mechanisms of the human intestinal H⁺-coupled oligopeptide transporter hPEPT1. *J Biol Chem* 271: 5430-5437.
- Mackey JR, Baldwin SA, Young JD, and Cass CE** (1998) Nucleoside transport and its significance for anticancer drug resistance. *Drug Resistance Updates* 1: 310-324.
- Mitchell P** (1990) Osmochemistry of solute translocation. *Res Microbiol* 141: 286-289.
- Pajor AM, and Wright EM** (1992) Cloning and functional expression of a mammalian Na⁺/nucleoside cotransporter. A member of the SGLT family. *J Biol Chem* 267: 3557-3560.
- Panayotova-Heiermann M, Loo DD, and Wright EM** (1995) Kinetics of steady-state currents and charge movements associated with the rat Na⁺/glucose cotransporters. *J Biol Chem* 270: 27099-27105.
- Ritzel MWL, Yao SYM, Huang MY, Elliot JF, Cass CE, and Young JD** (1997) Molecular cloning and functional expression of cDNAs encoding a human Na⁺-nucleoside cotransporters (hCNT1). *Am J Physiol* 272: C707-C714.
- Ritzel MWL, Yao SYM, Ng AML, Mackey JR, Cass CE, and Young JD** (1998) Molecular cloning, functional expression and chromosomal localization of a cDNA encoding a human Na⁺ nucleoside cotransporters (hCNT2) selective for purine nucleosides and uridine. *Mol Membr Biol* 15: 203-211.

- Ritzel MWL, Ng AML, Yao SYM, Graham K, Loewen SK, Smith KM, Ritzel RG, Mowles DA, Carpenter P, Chen X-Z, Karpinski E, Hyde RJ, Baldwin SA, Cass CE, and Young JD (2001)** Molecular identification and characterization of novel human and mouse concentrative Na⁺-nucleoside cotransporters proteins (hCNT3 and mCNT3) broadly selective for purine and pyrimidine nucleosides (system *cib*). *J Biol Chem* 276: 2914-2927.
- Shryock JC, and Belardinelli L (1997)** Adenosine and adenosine receptors in the cardiovascular system: biochemistry, physiology and pharmacology. *Am J Cardiol* 79: 2-10.
- Sundaram M, Yao SYM, Ingram JC, Berry ZA, Abidi F, Cass CE, Baldwin SA, and Young JD (2001)** Topology of a human equilibrative, nitrobenzylthioinosine (NBMPR)-sensitive nucleoside transporter (hENT1) implicated in the cellular uptake of adenosine and anti-cancer drugs. *J Biol Chem* 276: 45270-45275.
- Wang J, Su SF, Dresser MJ, Schaner ME, Washington CB, and Giacomini KM (1997)** Na⁺-dependent purine nucleoside transporter from human kidney: cloning and functional characterization. *Am J Physiol* 273: F1058-F1065.
- Williams TC and Jarvis SM (1991)** Multiple sodium-dependent nucleoside transport systems in bovine renal brush-border membrane vesicles. *Biochem J* 274: 27-33.
- Yamato I (1992)** Ordered binding model as a general mechanistic mechanism for secondary active transport systems. *FEBS Lett* 298: 1-5.
- Yamato I, and Anraku Y (1989)** Dependence on pH of substrate binding to a mutant lactose carrier, lacYun, in *Escherichia coli*. A model for H⁺/lactose symport. *Biochem J* 258: 389-396.
- Yao SYM, Ng AML, Ritzel MWL, Gati WP, Cass CE, and Young JD (1996)** Transport of adenosine by recombinant purine- and pyrimidine-selective sodium/nucleoside cotransporters from rat jejunum expressed in *Xenopus laevis* oocytes. *Mol Pharmacol* 50: 1529-1535.
- Yao SYM, Ng AML, Muzyka WR, Griffiths M, Cass CE, Baldwin SA, and Young JD (1997)** Molecular cloning and functional characterization of nitrobenzylthioinosine (NBMPR)-sensitive (*es*) and NBMPR-insensitive (*ei*) equilibrative nucleoside transporter proteins (rENT1 and rENT2) from rat tissues. *J Biol Chem* 272: 28423-28430.
- Yao SYM, Ng AML, Sundaram M, Cass CE, Baldwin SA, and Young JD (2002a)** Functional and molecular characterization of nucleobase transport by recombinant human and rat ENT1 and ENT2 equilibrative nucleoside transport proteins: chimeric constructs reveal a role for the ENT2 helix 5-6 region in nucleobase translocation. *J Biol Chem* (in press).
- Yao SYM, Ng AML, Loewen SK, Cass CE, Baldwin SA, and Young JD (2002b)** An ancient marine pre-vertebrate Na⁺/nucleoside cotransporter (hfCNT) from the Pacific hagfish (*Eptatretus stouti*). *Am J Physiol* 283: C155-C168.

CHAPTER IV: *

Molecular identification and characterization of novel human and mouse concentrative Na⁺-nucleoside cotransporter protein (hCNT3 and mCNT3) broadly selective for purine and pyrimidine nucleosides (system *cib*). **

* *A version of this chapter has been published. Sections describing H⁺-coupled CNT3-mediated nucleoside transport and the functional characteristics of chimeric constructs between hCNT3/hCNT1 were not presented in the original publication and will form the basis of a separate publication of which I will be first author.*

Ritzel MW, Ng AML, Yao SYM, Graham K, Loewen SK, Smith KM, Ritzel RG, Mowles DA, Carpenter P, Chen XZ, Karpinski E, Hyde RJ, Baldwin SA, Cass CE, Young JD (2001) *J Biol Chem* 276: 2914-2927.

** My contribution to the studies described in this chapter was to work with Dr. Sylvia Yao to undertake the functional characterization of the human and mouse CNT3 transporters by radioisotope flux techniques. In addition, I was responsible for the phylogenetic/structural analysis of the CNT3 proteins. The sections describing H⁺-coupled nucleoside transport by CNT3 and hCNT3/hCNT1 chimeras are also my own work.

Introduction

Most nucleosides, including those with antineoplastic and/or antiviral activities (Handschumacher *et al.*, 1993; Groothuis and Levy, 1997), are hydrophilic, and specialized plasma membrane nucleoside transporter (NT) proteins are required for uptake into or release from cells (Cass *et al.*, 1995; Baldwin *et al.*, 1999). NT-mediated transport is therefore a critical determinant of metabolism and, for nucleoside drugs, their pharmacologic actions (Mackey *et al.*, 1998a). NTs also regulate adenosine concentrations in the vicinity of cell surface receptors and have profound effects on neurotransmission, vascular tone and other processes (Fredholm, 1997; Shryock and Belardinelli, 1997).

Seven nucleoside transport processes that differ in their cation dependence, permeant selectivities and inhibitor sensitivities have been observed in human and other mammalian cells and tissues. The major concentrative systems (*cit*, *cif*, *cib*) are inwardly-directed Na⁺-dependent processes and have been primarily described in specialized epithelia such as intestine, kidney, liver and choroid plexus, in other regions of the brain, and in splenocytes, macrophages and leukemic cells (Cass *et al.*, 1995; Baldwin *et al.*, 1999). Concentrative NT transcripts have also been found in heart, skeletal muscle, placenta and pancreas. The equilibrative (bidirectional) transport processes (*es*, *ei*) have generally lower substrate affinities and occur in most, possibly all, cell types (Cass *et al.*, 1995; Baldwin *et al.*, 1999). Epithelia (*e.g.* intestine, kidney) and some nonpolarized cells (*e.g.* leukemic cells) coexpress both concentrative and equilibrative NTs, whereas other nonpolarized cells (*e.g.* erythrocytes) exhibit only equilibrative NTs (Cass *et al.*, 1995; Baldwin *et al.*, 1999). Systems *cit* and *cif* are generally pyrimidine nucleoside selective and purine nucleoside selective, respectively, while systems *cib*, *es* and *ei* transport both pyrimidine and purine nucleosides. System *ei* also transports nucleobases.

Molecular cloning studies have isolated cDNAs encoding the human and rat proteins responsible for four of these NT processes (*cit*, *cif*, *es*, *ei*) (Huang *et al.*, 1994; Che *et al.*, 1995; Yao *et al.*, 1996a; Griffiths *et al.*, 1997a, 1997b; Ritzel *et al.*, 1997; Wang *et al.*, 1997; Yao *et al.*, 1997, Crawford *et al.*, 1998; Ritzel *et al.*, 1998). These proteins and their homologs in other mammalian species comprise two previously unrecognized families of integral membrane proteins (CNT and ENT) with quite different predicted architectural designs (Cass *et al.*, 1995;

Baldwin *et al.*, 1999). The relationships of these NT proteins to the processes defined by functional studies are: CNT1 (*cit*), CNT2 (*cif*), ENT1 (*es*), and ENT2 (*ez*). While the NT protein(s) responsible for mammalian *cib* have remained elusive, we have recently identified a CNT protein with *cib*-type transport activity from the ancient marine vertebrate, the Pacific hagfish (*Eptatretus stouti*) (Loewen *et al.*, 1999; Yao *et al.*, 2002; as described in *Chapter V*). The CNT family also includes the *Escherichia coli* proton/nucleoside symporter NupC (Craig *et al.*, 1994). Human and rat CNT1 (650 and 648 residues, 71 kDa), designated hCNT1 and rCNT1, respectively, are 83% identical in amino acid sequence (Huang *et al.*, 1994; Ritzel *et al.*, 1997), and contain 13 putative TMs with an exofacial glycosylated tail at the carboxyl-terminus (Loewen *et al.*, 1999; Hamilton *et al.*, 2001). hCNT2 (658 residues) (Wang *et al.*, 1997; Ritzel *et al.*, 1998) is 83% identical to rCNT2 (659 residues) (Che *et al.*, 1995; Yao *et al.*, 1996a) and 72% identical to hCNT1 (Ritzel *et al.*, 1997). The hagfish transporter hCNT (683 residues) (Loewen *et al.*, 1999) is 50-52% identical to h/rCNT1/2 and has a similar predicted membrane topology. NupC (Craig *et al.*, 1994), in contrast, is a smaller protein with 27% identity to mammalian CNTs, with the major difference being the absence of the equivalents of TM 1-3 and the amino- and carboxyl-terminal regions of the other proteins.

As described in *Chapter II*, the characteristics of hCNT1/2 chimeras and sequence comparisons between h/rCNTs and hCNT have identified two sets of adjacent residues in TMs 7 and 8 of hCNT1 that, when converted to the corresponding residues in hCNT2, changed the specificity of the transporter from *cit* to *cif* (Loewen *et al.*, 1999). Mutation of the two residues in TM 7 alone produced a protein with intermediate, *cib*-like activity. In this *cit/cib* conversion, mutation of hCNT1 Ser³¹⁹ to Gly was sufficient to enable transport of purine nucleosides, while mutation of the adjacent residue Gln³²⁰ to Met (which had no effect on its own) augmented this transport. TMs 7 and 8 have also been identified as potential determinants of substrate selectivity in rCNT1/2 (Wang and Giacomini, 1997), and mutation of rCNT1 Ser³¹⁸ (the rat counterpart of hCNT1 Ser³¹⁹) resulted in a *cib*-type phenotype similar to that seen with the hCNT1 Ser³¹⁹ mutation (Wang and Giacomini, 1999).

Although an earlier study had identified a member of the SGLT glucose transporter family, SNST1, as a candidate *cib*-type transporter (Pajor and Wright, 1992), its nucleoside-transport activity is very low and we hypothesized that the missing mammalian concentrative NT was

more likely to be a CNT transporter. This chapter outlines the cDNA cloning and functional characterization of new human and mouse members of the CNT transporter family. The encoded proteins, designated hCNT3 and mCNT3, respectively, exhibit strong *cib*-type functional activity when expressed in *Xenopus* oocytes and have primary structures that place them together with hCNT in a CNT subfamily separate from h/rCNT1/2.

Materials and Methods

Molecular Cloning of hCNT3 – BLAST searches of CNT sequences in the GenBank™ database identified overlapping human ESTs from mammary gland (AI905993) and colon adenocarcinoma (AW083022) different from established members of the CNT transporter family. Together, they formed a composite cDNA fragment 807-bp in length with an open reading frame of 245 residues followed by 69-bp of untranslated 3'-sequence. The cDNA was 62% identical in nucleotide sequence to corresponding regions of the hCNT1 (U62968) and hCNT2 (AF036109) cDNAs, and 68% identical to the hCNT (AF132298) cDNA. The encoded amino acid sequence was 79% identical to the carboxyl-terminus of hCNT, and 58 and 62% identical, respectively, to hCNT1 and hCNT2.

These indications of a novel human CNT distinct from hCNT1 and hCNT2 were tested by RT-PCR in a panel of total RNA samples from human mammary gland, small intestine, kidney (Clontech, Palo Alto, CA) and liver (Ritzel *et al.*, 1998). Since the close sequence similarity between the EST composite sequence and hCNT suggested that the new CNT might correspond to system *cib*, we also performed RT-PCR on differentiated human myeloid HL-60 cells, a source of functional *cib*-type transport activity (see below). First strand cDNA was synthesized using the Superscript Preamplification system (GIBCO/BRL, Burlington, ON) and oligo(dT) as primer. The PCR reaction (30 μ l) contained 50 ng of template first-strand cDNA, 2.5 U of *Taq*-DeepVent DNA polymerase (100:1) and 10 pmol each of the 5'- and 3'-oligonucleotide primers 5'-GAAACATGTTTGACTACCCACAG-3' and 5'-GTGGAGTTGAAGGCATTCTCTAAAACGT-3'. Amplification for one cycle at 94°C for 55 s, 54°C for 55 s and 72°C for 70 s, two cycles at 94°C for 55 s, 55°C for 55 s and 72°C for 70 s, and 30 cycles at 94°C for 55 s, 58°C for 55 s and 72°C for 70 s (Robocycler™ 40 Temperature Cycler, Stratagene, La Jolla, CA) generated visible PCR products of the predicted

size (480-bp) from four of the samples (differentiated HL-60 cells, mammary gland, small intestine, liver).

We extended the partial EST cDNA sequence by 5'-RACE amplification of mRNA from differentiated HL-60 cells using the FirstChoice RLM-RACE kit (Ambion, Austin, TX). Poly(A)⁺-selected RNA was treated with CIP to degrade 5'-truncated transcripts, followed by TAP to remove cap from the remaining full-length mRNAs. A synthetic RNA adaptor from the kit was then ligated to the full-length 5'-monophosphate transcript population using T4 RNA ligase, followed by first strand cDNA synthesis with oligo(dT) as primer. For the initial PCR, the 5'-primer was the outer adaptor primer provided by the kit and the gene-specific 3'-primer was 5'-GATATATATTGCTGCACACCGTTTACAA-3'. Amplification by *Taq-DeepVent* DNA polymerase (100:1) was for 40 cycles at 94°C for 55 s, 65°C for 55 s and 72°C for 3 min, and 1 cycle at 72°C for 10 min, the reaction mixture being heated to 94°C for 1 min before addition of the *Taq-DeepVent* DNA polymerase mixture. The PCR reaction mixture was resolved on a 1% agarose gel, and faint bands between 1.5-2.0 kb in size were isolated and purified (QIAEX II Gel Extraction kit, Qiagen Inc., Mississauga, ON). This product was then reamplified by nested PCR (35 cycles at 94°C for 55 s, 65°C for 55 s and 72°C for 3 min, 1 cycle at 72°C for 10 min) using an inner 5'-primer from the kit and the gene-specific 3'-primer 5'-TTAGCTCAAAACTCAGCTGTGGGTAGTC-3'. A defined band of ~ 1.7 kb was isolated, cloned into pGEM-T (Promega, Madison, WI) and sequenced by *Taq* DyeDeoxyterminator cycle sequencing using an automated Model 373A DNA Sequencer (Applied Biosystems, Foster City, CA). The inset overlapped the 807-bp EST sequence by 114 bp and generated an additional 1633 bp of upstream sequence. The new composite 2440-bp sequence was 66% identical to the hfcNT cDNA and contained an open reading frame of 691 amino acids. cDNAs containing the complete coding sequence were then obtained by RT-PCR from differentiated HL-60 cells and mammary gland, as previously described, using 5'- and 3'-primers flanking the open reading frame (5'-CTAAATGAAGAGCGCTTGGGACCT-3' and 5'-AGCATCTGTACTTCAGAGTTCCACTGG-3'). The resulting ~ 2.2-kb products were ligated into pGEM-T and sequenced in both directions to give identical 691-residue open reading frames flanked by 92 bp of untranslated 5'-nucleotide sequence and 41 bp of untranslated 3'-sequence.

As expected from their identical nucleotide and predicted amino acid sequences, there was no difference in hCNT3 transport function between cDNA clones isolated from HL-60 cells or mammary gland. Radioisotope transport studies reported in this paper were performed with the HL-60 clone in pGEM-T. pGEM-HE was also used for electrophysiological studies of hCNT3.

Molecular Cloning of mCNT3 – BLAST searches of mouse ESTs in the GenBank™ database identified 630- and 635-bp sequences from two mammary gland IMAGE clones with 73 and 83% sequence identity to parts of the hCNT3 cDNA sequence. IMAGE clone 1514965 aligned with the 5'-coding region, while 1515408 ended 54 bp short of the predicted stop codon. Both clones were obtained from the IMAGE Consortium through the American Type Culture Collection (Manassas, VA). PCR showed that they were incomplete, and sequencing of 1515408 gave an additional 85 bp of sequence to complete the 3'-end of the open reading frame. A cDNA with the complete coding sequence was then obtained by RT-PCR from mouse liver RNA (Jackson Laboratories, Bar Harbour, ME) with 5'-primer 5'-AGGATGTCCAGGGCAGACCCGGGAAAGA-3' and 3'-primer 5'-AGATCACAATTTATTAGGGATCCAATTG-3'. First strand cDNA was synthesized using the ThermoScript RT-PCR System (Life Technologies, Burlington, ON), and amplification by *Taq-DeepVent* DNA polymerase (100:1) was for 2 cycles at 94°C for 2 min, 64°C for 1 min and 72°C for 2.5 min, 2 cycles at 94°C for 1 min, 62°C for 1 min, and 72°C for 2.5 min, 30 cycles at 94°C for 1 min, 60°C for 1 min, and 72°C for 2.5 min, and one final extension cycle for 10 min at 72°C. The resulting ~ 2.0-kb product was ligated into pGEM-T and subcloned into the enhanced *Xenopus* expression vector pGEM-HE (Liman *et al.*, 1992). Each was sequenced in both directions, giving identical 703 amino acid residue open reading frames flanked by short 3-bp regions of untranslated 5'- or 3'-nucleotide sequence. By providing additional untranslated 5'- and 3'-sequences from a *Xenopus* β -globin gene, the pGEM-HE construct gave greater functional activity and was used in subsequent transport characterization of the mouse protein.

Construction of Chimeric hCNT3 and hCNT1 Transporters – hCNT1 cDNA was subcloned into the vector pGEM-HE (Liman *et al.*, 1992) prior to chimera construction with

hCNT3 (which was already in pGEM-HE) to enhance expression in *Xenopus* oocytes. Overlap primers (sense; 5'-AAGATTGCCTGGCTGATGCAAGTCACCATGGGCACCAC-3'; antisense; 5'-GTGACTTGCATCAGCCAGGCAATCTTTCTAATAATCCA-3') were designed at a splice site between Lys³¹⁴ and Val³¹⁵ of hCNT3 in the loop linking TM6 and TM7 (arrow in Fig. 4-20) to create reciprocal 50:50 chimeras by a two-step overlap extension PCR method (Horton *et al.*, 1989) using the universal pUC/M13 forward and reverse primers and high fidelity *Pyrococcus furiosus* DNA polymerase. Chimeric constructs containing the restriction site *KpnI* downstream of the M13 forward primer and the restriction site *SphI* upstream of the M13 reverse primer were subcloned into the respective restriction sites of the pGEM-HE vector. The chimeras were sequenced in both directions to verify the splice sites and ensure that no mutations had been introduced.

Expression of Recombinant hCNT3 and mCNT3 in *Xenopus* Oocytes – hCNT3 and mCNT3 plasmid DNAs were linearized with *NotI* (pGEM-T) or *NheI* (pGEM-HE), and transcribed with T7 polymerase mMMESSAGE mMACHINE™ (Ambion). Stage VI oocytes of *Xenopus laevis* (Huang *et al.*, 1994) were microinjected with 20 nl of water or 20 nl of water containing capped RNA transcripts (20 ng) and incubated in modified Barth's medium (changed daily) at 18°C for 72 h prior to the assay of transport activity.

hCNT3 and mCNT3 Radioisotope Flux Studies – Transport was traced using the appropriate [¹⁴C/³H]-labeled nucleoside, nucleoside drug or nucleobase (Moravsek Biochemicals, Brea, CA or Amersham Pharmacia Biotech, Arlington Heights, IL) at a concentration of 1 and 2 µCi/ml for [¹⁴C]-labeled and [³H]-labeled compounds, respectively. [³H]Gemcitabine (2',3'-difluorodeoxycytidine) was a gift from Eli Lilly Inc. (Indianapolis, IN). Radiochemicals were 98-99% pure (see HL-60 transport studies). Flux measurements were performed at room temperature (20°C) as described previously (Huang *et al.*, 1994; Ritzel *et al.*, 1997) on groups of 12 oocytes in 200 µl of transport medium containing 100 mM NaCl, 2 mM KCl, 1 mM CaCl₂, 1 mM MgCl₂, and 10 mM HEPES, pH 7.5. Except where otherwise indicated, the nucleoside concentration was 20 µM. At the end of the incubation period, extracellular label was removed by six rapid washes in ice-cold transport medium, and individual oocytes were dissolved in 5% (w/v) SDS for quantitation of oocyte-associated radioactivity by liquid scintillation counting (LS 6000 IC, Beckman, Mississauga, ON). Initial

rates of transport (influx) were determined using an incubation period of 5 min (Huang *et al.*, 1994). Choline replaced sodium in Na⁺-dependence experiments, and the transport medium for adenosine uptake contained 1 μM deoxycoformycin to inhibit adenosine deaminase activity. The flux values shown are means ± S.E. of 10-12 oocytes from one representative experiment. Significant differences in mean flux values were determined by Student's t-test (P = 0.05). Each experiment was performed at least twice on different batches of cells. Kinetic (K_m and V_{max}) and Na⁺-activation parameters (K_{50} and Hill coefficient) ± S.E. were determined using ENZFITTER (Elsevier-Biosoft, Cambridge, UK) and SigmaPlot (SPSS Inc., Chicago, IL) software, respectively.

Measurement of hCNT3-induced Sodium and Proton Currents – Oocytes were voltage clamped using the two electrode voltage clamp. Membrane currents were measured at room temperature by use of a GeneClamp 500B oocyte clamp (Axon Instruments, Foster City, CA). The microelectrodes were filled with 3 M KCl and had resistances that ranged from 1 – 2.5 MΩ. The GeneClamp 500B was interfaced to a computer via a Digidata 1200 A/D converter and controlled by Axoscope software (Axon Instruments, Foster City, CA). Current signals were filtered at 20 Hz (four-pole Bessel filter) and sampled at intervals of 20 ms. For data presentation, the signals were further filtered at 0.5 Hz by use of pCLAMP software (Axon Instruments). Cells were not used if resting membrane potentials were unstable or less than – 30 mV. For measurements of hCNT3-generated currents, oocyte membrane potentials were clamped at – 50 mV. Oocytes were perfused with the same medium used for radioisotope flux studies, and transport assays were initiated by changing the substrate-free solution to one containing nucleoside (200 μM). In experiments examining Na⁺- and H⁺-dependence, sodium in the transport buffer was replaced with equimolar choline and pH was varied from 5.5 to 8.5.

Cation:Nucleoside Coupling Ratios – Na⁺:nucleoside and H⁺:nucleoside coupling ratios for hCNT3 and mCNT3 were determined by radiotracer transport-induced current measurements under voltage-clamp conditions in transport medium containing [¹⁴C]-labeled uridine (200 μM, 1 μCi/ml). Individual oocytes were placed in a perfusion chamber and voltage-clamped at a holding potential of –50 mV or –90 mV in the appropriate substrate-free transport medium for a 10 min period to monitor baseline currents. The transport medium

was then exchanged with medium of the same composition containing radiolabeled uridine. Current was measured for 3 min, followed immediately by reperfusion with substrate-free transport medium until current returned to baseline. The oocyte was recovered from the chamber and solubilized with 1% SDS for liquid scintillation counting. The total movement of charge across the plasma membrane was calculated from the current-time integral and correlated with the measured radiolabeled flux for each oocyte to calculate the charge:flux ratio. [¹⁴C]-labeled uridine uptake in H₂O-injected oocytes was used to correct for endogenous uptake of uridine over the same incubation period. The coupling ratios presented are means ± S.E. of 10 or more oocytes.

HL-60 Cell Culture and Differentiation – The human promyelocytic cell line, HL-60, obtained from the American Type Culture Collection, was propagated as suspension cultures in RPMI 1640 medium, supplemented with 10% foetal calf serum using reagents purchased from Life Technologies (Gaithersburg, MD). Stock cultures were maintained in 5% CO₂ without antibiotics at 37°C, subcultured every 3-4 days, and demonstrated to be mycoplasma-free. Cell numbers were determined using a Coulter Counter Model Z2 (Coulter Electronics Inc., Luton, UK).

To induce differentiation, HL-60 cells (3×10^6) growing in logarithmic phase were placed in 10-cm Falcon Primaria tissue culture plates (Becton Dickinson, Mississauga, ON) in the presence of PMA (200 ng/ml) (Sigma Chemical Co., Oakville, ON) freshly dissolved in acetone. After 48 h, the plates were washed once with transport buffer (see below) to remove non-adherent cells and then incubated for 15 min in the presence or absence of 100 μM dilazep. Transport assays were performed on the remaining adherent cells. Total RNA and mRNA were prepared from exponentially growing parent and adherent HL-60 cells using the RNeasy Mini Protocol (Qiagen) and Fast Track 2.0 Isolation kit (Invitrogen, Carlsbad, CA), respectively.

HL-60 Radioisotope Flux Studies – Nucleoside uptake by differentiated HL-60 cells was measured as previously described (Graham *et al.*, 2000) by exposing replicate cultures at room temperature to [³H]-labeled permeant (10 μM, 1 μCi/ml) in sodium or sodium-free transport medium (130 mM NaCl or 130 mM NMDG/HCl, and 3 mM K₂HPO₄, 2 mM

CaCl₂, 1 mM MgCl₂, 20 mM Tris/HCl and 5 mM glucose, pH 7.4). Radiochemicals (Moravsek Biochemicals) were 98-99% pure as assessed by high-performance liquid chromatography using water-methanol gradients on a C18 reverse phase column, and transport for timed intervals of 1–6 min was terminated by immersion of the culture dish in an excess volume of ice-cold transport solution. Assays to detect concentrative transport were performed in the presence of 100 μM dilazep (a gift from Hoffman La Roche & Co., Basel, Switzerland) to block equilibrative transport of the test nucleoside. Transport by non-adherent parental HL-60 cells was performed as previously described (Boleti *et al.*, 1997) using the inhibitor-oil stop method. Values are presented as the means of triplicate measurements ± S.E.

Tissue and Cell Distribution of hCNT3 mRNA - A human multiple tissue expression (MTETM) RNA array (Clontech) and dot blots of mRNA (0.5 μg) from parent and differentiated HL-60 cells on BrightStar-Plus nylon transfer membrane (Ambion) were incubated with a cDNA probe corresponding to hCNT3 amino acid residues 359-549 labelled with ³²P using the T7QuickPrime kit (Pharmacia, Uppsala, Sweden). Hybridization at high stringency (68°C) was performed using ExpressHyb hybridization solution (Clontech) and 100μg/ml of sheared herring sperm DNA. Wash conditions were as described in the Clontech ExpressHyb user manual. Signals on exposed blots were converted to a high resolution tiff image (Hewlett Packard ScanJet 4C) and quantified using the public domain NIH Image program, version 1.60 (<http://rsb.info.nih.gov/nih-image/>). For Northern analysis, 5 μg samples of mRNA from human pancreas, bone marrow, trachea, intestine, liver, brain, heart and kidney (Clontech) were separated on a 0.8% formaldehyde-agarose gel, blotted on to BrightStar-Plus nylon transfer membrane and hybridized with the same hCNT3 probe (residues 359-549) under identical high stringency conditions.

Possible cross-hybridization between CNT family members was tested on dot blots of dilutions (0.5 μg – 5 ng RNA) of hCNT1, hCNT2 and hCNT3 *in vitro* transcripts. Three identical series of blots were incubated either with hCNT3 probe, or with equivalent probes for hCNT1 or hCNT2. The hCNT3 probe, which was 63 and 58% identical in nucleotide sequence to the corresponding regions of hCNT1 and hCNT2, respectively, showed no cross-hybridization with hCNT1 or hCNT2 transcripts. Similarly, there was no cross-reactivity between the hCNT1 and hCNT2 probes and hCNT3 RNA. Some cross-hybridization was

seen between the hCNT1 and hCNT2 probes (73% nucleotide sequence identity) and their respective transcripts at RNA loadings > 50 ng. Under the conditions of high stringency used in our experiments, the hCNT3 probe was therefore specific.

Quantitative Real Time RT-PCR – In TaqMan™ quantitative RT-PCR (Applied Biosystems), an oligonucleotide probe, labeled with a fluorescent tag at the 5'-end and a quenching molecule at the 3'-end, is located between two PCR primers. The 5'-nucleotidase activity of *Taq* polymerase cleaves the fluorescent dye from the probe during each PCR cycle. The fluorescent signal generated is monitored in real time and is proportional to the amount of starting template in the sample.

RNA from parent or differentiated HL-60 cells was reverse transcribed using the TaqMan™ Gold RT-PCR kit (Applied Biosystems) and subjected to real time PCR using an Applied Biosystems PRISM 7700 Sequence Detection System and TaqMan™ Universal PCR Master Mix kit. Amplification conditions were a single cycle at 50°C for 2 min and 95°C for 10 min, followed by 40 cycles at 95°C for 15 s and 1 min at 60°C using hCNT3 probe and primers designed using Primer Express software (Applied Biosystems). The hCNT3 probe 5'-6FAM-CGGACTCACATCCATGGCTCCTTC-TAMRA-3' was purchased from Applied Biosystems, while the 5'- and 3'-primers were 5'-GGGTCCTAGGAATCGTGATC-3' and 5'-CGAGGCGATATCACGCTTTC-3', respectively. GADPH and 18S ribosomal RNA probes and primers, used as internal controls, were purchased as a TaqMan™ RNA Control Reagent kit. Relative quantification of hCNT3 message was determined as previously described (Fink *et al.*, 1998).

Chromosomal Fluorescence *in situ* Hybridization – Analysis of normal human lymphocyte metaphase chromosomes was performed by methods described previously (Roy *et al.*, 1996) using a PCR probe corresponding to hCNT3 amino acid residues 86 – 685. Chromosomal localization of the gene was also determined by screening an RPCI-11 human male BAC library (Plass *et al.*, 1997).

Results and Discussion

Membrane transport studies in various human and other mammalian cell and tissue preparations have produced evidence that concentrative (Na^+ -linked) cellular uptake of nucleosides and nucleoside drugs is mediated by at least three distinct mechanisms (Cass *et al.*, 1995; Baldwin *et al.*, 1999). Systems *cit* and *cif* are found primarily in specialized epithelia such as intestine, liver and kidney and have characteristic overlapping substrate specificities for pyrimidine and purine nucleosides, respectively. As well, a broadly selective transport activity for both pyrimidine and purine nucleosides (system *cib*) has been described (Cass *et al.*, 1995; Baldwin *et al.*, 1999). Expression cloning and other recombinant DNA strategies have recently established that systems *cit* and *cif* are mediated by isoforms of the CNT transporter family, designated in humans as hCNT1 and hCNT2, respectively (Huang *et al.*, 1994; Che *et al.*, 1995; Yao *et al.*, 1996a, Ritzel *et al.*, 1997; Wang *et al.*, 1997; Ritzel *et al.*, 1998). This chapter describes the molecular identification and characterization of the human and mouse *cib* transporters, and demonstrate that they represent a new mammalian isoform of the CNT transporter family (hCNT3 and mCNT3, respectively).

Molecular Identification of hCNT3 and mCNT3 - The possibility that *cib* might be a CNT transporter (Loewen *et al.*, 1999) led to identification of ESTs encoding partially overlapping regions at the carboxyl-terminus of a new, previously unrecognized human CNT distinct from hCNT1 or hCNT2. The full-length cDNA obtained by 5'-RACE/RT-PCR amplification of PMA-differentiated human myeloid HL-60 cells and by RT-PCR of human mammary gland encoded a 691-residue protein (77 kDa), designated here as hCNT3. Differentiated HL-60 cells represent a functionally defined source of *cib* transport activity (see below), while human mammary gland was the origin of one of the carboxyl-terminus ESTs. The hCNT3 sequence enabled us, in turn, to identify ESTs from mouse mammary gland encoding the amino- and carboxyl-terminus ends of a mouse homolog. The corresponding full-length mouse cDNA, obtained by RT-PCR from liver (also a source of hCNT3 transcript), encoded a 703-residue protein designated here as mCNT3.

hCNT3 and mCNT3 Amino Acid Sequences – hCNT3 was 57% identical in amino acid sequence to hCNT and 48 and 47% identical to hCNT1 and hCNT2, respectively (Fig. 4-

1). Protein structure algorithms predicted a topology for hCNT3 similar to that of hfCNT and hCNT1/2 (Hamilton *et al.*, 2001), with relatively large extramembraneous amino- and carboxy-termini (carboxyl-terminus external) linked by 13 TMs and short hydrophilic sequences (< 22 residues), with the exception of larger extracellular loops between TMs 5-6, 9-10 and 11-12 (Fig. 4-2). Residues within TMs 4-13 were particularly highly conserved between hCNT3 and hfCNT (67% sequence identity), while TMs 1-3 and the amino- and carboxyl-termini were much more divergent. The conserved TM 4-13 domains of hCNT3 and hfCNT corresponded closely to the predicted membrane architecture of the shorter *E coli* CNT proton/nucleoside co-transporter NupC (Craig *et al.*, 1994), suggesting that these regions represent the functionally important core structure of the proteins. We engineered an amino-terminal truncated form of rCNT1 and established that the TM 1-3 region is not required for transport activity (Hamilton *et al.*, 2001). mCNT3 contained additional amino acids at the amino terminus (Fig. 4-1) and was 78% identical in sequence to hCNT3, 57% identical to hfCNT and 48% identical to mCNT2 (AF079853), the other known mouse CNT.

Since we first identified rCNT1 from rat jejunum by expression selection in *Xenopus* oocytes in 1994, more than 40 members of the CNT protein family have been identified from mammals, lower vertebrates, insects, nematodes, pathogenic yeast and bacteria. As shown in Fig. 4-3, phylogenetic analysis identified discrete clusters of proteins, including two for bacteria and one for vertebrate transporters. hCNT3 and mCNT3 were placed together with hfCNT in a different vertebrate CNT subfamily from the human and other mammalian CNT1 and CNT2 proteins. Characteristically conserved motifs of the CNT transporter family present in hCNT3 and mCNT3 included GX₂₁GX₂FXFG between TMs 5 and 6, (G/A)XKX₃(N/T)E(F/Y)(V/F/T)(A/G/S)(Y/M/F) between TMs 11 and 12, and (G/S)F(A/S)N(F/I/P)(S/G)(S/T)X(G/A) in TM 12. In common with other CNTs, hCNT3 and mCNT3 also contained multiple consensus sites for N-linked glycosylation, grouped at the carboxyl-terminus (hCNT3 Asn⁶³⁶ and Asn⁶⁶⁴, mCNT3 Asn⁶⁴⁸ and Asn⁶⁷⁶). The extracellular location of this region has been confirmed by mutagenesis of rCNT1, which is glycosylated at Asn⁶⁰⁵ and Asn⁶⁴³ (Hamilton *et al.*, 2001).

In *Chapter II* (Loewen *et al.*, 1999), I identified two adjacent pairs of residues (Ser³¹⁹/Gln³²⁰ and Ser³⁵³/Leu³⁵⁴) in the TM 7-9 region of hCNT1 that, when mutated together to the

corresponding residues in hCNT2 (Gly³¹³/Met³¹⁴ and Thr³⁴⁷/Val³⁴⁸), converted hCNT1 (*cit*) into a transporter with *cif*-type functional characteristics. An intermediate broad specificity *cib*-like transport activity was produced by mutation of the two TM 7 residues alone: mutation of Ser³¹⁹ to Gly allowed for transport of purine nucleosides and this was augmented by mutation of Gln³²⁰ to Met. Mutation of Ser³⁵³ in TM 8 to Thr converted the *cib*-like transport of the TM 7 double mutant into one with *cif*-like characteristics, but with relatively low adenosine transport activity. Mutation of Leu³⁵⁴ to Val increased the adenosine transport capability of the TM 7/8 triple mutant, producing a full *cif* transport phenotype. On its own, mutation of Ser³⁵³ converted hCNT1 into a transporter with novel uridine-selective transport properties. The sequences of hCNT3 and mCNT3 at these positions were intermediate between hCNT1 and hCNT2, one member of each pair of residues being identical to the corresponding residue in hCNT1 and the other to that in hCNT2. These sequences in hCNT3 and mCNT3 were identical to hCNT (Gly³⁴⁰/Gln³⁴¹ and Ser³⁷⁴/Val³⁷⁵ in the case of hCNT3).

Functional Expression and Substrate Specificity of Recombinant hCNT3 and mCNT3 – hCNT1 and hCNT2 display *cit*- and *cif*-type Na⁺-dependent nucleoside transport activities (Huang *et al.*, 1994; Ritzel *et al.*, 1997). Therefore, while both hCNT1 and hCNT2 transport uridine and certain uridine analogs, they are otherwise selective for pyrimidine (hCNT1) and purine (hCNT2) nucleosides (except for modest transport of adenosine by hCNT1). hCNT, in contrast, exhibits *cib*-type Na⁺-dependent nucleoside transport activity and is broadly selective for both pyrimidine and purine nucleosides.

Fig. 4-4A shows a representative transport experiment in *Xenopus* oocytes measuring uptake of uridine and a panel of other radiolabeled pyrimidine and purine nucleosides (cytidine, thymidine, adenosine, guanosine and inosine) and nucleobases (uracil and hypoxanthine) in cells injected with water alone (control) or with water containing hCNT3 transcripts. Uptake of uridine (20 μM, 30 min flux) by hCNT3-expressing oocytes was Na⁺-dependent (60.7 ± 4.5 and 6.1 ± 0.7 pmol/oocyte in Na⁺ and choline medium, respectively) and concentrative (60.7 pmol/oocyte corresponds to an in-to-out concentration ratio ~ 3:1, calculated assuming an oocyte water content of 1 μl). In Na⁺ medium, uridine uptake in control water-injected oocytes was only 0.5 ± 0.1 pmol/oocyte, giving a mediated flux (uptake by RNA-injected oocytes minus uptake in water-injected oocytes) of 60.2 pmol/oocyte, and a

mediated-to-basal flux ratio of 120:1. Consistent with *cib*-type functional activity, each of the other pyrimidine and purine nucleosides tested (cytidine, thymidine, adenosine, guanosine and inosine) gave similar mediated fluxes. mCNT3 (Fig. 4-4B) exhibited a similar pattern of Na⁺-dependent *cib*-type functional activity, and neither protein transported uracil or hypoxanthine.

Fig. 4-5 compares the differences in substrate specificity between hCNT3, mCNT3, hfCNT, hCNT1 and hCNT2 by measuring the mediated uptake of three diagnostic nucleoside permeants (uridine, thymidine and inosine). All five proteins transported uridine. However, hCNT1 (*cit*) exhibited pyrimidine nucleoside selective characteristics (marked thymidine uptake, low inosine transport), while hCNT2 (*cif*) was purine nucleoside selective (low thymidine uptake, marked inosine transport). hCNT3, mCNT3 and hfCNT exhibited similar *cib*-type profiles, with marked transport of both thymidine and inosine. Subsequent in depth transport experiments focused on the human transporter hCNT3.

Kinetic Properties and Inhibitor Sensitivity of Recombinant hCNT3 – Fig. 4-6 shows representative concentration dependence curves for uridine, cytidine, thymidine, adenosine, guanosine and inosine, measured as initial rates of transport (5-min flux) in hCNT3-expressing oocytes and in control water-injected cells. Kinetic constants for the hCNT3-mediated component of influx are presented in Table 4-1. K_m values varied between 15 and 53 μM (cytidine, adenosine < uridine, thymidine < guanosine, inosine) and were within the range expected for native *cib*-type transporters (Wu *et al.*, 1992; Huang *et al.*, 1993; Hong *et al.*, 2000) and for hfCNT in oocytes (17-54 μM) (as described in *Chapter V*). They were also similar to K_m values obtained previously for permeants of recombinant mammalian CNT1/2 transporters. For example, the hCNT3 K_m for uridine was 22 μM compared to 37-45 μM for hCNT1, rCNT1 and hCNT2 (Huang *et al.*, 1994; Ritzel *et al.*, 1997; 1998). hCNT3 K_m values for thymidine and inosine were 21 and 53 μM , respectively, compared to 13 μM for thymidine transport by rCNT1 (Fang *et al.*, 1996) and 20 μM for inosine transport by rCNT2 (Wang and Giacomini, 1997). hCNT3 V_{max} values were in the range 24 and 51 pmol/oocyte.5 min⁻¹ (uridine, thymidine < cytidine, adenosine < guanosine, inosine), giving $V_{\text{max}}:K_m$ ratios of 0.9 to 2.1 (Table 4-1). These data support the *cib*-type specificity profile of hCNT3 shown in Fig. 4-4A and demonstrate that hCNT3 transports different pyrimidine and purine nucleosides with very similar efficiencies. For all of the nucleosides tested (Figs. 4-6A – F), influx in water-

injected oocytes was linear with concentration, consistent with non-mediated simple diffusion through the lipid bilayer.

In addition to the three major mammalian concentrative nucleoside transport systems *cit*, *cif* and *cib*, there are two minor Na⁺-dependent nucleoside transport processes (*cs_g* and *cs*), which have been described only in leukemic cells (Paterson *et al.*, 1993; Flanagan and Meckling-Gill, 1997). While their permeant preferences have not been well defined, the *cs_g* process (Flanagan and Meckling-Gill, 1997) accepts guanosine and the *cs* process (Paterson *et al.*, 1993) accepts adenosine analogs as permeants. In contrast to *cit*, *cif* and *cib*, both are inhibited by nanomolar concentrations of NBMPR (Paterson *et al.*, 1993; Flanagan and Meckling-Gill, 1997). hCNT3 was unaffected by NBMPR or other equilibrative nucleoside transport inhibitors, dipyridamole and dilazep, at concentrations up to 10 μM (100 μM for dilazep, which is more soluble), eliminating hCNT3 as a possible contributor to *cs_g* or *cs* transport activity (Fig. 4-7).

hCNT3 Na⁺:Nucleoside Cotransport – Na⁺/nucleoside coupling ratios of 1:1 have been described for various *cit* and *cif* transport activities in different mammalian cells and tissues (reviewed in Cass, 1995). In contrast, a coupling ratio of 2:1 has been reported for system *cib* in choroid plexus and microglia (Wu *et al.*, 1992; Hong *et al.*, 2000). In Figs. 4-8A & C, we show for both hCNT3 and mCNT3 that the relationship between uridine influx (10 μM) and Na⁺ concentration was sigmoidal. Fitting the data to the Hill equation, $v = V_{\max} \cdot [\text{Na}^+]^n / (K_{50}^n + [\text{Na}^+]^n)$, gave Hill coefficients (*n*) of 2.2 ± 0.2 (hCNT3) and 2.3 ± 0.1 (mCNT3), indicating a Na⁺/nucleoside coupling ratio of at least 2:1. Similar values of *n* (2.0 ± 0.2 and 2.0 ± 0.1, respectively) were determined from the slopes of Hill plots of the data (Figs. 4-8B & D), and in five independent experiments, Hill plot transformations gave a mean hCNT3 Hill coefficient of 2.1 ± 0.3. Since rCNT1 exhibited a Hill coefficient of 1 in similar experiments (Yao *et al.*, 1996), our data establish, for the first time, that the stoichiometry of Na⁺/nucleoside coupling is different in different CNT family members. In this respect, the CNTs resemble the SGLT glucose transporter family, where examples of proteins with 2:1 and 1:1 Na⁺/sugar coupling ratios (SGLT1/3 and SGLT2, respectively) have been described (Kanai *et al.*, 1994; Chen *et al.*, 1995; Mackenzie *et al.*, 1996, 1998; Diez-Sampedro *et al.*, 2001; Wright *et al.*, 2001). Similarly, the PepT2 and PepT1 proton-linked peptide transporters have

2:1 and 1:1 H⁺/peptide coupling ratios, respectively (Chen *et al.*, 1995). There was an interesting difference in K_{50} value for Na⁺ activation between hCNT3 and mCNT3 (16 ± 1 and 7 ± 1 mM, respectively), although both transporters were fully saturated with Na⁺ at cation concentrations approaching the physiological concentration range (Figs. 4-8A & C).

In addition to radioisotope flux studies, we also used the two-electrode voltage-clamp technique to investigate the Na⁺-dependence of hCNT3-mediated nucleoside transport. As shown in Fig. 4-9, external application of uridine, thymidine and inosine (200 μ M) to oocytes expressing recombinant hCNT3 induced inward currents for all three nucleosides that returned to baseline upon removal of permeant. No currents were seen in water-injected oocytes, or when Na⁺ in the extracellular medium was replaced by choline at pH 7.5, demonstrating that hCNT3 functions as a broad specificity electrogenic Na⁺/nucleoside symporter at physiological conditions.

Subsequent experiments determined directly the Na⁺/nucleoside coupling ratio of hCNT3 by simultaneous measurement of Na⁺ currents and [¹⁴C]uridine influx under voltage clamp conditions as described previously for the SDCT1 rat kidney dicarboxylate transporter (Chen *et al.*, 1998). As shown in Fig. 4-10A and B, where each data point represents a single oocyte, the slope of inward charge *versus* uridine flux was 1.63 ± 0.13 when oocytes were clamped at -50 mV and 2.01 ± 0.17 at -90 mV. Under hyperpolarized conditions, therefore, hCNT3 was confirmed to have a coupling stoichiometry of two Na⁺ ions to one molecule of nucleoside transported. As also occurs for the SGLT1 glucose transporter (Hirayama *et al.*, 1994), the lower coupling ratio of ~ 1.6 measured at -50 mV may reflect incomplete dissociation of Na⁺ from the inward-facing conformation of the transporter at less negative membrane potential. A two-Na⁺/one-nucleoside symporter will have a greater ability to transport permeant against its concentration gradient than a one-Na⁺/one-nucleoside symporter, and they may have evolved to transport nucleosides under different conditions. As described in a later Chapter, hCNT also exhibited a 2:1 stoichiometry, suggesting that a 2:1 coupling ratio is a general feature of the CNT3/hCNT subfamily shown in Fig. 4-4A. In marked contrast, preliminary charge *versus* uridine flux experiments confirm the expected, but different Na⁺:uridine transport ratio of 1:1 for hCNT1 (unpublished data).

pH- and Lithium-Dependence of Recombinant hCNT3 and mCNT3 – The two-microelectrode voltage-clamp technique was also used to assess the effects of protons as a possible driving force for hCNT3 and mCNT3. To do this, transporter-mediated currents were measured in the absence of sodium, at external pH values ranging from 5.5 to 8.5. As shown in Figs. 4-11A & B, hCNT3- and mCNT3-producing oocytes exhibited an inward uridine-evoked current under Na⁺-free conditions (choline chloride transport medium) that was pH dependent (pH 5.5 > pH 8.5) and absent from control water-injected oocytes. These currents, consistent with H⁺/uridine symport, were also seen for mCNT3-mediated transport of thymidine and inosine (Fig. 4-11C & D), demonstrating the ability of CNT3 proteins to extend proton coupling to other diagnostic *cib*-type pyrimidine and purine nucleoside permeants. At pH 7.5, the pH used in standard Na⁺-replacement experiments, the average hCNT3 proton current in the absence of Na⁺ was < 4% of that with Na⁺ present. This small current was not detected above background in some electrophysiological recordings (Fig. 4-9).

Parallel hCNT3 and mCNT3 radioisotope transport experiments confirmed H⁺/uridine symport by demonstrating a corresponding increase in [¹⁴C]-labeled uridine influx in Na⁺-free medium as the pH was lowered from 8.5 to 5.5 (Fig. 4-12). hCNT1 and hCNT2, in contrast, show no uridine flux in choline-containing medium regardless of pH, demonstrating that these transporters, unlike h/mCNT3, are strictly Na⁺-dependent. The effect of pH on hCNT3- and mCNT3-mediated uridine transport was similar in NMDG and choline chloride transport medium, whereas NaCl-replacement by equimolar LiCl at pH 8.5 showed a marked increase in uridine uptake compared to fluxes in choline chloride buffer at the same pH. This finding suggests that Li⁺ can also act as a Na⁺ substitute. In contrast, Li⁺ substitution had no effect on hCNT1 or hCNT2. Therefore, hCNT1 and hCNT2 are Na⁺-specific, while hCNT3 and mCNT3 can couple nucleoside transport to H⁺ or Li⁺ in addition to Na⁺. hCNT3 therefore resembles the SGLT1 and SGLT3 glucose transporters and the bacterial MelB melibiose transporter, which can also use Na⁺, Li⁺, and H⁺ as the coupling cation (Hirayama *et al.*, 1994; Kanai *et al.*, 1994; Pourcher *et al.*, 1995; Hirayama *et al.*, 1997).

Complementary to the results presented in Fig. 4-10A to determine the 2:1 Na⁺/nucleoside coupling ratio of hCNT3, we also performed charge/flux analyses to measure the corresponding stoichiometry for H⁺-coupled uridine transport (Fig. 4-10C and D). Performed

in Na^+ -free (choline chloride) transport medium at pH 5.5 and clamped at -50 and -90 mV, the results gave regression lines with slopes of 1.07 ± 0.11 and 0.91 ± 0.10 , respectively, suggesting a lower 1:1 coupling ratio for H^+ /nucleoside cotransport, which did not change at more negative membrane potentials. If, by analogy with Na^+ , two H^+ ions interact with the transporter, it is possible that one of the two bound protons may not dissociate from the protein during the translocation cycle.

hCNT3-mediated Transport of Anticancer and Antiviral Nucleoside Drugs – The difference in substrate specificity between CNT1 and CNT2 for physiological pyrimidine and purine nucleosides is reflected in their complementary roles for transport of pyrimidine and purine antiviral and anticancer nucleoside drugs. For example, we have used *Xenopus* oocyte expression to establish that mammalian CNT1/2 proteins transport antiviral dideoxynucleosides: h/rCNT1 transports the AIDS drugs AZT (3'-azido-3'-deoxythymidine) and ddC (2',3'-dideoxycytidine), but not ddI (2',3'-dideoxyinosine), while hCNT2 transports only ddI (Huang *et al.*, 1994, Yao *et al.*, 1996b; Ritzel *et al.*, 1997, 1998). Gemcitabine, a cytidine analog used in therapy of solid tumors, is a good hCNT1 permeant, but is not transported by hCNT2 either in oocytes (Mackey *et al.*, 1999) or in transfected HeLa cells (Mackey *et al.*, 1998b). As shown in Fig. 4-13, hCNT3, a *cib*-type NT, efficiently transported both pyrimidine (5-fluorouridine, 5-fluoro-2'-deoxyuridine, zebularine, gemcitabine) and purine (cladribine, fludarabine) anticancer nucleoside drugs. Lower, but still significant, uptake was observed for pyrimidine (AZT, ddC) and purine (ddI) antiviral nucleoside drugs, the magnitudes of the fluxes being similar to those found previously for hCNT1 (AZT, ddC) and hCNT2 (ddI) (Huang *et al.*, 1994; Ritzel *et al.*, 1997). Only ganciclovir, an antiviral drug with an acyclic ribose moiety, was not transported. Therefore, by virtue of its ability to transport both pyrimidine and purine nucleosides, hCNT3 is capable of transporting a broader range of therapeutic nucleosides than either hCNT1 or hCNT2. Consistent with the present results, thymidine transport by the microglial *cib* transporter was inhibited by AZT (Hong *et al.*, 2000).

In a final series of drug uptake experiments, we used the two electrode voltage clamp to investigate Na^+ and H^+ currents associated with hCNT3- and mCNT3-mediated transport of gemcitabine, AZT, and ddC (Fig. 4-14). Because AZT and ddC exhibited lower isotope fluxes than gemcitabine (Fig. 4-13), 1 mM concentrations of AZT and ddC were used to promote

larger current responses (*cf* 100 μ M for gemcitabine). In sodium-perfused medium at pH 7.5, all three nucleoside drugs elicited an electrogenic response with currents ranging from 78-154 nA (ddC < AZT < gemcitabine). In contrast, only gemcitabine generated a current response when Na⁺ was replaced by H⁺ (choline chloride transport medium, pH 5.5), suggesting that protons may not be able to support transport of AZT and ddC. This was confirmed by [³H]ddC uptake assays, which found no hCNT3-mediated transport of ddC in choline chloride transport medium at pH 5.5 (Fig. 4-15). In a phenomenon possibly related to the different abilities of Na⁺ and H⁺ to support hCNT3-mediated transport of AZT and ddC, Hong *et al.* (2001) have reported that inwardly-directed H⁺ gradients inhibit AZT uptake by microglia. Microglia have *cib*-type activity as a major component of their nucleoside transport machinery (Hong *et al.*, 2000).

Characterization of hCNT3/hCNT1 Chimeras – The predicted amino acid sequences of hCNT3 and hCNT1 are 48% identical and 57% similar, with strongest residue similarity within TMs of the carboxyl-terminal halves of the proteins. The major differences lie in the putative amino- and carboxyl-terminal tails of the proteins and in the first three TMs (Fig. 4-16). To localize domains involved in cation recognition and substrate specificity, a chimera (hCNT3/1) in which the carboxyl-terminal half of hCNT3 (incorporating TMs 7-13) was replaced with that of hCNT1 was constructed. The splice site between the two proteins following hCNT3 residue Lys³¹⁴ was engineered at the beginning of the putative extramembraneous loop prior to TM 7 to divide the proteins into two approximately equal halves as predicted by the topology model in Fig. 4-16, and to minimize disruption of native TMs and loops. As predicted by earlier hCNT1/2 mutagenesis studies (Loewen *et al.*, 1999 and *Chapter II*), chimera hCNT3/1 exhibited hCNT1-like substrate specificity (Ritzel *et al.*, 1997). This is illustrated in Fig. 4-17A, which shows the transportability of a panel of physiological purine and pyrimidine nucleosides (adenosine, cytidine, guanosine, inosine, thymidine and uridine). Fluxes were similar in profile to those exhibited by wild-type hCNT1 (uridine, thymidine, cytidine >> adenosine, and no detectable transport of guanosine or inosine). A reciprocal chimera to hCNT3/1 (hCNT1/3), representing a 50:50 construct incorporating the amino-terminal half of hCNT1 and the carboxyl-terminal half of hCNT3), was non-functional and was not studied further.

In addition to substrate specificity, we also tested chimera hCNT3/1 for possible H⁺-dependence. Fig. 4-17B shows relative levels of uridine transport (20 μM) by hCNT1, hCNT3, and chimera hCNT3/1 in Na⁺-containing (pH 7.5) and Na⁺-free (pH 7.5 and 5.5) media. Only wild-type hCNT3 exhibited elevated transport activity at pH 5.5 in the absence of Na⁺, demonstrating that the structural features determining H⁺-dependence reside in the carboxyl-terminal half of the protein.

Tissue and Cell Distribution – The *cib* process has been described functionally in rabbit choroid plexus (Wu *et al.*, 1992), rat MSL-9 microglia cells (Hong *et al.*, 2000), *Xenopus* oocytes injected with rat jejunal mRNA (Huang *et al.*, 1993), and colorectal carcinoma CaCo cells (Belt *et al.*, 1993) and, after induction of differentiation, in human HL-60 cells (see below). The human and mouse ESTs that led to the identification of h/mCNT3 were from human/mouse mammary gland and human colon adenocarcinoma, while the full-length transporter cDNAs were isolated from differentiated HL-60 cells and mammary gland (hCNT3), and liver (mCNT3). Fig. 4-18 shows a multiple tissue expression RNA array for 76 human tissues and cells probed with hCNT3 cDNA (a second commercial RNA array from the same supplier gave essentially identical results). As described in *Materials and Methods*, this analysis was performed under conditions of high stringency where there was no cross-hybridization between hCNT3 and hCNT1 or hCNT2. The distribution pattern of hCNT3 transcripts, although selective, was surprisingly widespread. Highest levels were found in a number of normal tissues, including mammary gland, pancreas, bone marrow and trachea, with substantial levels in various regions of the intestine (but very much less in kidney), and more modest levels in liver, lung, placenta, prostate, testis and other tissues, including some regions of the brain and heart. hCNT3 transcripts were generally present in fetal tissues, but were low in various cultured cell lines, including K562, HeLa and undifferentiated HL-60 (see also below). In contrast, h/rCNT1 and h/rCNT2 transcripts are found primarily in specialized epithelia, including small intestine, kidney and liver (Huang *et al.*, 1994; Che *et al.*, 1995; Yao *et al.*, 1996a, Ritzel *et al.*, 1997; Wang *et al.*, 1997; Ritzel *et al.*, 1998). Other reported sources of h/rCNT1 and h/rCNT2 transcripts include brain, spleen, heart, pancreas and skeletal muscle (Che *et al.*, 1995, Wang *et al.*, 1997; Anderson *et al.*, 1996). A systematic analysis of CNT1/2 transcript

distribution similar to that shown in Fig. 4-18 for hCNT3 would be helpful to more fully characterize the different expression patterns of the three transporters.

In parallel with the multiple tissue expression RNA array, we also investigated the distribution of hCNT3 transcript in selected tissues by Northern blotting. This less sensitive technique detected hCNT3 transcripts in pancreas, bone marrow and trachea, but not in intestine, liver, brain or heart (Fig. 4-19). Kidney, as expected from Fig. 4-18, was also negative. In pancreas, bone marrow and trachea, three bands were apparent, a major 5.3-kb transcript and secondary bands at 6.5-kb and 4.8-kb. Although two of the bands were similar in size to the major transcripts of hCNT1 (3.4-kb) and hCNT2 (4.5-kb) (Ritzel *et al.*, 1998), the blot was probed at high stringency under conditions where there was no cross-reactivity with hCNT1/2 (see *Materials and Methods*). It is likely, therefore, that they represent alternate hCNT3 gene transcripts rather than cross-hybridization with other CNT family members. The absence of bands in kidney, which contains transcripts for both hCNT1 and hCNT2 (Ritzel *et al.*, 1998), is further evidence of the hCNT3 probe's specificity. The same tissues (plus mammary gland) were also analyzed by TaqMan™ quantitative RT-PCR using hCNT3-specific primers as described below for HL-60 cells. Relative levels of hCNT3 transcript by this method were pancreas > bone marrow, trachea, intestine > mammary gland >> liver, brain, heart > kidney (data not shown).

HL-60 cells (Functional Studies) – The human promyelocytic leukemia cell line, HL-60, can be induced to differentiate into adherent monocyte/macrophage-like cells treatment with phorbol esters (Lotem *et al.*, 1979; Rovera *et al.*, 1979). Upon differentiation, the cells exhibit a decrease in equilibrative, Na⁺-independent nucleoside transport that is accompanied by an increase in concentrative, Na⁺-dependent transport of both pyrimidine and purine nucleosides (Lee *et al.*, 1991). To rigorously identify the concentrative transport process(es) contributing to this uptake, we first determined the uridine transport profile of parent and PMA-treated HL60 cells under conditions previously shown to be optimal for induction of the concentrative transport activity (Lee *et al.*, 1991). Equilibrative transport was measured by replacing Na⁺ in the transport medium with NMDG, and concentrative transport was determined in the presence of Na⁺, but with the addition of dilazep (100 μM) to inhibit equilibrative transport activity. We have shown that this concentration of dilazep has no effect on hCNT3 transport

activity (Fig. 4-7). Although previous studies have reported a small amount of Na⁺-dependent transport activity in untreated HL-60 cells (Lee *et al.*, 1991, 1994), our assays did not detect any concentrative transport in the parent cell line, which exhibited only equilibrative uptake of 10 μM uridine (Fig. 4-20A). However, there was a notable increase in Na⁺-dependent uridine transport in differentiated, adherent HL-60 cells (Fig. 4-20B). Uptake of thymidine and formycin B (a non-metabolized analog of inosine) was then used to define which of the concentrative transport processes (*cit*, *cif*, *cib*) was active in differentiated HL-60 cells (Figs. 4-20C & D). Both nucleosides were taken up by the concentrative process(es) of differentiated HL-60 cells. Transport of thymidine was totally inhibited by unlabelled thymidine, inosine and uridine, while formycin B uptake was reciprocally inhibited by thymidine. Thus, *cib* (rather than *cit* + *cif*) was the dominant concentrative transport activity in differentiated HL-60 cells. Consistent with this result, concentrative uridine transport was inhibited by uridine, thymidine and inosine (data not shown). Dot blot analysis (Fig. 4-18A) and non-quantitative RT-PCR (Fig. 4-21A) established that the appearance of *cib* functional activity correlated with substantially increased levels of hCNT3 transcripts in differentiated *versus* parent HL-60 cells, the latter exhibiting only small amounts of hCNT3 mRNA. In RT-PCR experiments, parent and differentiated HL-60 cells were negative for hCNT2 mRNA and expressed only very small amounts of hCNT1 mRNA, most likely as a consequence of bleed-through transcription (data not shown). These results provided further evidence that the concentrative nucleoside transport activity seen in differentiated HL-60 cells was mediated by *cib*, and not by (*cit* + *cif*).

HL-60 cells (TaqMan™ Quantitative Real Time RT-PCR) – The relative levels of hCNT3 transcripts in HL-60 parent and differentiated cells were determined by quantitative real time RT-PCR (Fig. 4-21B). GAPDH and hCNT3 were demonstrated to amplify with equal efficiency, and GAPDH was, therefore, used as the internal control to normalize levels of expression of hCNT3 mRNA between samples. To compare samples, a threshold line was set at the phase of the PCR reaction during which the fluorescent signal accumulated exponentially. As shown in Fig. 4-21B, there was a substantial difference between the HL-60 parent and differentiated samples in the PCR cycle numbers at the threshold line, and three independent experiments gave a mean (\pm S.E.) ratio of 4.08 ± 0.09 , indicating (since PCR amplification is an exponential process) that there was 16.9 ± 1.1 more hCNT3 mRNA in

differentiated *versus* parent HL-60 cells. Similar results were obtained when the data were normalized to 18S-gene expression (data not shown). The human tumor cell lines K562 (erythroleukemia) and HeLa (cervical carcinoma) were also tested in this assay (data not shown) and gave signals that were close to background levels (see also Fig. 4-18A). These results, taken with those of the transport experiments, indicated that the small amount of hCNT3 transcription in the HL-60 parent cells did not result in enough protein to be functionally detected whereas the differentiated cells that expressed 16-fold more hCNT3 mRNA had a readily measurable *cib* transport process. Since the analyses were performed on exponentially growing parent and differentiated cells, the difference in transcript levels between parent and differentiated HL-60 cells could not be attributed to cell proliferation.

Chromosomal Localization of the hCNT3 Gene – While the genes encoding hCNT1 and hCNT2 have both been mapped to chromosome 15 (15q25-26 (Ritzel *et al.*, 1997) and 15q15 (Ritzel *et al.*, 1998), respectively), FISH analysis localized the hCNT3 gene to 9q22.2. The same chromosomal band location was determined by screening a human BAC library. Searches of the Sanger Centre human genomic sequence database and the Unfinished High Throughput Genomic Sequence GenBank™ database identified two chromosome 9 clones (GenBank™ accession numbers AL356134 and AL353787) containing multiple hCNT3 genomic fragments that, when aligned, revealed 27.3-kb of composite hCNT3 gene sequence containing 74% of the hCNT3 coding sequence. The coding sequence that was obtained was an exact match with corresponding regions of the hCNT3 cDNA sequence. Analysis of hCNT3 5'-genomic sequence in the potential upstream promoter region of the gene revealed the presence of a PMA-RE eukaryotic phorbol myristate acetate (ester) response element (Deutsch *et al.*, 1988) with the sequence 5'-TGAGTCA-3' that may potentially contribute to the transcriptional regulation of hCNT3 seen in HL-60 cells. Studies are in progress to compare the organization of the hCNT3 gene with that for hCNT1 (32-kb), which has been determined to contain 18 exons separated by 17 introns (GenBank™ accession numbers 187967–187978).

Conclusions – The CNT protein family in humans is represented by three members, hCNT1, hCNT2 and the presently described hCNT3. Searches of the Unfinished High Throughput Genomic Sequence GenBank™ database have so far revealed no other closely-

related members of this family in humans. hCNT3 is a transcriptionally regulated electrogenic transport protein that, unlike hCNT1 and hCNT2, has a broad permeant selectivity for pyrimidine and purine nucleosides and nucleoside drugs. Hill-type analyses and charge/flux determinations established a Na⁺:uridine coupling ratio of 2:1, compared to 1:1 for hCNT1/2. These characteristics, and the induction of hCNT3 mRNA in HL-60 cells following phorbol ester treatment, identified hCNT3 as the physiological human *cib* transporter. A mouse homolog of hCNT3 (mCNT3) was also cloned, suggesting that CNT3 is widely distributed in mammals.

hCNT3, unlike hCNT1/2, was also H⁺- (and Li⁺-) dependent and had a calculated H⁺:uridine coupling ratio of 1:1 that did not appear to support transport of antiviral nucleoside drugs. Chimeric studies between hCNT3 and hCNT1 located the domains involved in cation recognition and substrate specificity to within the carboxyl-terminal half of the protein.

A candidate *cib*-type transporter SNST1 that is related to the Na⁺-dependent glucose transporter SGLT1 was identified in 1992 in rabbit kidney (Pajor and Wright, 1992). There is no sequence similarity between SNST1 and either the CNT or ENT protein families. Although recombinant SNST1, when expressed in oocytes, stimulated low levels of Na⁺-dependent uptake of uridine that was inhibited by pyrimidine and purine nucleosides (*i.e.* *cib*-type pattern), the function of this protein remains unclear because the rate of uridine transport in oocytes was only two-fold above endogenous (background) levels, whereas a > 100-fold stimulation was observed with h/mCNT3. It is likely that the true physiological substrate of SNST1 is a low molecular weight metabolite for which there is overlapping permeant recognition with nucleosides.

hCNT3 and mCNT3 are more closely related to the hagfish transporter hCNT than to mammalian CNT1/2 and thus form a separate CNT subfamily. Hagfish diverged from the main line of vertebrate evolution about 550 million years ago and represent the most ancient class of extant vertebrates. The high degree of amino acid sequence similarity between h/mCNT3 and hCNT in the TM 4-13 region (67% sequence identity) may indicate functional constraints on the primary structure of this domain and suggests that *cib*-type concentrative NTs fulfill important physiological functions. The tissue distribution of hCNT3 transcripts

was more widespread than anticipated from previous studies of *cib* functional activity, and is different from that of either CNT1 or CNT2. While transcripts for mammalian CNT1 and CNT2 have been described in jejunum, kidney, liver and brain (CNT1) and jejunum, kidney, liver, spleen, heart, skeletal muscle and pancreas (CNT2), the highest levels of hCNT3 transcripts were found in pancreas, bone marrow, trachea, mammary gland and duodenum. Clinically, hCNT3 may be expected to contribute to the concentrative cellular uptake of both anticancer and antiviral nucleoside drugs. Future studies of the transcriptional regulation of the hCNT3 gene will enhance our understanding of its physiological function(s) and therapeutic potential.

Table 4-1 – Kinetic Properties of hCNT3

Substrate	Apparent K_m^a (μM)	V_{max}^a ($pmol/oocyte.5min^{-1}$)	$V_{max}:K_m$
Uridine	22 ± 5	25.8 ± 1.3	1.19
Cytidine	15 ± 3	32.8 ± 1.0	2.13
Thymidine	21 ± 6	24.2 ± 1.4	1.14
Adenosine	15 ± 2	30.4 ± 0.7	2.01
Guanosine	43 ± 7	51.4 ± 1.8	1.20
Inosine	53 ± 13	44.8 ± 2.5	0.85

^a, from Fig. 4-6.

Figure 4-1. hCNT3 and mCNT3 are members of the CNT family of nucleoside transporters. Alignment of the predicted amino acid sequences of hCNT3 (GenBank™ accession AF305210) and mCNT3 (GenBank™ accession AF305211) with those of hCNT1 (GenBank™ accession U62968), hCNT2 (GenBank™ accession AF036109) and hCNT (GenBank™ accession AF132298) using the GCG PILEUP program. Potential membrane-spanning α -helices are *numbered*. Putative glycosylation sites in predicted extracellular domains of hCNT3, mCNT3, hCNT1, hCNT2 and hCNT are shown in *lowercase (n)*, and their positions highlighted by an *asterisk* above the aligned sequences. Residues in hCNT3 identical to one or more of the other transporters are indicated by *black boxes*.

```

hcNT1 -----MENDPSRRRESISLTPVAK--GLENMGADFLLESLEE
hcNT3 -----MELRSTAAFRRAEGYSNVGFQNEENFLEENNTSGNSISRAV
mCNT3 MSRADPGKNSEPSSESKMSHELRPT--APSDLGRSNEAFQDE--LEFRQNTSPGNSIVPNTVV
hcCNT -----MSAFKARQVE--NPSYEDPD--EKGKPDLEMSKTNGI
hcNT2 -----MEKASGR--QSIALSTVET--GTVNPGLELME--KE

```

```

hcNT1 GGLPRSDLSPAERIRSSWSEAAFKPFPSRWRNLQPALRRAR-----SFCREHM
hcNT3 OSREHTNNTKQDEEQVTVVQDSPRNRKHMEDDDSEEMQCKGCLER---RYDTVCGFCRKHK
mCNT3 OSGEQGHAKQDDRQITIEQEPLGNKEDEPDDSEDEHQKGFLE---KYDTICEFCRKH
hcCNT GVDNPSYYKNPEKYLGNENEEGKSNNDNEEEEGEEDQGAVERCVNKFYGGIHNFKYKRNK
hcNT2 VEPEGSKRTDAGGHSLSGDGLGPESTYQR--RSRWPFPSKAR-----SFCCKTHA

```

```

                                Helix 1                                Helix 2
hcNT1 QLEFRWIGTGLICTGLSAFLLVACLLEDFQRALALFVLTFCVVLTFGLGHRLLKRLRLGPKLRRF
hcNT3 TTLRSHIHWGILLLAGYLVMSVISACVLFNFRRALPLFVITVAEIFEVVWDHLMKAYEHRIDEM
mCNT3 VVLRSTIWAVALLTGFLALVIAACATNFRRALPLFVITLVTFIFVVDHLMKAYEQRIDDF
hcCNT KIITHYTFLLGLLVGYFALVIAACIVNFKQSLALFLVLTLIATIFFFDLFTIAKYGDKIAEA
hcNT2 SLFKKLTLLGLLCLAYAAAYLLAACILNFRQALALFVITCLVIFVVLVHSFLKRLGKLLTRC

```

```

                                Helix 3                                Helix 4
hcNT1 LKFRQGHPRLLLWFKRGLALAAFLGLVVLWLSLDTTSQR--PEQLVVSFAGICVEIALLFACS
hcNT3 LSPGRRLLNSHWFWLKWVWSSSLVLAIVIFLWLSLDTAKLGGQQLVVSFGGLIMYIVLLFLFS
mCNT3 LSPGRRLLDRHWFWLKWVWSSSLIILAVILWLSLDTAKLGGQQLVVSFGGLIMYIVLLFLFS
hcCNT LKFRQGHPRLLLWFKRGLALAAFLGLVVLWLSLDTTSQR--PEQLVVSFAGICVEIALLFACS
hcNT2 LKFRQGHPRLLLWFKRGLALAAFLGLVVLWLSLDTTSQR--PEQLVVSFAGICVEIALLFACS

```

```

                                Helix 5
hcNT1 KHHC AVSWRAVSWGLGLQFVLGLLIRTEPGFIAFEWLGEEQIRIFLSYTKAGS SFVFGEA
hcNT3 KHHPTRVYWRPVFWGIGLQFLLGLLILRTRPGFVAFDWMGRQVQTFELKYTDGAREVFGKE
mCNT3 KHHPTRVYWRPVFWGIGLQFLLGLLILRTRPGFVAFDWMGRQVQTFELKYTDGAREVFGKE
hcCNT KHHPTRVYWRPVFWGIGLQFLLGLLILRTRPGFVAFDWMGRQVQTFELKYTDGAREVFGKE
hcNT2 KHHS AVSWRAVSWGLGLQFVLGLLIRTEPGFIAFEWLGEEQIRIFLSYTKAGS SFVFGEDT

```

```

                                Helix 6                                Helix 7
hcNT1 LVKDVFAFQVLPPIVVFSCVISVLYHVGLMQWVILKIAWLMQVMTGTTATETLSVAGNIF
hcNT3 YTDHFFFAFKLPIVVFVSTVMSMLYLYLGLMQWVILKIAWLMQVMTGTTATETLSVAGNIF
mCNT3 YTDHFFFAFKLPIVVFVSTVMSMLYLYLGLMQWVILKIAWLMQVMTGTTATETLSVAGNIF
hcCNT YTDHFFFAFKLPIVVFVSTVMSMLYLYLGLMQWVILKIAWLMQVMTGTTATETLSVAGNIF
hcNT2 LVKDVFAFQVLPPIVVFSCVISVLYHVGLMQWVILKIAWLMQVMTGTTATETLSVAGNIF

```

```

                                Helix 8                                Helix 9
hcNT1 VSGTEAPLLLRPYLADMTLSEVHVVMVTGGYATFAGSLLGAYISFGIDATSLIAASVMAAP
hcNT3 VSGTESPLLVRPYLPHYITKSELHAIMTAGFSTIAGSVLGAAYISFGVSSHLLTASVMSAP
mCNT3 VSGTESPLLVRPYLPHYITKSELHAIMTAGFSTIAGSVLGAAYISFGVSSHLLTASVMSAP
hcCNT VSGTESPLLVRPYLADMTLSEVHVVMVTGGYATFAGSLLGAYISFGIDATSLIAASVMAAP
hcNT2 VGMTEAPLLLRPYLADMTLSEVHVVMVTGGYATFAGSLLGAYISFGIDATSLIAASVMAAP

```

```

                                Helix 10
hcNT1 CALALS KL VY PEVEESKFRREEGVKLTYGDAQSLIEAASSTGAAISVKVVAANIAANLIAFL
hcNT3 ASLAAAKLFWPETEKPKITLTKNANRMEKSGDSGNLLEAASSTGASSISLVANIAANLIAFL
mCNT3 AALAVAKLFWPETEKPKITLTKSAMKMEKSGDSGNLLEAASSTGASSISLVANIAANLIAFL
hcCNT AALAIKLTWPETKPKKSTQTSIKLEKQGENNLVEAASSTGASSISLVANIAANLIAFL
hcNT2 CALALS KL VY PEVEESKFKSEEGVLELPRGKER NVLEAASSTGAVDAIGLATHVAANLIAFL

```

```

                                Helix 11
hcNT1 AVLDFFINAAALS WLGDMVDIQGLSFLICSYLRLPVAFLMGVAWEEDCPVVAELLGIKLFLN
hcNT3 ALLSFMNSALS WFGNMF DYPQLSFLICSYIFMPPFSFMMGVVEWQDSFMVARLIGYKTFEN
mCNT3 ALLSFMNSALS WFGSMEFNYPQLSFLICSYIFMPPFSFMMGVVEWQDSFMVARLIGYKTFEN
hcCNT AVLDFFINAAALS WLGDMVDIQGLSFLICSYLRLPVAFLMGVAWEEDCPVVAELLGIKLFLN
hcNT2 AVLDFFINAAALS WLGDMVDIQGLSFLICSYLRLPVAFLMGVAWEEDCPVVAELLGIKLFLN

```

```

                                Helix 12
hcNT1 EFVAYQDLSKYKQRRLA GAEEWVGNRKQWISVRAEVLTFEALCGGFANFSSLIGIMLGLLTS
hcNT3 EFVAYEHLKSWIHLRKEGGPKFVNGVQQYISIRSEIATYALCGGFANFSSLIGIVIGGLTS
mCNT3 EFVAYDHLKSLINLRKAAGPKFVNGVQQYISIRSEIATYALCGGFANFSSLIGIVIGGLTS
hcCNT EFVAYQRLSEYIHNRESGGPLEVDEGKQYMSVRSERAIATYALCGGFANFSSLIGIMIGGLS
hcNT2 EFVAYQQLSQYKKNKFLS GMEEWIEGKQWISVRAEIIITTFSLCGGFANLSSLIGITLGLLTS

```

```

                                Helix 13
hcNT1 M V P Q R K S D F S Q I V L R A L F T G A C V S L V N A C M A G I L Y - - - M P R G A E V D C M S L L A T T L S S S S F
hcNT3 M A P S R R K R D I A S G A V R A L I A G T V A C F M T A C I A G I L S S T P V D I N C H V L E N A F A S T F P P G A T T
mCNT3 I A P S R R K R D I A S G A M R A L I A G T I A C F M T A C I A G I L S D T P V D I N C H V L E - - - N G R V L S R T T
hcCNT L A P H R K R S D I A S C G I P A L I A G T I A C F S T A C I A G V L Y - I P E L Y C P N L L M S T L E N G T T V R T T
hcNT2 I V P H R K R S D L S K V V V R A L E T G A C V S L I S A C M A G I L Y - - - P R G A E A D C V S F P A T S E T n R A Y

```

```

hcNT1 E I Y Q C C R E A F Q S - - - V N P - - - - - E F S P E A L D N C C R F Y A H T I C A Q - - - - -
hcNT3 K V I A C C Q S L S S T V A R G P G E V I P G G S - - - - H S L Y S L K G C C T L L P S T F N C N G I S N T F
mCNT3 E V S C C Q N L F n S T V A R G P N D V P G G S - - - - F S L Y A L M S C C N L L K P P T L C N G W I P R K E
hcCNT N L M S C C T D L F K S T T M L T P K N I T F T E - - - - G F n T T M L N G C C T F F - P S G F L C A S E V R P E -
hcNT2 E T Y M C C R G L F Q S T S L n G T N P P S F S G P W E D K E F S A M A L T N C C G F Y R N T V C A - - - - -

```

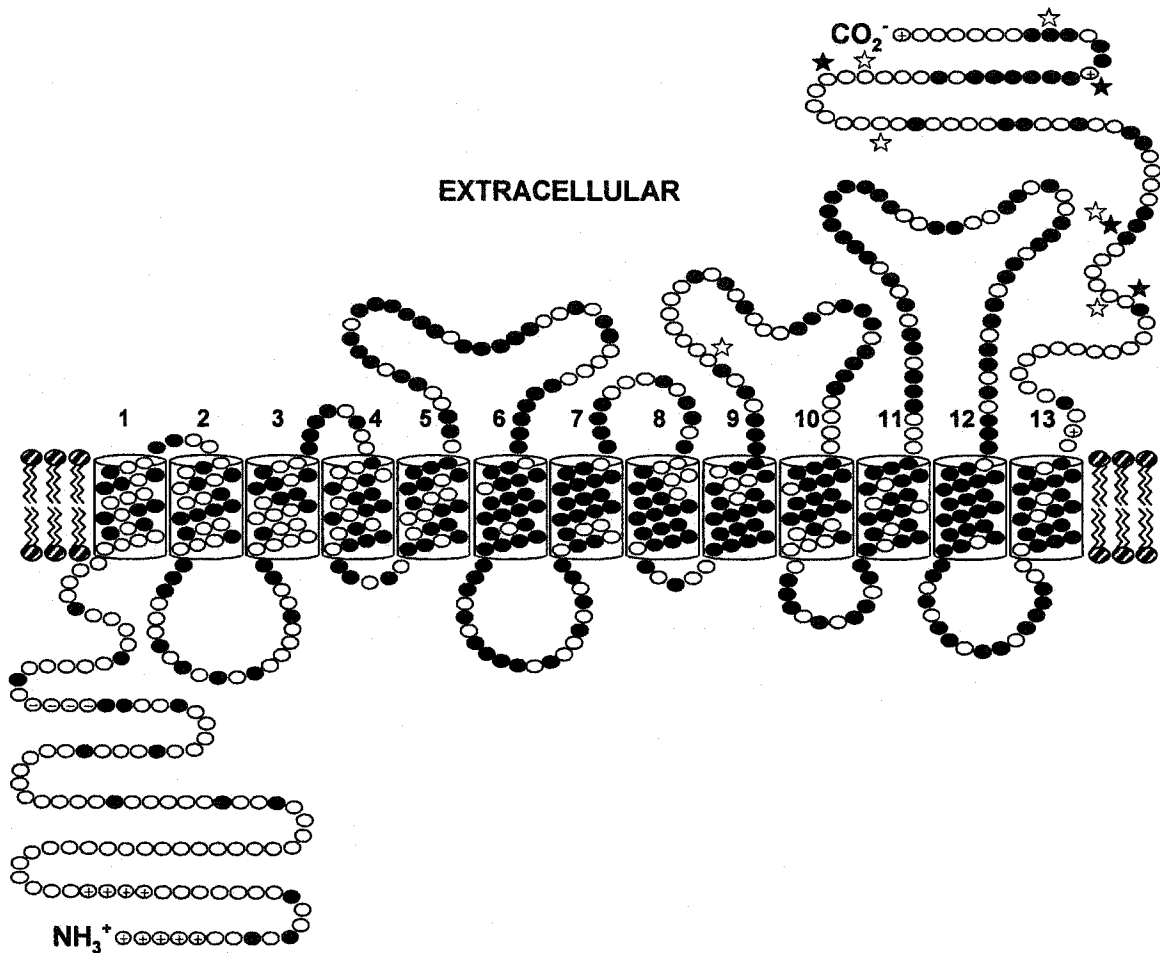
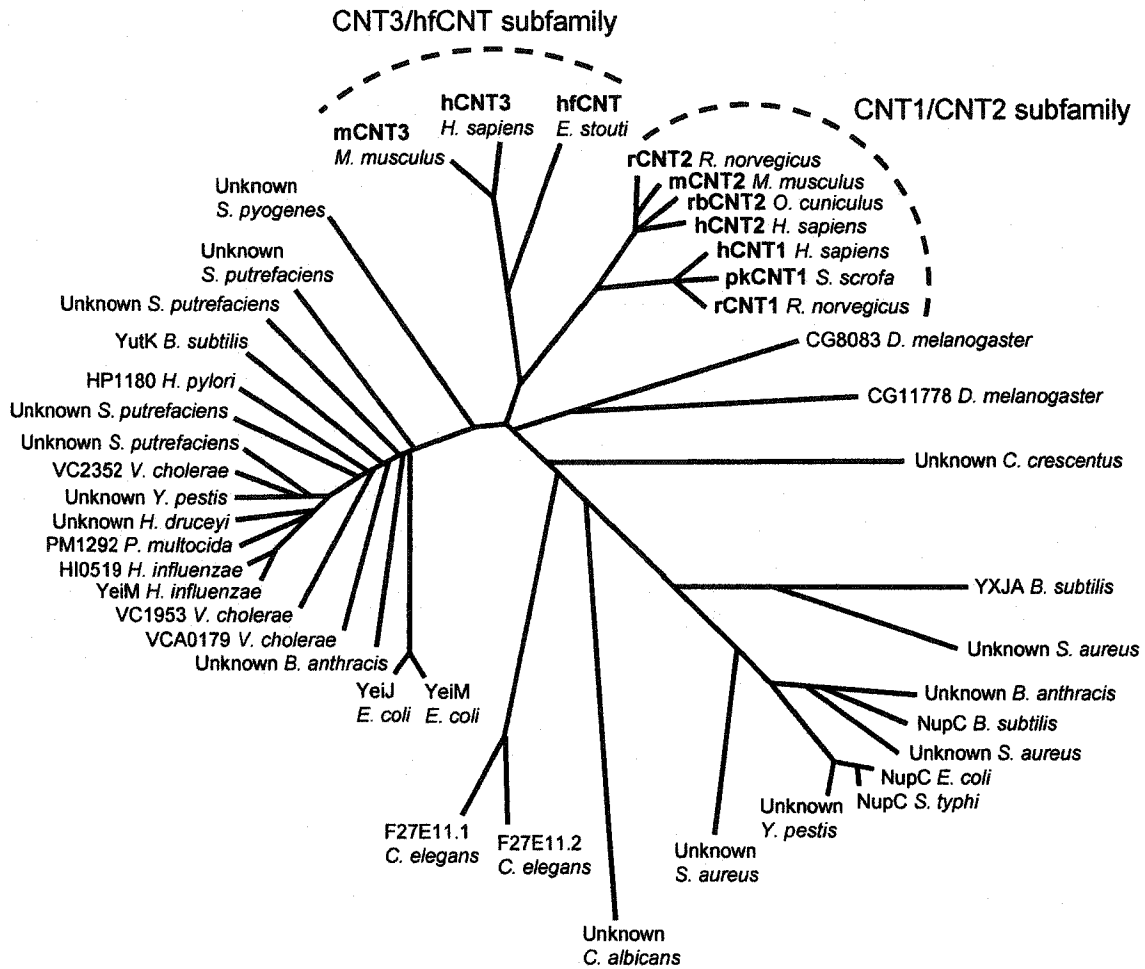


Figure 4-2. Topological model of hCNT3 and hfCNT. Potential membrane-spanning α -helices are numbered, and putative glycosylation sites in predicted extracellular domains in hCNT3 and hfCNT are indicated by *solid* and *open stars*, respectively. Residues identical in the two proteins are shown as *solid circles*. Residues corresponding to insertions in the sequence of hCNT3 or hfCNT are indicated by *circles* containing “+” and “-” signs, respectively.

Figure 4-3. Phylogenetic tree showing relationships between hCNT3 and mCNT3 and other eukaryotic and prokaryotic members of the CNT transporter family. In addition to those listed in *Figure 4-1*, these are: rCNT1 (rat CNT1, GenBank™ accession U10279); pkCNT1 (pig kidney CNT1, GenBank™ accession AF009673); rCNT2 (rat CNT2, GenBank™ accession U25055); mCNT2 (mouse CNT2, GenBank™ accession AF079853); rbCNT2 (rabbit CNT2, GenBank™ accession AF161716); F27E11.1 (*Caenorhabditis elegans*, GenBank™ accession AF016413); CG11778_DROME (*Drosophila melanogaster*, GenBank™ accession AAF58996); CG8083_DROME (*Drosophila melanogaster*, GenBank™ accession AAF58997); F27E11.2 (*Caenorhabditis elegans*, GenBank™ accession AF016413); YEIM_HAEIN (*Haemophilus influenzae*, Swissprot accession P44742); HP1180_HELPY (*Helicobacter pylori*, GenBank™ accession AE000623); YEIM_ECOLI (*Escherichia coli*, Swissprot accession P33024); YEIJ_ECOLI (*Escherichia coli*, Swissprot accession P33021); YXJA_BACSU (*Bacillus subtilis*, Swissprot accession P42312); NUPC_ECOLI (*Escherichia coli*, Swissprot accession P33031); NUPC_BACSU (*Bacillus subtilis*, Swissprot accession P39141); HI0519_HAEIN (*Haemophilus influenzae*, GenBank™ accession U32734); YUTK_BACSU (*Bacillus subtilis*, GenBank™ accession Z99120); VC2352_VIBCH (*Vibrio cholerae*, GenBank™ accession AAF95495); VC1953_VIBCH (*Vibrio cholerae*, GenBank™ accession AAF95101); VCA0179_VIBCH (*Vibrio cholerae*, GenBank™ accession AAF96092); UNKNOWN_STREP (*Streptococcus pyogenes*, open reading frame (284) present in contig0001 from the *S. pyogenes* genome sequencing project, Oklahoma University); UNKNOWN_YERPE (*Yersinia pestis*, open reading frame present in contig971 from the *Y. pestis* genome sequencing project, Sanger Centre); UNKNOWN_YERPE (*Yersinia pestis*, open reading frame present in contig976 from the *Y. pestis* genome sequencing project, Sanger Centre); UNKNOWN_SALTY (*Salmonella typhi*, open reading frame present in contig18 (CT18) from the *S. typhi* genome sequencing project, Sanger Centre); UNKNOWN_BACAN (*Bacillus anthracis*, open reading frame in contig1985 from the *B. anthracis* genome sequencing project, TIGR); UNKNOWN_BACAN (*Bacillus anthracis*, open reading frame in contig1745 from the *B. anthracis* genome sequencing project, TIGR); UNKNOWN_CAUCR (*Caulobacter crescentus*, open reading frame present in contig12574 from the *C. crescentus* genome sequencing project, TIGR); UNKNOWN_STAAU (*Staphylococcus aureus*, open reading frame present in contig6185 from the *S. aureus* genome sequencing project, TIGR); UNKNOWN_STAAU (*Staphylococcus aureus*, open reading frame present in contig6213 from the *S. aureus* genome sequencing project, TIGR); UNKNOWN_STAAU (*Staphylococcus aureus*, open reading frame present in contig6186 from the *S. aureus* genome sequencing project, TIGR); UNKNOWN_SHEPU (*Shewanella putrefaciens*, open reading frame present in contig6401 from the *S. putrefaciens* genome sequencing project, TIGR); (continued on adjacent page)



UNKNOWN_SHEPU (*Shewanella putrefaciens*, open reading frame present in contig6410 from the *S. putrefaciens* genome sequencing project, TIGR); UNKNOWN_SHEPU (*Shewanella putrefaciens*, open reading frame present in contig6413 from the *S. putrefaciens* genome sequencing project, TIGR); UNKNOWN_SHEPU (*Shewanella putrefaciens*, open reading frame present in contig6438 from the *S. putrefaciens* genome sequencing project, TIGR); PM1292_SHEPU (*Pasteurella multocida*, open reading frame gene product PM1292 from the *P. multocida* genome sequencing project, University of Minnesota); UNKNOWN_CANAL (*Candida albicans*, open reading frame present in contig5-2704 from the *C. albicans* genome sequencing project, Stanford); UNKNOWN_HAEDU (*Haemophilus ducreyi*, open reading frame present in contig730 from the *H. ducreyi* genome sequencing project, University of Washington). The phylogenetic tree was constructed from a multiple alignment of the 43 CNT sequences using ClustalX version 1.81 for Windows (Thompson *et al.*, 1997) and KITSCH, PHYLIP version 3.57c (Felsenstein, 1989) software. The CNT3/hfCNT and CNT1/2 subfamilies are highlighted.

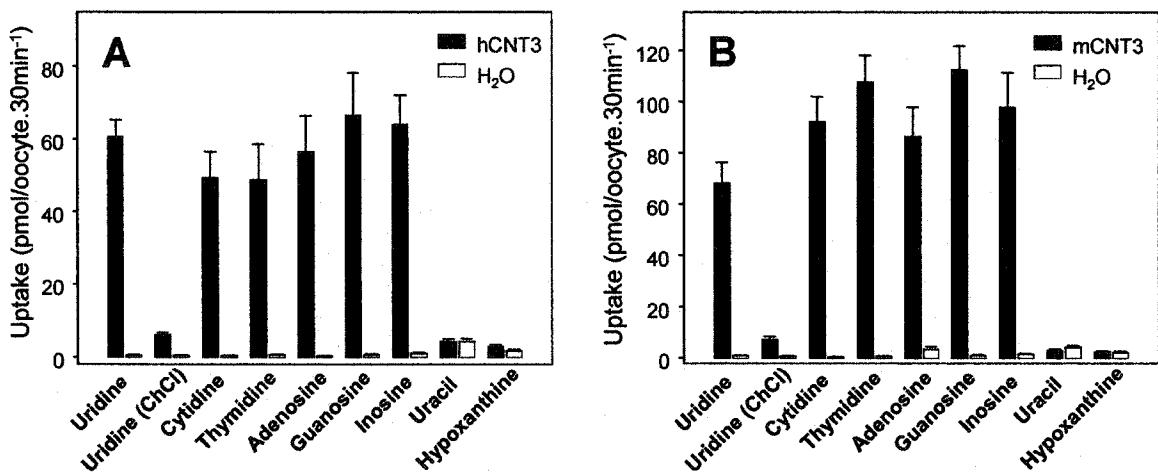


Figure 4-4. Uptake of ¹⁴C/³H-labeled nucleosides and nucleobases by recombinant hCNT3 and mCNT3 expressed in *Xenopus* oocytes. Uptake of nucleosides and nucleobases (20 μM, 20°C, 30 min) in oocytes injected with RNA transcripts or water alone was measured in transport medium containing 100 mM NaCl or 100 mM choline chloride (ChCl).

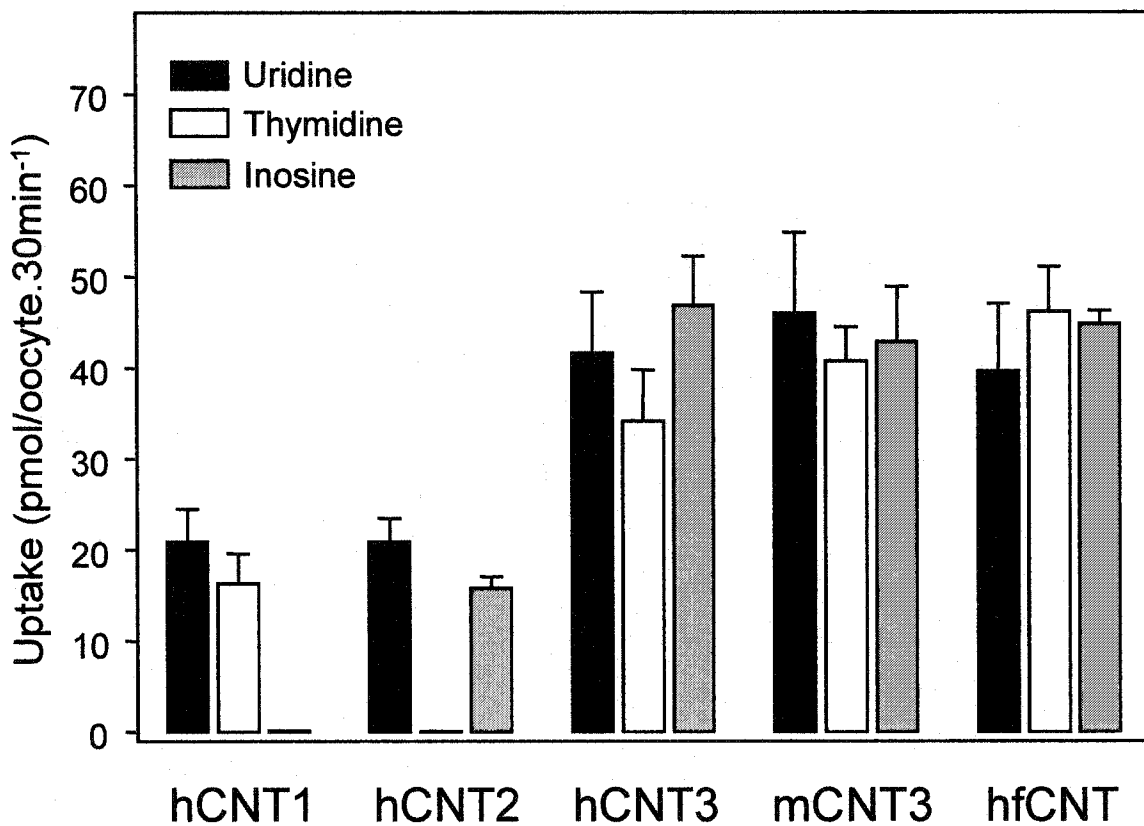


Figure 4-5. Nucleoside selectivity of recombinant hCNT3, mCNT3, hCNT1, hCNT2 and hfCNT. Transporter-mediated nucleoside uptake (20 μ M, 20°C, 30 min) was measured in transport medium containing 100 mM NaCl. Mediated transport was calculated as uptake in RNA-injected oocytes minus uptake in water-injected oocytes.

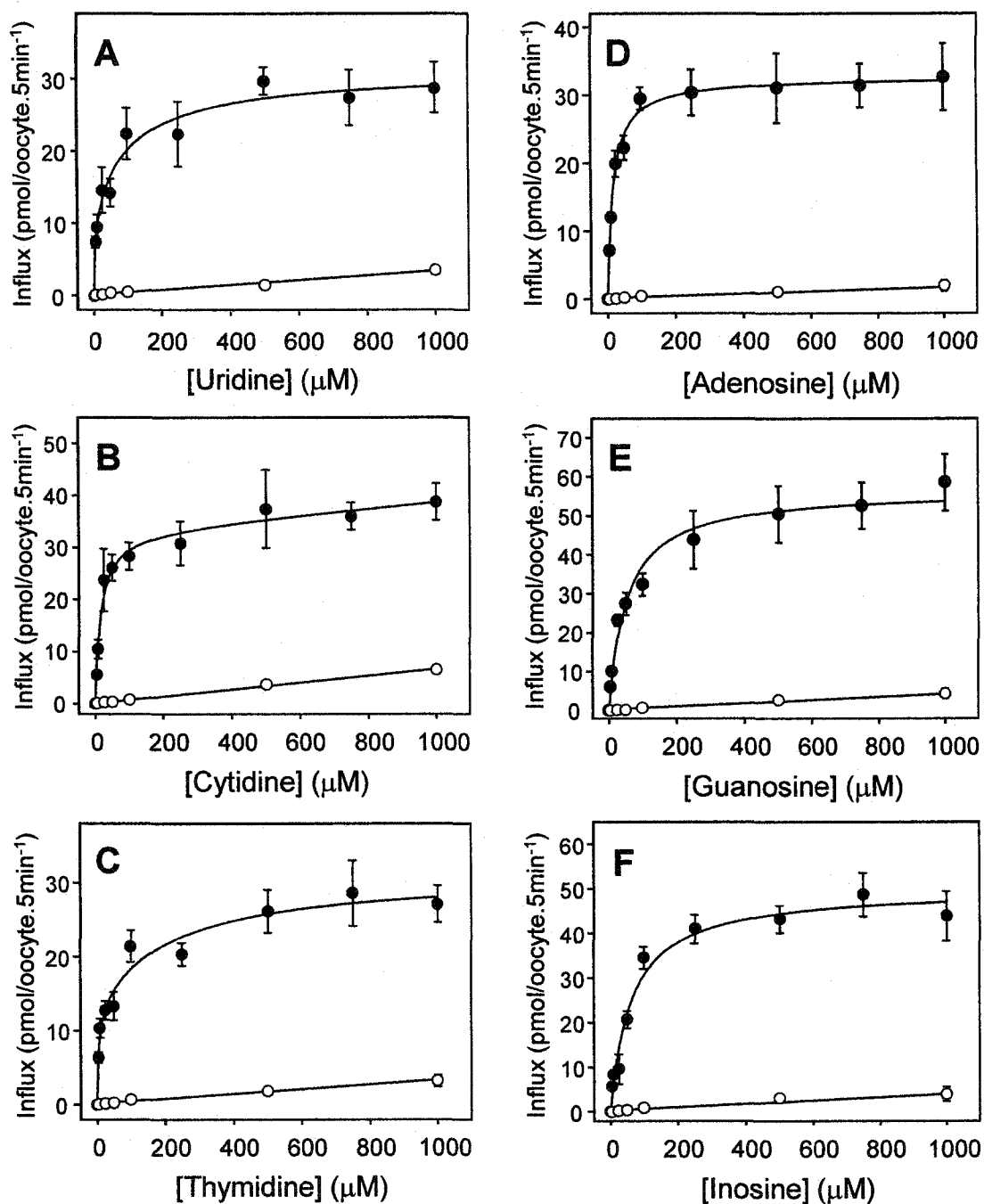


Figure 4-6. Kinetic properties of recombinant hCNT3. Initial rates of nucleoside uptake (5-min fluxes, 20°C) in oocytes injected with RNA transcripts (*solid circles*) or water alone (*open circles*) were measured in transport medium containing 100 mM NaCl. Kinetic parameters calculated from the mediated component of transport (uptake in RNA-injected oocytes minus uptake in water-injected oocytes) are presented in *Table 4-1*.

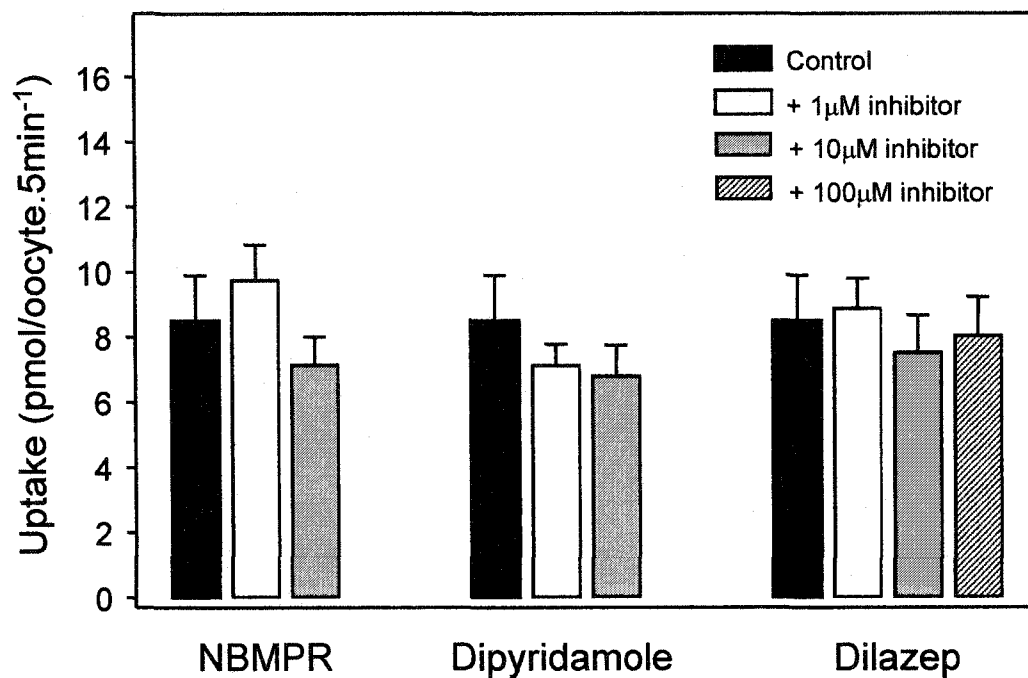


Figure 4-7. Recombinant hCNT3 is not inhibited by NBMPR, dipyridamole or dilazep. Initial rates of transporter-mediated uridine uptake (20 μ M, 20°C, 5 min) were measured in transport medium containing 100 mM NaCl in the absence or presence of 1 – 10 μ M NBMPR and dipyridamole, or 1 – 100 μ M dilazep. Oocytes were incubated with inhibitor for 30 min before addition of permeant. Mediated transport was calculated as uptake in RNA-injected oocytes minus uptake in water-injected oocytes (uptake of uridine by water-injected oocytes was unaffected by NBMPR, dipyridamole or dilazep).

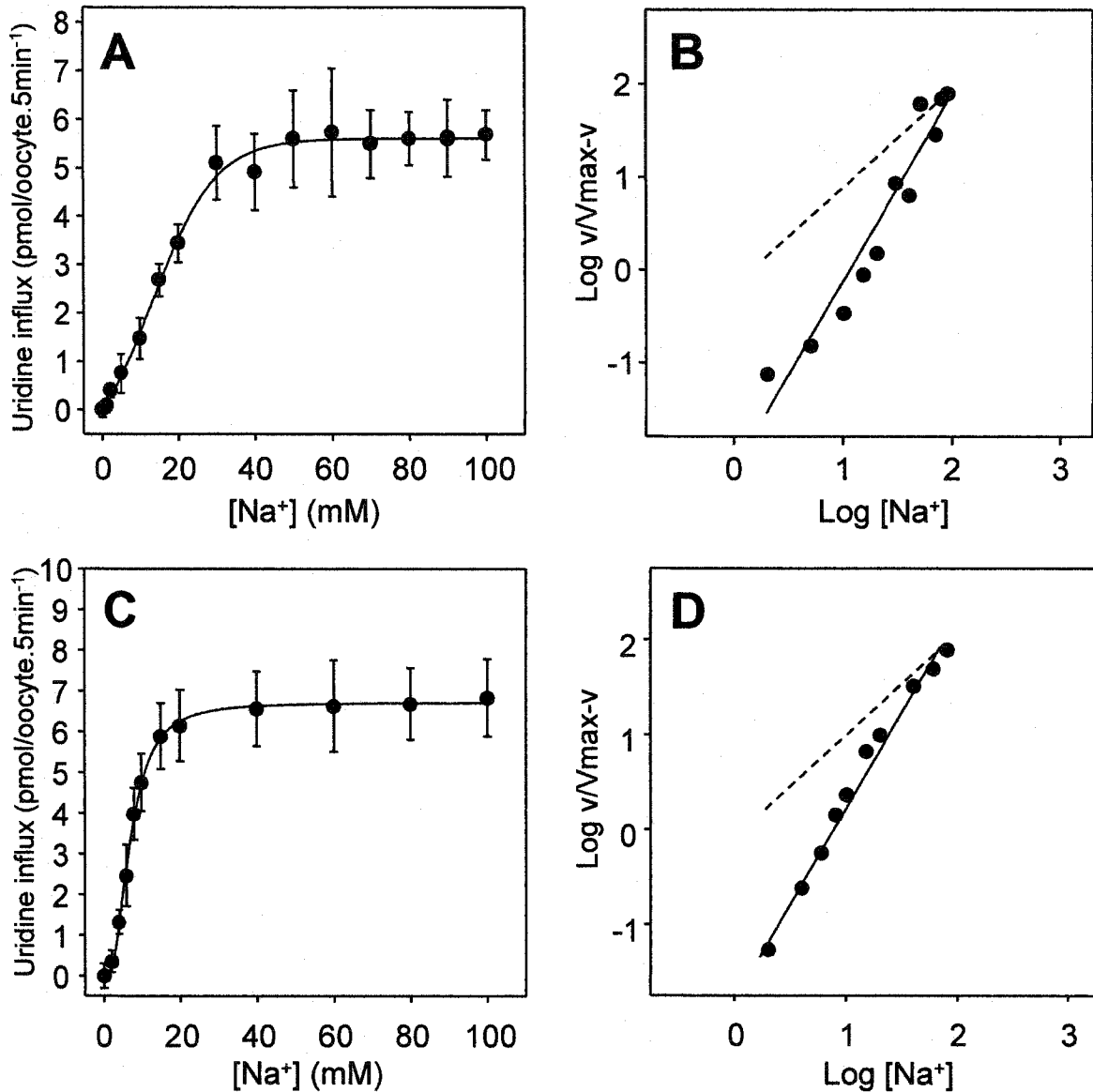


Figure 4-8. Sodium dependence of influx of uridine mediated by recombinant hCNT3 and mCNT3. Initial rates of transporter-mediated uptake of uridine (10 μ M, 20°C, 5 min) by hCNT3 (A) and mCNT3 (C) were measured in transport media containing 0 - 100 mM NaCl, using choline chloride to maintain isosmolality. Mediated transport was calculated as uptake in RNA-injected oocytes minus uptake in water-injected oocytes (uptake of uridine by water-injected oocytes was not Na⁺-dependent). B and D are Hill plots of the hCNT3 and mCNT3 data, respectively. K_{50} values and Hill coefficients (n) are given in the text. Broken lines in B and D correspond to n values of 1.

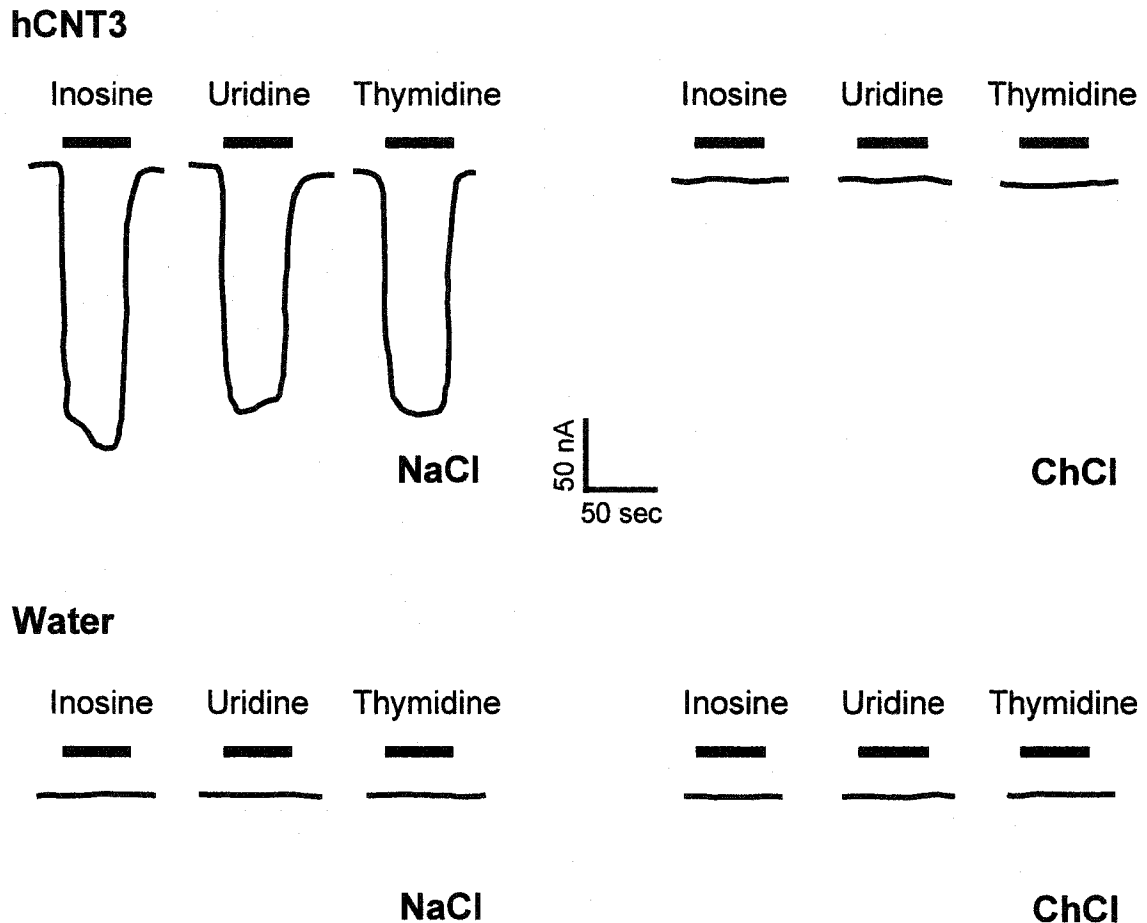


Figure 4-9. Sodium currents induced by exposure of recombinant hCNT3 to nucleoside permeants. *Upper panel (left)*, Inward currents caused by perfusing an hCNT3-expressing oocyte at room temperature with 200 μ M inosine, uridine or thymidine in Na^+ -containing transport medium (NaCl). *Upper panel (right)*, The same oocyte perfused with 200 μ M inosine, uridine or thymidine in transport medium with Na^+ replaced by choline (ChCl). No inward currents were generated. *Lower panels (left) and (right)*, The same experiment described in *Upper panels (left) and (right)* above, but with a control water-injected oocyte. No inward currents were generated.

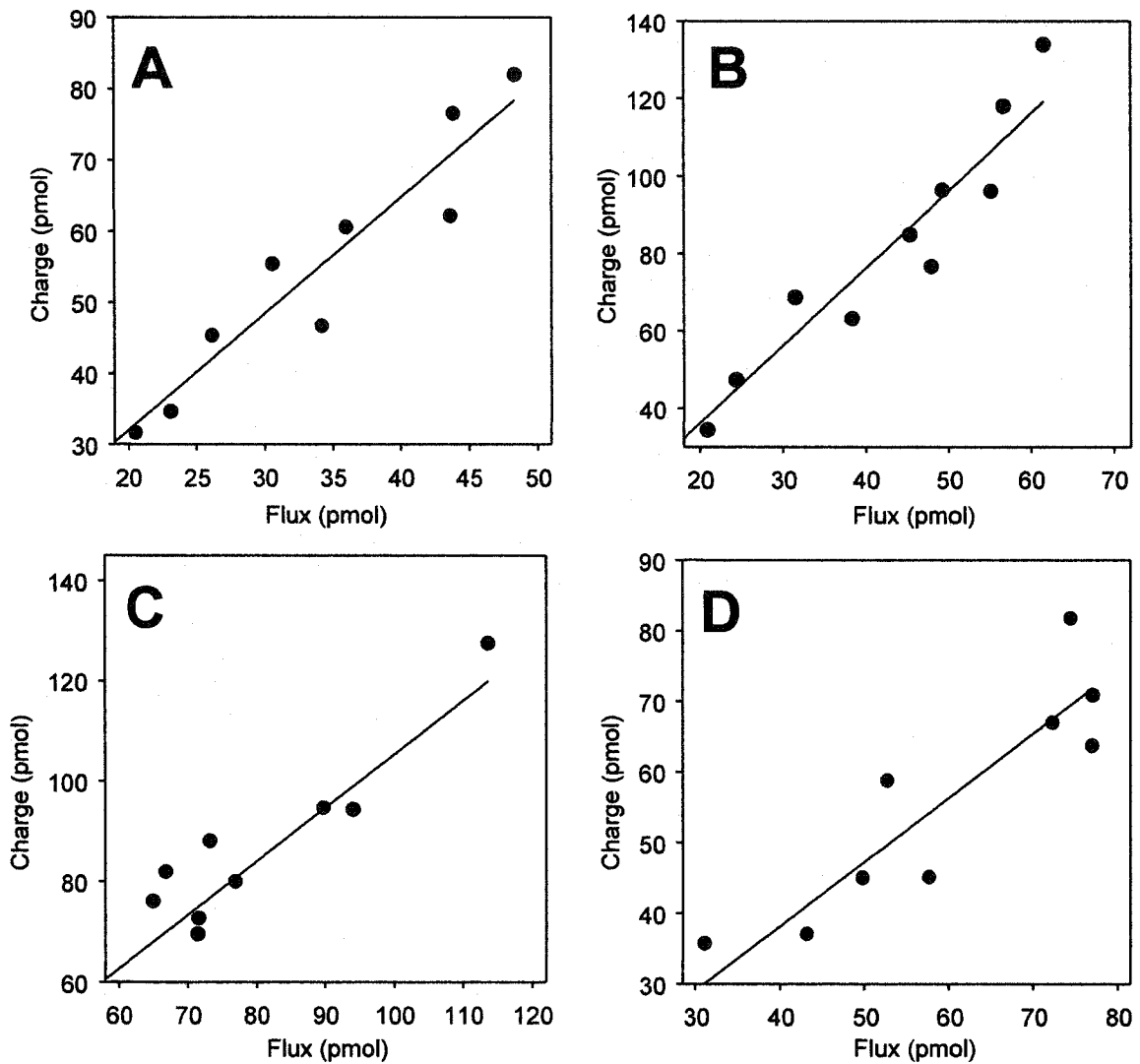


Figure 4-10. Stoichiometry of Na^+ /uridine and H^+ /uridine cotransport by recombinant hCNT3. Uridine-dependent charge and [^{14}C]-uridine uptake were simultaneously determined at $V_m = -50$ mV (*panels A and C*) or -90 mV (*panels B and D*) in the presence of Na^+ (NaCl transport medium, pH 7.5) (*panels A and B*) or H^+ (choline chloride (ChCl) transport medium, pH 5.5) (*panels C and D*) for 3 min. Integration of the uridine-evoked inward current with time was used to calculate the net cation influx by converting picocoulombs to picomoles using the Faraday constant. Mediated [^{14}C]-uridine uptake was calculated as uptake in hCNT3-producing oocytes minus uptake in water-injected oocytes. Each data point represents one oocyte. Slopes of the regression lines in *panels A-D* are given in the text.

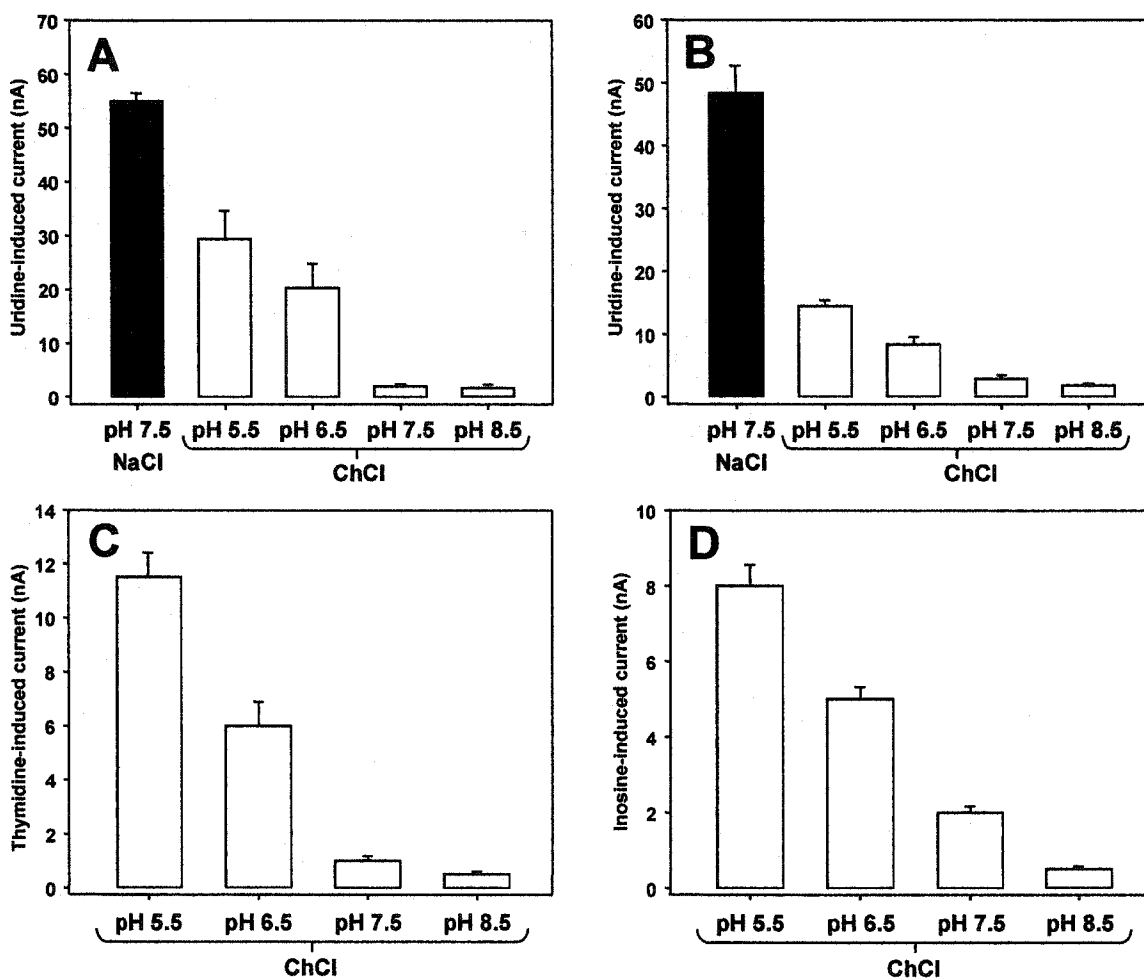


Figure 4-11. pH dependence of recombinant hCNT3 and mCNT3. Average inward currents measured by perfusing hCNT3-expressing oocytes (A) or mCNT3-expressing oocytes (B) at room temperature with 200 μ M uridine in transport medium containing 100 mM NaCl (black bars) or 100 mM choline chloride (open bars; ChCl). Medium pH values are indicated under each bar. No inward currents were present in H₂O-injected oocytes (data not shown). C and D (hCNT3- and mCNT3-expressing oocytes, respectively) are the same experiment described above, except in medium containing choline chloride only (open bars) and using 200 μ M concentrations of thymidine and inosine, respectively. Each value represents the mean \pm S.E. of 5-6 oocytes.

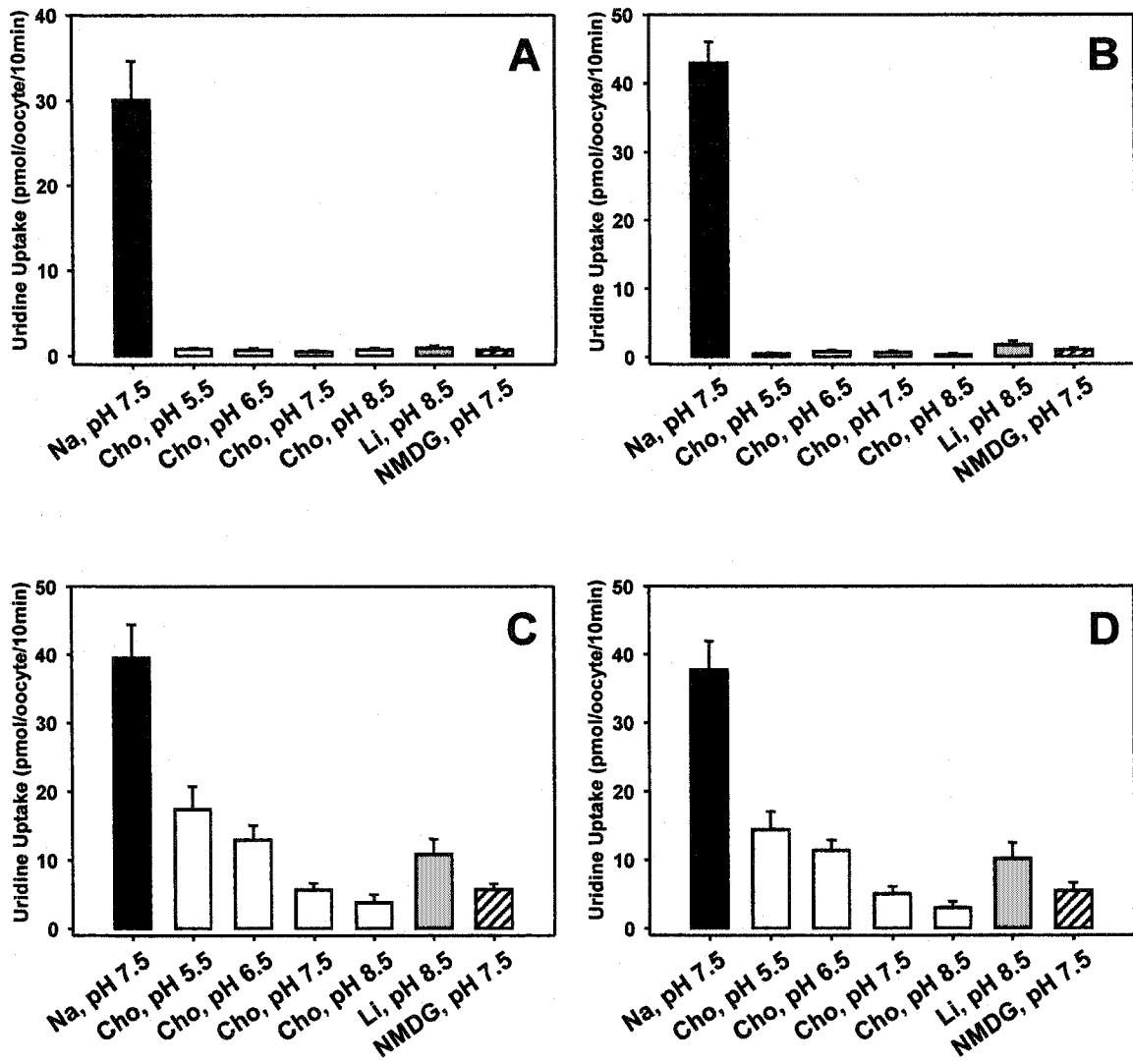


Figure 4-12. Effects of sodium, pH and lithium on the transport activities of oocytes expressing recombinant hCNT1, hCNT2, hCNT3, and mCNT3. Mediated fluxes of uridine (20 μ M, 20°C, 30 min) in oocytes injected with hCNT1 (A), hCNT2 (B), hCNT3 (C), or mCNT3 (D) RNA transcripts was measured in transport media containing 100 mM NaCl (black bars), 100 mM choline chloride (open bars; ChCl), 100 mM LiCl (gray bars), or 100 mM NMDG (hatched bars; N-methyl-D-glucamine). Mediated transport was calculated as uptake in RNA-injected oocytes minus uptake in water-injected oocytes. Each value represents the mean \pm S.E. of 10-12 oocytes.

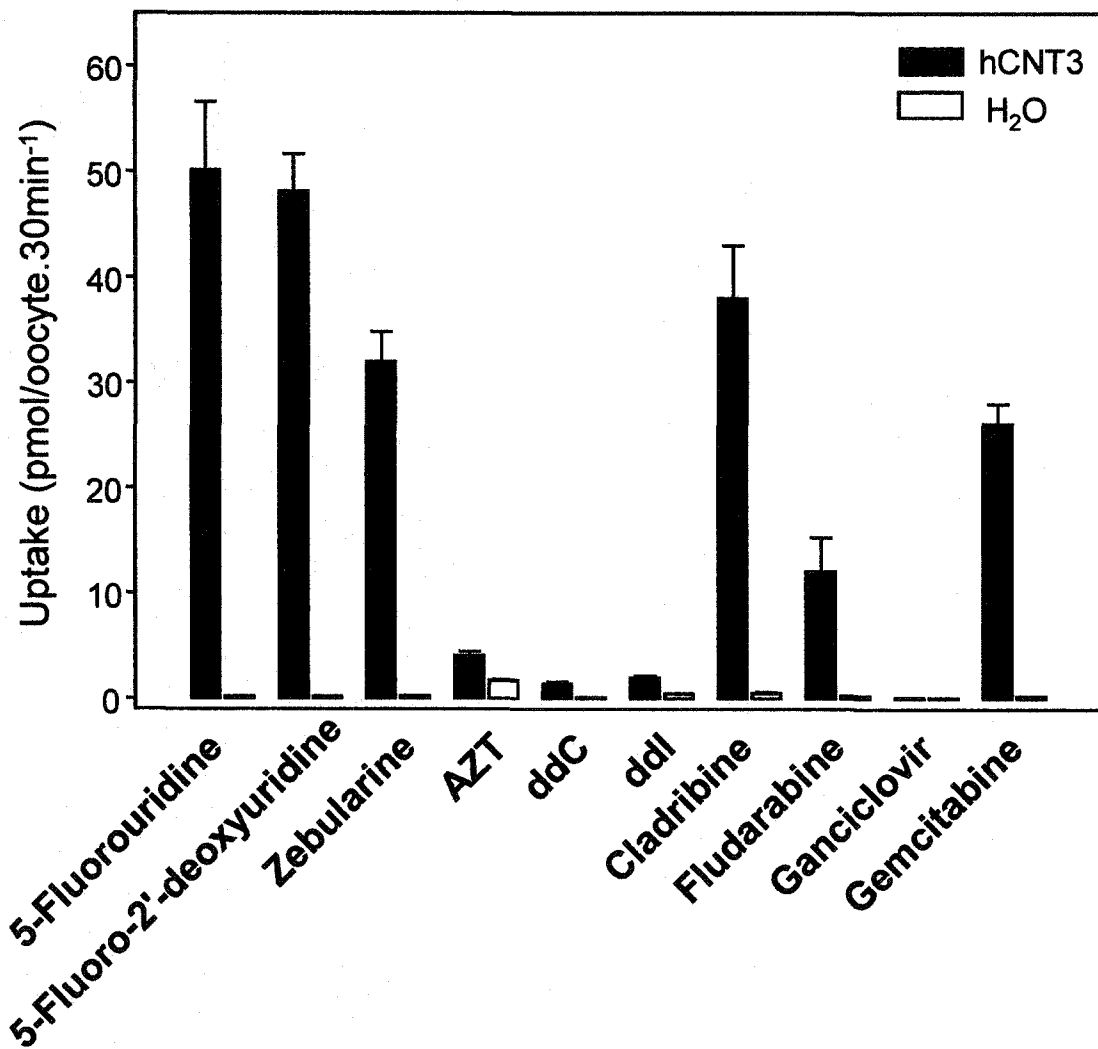


Figure 4-13. Uptake of ³H-labeled anticancer and antiviral nucleoside drugs by recombinant hCNT3 expressed in *Xenopus* oocytes. Uptake of nucleoside drugs (20 μM, 20°C, 30 min) in oocytes injected with RNA transcripts or water alone was measured in transport medium containing 100 mM NaCl.

hCNT3

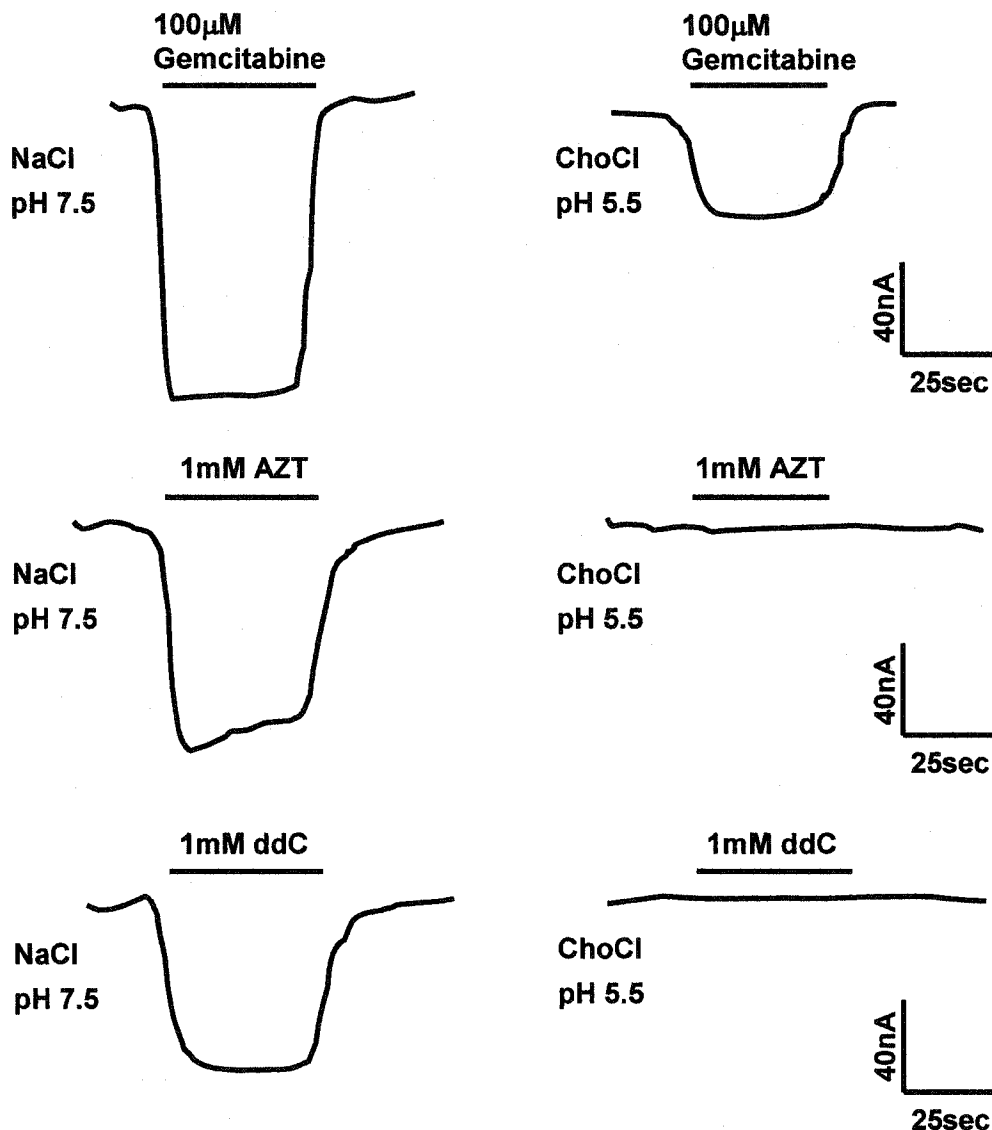


Figure 4-14. Representative nucleoside drug-induced currents in an hCNT3-producing *Xenopus* oocyte. Inward currents induced by gemcitabine (100 μ M), AZT (1 mM), or ddC (1 mM) were measured for 1 min at a membrane potential of -50 mV in transport medium containing either 100 mM NaCl at pH 7.5 (*left column*) or 100 mM choline chloride (ChCl) at pH 5.5 (*right column*). No currents were seen in water-injected oocytes. Values for uridine-evoked currents in control oocytes expressing hCNT3 were 180-230 nA in NaCl medium at pH 7.5 and 80-110 nA in choline chloride medium at pH 5.5 (*data not shown*).

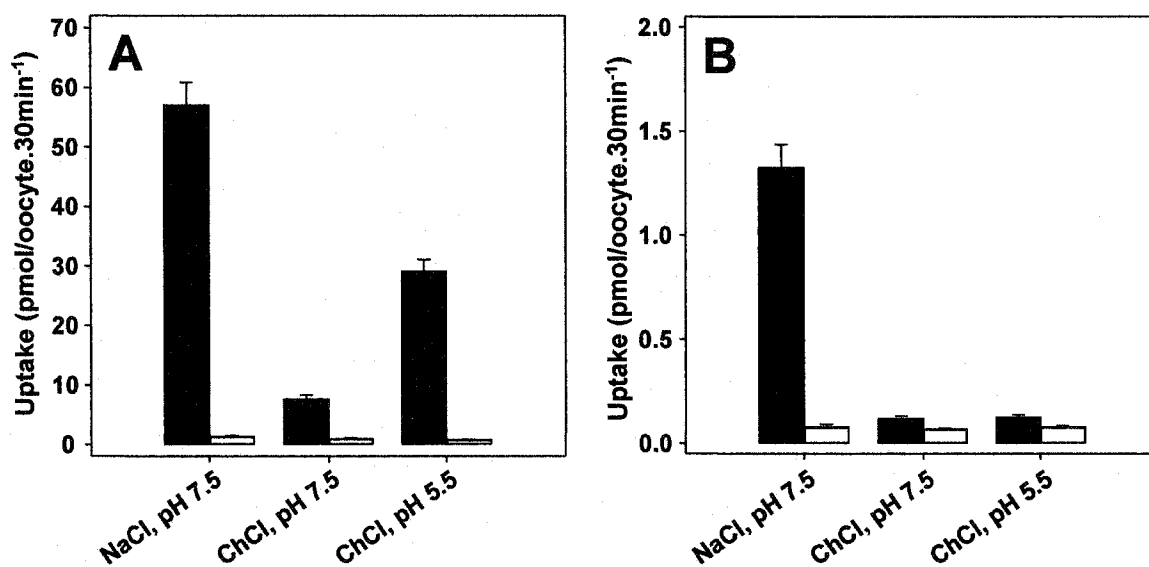


Figure 4-15. Na⁺- and H⁺-dependence of radiolabeled ddC and uridine uptake by recombinant hCNT3 expressed in *Xenopus* oocytes. Uptake of ¹⁴C-labeled uridine (A) and ³H-labeled ddC (B) (20 μM, 20°C, 30 min) in oocytes injected with RNA transcript (*black bars*) or water alone (*open bars*) was measured in transport medium containing 100 mM NaCl, pH 7.5 or 100 mM choline chloride (ChCl), pH 7.5/5.5.

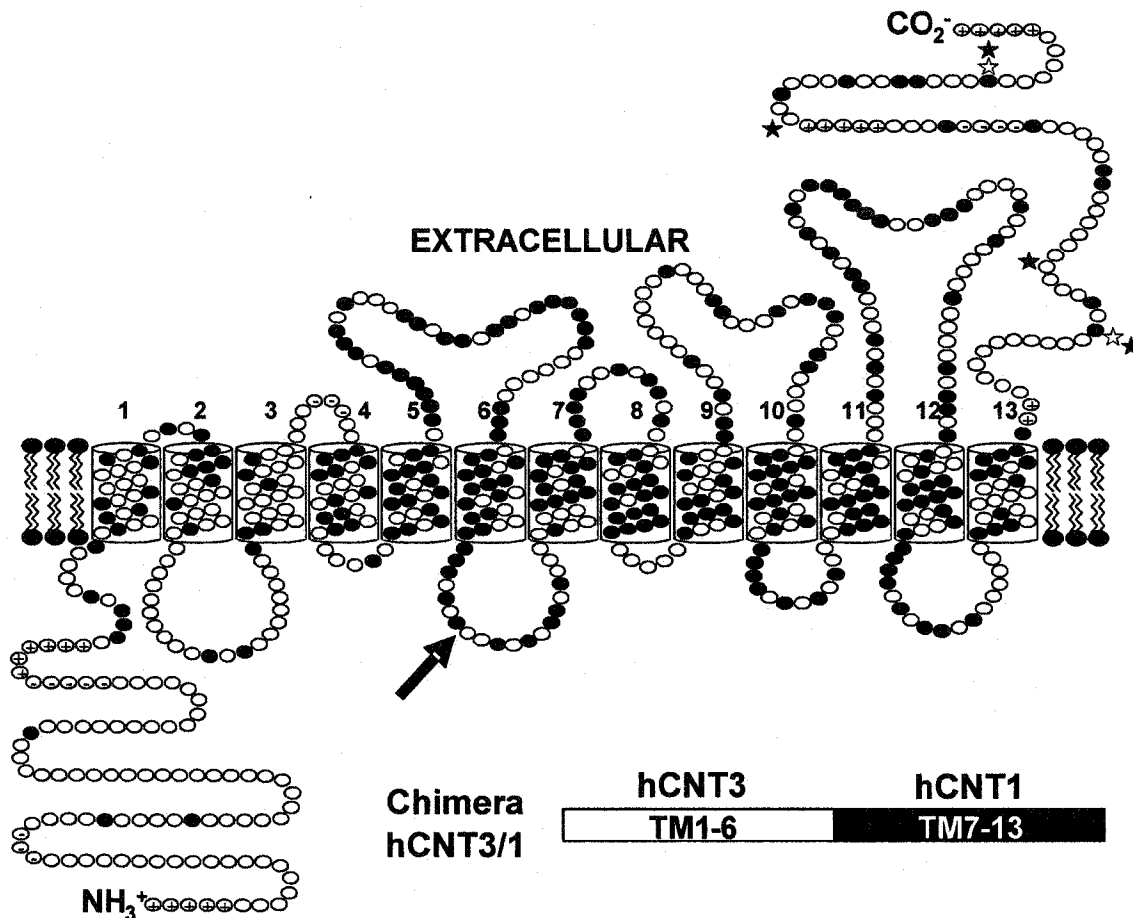


Figure 4-16. Topographical model of hCNT3 and hCNT1. Potential membrane-spanning α -helices are *numbered*, and putative glycosylation sites in predicted extracellular domains in hCNT3 and hCNT1 are indicated by *solid* and *open stars*, respectively. Residues identical in the two proteins are shown as *solid circles*. Residues corresponding to insertions in the sequence of hCNT3 or hCNT1 are indicated by *circles* containing “+” and “-” signs, respectively. The *arrow* represents splice site used for construction of the chimera. A schematic of the chimera is shown below.

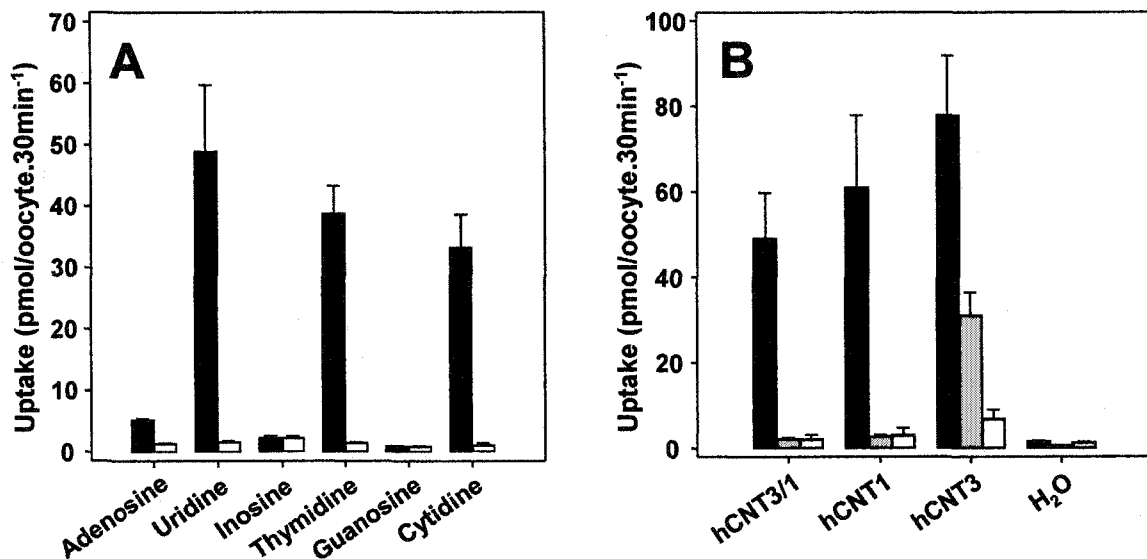
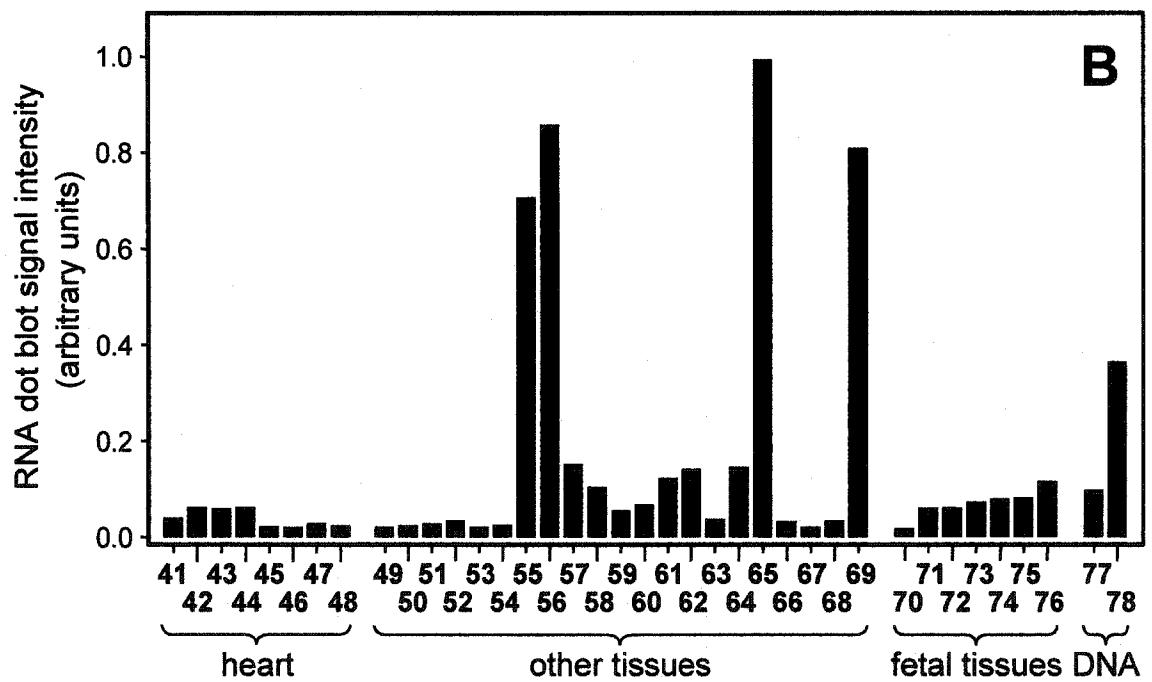
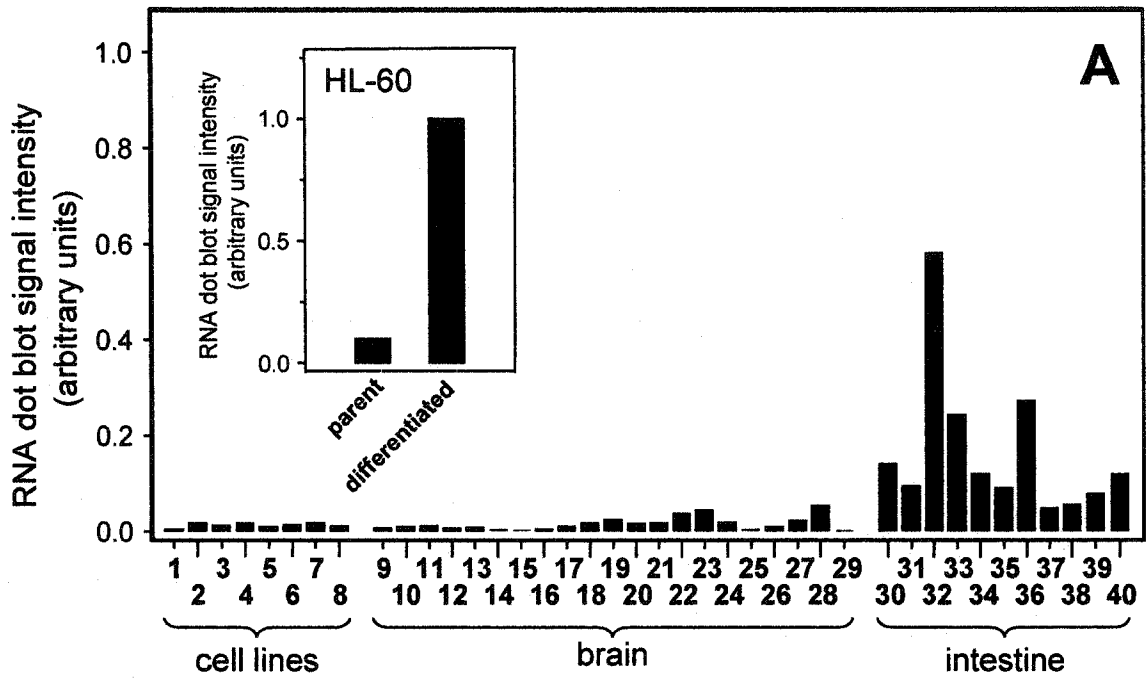


Figure 4-17. Uptake of nucleosides by chimera hCNT3/1. *A*, Nucleoside uptake (20 μ M, 20°C, 30 min) was measured in transport medium containing 100 mM NaCl in oocytes injected with RNA transcript (*black bars*) or water alone (*open bars*). *B*, Transporter-mediated nucleoside uptake (20 μ M, 20°C, 30 min) was measured in transport medium containing 100 mM NaCl, pH 7.5 (*black bars*) and 100 mM choline chloride at pH 7.5 (*gray bars*) and 5.5 (*open bars*). Mediated transport was calculated as uptake in RNA-injected oocytes minus uptake in water-injected oocytes. Each value in *panels A* and *B* is the mean \pm S.E. of 10-12 oocytes.

Figure 4-18. Tissue distribution of hCNT3 mRNA. *A* and *B*, A commercial human multiple tissue expression RNA array probed with a ³²P-labeled cDNA corresponding to hCNT3 amino acid residues 359-549. The *inset* in *A* is a dot blot of mRNA (0.5 μg) from suspension parent and adherent differentiated HL-60 cells probed with the same cDNA. The *numbered samples* are: 1, leukemia (undifferentiated HL-60); 2, HeLa S3; 3, leukemia (K-562); 4, leukemia (MOLT-4); 5, Burkitt's lymphoma (Raji); 6, Burkitt's lymphoma (Daudi); 7, colorectal adenocarcinoma (SW480); 8, lung carcinoma (A549); 9, whole brain; 10, cerebral cortex; 11, frontal lobe; 12, parietal lobe; 13, occipital lobe; 14, temporal lobe; 15, paracentral gyrus of cerebral cortex; 16, pons; 17, cerebellum (left); 18, cerebellum (right); 19, corpus callosum; 20, amygdala; 21, caudate nucleus; 22, hippocampus; 23, medulla oblongata; 24, putamen; 25, substantia nigra; 26, accumbens nucleus; 27, thalamus; 28, pituitary gland; 29, spinal cord; 30, esophagus; 31, stomach; 32, duodenum; 33, jejunum; 34, ileum; 35, ilocecum; 36, appendix; 37, colon (ascending); 38, colon (transverse); 39, (descending); 40, rectum; 41, heart; 42, aorta; 43, atrium (left); 44, atrium (right); 45, ventricle (left); 46, ventricle (right); 47, interventricular septum; 48, apex of the heart; 49, kidney; 50, skeletal muscle; 51, spleen; 52, thymus; 53, peripheral blood leukocyte; 54, lymph node; 55, bone marrow; 56, trachea; 57, lung; 58, placenta; 59, bladder; 60, uterus; 61, prostate; 62, testis; 63, ovary; 64, liver; 65, pancreas; 66, adrenal gland; 67, thyroid gland; 68, salivary gland; 69, mammary gland; 70, fetal brain; 71, fetal heart; 72, fetal kidney; 73, fetal liver; 74, fetal spleen; 75, fetal thymus; 76, fetal lung; 77, human DNA (100ng) ; 78, human DNA (500ng).



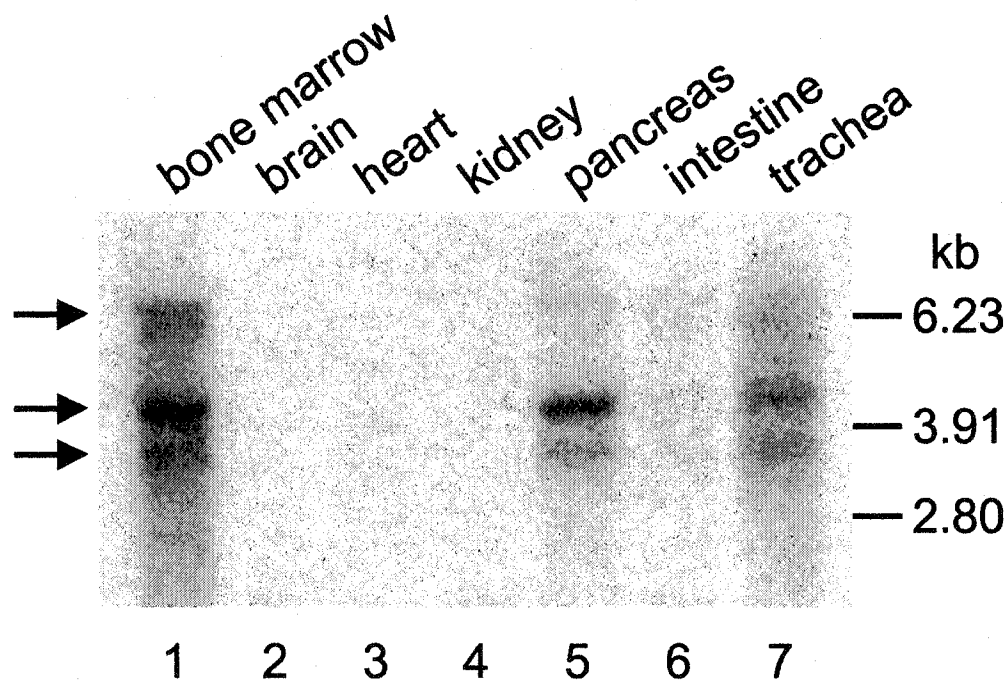


Figure 4-19. High stringency Northern analysis of mRNA from human tissues probed with ^{32}P -labeled hCNT3 cDNA. Samples of human tissue mRNA (5 μg) were separated on a 0.8% formaldehyde-agarose gel and blotted on to BrightStar-Plus nylon transfer membrane. Hybridization with a radiolabeled cDNA probe for the coding sequence of hCNT3 amino acid residues 359-549 was performed under high stringency conditions where there was no cross-reactivity with hCNT1 or hCNT2. *Arrows* indicate the positions of three bands in pancreas, bone marrow with sizes of 3.5-, 4.2- and 6.5-kb.

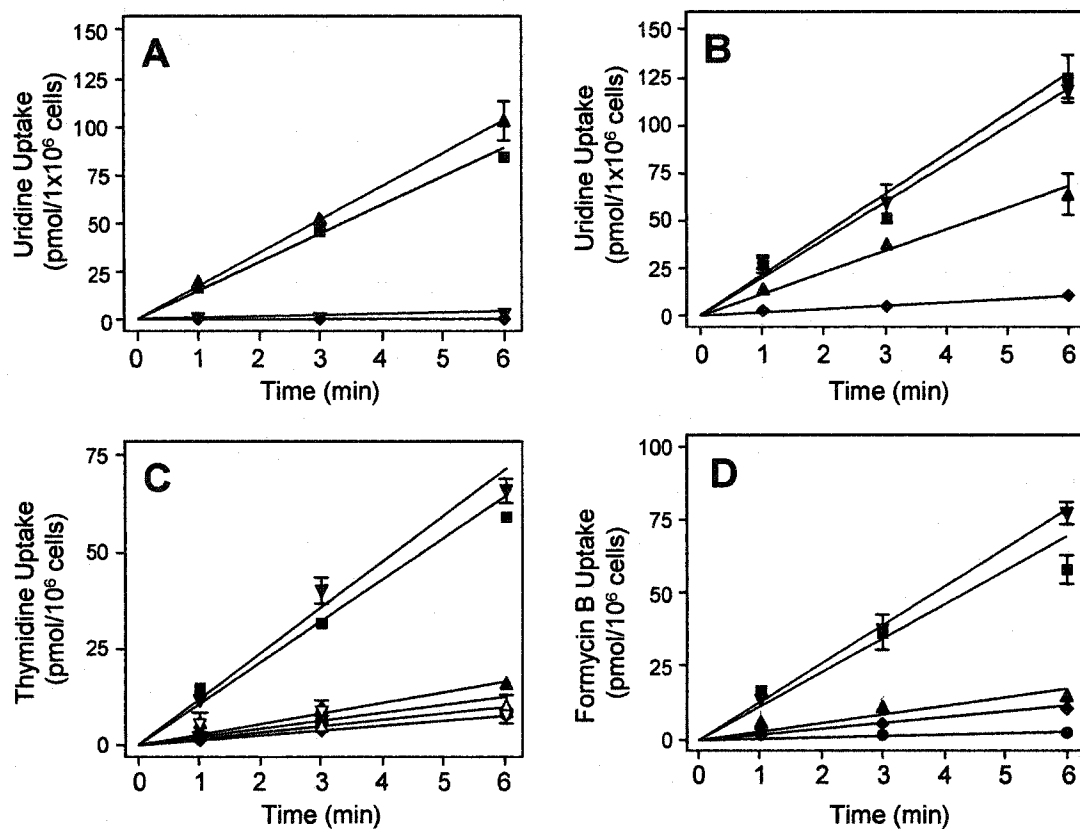
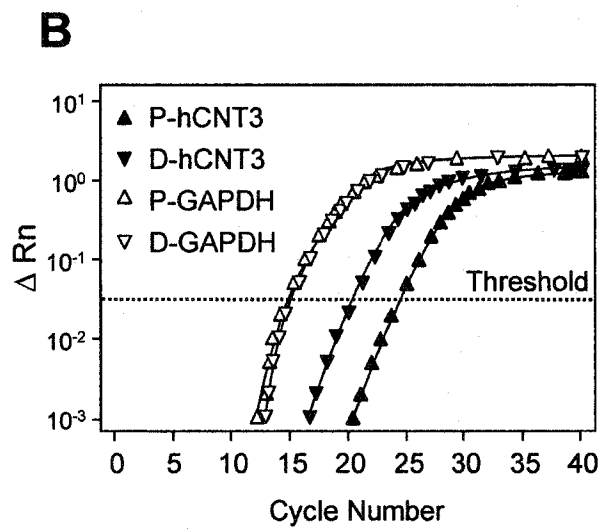
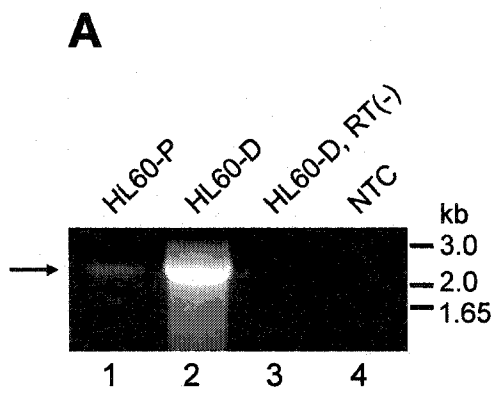


Figure 4-20. Time courses of ^3H -labeled uridine, thymidine and formycin B uptake by HL-60 cells. *A* and *B*, Uptake of 10 μM uridine (20°C) by suspension parent (*A*) and adherent differentiated (*B*) HL-60 cells. Total transport (*square*, no inhibitor, Na^+ -containing medium) was compared to equilibrative transport (*upward triangle*, no inhibitor, NMDG-containing medium), concentrative transport (*downward triangle*, 100 μM dilazep, Na^+ -containing medium), and diffusion (*diamond*, 100 μM dilazep, NMDG -containing medium). *C* and *D*, Uptake of 10 μM thymidine (*C*) and formycin B (*D*) by the concentrative transport process in adherent differentiated HL-60 cells. Uptake of each permeant was measured at 20°C to demonstrate total transport (*square*, no inhibitor, Na^+ -containing medium), equilibrative transport (*upward triangle*, no inhibitor, NMDG-containing medium), concentrative transport (*downward triangle*, 100 μM dilazep, Na^+ -containing medium), and diffusion (*diamond*, 100 μM dilazep, Na^+ -containing medium). In addition, concentrative transport, in the presence of Na^+ and 100 μM dilazep, of each permeant was assessed in the presence of competing unlabeled nucleosides including 1 mM thymidine (*circle*), 1 mM inosine (*open downward triangle*) and 1 mM uridine (*open upward triangle*).

Figure 4-21. Non-quantitative RT-PCR and TaqMan™ quantitative RT-PCR of hCNT3 transcripts in HL-60 cells. *A*, RNA from suspension parent (HL60-P, *lane 1*) and adherent differentiated (HL60-D, *lane 2*) cells in exponential growth was subjected to RT followed by PCR using hCNT3 primers flanking the hCNT3 open reading frame (see *Materials and Methods*), and the products were run on an ethidium bromide-stained agarose gel. hCNT3-specific PCR products migrated at the expected size of ~ 2.2 kb (*arrow*). The negative controls were RNA preparations from differentiated HL-60 cells that were subjected to PCR but not RT (RT(-), *lane 3*) and that did not contain template (NTC, *lane 4*). A predominant band was amplified from the HL-60 differentiated cells (*lane 2*), whereas a faint band of the same size was amplified from the HL-60 parent sample (*lane 1*). The RT-free (*lane 3*) and template-free (*lane 4*) preparations were both negative. *B*, Real time quantitative PCR was performed on cDNA from HL-60 parent (P, *upward triangles*) or differentiated (D, *downward triangles*) cells in exponential growth using primers and probes specific for either hCNT3 (*solid symbols*) or GAPDH (*open symbols*). The ΔRn , or change in reporter fluorescence normalized to the cycle-to-cycle signal from a passive reference dye, is plotted against the PCR cycle number. The cycle threshold, Ct , values were assessed at the point at which ΔRn values crossed the threshold value, which was above background and within the exponential phase of the reaction. The values plotted are from representative samples. The results of three experiments, each with duplicate samples, were used to calculate the difference in hCNT3 transcript expression between the two cell populations (see *Results and Discussion*). The template-free control values were at background levels.



Bibliography

- Anderson CM, Xiong W, Young JD, Cass CE, and Parkinson FE** (1996) Demonstration of the existence of mRNAs encoding N1/*cif* and N2/*cit* sodium/nucleoside cotransporters in rat brain. *Mol Brain Res* 42: 358-361.
- Baldwin SA, Mackey JR, Cass CE, and Young JD** (1999) Nucleoside transporters: molecular biology and implications for therapeutic development. *Mol Med Today* 5: 216-224.
- Belt JA, Marina NM, Phelps DA, and Crawford CR** (1993) Nucleoside transport in normal and neoplastic cells. *Adv Enzyme Regul* 33: 235-252.
- Boleti H, Coe IR, Baldwin SA, Young JD and Cass CE** (1997) Molecular identification of the equilibrative NBMPR-sensitive (*ei*) nucleoside transporter and demonstration of an equilibrative NBMPR-insensitive (*ei*) transport activity in human erythroleukemia (K562) cells. *Neuropharmacology* 38: 1167-1179.
- Cass CE** (1995) Nucleoside transport. In *Drug Transport in Antimicrobial and Anticancer Chemotherapy* (Georgopapadakou, NH, ed) pp. 404-451, Marcel Dekker, New York.
- Che M, Ortiz DF, and Arias IM** (1995) Primary structure and functional expression of a cDNA encoding the bile canalicular, purine-specific Na⁺-nucleoside cotransporters. *J Biol Chem* 270: 13596-13599.
- Chen XZ, Coady MJ, Jackson F, Berteloot A and Lapointe JY** (1995) Thermodynamic determination of the Na⁺: glucose coupling ratio for the human SGLT1 cotransporter. *Biophys J* 69: 2405-2414.
- Chen XZ, Shayakul C, Berger UV, Tian W, and Hediger MA** (1998) Characterization of a rat Na⁺-dicarboxylate cotransporters. *J Biol Chem* 273: 20972-20981.
- Chen XZ, Zhu T, Smith DE, and Hediger MA** (1999) Stoichiometry and kinetics of the high-affinity H⁺-coupled peptide transporter PepT2. *J Biol Chem* 274: 2773-2779.
- Craig JE, Zhang Y, and Gallagher MP** (1994) Cloning of the *nupC* gene of *Escherichia coli* encoding a nucleoside transport system, and identification of an adjacent insertion element, IS 186. *Mol Microbiol* 11: 1159-1168.
- Crawford CR, Patel DH, Naeve C, and Belt JA** (1998) Cloning of a human equilibrative, nitrobenzylmercaptapurine riboside (NBMPR)-insensitive nucleoside transporter *ei* by functional expression in a transport-deficient cell line. *J Biol Chem* 273: 5288-5293.
- Deutsch PJ, Hoeffler JP, Jameson JL, and Habener JF.** (1988) Cyclic AMP and phorbol ester-stimulated transcription mediated by similar DNA elements that bind distinct proteins. *Proc Natl Acad Sci USA* 85: 7922-7926.

- Diez-Sampedro A, Eskandari S, Wright EM, and Hirayama BA** (2001) Na⁺-to-sugar stoichiometry of SGLT3. *Am J Physiol Renal Physiol* 280: F278-F282.
- Fang X, Parkinson FE, Mowles DA, Young JD, and Cass CE** (1996) Functional characterization of a recombinant sodium-dependent nucleoside transporter with selectivity for pyrimidine nucleosides (cNT1rat) by transient expression in cultured mammalian cells. *Biochem J* 317: 457-465.
- Felsenstein J** (1989) Phylip-Phylogeny inference package (version 3.2). *Cladistics* 5: 164-166.
- Fink L, Seeger W, Ermert L, Hanze J, Stahl U, Grimminger F, Kummer W, Bohle RM** (1998) Real-time quantitative RT-PCR after laser-assisted cell picking. *Nat Med* 4: 1329-1333.
- Fredholm BB** (1997) Adenosine and neuroprotection. *Int Rev Neurobiol* 40 :259-80.
- Flanagan SA and Meckling-Gill KA** (1997) Characterization of a novel Na⁺-dependent, guanosine-specific, nitrobenzylthioinosine-sensitive transporter in acute promyelocytic leukemia cells. *J Biol Chem* 272: 18026-18032.
- Griffiths M, Beaumont N, Yao SYM, Sundaram M, Bouman CE, Davies A, Kwong FYP, Coe IR, Cass CE, Young JD, and Baldwin SA** (1997a) Cloning of a human nucleoside transporter implicated in the cellular uptake of adenosine and chemotherapeutic drugs. *Nat Med* 3: 89-93.
- Griffiths M, Yao SYM, Abidi F, Phillips SEV, Cass CE, Young JD, and Baldwin SA** (1997b) Molecular cloning and characterization of a nitrobenzylthioinosine-insensitive (*et*) equilibrative nucleoside transporter from human placenta. *Biochem J* 328: 739-743.
- Graham KA, Leithoff J, Coe IR, Mowles D, Mackey JR, Young JD and Cass CE** (2000) Differential transport of cytosine-containing nucleosides by recombinant human concentrative nucleoside transporter protein hCNT1. *Nucleosides Nucleotides Nucleic Acids* 19: 415-434.
- Groothuis DR and Levy RM** (1997) The entry of antiviral and antiretroviral drugs into the central nervous system. *J Neurovirol* 3: 387-400.
- Hamilton SR, Yao SYM, Gallagher MP, Henderson PJF, Cass CE, Young JD, and Baldwin SA** (2001) Subcellular distribution and membrane topology of the mammalian concentrative Na⁺-nucleoside cotransporters rCNT1. *J Biol Chem* 276: 27981-27988.
- Handschumacher RE and Cheng CY** (1993) Purine and pyrimidine antimetabolites. In *Cancer Metabolism* (Holland E, Frei E, Bast RC, Kufe DW, Morton DL, and Weichselbaum RR, eds.) pp. 712-732, Lea & Febiger, Philadelphia.
- Hirayama BA, Loo DD, and Wright EM** (1994) Protons drive sugar transport through the Na⁺/glucose cotransporter (SGLT1). *J Biol Chem* 269: 21407-21410.
- Hirayama BA, Loo DD, and Wright EM** (1997) Cation effects on protein conformation and transport in the Na⁺/glucose cotransporter. *J Biol Chem* 272: 2110-2115.

- Hong M, Schlichter L, and Bendayan R** (2000) A Na⁺-dependent nucleoside transporter in microglia. *J Pharmacol Exp Ther* 292: 366-374.
- Hong M, Schlichter L, and Bendayan R** (2001) A novel zidovudine uptake system in microglia. *J Pharmacol Exp Ther* 296: 141-149.
- Horton RM, Hunt HD, Ho SN, Pullen JK, and Pease LR** (1989) Engineering hybrid genes without the use of restriction enzymes: gene splicing by overlap extension. *Gene* 77: 51-59.
- Huang QQ, Harvey CM, Paterson ARP, Cass CE, and Young JD** (1993) Functional expression of Na⁺-dependent nucleoside transport systems of rat intestine in isolated oocytes of *Xenopus laevis*. Demonstration that rat jejunum expresses the purine-selective system N1 (*cif*) and a second, novel system N3 having broad specificity for purine and pyrimidine nucleosides. *J Biol Chem* 268: 20613-20619.
- Huang QQ, Yao SYM, Ritzel MWL, Paterson ARP, Cass CE, and Young JD** (1994) Cloning and functional expression of a complementary DNA encoding a mammalian nucleoside transport protein. *J Biol Chem* 269: 17757-17760.
- Kanai Y, Lee WS, You G, Brown D, and Hediger MA** (1994) The human kidney low affinity Na⁺/glucose cotransporter SGLT2. Delineation of the major renal reabsorptive mechanism for D-glucose. *J Clin Invest* 93: 397-404.
- Lee CW, Sokoloski JA, Sartorelli AC, and Handschumacher RE** (1991) Induction of the differentiation of HL-60 cells by phorbol 12-myristate 13-acetate activates a Na⁺-dependent uridine-transport system. Involvement of protein kinase C. *Biochem J* 274: 85-90.
- Lee CW, Sokoloski JA, Sartorelli AC, and Handschumacher RE** (1994) Differentiation of HL-60 cells by dimethylsulfoxide activates a Na⁺-dependent nucleoside transport system. *In Vivo* 8: 795-801.
- Liman ER, Tytgat J and Hess P** (1992) Subunit stoichiometry of a mammalian K⁺ channel determined by construction of multimeric cDNAs. *Neuron* 9: 861-871.
- Loewen SK, Ng AML, Yao SYM, Cass CE, Baldwin SA and Young JD** (1999) Identification of amino acid residues responsible for the pyrimidine and purine nucleoside specificities of human concentrative Na⁺ nucleoside cotransporters hCNT1 and hCNT2. *J Biol Chem* 274: 24475-24484.
- Lotem J and Sachs L** (1979) Regulation of normal differentiation in mouse and human myeloid leukemic cells by phorbol esters and the mechanism of tumor promotion. *Proc Natl Acad Sci USA* 76: 5158-5162.
- Mackenzie B, Loo DDF, Panayotova-Heiermann M, and Wright EM** (1996) Biophysical characteristics of the pig kidney Na⁺/glucose cotransporter SGLT2 reveal a common mechanism for SGLT1 and SGLT2. *J Biol Chem* 271: 32678-32683.
- Mackenzie B, Loo DD, and Wright EM** (1998) Relationships between Na⁺/glucose cotransporter (SGLT1) currents and fluxes. *J Membr Biol* 162: 101-106.

- Mackey JR, Baldwin SA, Young JD, and Cass CE (1998a)** Nucleoside transport and its significance for anticancer drug resistance. *Drug Resistance Updates*, 1: 310-324.
- Mackey JR, Mani RS, Selner M, Molwes D, Young JD, Belt JA, Crawford CR, and Cass CE (1998b)** Functional nucleoside transporters are required for gemcitabine influx and manifestation of toxicity in cancer cell lines. *Cancer Res* 58: 4349-4357.
- Mackey JR, Yao SYM, Smith KM, Karpinski E, Baldwin SA, Cass CE, and Young JD (1999)** *J Natl* Gemcitabine transport in *Xenopus* oocytes expressing recombinant plasma membrane mammalian nucleoside transporters. *Cancer Inst USA* 91: 1876-1881.
- Pajor AM and Wright EM (1992)** Cloning and functional expression of a mammalian Na⁺-nucleoside cotransporters. A member of the SGLT family. *J Biol Chem* 267: 3557-3560.
- Paterson ARP, Gati WP, Vijayalakshmi D, Cass CE, Mant MJ, Young JD, and Belch AR (1993)** *Proc Am Assoc Cancer Res* 34: A84.
- Plass C, Weichenhan D, Catanese J, Costello JF, Yu F, Yu L, Smiraglia D, Cavenee WK, Caligiuri MA, deJong P, and Held WA (1997)** An arrayed human *NotI-EcoRV* boundary library as a tool for RLGS spot analysis. *DNA Res* 4: 253-255.
- Pourcher T, Leclercq S, Brandolin G, and Leblanc G (1995)** Melibiose permease of *Escherichia coli*: large scale purification and evidence that H⁺, Na⁺, and Li⁺ sugar symport is catalyzed by a single polypeptide. *Biochemistry* 34: 4412-4420.
- Ritzel MWL, Yao SYM, Huang MY, Elliot JF, Cass CE, and Young JD (1997)** Molecular cloning and functional expression of cDNAs encoding a human Na⁺-nucleoside cotransporters (hCNT1). *Am J Physiol* 272: C707-C714.
- Ritzel MWL, Yao SYM, Ng AML, Mackey JR, Cass CE, and Young JD (1998)** Molecular cloning, functional expression and chromosomal localization of a cDNA encoding a human Na⁺ nucleoside cotransporters (hCNT2) selective for purine nucleosides and uridine. *Mol Membr Biol* 15: 203-211.
- Rovera G, Santoli D, and Damsky C (1979)** Human promyelocytic leukemia cells in culture differentiate into macrophage-like cells when treated with a phorbol diester. *Proc Natl Acad Sci USA* 76: 2779-2783.
- Roy L, Sorokine-Durm I, and Voisin P (1996)** Comparison between fluorescence in situ hybridization and conventional cytogenetics for dicentric scoring: a first-step validation for the use of FISH in biological dosimetry. *Int J Radiat Biol* 70: 665-669.
- Shryock JC and Belardinelli L (1997)** Adenosine and adenosine receptors in the cardiovascular system: biochemistry, physiology and pharmacology. *Am J Cardiol* 79: 2-10.
- Thompson JD, Gibson TJ, Plewniak F, Jeanmougin F, and Higgins DG (1997)** The CLUSTAL_X windows interface: flexible strategies for multiple sequence alignment aided by quality analysis tools. *Nucleic Acids Res* 24: 4876-4882.

- Wang J, Su SF, Dresser MJ, Schaner ME, Washington CB, and Giacomini KM** (1997) Na⁺-dependent purine nucleoside transporter from human kidney: cloning and functional characterization. *Am J Physiol* 273: F1058-F1065.
- Wang J and Giacomini KM** (1997) Molecular determinants of substrate selectivity in Na⁺-dependent nucleoside transporters. *J Biol Chem* 272: 28845-28848.
- Wang J and Giacomini KM** (1999) Serine 318 is essential for the pyrimidine selectivity of the N2 Na⁺-nucleoside transporter. *J Biol Chem* 274: 2298-2302.
- Wright EM** (2001) Renal Na⁺-glucose cotransporters. *Am J Physiol Renal Physiol* 280: F10-F18.
- Wu X, Yuan G, Brett CM, Hui AC, and Giacomini KM** (1992) Sodium-dependent nucleoside transport in choroid plexus from rabbit. Evidence for a single transporter for purine and pyrimidine nucleosides. *J Biol Chem* 267: 8813-8818.
- Yao SYM, Ng AML, Ritzel MWL, Gati WP, Cass CE, and Young JD** (1996a) Transport of adenosine by recombinant purine- and pyrimidine-selective sodium/nucleoside cotransporters from rat jejunum expressed in *Xenopus laevis* oocytes. *Mol Pharmacol* 50: 1529-1535.
- Yao SYM, Cass CE, and Young JD** (1996b) Transport of the antiviral nucleoside analogs 3'-azido-3'-deoxythymidine and 2',3'-dideoxycytidine by a recombinant nucleoside transporter (rCNT) expressed in *Xenopus laevis* oocytes. *Mol Pharmacol* 50: 388-393.
- Yao SYM, Ng AML, Muzyka WR, Griffiths M, Cass CE, Baldwin SA, and Young JD** (1997) Molecular cloning and functional characterization of nitrobenzylthioinosine (NBMPR)-sensitive (*es*) and NBMPR-insensitive (*ei*) equilibrative nucleoside transporter proteins (rENT1 and rENT2) from rat tissues. *J Biol Chem* 272: 28423-28430.
- Yao SYM, Ng AML, Loewen SK, Cass CE, Baldwin SA, and Young JD** (2002) An ancient marine pre-vertebrate Na⁺/nucleoside cotransporter (hfcNT) from the Pacific hagfish (*Eptatretus stouti*). *Am J Physiol* 283: C155-C168.

CHAPTER V:*

An ancient prevertebrate Na⁺-nucleoside cotransporter (hfcNT) from the Pacific hagfish (*Eptatretus stouti*).**

* *A version of this chapter has been published.*

Yao SYM, Ng AML, Loewen SK, Cass CE, Baldwin SA, and Young JD (2002) *Am J Physiol Cell Physiol* 283: C155-C168.

** I worked together with Dr. Sylvia Yao to undertake the functional studies described in this chapter. I was also responsible for the phylogenetic and sequence analysis of hfcNT as well as construction of the hfcNT/hcNT1 chimera and its functional characterization.

Introduction

Most natural and synthetic nucleosides are hydrophilic and require specialized nucleoside transport (NT) proteins for passage across cell membranes (Griffith and Jarvis, 1996; Cheeseman *et al.*, 2000). NT-mediated transport is therefore a critical determinant of intracellular nucleoside metabolism and the pharmacologic actions of antineoplastic and antiviral nucleoside drugs (Mackey *et al.*, 1998; Baldwin *et al.*, 1999). By modulating the concentration of adenosine in the vicinity of cell surface receptors, NTs also have important physiological effects on neurotransmission, vascular tone and other processes (Shryock and Berladinelli, 1997; Dunwiddie and Masino, 2001). Five major nucleoside transport processes that differ in their cation dependence, permeant selectivities and inhibitor sensitivities have been observed in human and other mammalian cells and tissues (Griffith and Jarvis, 1996; Cheeseman *et al.*, 2000). Three are concentrative (Na^+ -dependent) (systems *cit*, *cif* and *cib*) and two are equilibrative (Na^+ -independent) (systems *es* and *ei*). The former are found primarily in specialized epithelia such as intestine, kidney, liver, choroid plexus and in leukemic cells, while the latter are present in most, possibly all, cell types (Griffith and Jarvis, 1996; Baldwin *et al.*, 1999; Cheeseman *et al.*, 2000). Systems *cit* and *cif* transport adenosine and uridine, but are otherwise pyrimidine or purine nucleoside selective, respectively. Systems *cib*, *es* and *ei* are broadly selective for both pyrimidine and purine nucleosides. The *ei* system also transports nucleobases (Yao *et al.*, 2002).

Molecular cloning studies have isolated cDNAs encoding the human proteins responsible for each of these NT processes (*cit*, *cif*, *cib*, *es*, *ei*) (Griffiths *et al.*, 1997a, 1997b; Ritzel *et al.*, 1997; Wang *et al.*, 1997; Crawford *et al.*, 1998; Ritzel *et al.*, 1998, 2001). These proteins and their orthologs in other mammalian species (Huang *et al.*, 1994; Che *et al.*, 1995; Yao *et al.*, 1996, 1997; Ritzel *et al.*, 2001) comprise two new, previously unrecognized families of integral membrane proteins designated CNT (concentrative nucleoside transporter family) and ENT (equilibrative nucleoside transporter family). The relationships of these NT proteins to the processes defined by functional studies are: CNT1 (*cit*), CNT2 (*cif*), CNT3 (*cib*), ENT1 (*es*), and ENT2 (*ei*). The two protein families are unrelated and have different membrane architectures (Hamilton *et al.*, 2001; Sundaram *et al.*, 2001), mammalian CNTs having 13 predicted transmembrane helices (TMs) with an intracellular N-terminus and an exofacial glycosylated

tail at the carboxyl-terminus (Hamilton *et al.*, 2001). NupC, a CNT family member from *Escherichia coli*, has a similar membrane topology to mammalian CNTs, but lacks TMs 1-3 (Hamilton *et al.*, 2001).

Human (h) CNT1 contains 650 amino acid residues and is 83% identical in sequence to rat (r) CNT1 (648 residues) (Huang *et al.*, 1994; Ritzel *et al.*, 1997). hCNT2 (658 residues) is 83% identical to rCNT2 (659 residues) and 72% identical to hCNT1 (Che *et al.*, 1995; Yao *et al.*, 1996; Wang *et al.*, 1997; Ritzel *et al.*, 1998; 49). hCNT3 (691 residues) is 78% identical to rCNT3 and mouse (m) CNT3 (both 703 residues) and about 50% identical to h/rCNT1 and h/rCNT2 (Ritzel *et al.*, 2001). These CNTs are unrelated to SNST1 (now SGLT2), a previous candidate *cib*-type nucleoside transport protein from rabbit kidney (Pajor and Wright, 1992), and mutagenesis of amino acid residues in TMs 7 and 8 of hCNT1 has been shown to sequentially change the specificity of the transporter from *cit* to *cib* to *cif* (Loewen *et al.*, 1999). While CNTs have been most thoroughly characterized in mammals (and *E. coli*), recent genome sequencing projects have revealed that putative CNT family members are also widely distributed in lower eukaryotes, including insects (*Drosophila melanogaster*), nematodes (*Caenorhabditis elegans*) and pathogenic yeast (*Candida albicans*).

Hagfish (Hyperotreti) are eel-like jawless marine animals that diverged from the main line of vertebrate evolution approximately 550 million years ago (Barack *et al.*, 1991; Forey *et al.*, 1993; Shu *et al.*, 1999; Janvier, 2001). They are the most ancient extant member of the subphylum Craniata, which includes humans and other vertebrates, having evolved from animals that represent the transition between early chordates and the first true vertebrates. As such, hagfish represent a unique research resource in molecular studies of early vertebrate evolution. Hagfish plasma is in approximate osmotic equilibrium with sea water (500 mM NaCl) and studies with their red blood cells have revealed a number of novel membrane transport characteristics (Young *et al.*, 1987; Ellory and Wolowyl, 1991; Fincham *et al.*, 1991; Young *et al.*, 1991, 1994; Tiihonen *et al.*, 2000). While these investigations have provided functional insights into hagfish membrane transport biology, there is little known structurally about hagfish transport proteins. In fact, the GenBank™ database lists only their mitochondrion genome and 14 complete hagfish cDNA sequences, including that of a hagfish equilibrative glucose transport protein (hfGLUT) (GenBank™ accession number AY059413).

This chapter describes the first hagfish transport protein to be characterized in detail at the molecular level. hfcNT, a member of the CNT family, exhibited strong *cib*-type transport activity when produced in *Xenopus* oocytes. Differences in cation interactions between hfcNT and hCNT1 were exploited in a chimeric study to demonstrate that determinants of the Na⁺ binding and coupling were located within the carboxyl-terminal half of the protein.

Materials and Methods

Molecular Cloning of hfcNT – The cDNA encoding hfcNT was obtained by first amplifying a partial hfcNT cDNA. The template was a directional Stratagene lambda vector Uni-ZAP® XR cDNA library prepared in this laboratory using mRNA isolated from hagfish intestinal tissue (mucosal scrapings). Two rounds of nested PCR were employed using a pair of internal primers against regions of conserved sequence among mammalian and bacterial CNTs: Q1 (antisense; rCNT1 nucleotide sequence 5'-TTTGCCAACTTCAGATCCATCGGG-3' corresponding to motif FANFSSIG in TM12) and Q2 (sense; hCNT1 nucleotide sequence 5'-AACATCGCTGCCAACCTGATTGC-3' corresponding to motif NIAANLIA in TM10). Initial amplification of diluted (1000-fold) hagfish phage cDNA library with Q2 as the sense primer and T7 oligonucleotide sequence corresponding to a region of the Uni-ZAP® XR insertion vector downstream of the *Xho*I cloning site as the antisense primer involved 1 cycle of 94°C for 5 min, 56°C for 1 min and 72°C for 1 min 30 s, 33 cycles of 94°C for 1 min, 56°C for 1 min and 72°C for 1 min 30 s, and a final extension cycle at 72°C for 10 min. A portion (10 %) of the first round PCR product was then subjected to a second round of amplification with Q1 and Q2 for 28 cycles under the same conditions. A 366-bp product was identified, cloned into pGEM-T vector (Promega) and sequenced by Taq Dyedexyterminator cycle sequencing using an automated model 373A DNA Sequencer (Applied Biosystems Inc.). This fragment, which showed 61%, 62% and 39% sequence identity to the corresponding regions of hCNT1, rCNT1 and NupC, respectively, was radiolabeled with ³²P (T7QuickPrime Kit, Amersham Pharmacia Biotech) and used as a hybridization probe to screen the hagfish intestinal cDNA library. Ten positive clones were identified, three of which contained full-length hfcNT cDNA. One of these clones in Uni-ZAP® XR vector was excised to generate a subclone in the pBluescript® SK(-)

vector according to the manufacturer's instructions. This 2.5 kb subclone was sequenced in both directions to give a 683-amino acid residue open reading frame flanked by 21 bp of untranslated 5'-nucleotide sequence and 443 bp of untranslated 3'-nucleotide sequence containing a poly(A)⁺ tail.

Other hagfish CNTs – The presence of transcripts for other possible CNT isoforms in hagfish intestinal mucosa was tested using a pair of internal primers against regions of amino acid sequence common to hfcNT and human and rat CNT1-3: Q3 (antisense; hfcNT nucleotide sequence 5'-CTCTGCGGTTTTGCTAATTT-3' corresponding to motif LCGFAN in TM 12) and Q4 (sense; hfcNT nucleotide sequence 5'-AACCTCATCGCTTTCCTGGC-3' corresponding to motif NLLAFLA in TM 10). RT-PCR yielded product of the expected size (~ 360-bp). This was subcloned into pGEM-T vector. Twelve clones were selected at random and sequenced.

Construction of Chimeric hfcNT and hCNT1 Transporters – cDNAs of hfcNT and hCNT1 were subcloned into the vector pGEM-HE (Liman *et al.*, 1992) prior to chimera construction to enhance expression in *Xenopus* oocytes. Overlap primers (sense; 5'-TGGCTTATGCAAGTCACCATG-3'; antisense; 5'-GGTACCCATGGTGACTIONTGCATAAGCCA-3') were designed at a splice site between Gly³¹¹ and Trp³¹² of hfcNT in the loop linking TM6 and TM7 (*arrow* in Fig. 5-9A) to create reciprocal 50:50 chimeras by a two-step overlap extension PCR method (Horton *et al.*, 1989) using the universal pUC/M13 forward and reverse primers and high fidelity *Pyrococcus furiosus* DNA polymerase. Chimeric constructs containing the restriction site *Kpn*I downstream of the M13 forward primer and the restriction site *Sph*I upstream of the M13 reverse primer were subcloned into the respective restriction sites of the pGEM-HE vector. The chimeras were sequenced in both directions to verify the splice sites and ensure that no mutations had been introduced.

In Vitro Transcription and Expression in *Xenopus* Oocytes – hfcNT and chimeric cDNAs were expressed in *Xenopus laevis* oocytes according to standard protocols (Yao *et al.*, 2000). Healthy defolliculated stage VI oocytes of *Xenopus laevis* were microinjected with 20 nl water or 20 nl water containing RNA transcripts (1 ng/nl) and incubated in modified Barth's medium at 18°C for 72 h prior to the assay of transport activity.

Radioisotope Flux Studies – Transport was traced using the appropriate [$^{14}\text{C}/^3\text{H}$]-labeled nucleoside, nucleoside drug or nucleobase (Moravsek Biochemicals or Amersham Pharmacia Biotech) at either 1 or 2 $\mu\text{Ci}/\text{ml}$ for [^{14}C]-labeled and [^3H]-labeled compounds, respectively. Flux measurements were performed at room temperature (20°C) as described previously (Huang *et al.*, 1994, Yao *et al.*, 2000) on groups of 12 oocytes in 200 μl of transport medium containing 100 mM NaCl, 2 mM KCl, 1 mM CaCl_2 , 1 mM MgCl_2 , and 10 mM HEPES, pH 7.5. Unless otherwise indicated, permeant concentrations were 10 μM . At the end of incubation periods, extracellular label was removed by six rapid washes in ice-cold transport medium, and individual oocytes were dissolved in 5% (w/v) SDS for quantitation of oocyte-associated radioactivity by liquid scintillation counting (LS 6000 IC, Beckman). Initial rates of transport (influx) were determined using an incubation period of 1 min (Huang *et al.*, 1994). Choline replaced sodium in Na^+ -dependence experiments, and the transport medium for adenosine uptake contained 1 μM deoxycoformycin to inhibit adenosine deaminase activity. The flux values shown are means \pm S.E. of 10-12 oocytes from one representative experiment. Significant differences in mean flux values were determined by Student's t-test ($P = 0.05$). Each experiment was performed at least twice on different batches of cells. Kinetic parameters were determined using programs of the ENZFITTER software package (Elsevier-Biosoft, Cambridge, UK).

Measurement of hfcNT-induced Sodium Currents – Membrane currents were measured in voltage clamped oocytes at room temperature using the two-electrode voltage clamp (CA-1B oocyte clamp, Dagan Corp.). The microelectrodes were filled with 3 M KCl and had resistances that ranged from 0.5 – 1.5 $\text{M}\Omega$. The CA-1B was interfaced to a computer via a Digidata 1200B A/D converter and controlled by Axoscope software (Axon Instruments). Current signals were filtered at 20 Hz (four-pole Bessel filter) and sampled at intervals of 10 msec. For data presentation, the signals were further filtered at 0.5 Hz by use of pCLAMP software (Axon Instruments). Following microelectrode penetration, resting membrane potential was measured over a 15-min period prior to the start of the experiment. Cells were not used if the resting membrane potential was unstable or less than -30 mV. For measurements of hfcNT-generated currents, the oocyte membrane potential was clamped at -50 mV. Oocytes were perfused with the same medium used for radioisotope flux studies,

and transport was initiated by changing substrate-free solution to one containing nucleoside (200 μM). In experiments examining Na^+ - and H^+ -dependence, sodium in the medium was replaced by choline and pH was varied from 5.5 to 8.5. For the determination of charge to uridine uptake ratio, currents were monitored and recorded after an oocyte was clamped at -50 mV in substrate-free transport medium for a 10 min period. The solution was then exchanged with transport medium of the same composition containing radiolabeled uridine. Current was measured for 3 min, followed immediately by reperfusion with substrate-free transport medium until current returned to baseline. The oocyte was recovered from the chamber and solubilized with 5% SDS for liquid scintillation counting. The total movement of charge across the plasma membrane was calculated by integrating the uridine-evoked current over the uptake period. Charge was converted into pmol to compare with radiolabeled uridine uptake. Uptake of [^{14}C]-labeled uridine in control H_2O -injected oocytes was used to correct for endogenous basal uptake of uridine over the same incubation period. The coupling ratio of hfcNT was calculated from data collected from 10 individual oocytes.

Results and Discussion

Previous studies of nucleoside transport in hagfish have been limited to red blood cells, which possess an equilibrative NBMPR-insensitive (*ei*-type) nucleoside transport process (Fincham *et al.*, 1991). The goal of the present study was to use recombinant DNA technology in combination with heterologous expression in *Xenopus* oocytes to attempt the cDNA cloning and functional characterization of a hagfish concentrative nucleoside transport protein.

Molecular Identification of hfcNT – The first step of our cDNA cloning strategy exploited regions of amino acid sequence similarity between CNT family members to isolate a partial length hagfish CNT cDNA from intestinal epithelium, a tissue in mammals known to express multiple CNT proteins (Cheeseman *et al.*, 2000). The template for this PCR amplification was a cDNA library prepared from hagfish intestinal mucosa. The resulting 366-bp fragment generated by PCR amplification (see *Materials and Methods*) was used as a probe to screen our hagfish intestinal cDNA library. High-stringency hybridization screening yielded a 2516-bp cDNA, with an open reading frame of 2049 bp flanked by 21 bp of 5'-untranslated region and 446 bp of 3'-untranslated region containing a poly(A)⁺ tail. The encoded 683-

amino acid residue protein, designated hfCNT (Fig. 5-1), with 13 predicted TMs, had a putative molecular weight of 76 kDa and was 52% identical (62% similar) to hCNT1, 50% identical (59% similar) to hCNT2 and 57% identical (67% similar) to hCNT3. In addition to having multiple consensus sites for N-linked glycosylation at the carboxyl-terminus (Asn⁶²⁵, Asn⁶³⁰, Asn⁶⁵², Asn⁶⁶⁰, Asn⁶⁷⁰), hfCNT also contained an additional potential site of glycosylation on the putative extracellular loop between TMs 9 and 10 (Asn⁴¹¹) (Fig. 5-1). The extracellular location of the carboxyl-terminus has been confirmed by mutagenesis of rCNT1, which is glycosylated at Asn⁶⁰⁵ and Asn⁶⁴³ (Hamilton *et al.*, 2001).

The greater sequence similarity of hfCNT with hCNT3 than with hCNT1/2 extended to mCNT3 (Ritzel *et al.*, 2001) and rCNT3 (GenBankTM accession number AY059414) and was most pronounced in TMs 4-13 (Fig. 5-1). For example, hfCNT and hCNT3 exhibited an average sequence identity of 77% within these transmembrane helices, and in the whole region of 413 residues (including loops) there were only 32 non-conservative substitutions among the human, mouse, rat, and hagfish sequences. Seven motifs of eight or more consecutive identical residues were common to all four proteins: FFSTVMSM and YYLGLMQW in TM 6, GQTESPLL in TM 7, TIAGSVLGAYIS in TM 8, HLLTASVMSAPA in TM 9, KTFNFNEFVAY in the loop between TM 11 and TM 12 and IATYALCGFAN in TM 12. These motifs are likely to have structural and/or functional significance. The importance of the TM 4-13 region as a core structure to the CNT family in general is indicated by the ten TM membrane architecture of NupC, and by the functionality of a truncation construct of hCNT1 with TMs 1-3 removed (Hamilton *et al.*, 2001).

Since we first identified rCNT1 from rat jejunum by expression cloning in *Xenopus* oocytes (Ritzel *et al.*, 1997), more than 40 members of the CNT protein family have been identified by functional expression, sequence homology, and genome sequencing projects. At present, there are 14 CNT proteins that have been characterized functionally, and their phylogenetic relationships are illustrated in Fig. 5-2. The hfCNT and mammalian CNT3 proteins cluster in a discrete CNT subfamily different from that formed by mammalian CNT1 and CNT2. Also shown in Fig 5-2 is the relationship between these proteins and *C. elegans* CeCNT3 (Xiao *et al.*, 2001). In oocytes, CeCNT3 transports both pyrimidine and purine nucleosides (except cytidine). Although not truly broadly selective, CeCNT3 was designated "CNT3" in

anticipation that it would prove to be an ortholog of mammalian *cib* (Xiao *et al.*, 2001). However, as would be expected from an invertebrate sequence, CeCNT3 was not closely related to either hfcNT/CNT3 or CNT1/2.

Other Hagfish CNTs – Human and rat intestine contain transcripts for all three mammalian concentrative nucleoside transporters (CNT1-3). We therefore searched for other possible CNT isoforms in hagfish intestine using hfcNT primers corresponding to regions of amino acid sequence in TMs 10 and 12 identical in hfcNT and human and rat CNT1-3. Twelve randomly selected RT-PCR clones were sequenced. Each contained a 363-bp insert identical in nucleotide sequence to the corresponding region of hfcNT, establishing hfcNT as the major CNT transcript present in hagfish intestine.

Production of Recombinant hfcNT in *Xenopus* Oocytes – Mammalian CNT1 and CNT2 display pyrimidine nucleoside selective *cit*-type and purine nucleoside selective *cif*-type transport activities, respectively. hfcNT, in contrast, was found to be similar to human, mouse and rat CNT3 and to mediate *cib*-type transport of both pyrimidine and purine nucleosides. Fig. 5-3 shows representative time courses for uptake of uridine (a universal CNT1/2/3 permeant), thymidine (a diagnostic CNT1 permeant) and inosine (a diagnostic CNT2 permeant) in oocytes injected with either hfcNT RNA transcript or water. After 30 min, the uptake of uridine, thymidine and inosine in hfcNT-producing oocytes were 37 ± 6 , 58 ± 6 , and 62 ± 8 pmol/oocyte, respectively, values 95 – 380 fold higher than those in water-injected oocytes (0.2 – 0.4 pmol/oocyte). Substitution of Na^+ in the incubation medium by choline reduced the fluxes in RNA-injected oocytes by $\geq 98\%$. In the subsequent kinetic experiments (presented in Figs. 5-5 and 5-7), we used a 1-min incubation period to define initial rates of uridine, thymidine and inosine uptake.

Substrate Selectivity and Anti-viral Drug Transport of Recombinant hfcNT. Fig. 5-4 shows a representative transport experiment in *Xenopus* oocytes that measured uptake of a panel of radiolabeled pyrimidine and purine nucleosides in cells injected with water alone (control) or water containing hfcNT transcripts. Consistent with *cib*-type functional activity, hfcNT-producing oocytes transported all the pyrimidine and purine nucleosides tested (cytidine, thymidine, uridine, adenosine, deoxyadenosine, guanosine, and inosine) and gave

similar mediated fluxes (uptake in RNA-injected oocytes minus uptake in water-injected oocytes) for each nucleoside tested (18 ± 3 , 22 ± 2 , 17 ± 3 , 24 ± 5 , 22 ± 3 , 21 ± 3 , and 14 ± 2 pmol/oocyte.30 min⁻¹, respectively). In contrast, no mediated transport of uracil was detected, establishing the transporter's specificity for nucleosides over nucleobases.

Previously, we have used *Xenopus* oocyte expression to establish that the mammalian CNT1/2/3 proteins transport antiviral dideoxynucleosides: hCNT1 and rCNT1 transported 3'-azido-3'-deoxythymidine (AZT) and 2',3'-dideoxycytidine (ddC) but not 2',3'-dideoxyinosine (ddI), hCNT2 transported only ddI, and hCNT3 and mCNT3 transported all three compounds (Huang *et al.*, 1997; Ritzel *et al.*, 1997, 1998, 2001; Yao *et al.*, 2001). As shown in Fig. 5-4 by differences in radiolabeled drug uptake between oocytes injected with water alone (control) or water containing RNA transcript, hfCNT accepted both pyrimidine (AZT, ddC) and purine (ddI) dideoxynucleoside drugs as permeants. The magnitudes of the fluxes were smaller than for physiological nucleosides, but similar to those reported previously for hCNT1 (AZT, ddC), hCNT2 (ddI) and hCNT3 (AZT, ddC, ddI). Consistent with transporter-mediated pyrimidine and purine dideoxynucleoside drug uptake, control experiments confirmed that influx of AZT and ddI in hfCNT-producing oocytes was reduced to basal (water-injected oocyte) levels in the presence of excess unlabeled uridine (10 mM) (data not shown). These results indicated that hfCNT and other CNTs are relatively tolerant of the lack of the 3'-OH group on the sugar moiety of nucleosides, a feature also characteristic of the mammalian equilibrative ENT2 protein isoform (Yao *et al.*, 2001).

Kinetic Properties – Fig. 5-5 presents representative concentration dependence curves for uridine, inosine and thymidine transport, measured as initial rates of uptake (1-min fluxes) in hfCNT-producing oocytes and in control water-injected oocytes. Kinetic constants for the hfCNT-mediated component of uptake are presented in Table 5-1. Apparent K_m values for uridine, inosine and thymidine transport were similar (10, 35 and 45 μ M, respectively) and in the same range as values obtained previously for recombinant mammalian CNT1/2/3 proteins (Huang *et al.*, 1994; Che *et al.*, 1995; Yao *et al.*, 1996; Ritzel *et al.*, 1997; Wang *et al.*, 1997; Crawford *et al.*, 1998; Ritzel *et al.*, 1998). V_{max} values for the three nucleosides were similar. Influx of uridine, inosine and thymidine in control, water-injected oocytes was linear with concentration, consistent with non-mediated simple diffusion across the lipid layer.

hfCNT Na⁺:Nucleoside Cotransport – In mammalian cells, most plasma membrane transporters use the sodium electrochemical gradient to actively transport substrates into or out of cells, whereas in bacteria, H⁺ is the preferred ion of many coupled transporters (Hediger, 1994). A few mammalian transporters have been described that use H⁺ as the coupling ion, including oligopeptide transporters (Ono-Koyanagi *et al.*, 1997), iron transporters (Gunshin *et al.*, 1997), monocarboxylate transporters (Halestrap *et al.*, 1999) and a myo-inositol transporter (Uldry *et al.*, 2001). The three mammalian CNTs function as Na⁺-dependent nucleoside transporters, although recent electrophysiological studies in *Xenopus* oocytes have found that H⁺ and Li⁺ can substitute for Na⁺ for CNT3, but not for CNT1 or CNT2 (unpublished observation). In contrast, Na⁺ replacement and pH-dependence experiments suggest that *C. albicans* CaCNT (as described in *Chapter VII*), *C. elegans* CeCNT3 (Xiao *et al.*, 2001) and *E. coli* NupC (Yao *et al.*, 2000) are exclusively H⁺-dependent. In the case of CaCNT, this has been confirmed by electrophysiology (as described in *Chapter VII*).

As shown in Fig. 5-6, external application of adenosine, cytidine, guanosine, inosine, thymidine or uridine (200 μM) to hfCNT-producing oocytes generated quantitatively similar inward currents that returned to baseline upon removal of permeant. No currents were seen in water-injected oocytes, or when Na⁺ in the extracellular medium was replaced by choline, confirming that hfCNT3 functions as an electrogenic Na⁺/nucleoside symporter. In addition, no uridine-mediated currents were detected under Na⁺-free conditions over the pH range 5.5 to 8.5, indicating that hfCNT was unable to substitute H⁺ for Na⁺ (data not shown). A similar negative result was obtained when Li⁺ was substituted for Na⁺ (data not shown). Therefore, the CNT protein family includes members that are H⁺-dependent (CaCNT, CeCNT3, NupC), Na⁺-dependent (hfCNT, CNT1, CNT2) and Na⁺/H⁺ (and Li⁺) -dependent (CNT3). In prokaryotes, the melibiose transporter of *E. coli* can also use either H⁺ or Na⁺ as the coupling ion, depending on which sugar is being transported (Botfield *et al.*, 1990), while that of *K. pneumoniae* couples sugar transport to H⁺ and Li⁺ (Hama *et al.*, 1992). On the basis of sequence comparisons between the *E. coli* and *K. pneumoniae* proteins, site-directed mutagenesis identified a single residue in TM 2 that was important for Na⁺ recognition (Hama *et al.*, 1994). Since hfCNT and hCNT3 are very similar in amino acid sequence, particularly in the region from TM 4 to TM 13 (Fig. 5-1), it is likely that introduction of point mutations into hfCNT by site-

directed mutagenesis will identify individual amino acid residues that contribute to CNT cation specificity.

A Na^+ /nucleoside coupling ratio of 2:1 has been reported for system *cib* in choroid plexus and microglia (Wu *et al.*, 1992, Hong *et al.*, 2000), whereas coupling ratios of 1:1 have been described for various *cit* and *cif* transport activities in different mammalian cells and tissues (Cass, 1995). Similarly, Hill coefficients for Na^+ -activation of nucleoside transport by recombinant hCNT3 and mCNT3 were approximately 2, compared to approximately 1 for rCNT1 (Yao *et al.*, 1996; Ritzel *et al.*, 1997). K_{50} values for Na^+ -activation were in the range 7-16 mM. In the present study, we undertook similar Na^+ -activation experiments with hfcCNT. Consistent with the high Na^+ concentrations normally experienced by hagfish tissues (about 500mM NaCl), we found an almost linear relationship between nucleoside influx (uridine, inosine and thymidine) and Na^+ concentration, even up to 100 mM Na^+ , the maximum extracellular Na^+ concentration that is possible for *Xenopus* oocytes (Fig. 5-7). Thus the K_{50} value for Na^+ -activation of hfcCNT was > 100 mM. We have recently described a similar very high K_{50} value for a Na^+ -dependent pyruvate transport system in hagfish red blood cells, suggesting that this may be a general characteristic of hagfish Na^+ -dependent transporters (Tiihonen *et al.*, 2000).

Although it was not possible to determine a Hill coefficient for Na^+ -activation of hfcCNT, we used the two-microelectrode voltage-clamp technique to directly determine the Na^+ /nucleoside coupling ratio of hfcCNT by simultaneous measurement of Na^+ currents and [^{14}C]-uridine influx under voltage clamp conditions, as described previously for the SDCT1 rat kidney dicarboxylate transporter (Chen *et al.*, 1998). The results of these experiments presented in Fig. 5-8 demonstrated that hfcCNT has a Na^+ /nucleoside coupling ratio of 2:1 at (the slope of the regression line (\pm S.E.) is 2.1 ± 0.1) similar to that of hCNT3 and mCNT3, but different from the 1:1 coupling ratio of hCNT1 (Yao *et al.*, 1996; Ritzel *et al.*, 2001; unpublished data). Unlike the results for hCNT3 however (*Chapter IV*; Fig. 4-10), but consistent with the lower apparent affinity of hfcCNT for Na^+ , the hfcCNT Na^+ :uridine coupling ratio was not potential dependent (data not shown). In this respect, the CNTs resemble the SGLT glucose transporter family which has members with Na^+ /sugar coupling ratios of 2:1 (SGLT1 and SGLT3) and 1:1 (SGLT2) (Diez-Sampedro *et al.*, 2001). Similarly,

the proton-linked oligopeptide transporter PepT1 and PepT2 have 1:1 and 2:1 H⁺/peptide coupling ratios, respectively (Meredith and Boyd, 2000).

Characterization of hfCNT/hCNT1 Chimeras – As previously described in *Chapter II*, I have identified two adjacent pairs of residues (Ser³¹⁹/Gln³²⁰ and Ser³⁵³/Leu³⁵⁴) in the TM 7-9 region of hCNT1 that, when mutated together to the corresponding residues in hCNT2 (Gly³¹³/Met³¹⁴ and Thr³⁴⁷/Val³⁴⁸), converted hCNT1 (*cit*-type) into a transporter with *cif*-type functional characteristics (Loewen *et al.*, 1999). An intermediate broad specificity *cib*-like transport activity was produced by mutation of the two TM 7 residues alone. The amino acid residues of hfCNT at these four positions are Gly³³⁵/Gln³³⁶ in TM7 and Ser³⁶⁹/Val³⁷⁰ in TM 8, which represents the intermediate state between hCNT1 and hCNT2 to allow transport of both purine and pyrimidine nucleosides. In addition to differing in substrate specificity, the previous section showed hfCNT and hCNT1 exhibit differences in interactions with Na⁺, the hagfish transporter having a Na⁺/nucleoside coupling ratio of 2:1 (*vs.* 1:1 for hCNT1) and a high K₅₀ value for Na⁺-activation of > 100 mM.

The predicted amino acid sequences of hfCNT and hCNT1 are 52% identical and 62% similar, with strongest residue similarity within TMs of the carboxyl-terminal halves of the proteins. The major differences lie in the putative amino- and carboxyl-terminal tails of the proteins and in the first three TMs (Fig. 5-9). To localize domains involved in cation stoichiometry and binding affinity, a chimera (HF/H) in which the carboxyl-terminal half of hfCNT (incorporating TMs 7-13) was replaced with that of hCNT1 was constructed. The splice site between the two proteins following hfCNT residue Gly³¹¹ was engineered at the beginning of the putative extramembraneous loop prior to TM 7 to divide the proteins into two approximately equal halves as predicted by the topology model in Fig. 5-9, and to minimize disruption of native TMs and loops. The resulting chimera (HF/H) transported uridine when produced in *Xenopus* oocytes (Fig. 5-10), but displayed lower levels of functional activity than hfCNT and hCNT1 (most likely the result of reduced plasma membrane targeting) and required a longer incubation period (30 min *versus* 1 min) to obtain comparable levels of total uptake. A reciprocal chimera to HF/H (H/HF, a 50:50 construct incorporating the amino-terminal half of hCNT1 and the carboxyl-terminal half of hfCNT) was non-functional and was not studied further.

As predicted by the earlier mutagenesis studies (Loewen *et al.*, 1999), chimera HF/H exhibited hCNT1-like substrate specificity (Ritzel *et al.*, 1997). This is illustrated in Fig. 5-10, which shows the transportability of a panel of physiological purine and pyrimidine nucleosides (adenosine, cytidine, guanosine, inosine, thymidine and uridine). Fluxes were similar in profile to those exhibited by wild-type hCNT1 (uridine, thymidine, cytidine \gg adenosine and no detectable transport of guanosine or inosine). Furthermore, ddi (a substrate of hCNT but not hCNT1) was not transported by HF/H (Fig. 5-10).

In addition to substrate specificity, we also tested HF/H interactions with Na^+ . The relationship between cytidine, thymidine, uridine influx and Na^+ concentration (Fig. 5-11) was saturable and hyperbolic, with Hill coefficients (\pm S.E.) of 0.8 ± 0.1 (cytidine), 1.2 ± 0.2 (thymidine) and 1.0 ± 0.1 (uridine), indicating a Na^+ /nucleoside coupling ratio of 1:1 (*i.e.* hCNT1-like). These results indicated that the residue(s) determining coupling ratio also reside in the carboxyl-terminal half of the transporter. K_{50} values for Na^+ -activation of 4.0 ± 1.0 (cytidine), 8.7 ± 2.2 (thymidine) and 10.0 ± 1.7 (uridine) were also hCNT1-like, demonstrating that the structural features determining Na^+ -binding affinity are likewise in this half of the protein. Cysteine-scanning mutagenesis studies of *E. coli* lactose permease have found that coupling between substrate and H^+ translocation involved six irreplaceable residues located at five different helices from TM 4 to TM 10 (Kaback *et al.*, 2001). It is likely that the three dimensional conformations of the cation (and substrate) binding sites of hCNT are also composed of residues from multiple helices. Future site-directed and cysteine-scanning mutagenesis studies in the carboxyl-terminal half of hCNT will therefore not only identify amino acid residues involved in cation stoichiometry and binding affinity, but also provide information on helix packing within the translocation pore of the transporter.

Conclusions – Nucleosides are important precursors of nucleic acids and energy-rich cellular metabolites, and one (adenosine) has functions as a local hormone in a variety of tissues, including the gastrointestinal system (Griffith and Jarvis, 1996; Baldwin *et al.*, 1999; Cheeseman *et al.*, 2000). Cells obtain nucleosides from breakdown of dietary and endogenous nucleotides. The former are important nutrients and are absorbed as nucleosides by enterocytes of the intestinal mucosa. In mammals, enterocytes have a limited capacity for *de novo* nucleotide synthesis and require both dietary and endogenous nucleosides for their own

metabolism and differentiation (Cheeseman *et al.*, 2000). hfcNT is a CNT nucleoside transport protein from hagfish intestinal epithelium that belongs to the CNT3 subfamily. hfcNT was electrogenic, Na⁺-dependent, H⁺- and Li⁺-independent and exhibited a broad permeant selectivity for both pyrimidine and purine nucleosides. hfcNT had a 2:1 Na⁺/nucleoside coupling stoichiometry, identifying this characteristic, in addition to *cib*-type substrate selectivity, as a general functional feature of the hfcNT/CNT3 subfamily. A two Na⁺/one-nucleoside symporter such as hfcNT will have greater ability to transport permeants against its concentration gradient than a one Na⁺/one-nucleoside symporter, particularly when considered in the context of the very high concentration of Na⁺ present in hagfish extracellular fluids or intestinal lumen and the high K_{50} value for hfcNT Na⁺-activation. hfcNT differed from its mammalian orthologs in that it was unable to substitute H⁺ (and Li⁺) for Na⁺.

The differences in cation stoichiometry, binding affinity and specificity between hfcNT and mammalian CNTs will provide a basis for future site-directed mutagenesis studies to identify the amino acid residues involved. While there is greater sequence divergence between hfcNT and CNT1/2 than between hfcNT and CNT3, our functionally-active hfcNT/hCNT1 chimera HF/H has narrowed down the region of interest to the carboxyl-terminal halves of the proteins. Within TMs 7-13, there are only 51 residue differences between hfcNT and hCNT1 that could potentially account for the observed differences in Na⁺/nucleoside coupling ratio and binding affinity. Many of these residue differences occur in clusters, making it feasible to undertake multiple simultaneous mutations between the two proteins to rapidly identify the amino acid residues involved.

Hagfish (Hyperotreti) are pre-vertebrates that diverged from the main line of vertebrate evolution about 550 million years ago and represent the most ancient extant member of the craniate subphylum. The fossil record indicates that hagfish have undergone little evolutionary change in body structures (Shu *et al.*, 1999). In the phylogenetic analysis of functionally characterised CNT family members shown in Fig. 5-2, hfcNT clustered with mammalian CNT3 proteins. Since the period around the Hyperotreti – Vertebrata split was a time of very active gene duplication (Ono-Koyanagi *et al.*, 2000), it will be informative from an evolutionary perspective to establish in future studies whether or not hagfish also contain members of the CNT1/2 subfamily. The present finding by RT-PCR that hfcNT is the predominant CNT in

hagfish intestine may indicate the absence of other concentrative nucleoside transporter isoforms and contrasts with mammalian intestine which contains transcripts for CNT1, CNT2 and CNT3 (Ritzel *et al.*, 1997, 1998, 2001). Even in the absence of other CNTs, the functional characteristics described here for hfcNT would enable the efficient intestinal absorption of both pyrimidine and purine dietary nucleosides required by their scavenging carnivorous lifestyle and periodic feeding behaviour. The high degree of amino acid sequence similarity between hfcNT and mammalian CNT3 proteins, particularly in the TM 4-13 region may indicate functional constraints on the primary structure of this region and provides structural evidence that *cib*-type nucleoside transporters fulfill important physiological functions.

Table 5-1 – Kinetic Properties of hfCNT

Substrate	Apparent K_m^a (μM)	V_{max}^a ($pmol/oocyte.min^{-1}$)	$V_{max}:K_m$
Uridine	10 ± 1	5.0 ± 0.1	0.50
Thymidine	45 ± 7	4.9 ± 0.2	0.11
Inosine	35 ± 6	4.0 ± 0.2	0.11

^a, from Fig. 5-5.

Figure 5-1. hfcNT is a member of the CNT family of nucleoside transporters. Alignment of the predicted amino acid sequences of hfcNT (GenBank™ accession AF036109), hCNT3 (GenBank™ accession AF305210), mCNT3 (GenBank™ accession AF305211) and rCNT3 (GenBank™ accession AY059414) using the GCG PILEUP program. Potential membrane-spanning α -helices, identified as described previously (Hamilton *et al.*, 2001), are *numbered*. Putative glycosylation sites in predicted extracellular domains of hfcNT, hCNT3, mCNT3 and rCNT3 are shown in *lowercase (n)*, and their positions highlighted by an *asterisk* above the aligned sequences. Residues identical in hfcNT and one or more of the other transporters are indicated by *black boxes*.


```

rCNT3 MSRSDPDPGKNSPEPSKSKMSLELR-PTAPSDDQGRSNEAFQDED--LEEQNAPGNSSTVRSR
mCNT3 MSRADP--GKNSPEPSKSKMSLELR-PTAPSDDQGRSNEAFQDED--LEEQNTPGNSSTVRSR
hCNT3 -----MELRSTAAAPRAEGYSNVGFQNEENFLENENTSGNNSIRSR
hfCNT -----MSAFKARGVENPSYEDPD--EKGKPDLEMSKTN

rCNT3 VVQSGEQGRAKQDDRQITISQEPPLGPKEGTDEESEDERQKGFLEK---KYDVTVCFPCRK
mCNT3 VVQSGEQGHAKQDDRQITISQEPPLGPKEGTDEESEDERQKGFLEK---KYDTHCFPCRK
hCNT3 AVQSRREHTNTKQDEEQVTVNEQDSPRNRREHMEDEDEEMQKQGFLEK---RYDVTVCFPCRK
hfCNT GIGVDNPSYKKNPKYLGNESEEGKSNNDNEEEEGEEDQGAVERCVNKFYGGHNFYKRR

                Helix 1                                Helix 2
rCNT3 HRVILQHTIWAVALLTGFLALVIAACALNPFHRAALPLPFVITLVITIFFVVWDRLMAKYEQRID
mCNT3 HRVILQHTIWAVALLTGFLALVIAACALNPFHRAALPLPFVITLVITIFFVVWDRHLMMAKYEQRID
hCNT3 HKTTLRHIWGIILLAGYLVMLVLSACVLFNPHRALPLPFVITLVITIFFVVWDRHLMMAKYEQRID
hfCNT NKKIHYHTFLGLLVGYFALVIAACIVNPFKQSLALLVLTVAIIFVFWDLFIKYGDKIA

                Helix 3                                Helix 4
rCNT3 DVLSFGKRLLELRRHWFWLKKWVWCSLILAVILWLAALDTRARLGGQQQLSFGGLVMYIVLFLFL
mCNT3 DFLSPGRRLLDRHWFVWFKWVWSSLLILAVILWLAALDTRARLGGQQQLSFGGLVMYIVLFLFL
hCNT3 EMLSPGRRLLNSHWFVWFKWVWSSLVLAVIFWLAALDTRARLGGQQQLSFGGLVMYIVLFLFL
hfCNT EALKPKCFKLDNHWSTIRWVYGAALLAVILWLAALDTRARLGGANQVTFPFGGLIIVLFLFI

                Helix 5                                Helix 6
rCNT3 FSKHPTRVYWRPVPFEGIGLQFLLLGLLILRTRRPGFVAFDWMGKQVQTFLLGYTDAGAQFVFG
mCNT3 FSKHPTRVYWRPVPFEGIGLQFLLLGLLILRTRRPGFVAFDWMGKQVQTFLLGYTDAGARFVFG
hCNT3 FSKHPTRVYWRPVPFEGIGLQFLLLGLLILRTRRPGFVAFDWMGKQVQTFLLGYTDAGASRFVFG
hfCNT FSKHPTKVRWRIVIWGLLQFIFGLIILRTKPGLDAPNWLGIQVQTFLLGYTDAGASRFVFG

                Helix 7                                Helix 8
rCNT3 EKYTDHFFFAFKILPIVVFSTVMSMLYYLGLMQWIIIRKVGWMLLVTMGSSPIESVVAAGN
mCNT3 EKYTDHFFFAFKILPIVVFSTVMSMLYYLGLMQWIIIRKVGWMLLVTMGSSPIESVVAAGN
hCNT3 EKYTDHFFFAFKILPIVVFSTVMSMLYYLGLMQWIIIRKVGWMLLVTMGSSPIESVVAAGN
hfCNT DDFQDHFFAFAVLPVIVFSTVMSMMYYLGLMQWLLILKVGWMLQITMGTSPMESMVVACN

                Helix 9                                Helix 10
rCNT3 IFVQGTESPLLVRQPYLPHVTKSELHTIMTAGFATIAGSVLGAISFGVSSSTHLLTASVMS
mCNT3 IFVQGTESPLLVRQPYLPHVTKSELHTIMTAGFATIAGSVLGAISFGVSSSTHLLTASVMS
hCNT3 IFVQGTESPLLVRQPYLPHVTKSELHTIMTAGFATIAGSVLGAISFGVSSSTHLLTASVMS
hfCNT IFVQGTESPLLVRQPYLADLTISEMHSVMSSSGFATIAGSVLGAISLGIIPAAHLLTASVMS

                Helix 11
rCNT3 APAALAVARLFWPETEKPKKITLKNAMKMEENGDSRNLLEAATQGASSIIPLVANIAANLIA
mCNT3 APAALAVARLFWPETEKPKKITLKNAMKMEENGDSRNLLEAASQGASSIIPLVANIAANLIA
hCNT3 APASLAAAKLFWPETEKPKKITLKNAMKMEENGDSGNLLEAATQGASSIIPLVANIAANLIA
hfCNT APAALATSKTFWPETKKSknSTQTSIKLEKCGQENNLVBEAASQGASSAAPPVLVANIAANLIA

                Helix 12
rCNT3 FLALLSSEFVNSALSWSFGSMFDYPOLSFELICSYIFMPPSFMMGVVDWQDRFMVAKLIICYKTF
mCNT3 FLALLSSEFVNSALSWSFGSMFDYPOLSFELICSYIFMPPSFMMGVVDWQDSFMVAKLIICYKTF
hCNT3 FLALLSSEFVNSALSWSFGSMFDYPOLSFELICSYIFMPPSFMMGVVDWQDSFMVAKLIICYKTF
hfCNT FLAVLAFINATLSWLSGSMFDYPOLSFELICSYVLMPPAFMMGVVNYDDSPFLVAELLGMKTF

                Helix 13
rCNT3 FNEFVAYEHLKSKFLNLRKAAAGPKFVNGVQQYMSIRSEITATYALCGFANFGSLGIVIGGL
mCNT3 FNEFVAYEHLKSKFLNLRKAAAGPKFVNGVQQYMSIRSEITATYALCGFANFGSLGIVIGGL
hCNT3 FNEFVAYEHLKSKFLNLRKAAAGPKFVNGVQQYMSIRSEITATYALCGFANFGSLGIVIGGL
hfCNT FNEFVAYQLSEYTHNRESGGELFVDGVRQYMSVREAITATYALCGFANFGSLGIMIGGL

                Helix 14
rCNT3 TSIAPSRKRDIASGAMRALIAGTIACFMFACIAGMLSDTTPVAINCHVLE--SSKVLSh
mCNT3 TSIAPSRKRDIASGAMRALIAGTIACFMFACIAGMLSDTTPVDINCHVLE--NGRVLSh
hCNT3 TSMAPSRKRDIASGAVRALIAGTIACFMFACIAGMLSDTTPVDINCHVLENAFhNSTFPSh
hfCNT SSLAPHRSKSDIASCGIRRALIAGTIACFMSACIAGVLY-IPELYCPNLLMSTLFPnGTTVh

rCNT3 TTEVA S C C Q G L F n S T V A R G P N D V L P G G n F S L Y T L K S C C N L L K P P T L N C G W I P N I P
mCNT3 TTEV S C C Q N L F n S T V A K G P N D V P G G n F S L Y A L K S C C N L L K P P T L N C N W I P N K L
hCNT3 TTKV I A C C Q S L L S T V A K G P G E V I P G G n H S L Y S L K G C C T L L n P S T F N C N G I S N T F
hfCNT T T N L M S C C T D L F K S T T M L T P K n I T F T E G F n T T M L N G C C T F F - P S G F n C S E V R P E -

```

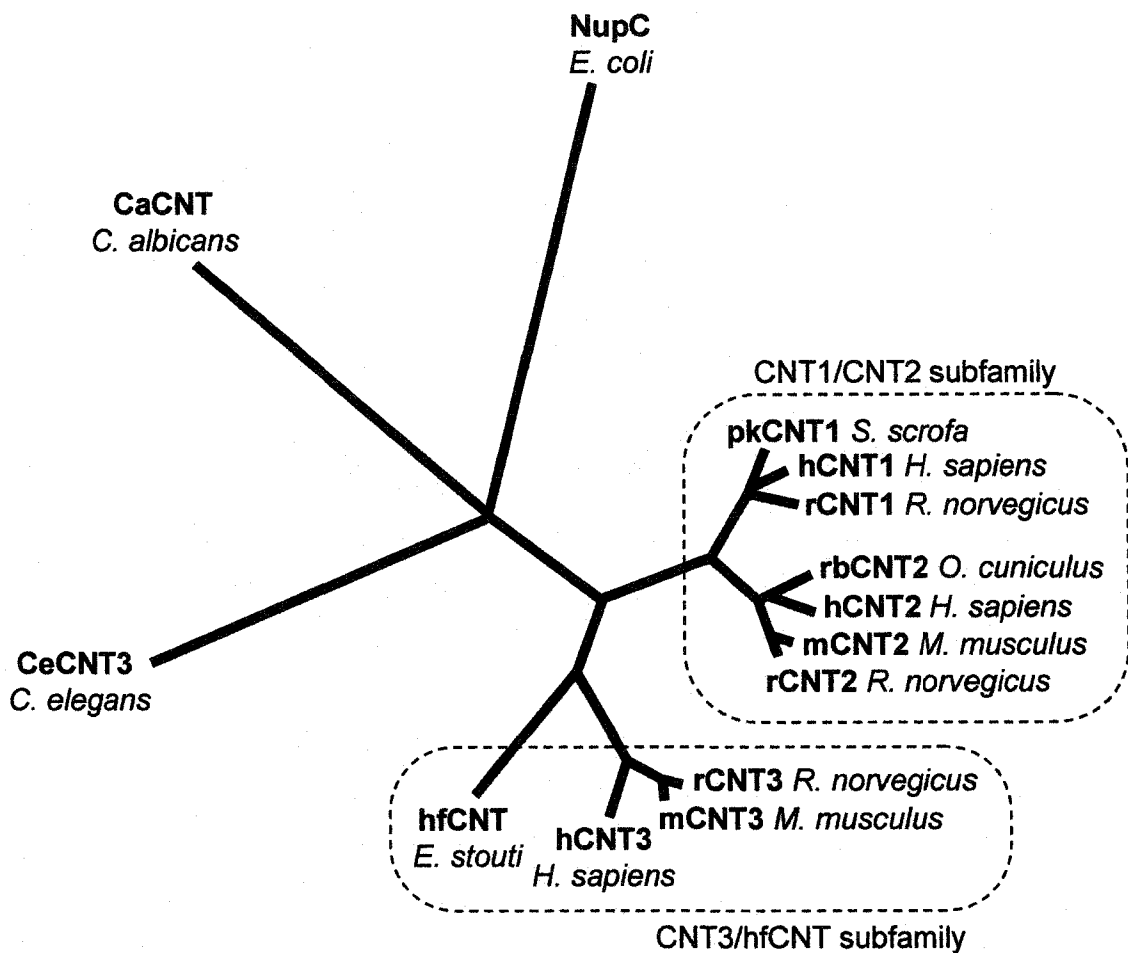
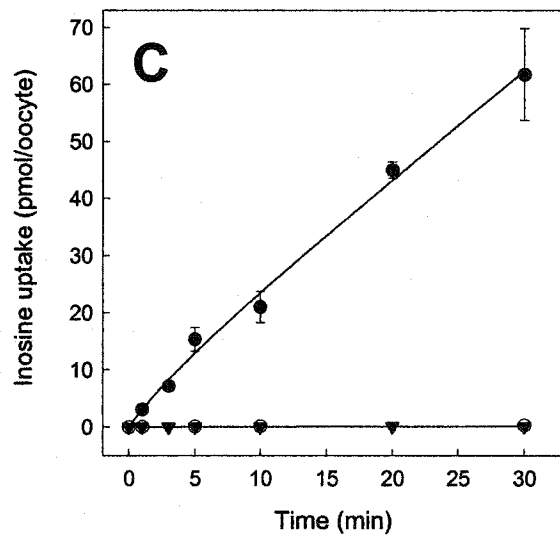
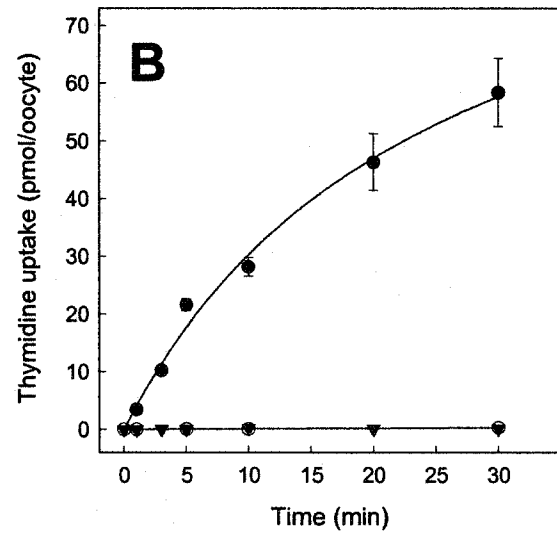
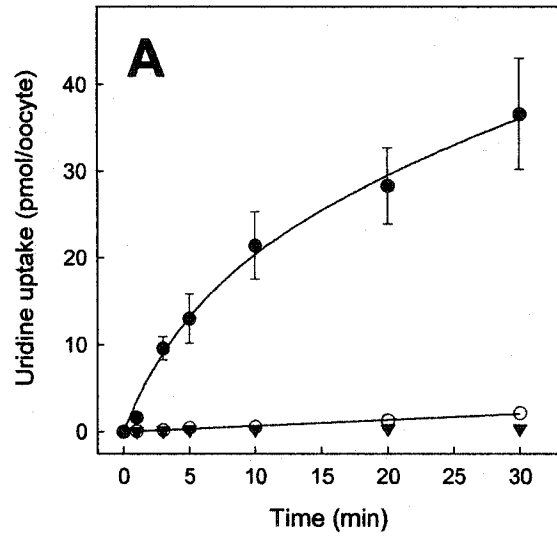


Figure 5-2. Phylogenetic tree showing relationships between hfcNT and other functionally characterized members of the CNT transporter family. In addition to those listed in *Figure 5-1*, these are: rCNT1 (rat CNT1, GenBank™ accession U10279); pkCNT1 (pig kidney CNT1, GenBank™ accession AF009673); hCNT1 (human CNT1 GenBank™ accession U62968); rCNT2 (rat CNT2, GenBank™ accession U25055); mCNT2 (mouse CNT2, GenBank™ accession AF079853); rbCNT2 (rabbit CNT2, GenBank™ accession AF161716); hCNT2 (human CNT2 GenBank™ accession number AF036109); F27E11.2 (*Caenorhabditis elegans*, GenBank™ accession AF016413); NUPC_ECOLI (*Escherichia coli*, Swissprot accession number P33031); CaCNT (*Candida albicans*, open reading frame present in contig5-2704 from the *C. albicans* genome sequencing project, Stanford). The phylogenetic tree was constructed from a multiple alignment of the 14 CNT sequences using ClustalX version 1.81 for Windows (Thompson *et al.*, 1997) and KITSCH, PHYLIP version 3.57c software (Felsenstein, 1989).

Figure 5-3. Time courses of uridine, thymidine and inosine uptake by recombinant hfCNT produced in *Xenopus* oocytes. Oocytes injected with 20 nl of water containing 20 ng of hfCNT RNA transcripts were incubated for 3 days at 18°C in MBM. Uptake of uridine (*A*), thymidine (*B*) and inosine (*C*) (10 μM, 20°C) was then measured in transport medium containing 100 mM NaCl (*solid circles*) or 100 mM choline chloride (*solid triangles*) and compared with uptake in NaCl medium by control oocytes injected with 20 nl of water alone (*open circles*). Each value is the mean ± S.E. of 10-12 oocytes, and error bars are not shown where S.E. values were smaller than that represented by the symbols.



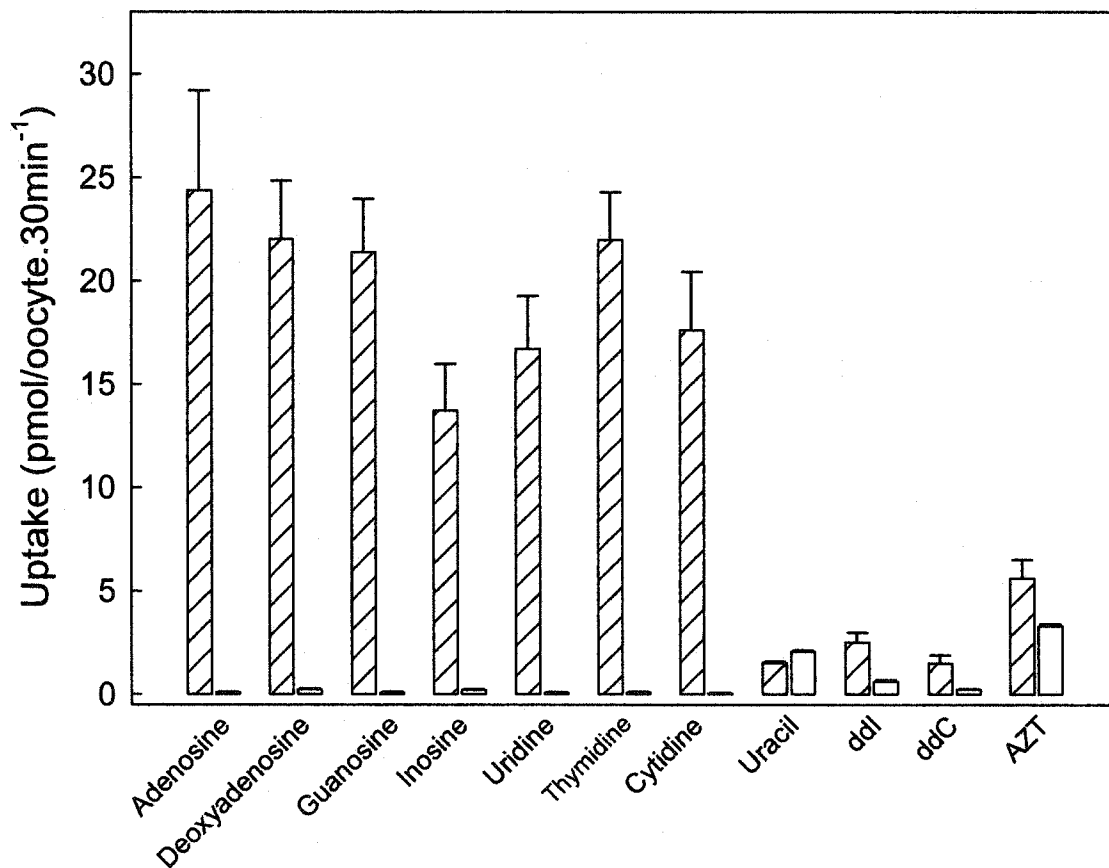
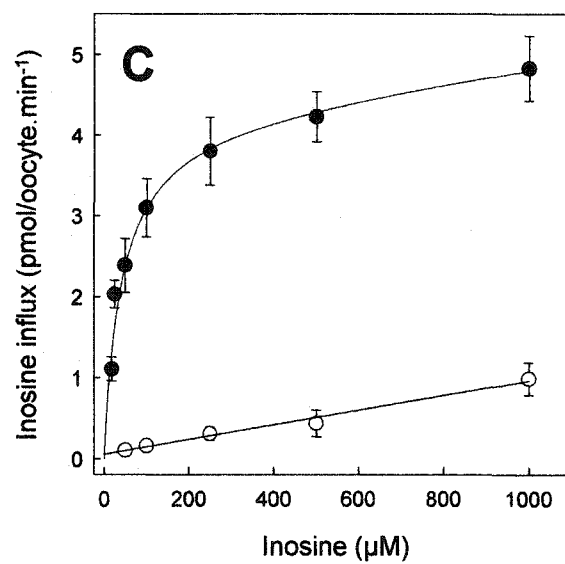
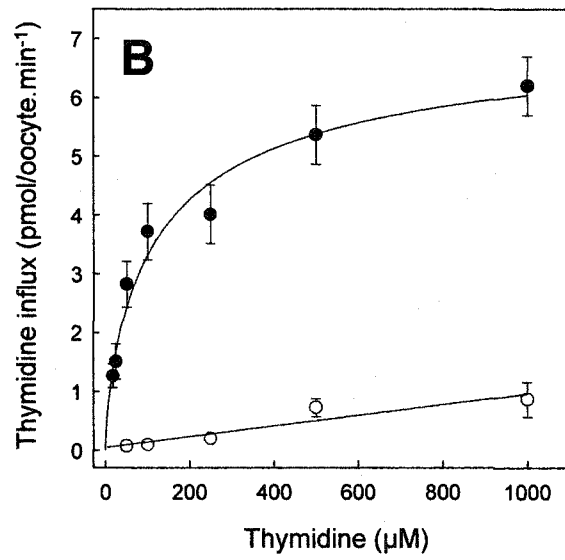
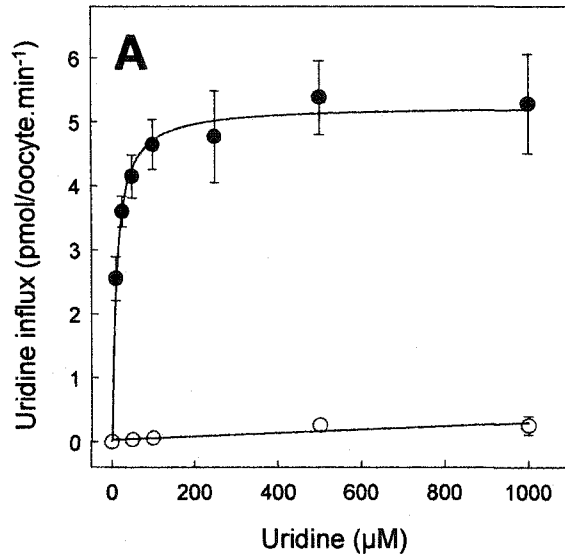


Figure 5-4. Uptake of nucleosides and anti-viral nucleoside drugs by hfcNT. Nucleoside and anti-viral nucleoside drug uptake ($10 \mu\text{M}$, 20°C , 30 min) in oocytes injected with RNA transcripts (*hatched bars*) or water alone (*open bars*) was measured in transport medium containing 100 mM NaCl. Each value is the mean \pm S.E. of 10-12 oocytes.

Figure 5-5. Kinetic properties of hfCNT. Initial rates of uridine (*A*), thymidine (*B*) and inosine uptake (*C*) (1 min fluxes, 20°C) in oocytes injected with RNA transcripts (*solid circles*) or water alone (*open circles*) were measured in transport medium containing 100 mM NaCl. Kinetic parameters calculated from the mediated component of transport (uptake in RNA-injected oocytes minus uptake in oocytes injected with water alone) are presented in *Table 5-1*. Each value is the mean \pm S.E. of 10-12 oocytes, and error bars are not shown where S.E. values were smaller than that represented by the symbols.



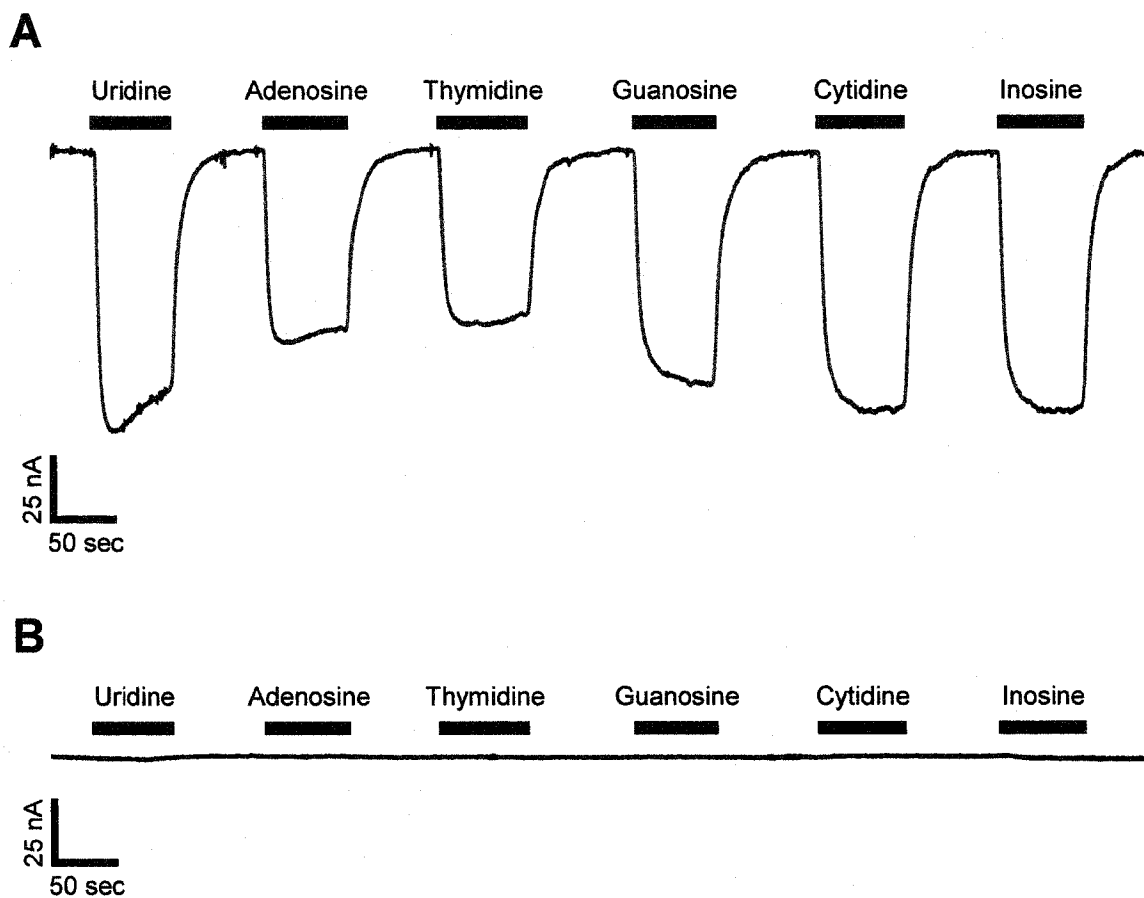
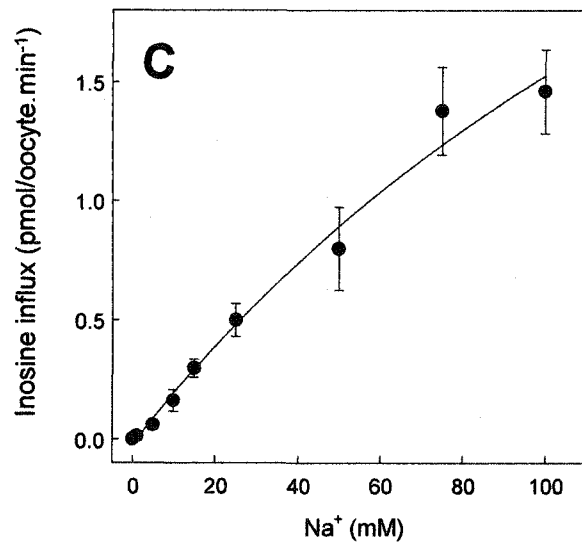
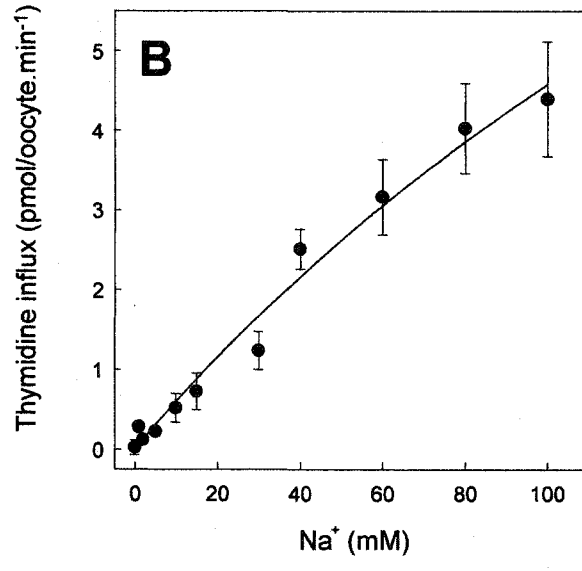
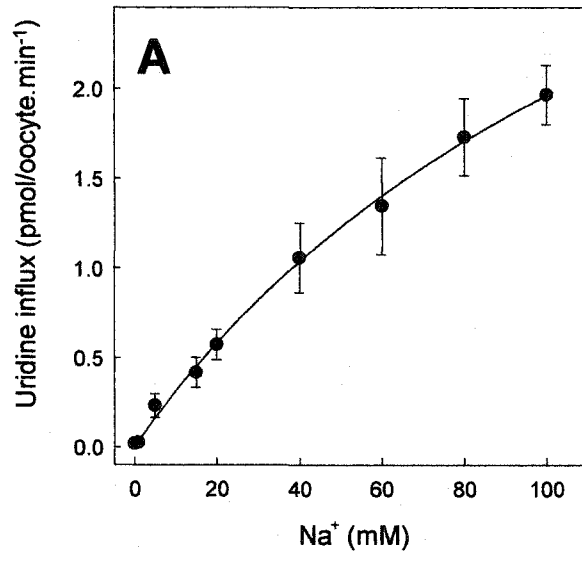


Figure 5-6. Sodium currents induced by exposure of recombinant hfcNT to nucleoside permeants. *A*, inward currents caused by perfusing an hfcNT-producing oocyte at room temperature with NaCl transport medium containing different pyrimidine and purine nucleosides at a concentration of 200 μ M. *B*, the same oocyte perfused with nucleosides (200 μ M) in choline chloride transport medium. No inward currents were generated. Similarly, no inward currents were generated when control water-injected oocytes were perfused with nucleosides either in the presence or in the absence of Na⁺ (traces not shown).

Figure 5-7. Sodium dependence of uridine, thymidine and inosine of influx by recombinant hfCNT. Initial rates of hfCNT-mediated uridine (*A*), thymidine (*B*) and inosine uptake (*C*) (10 μ M, 20°C, 1 min) were measured in transport medium containing 0 – 100 mM NaCl using choline chloride to maintain isomolarity. Mediated uptake was calculated as uptake in hfCNT-producing oocytes minus uptake in control water-injected oocytes. Each value is the mean \pm S.E. of 10-12 oocytes, and error bars are not shown where S.E. values were smaller than that represented by the symbols.



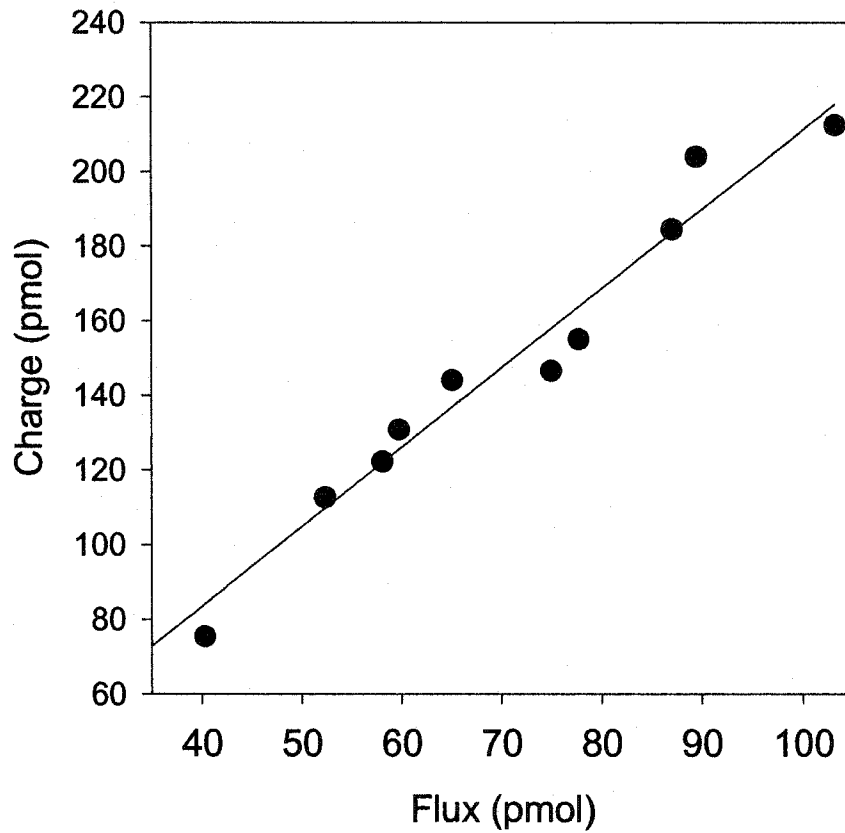


Figure 5-8. Stoichiometry of Na⁺/uridine cotransport by recombinant hfCNT. Uridine-dependent charge and [¹⁴C]uridine uptake were simultaneously determined at $V_m = -50$ mV in the presence of Na⁺ for 3 min. Integration of the uridine-evoked inward current with time was used to calculate the net cation influx by converting picocoulombs to picomoles using the Faraday constant. Mediated [¹⁴C]uridine uptake was calculated as uptake in hfCNT-producing oocytes minus uptake in water-injected oocytes.

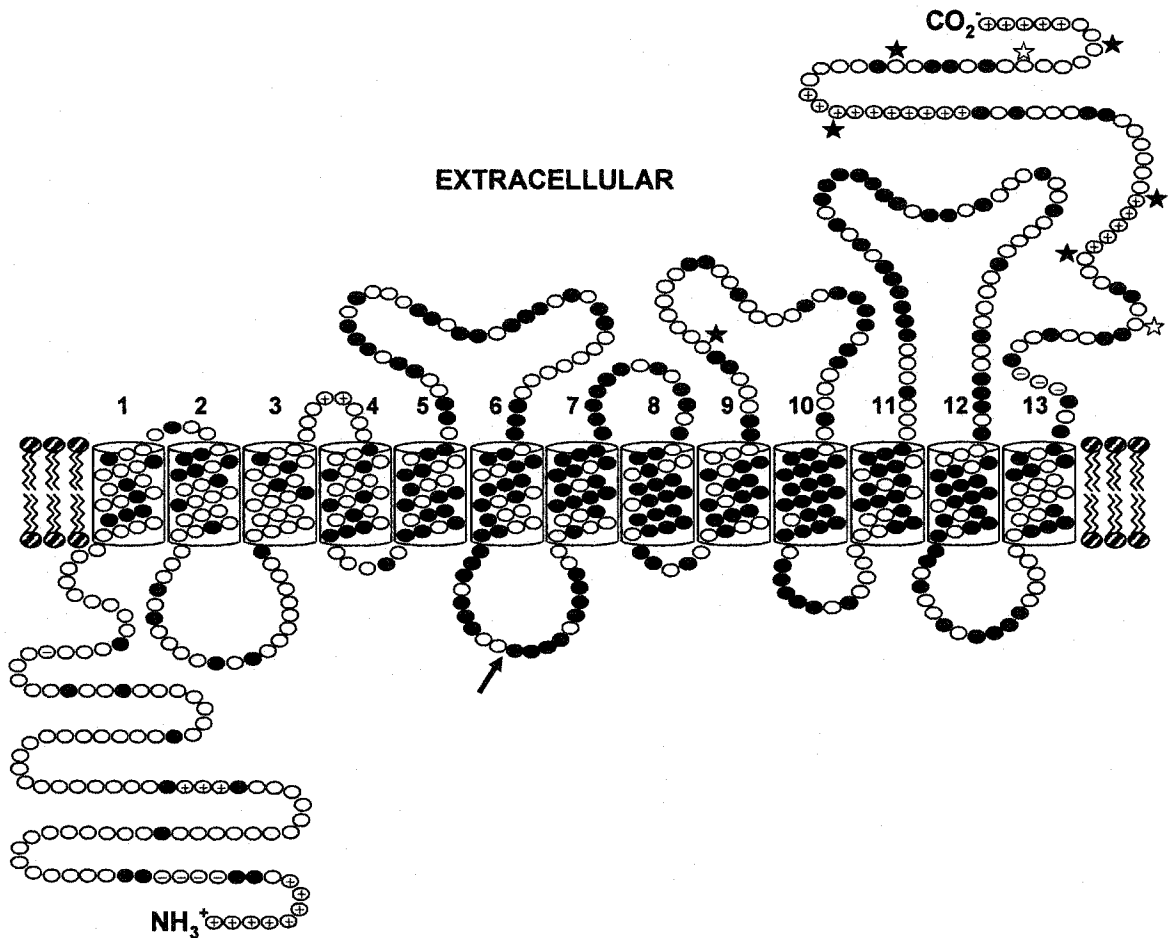


Figure 5-9. Topographical model of hfcNT and hCNT1. Potential membrane-spanning α -helices are *numbered*, and putative glycosylation sites in predicted extracellular domains in hfcNT and hCNT1 are indicated by *solid* and *open stars*, respectively. Residues identical in the two proteins are shown as *solid circles*. Residues corresponding to insertions in the sequence of hfcNT or hCNT1 are indicated by *circles* containing “+” and “-” signs, respectively. The *arrow* represents splice site used for construction of the chimera.

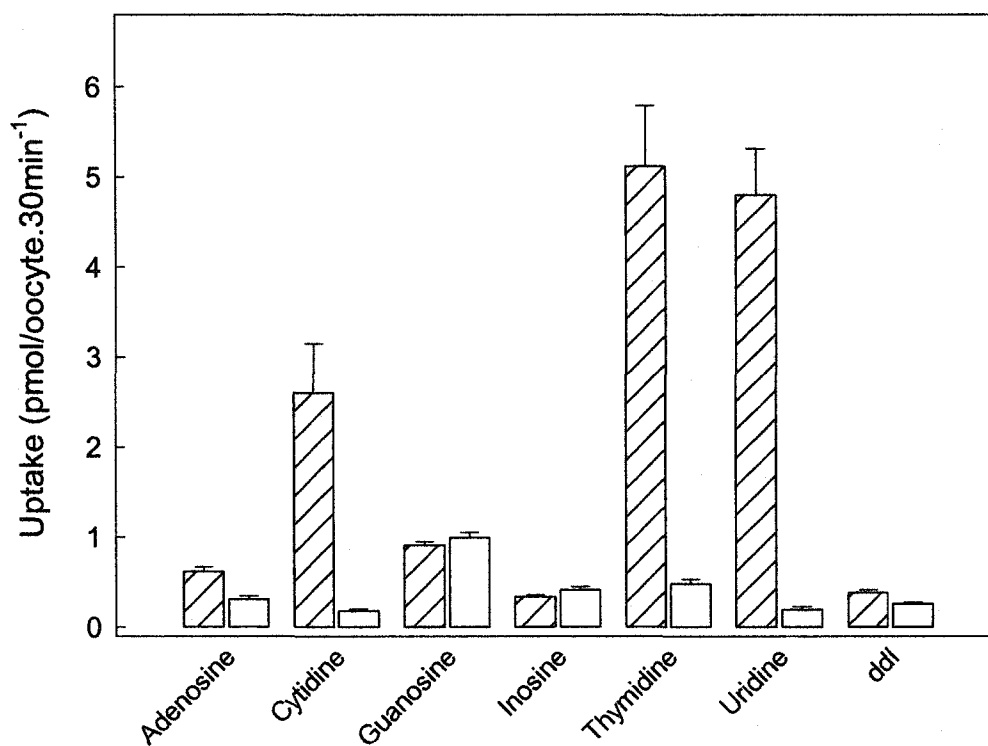
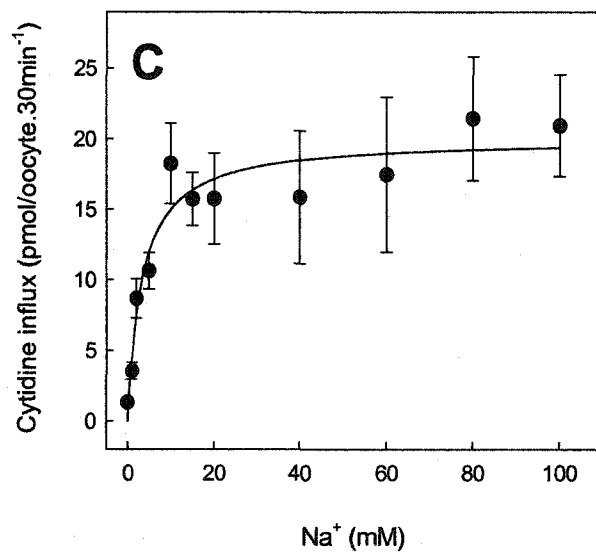
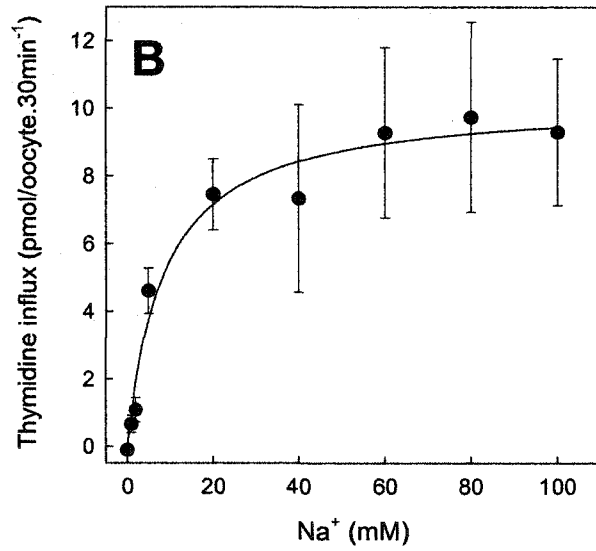
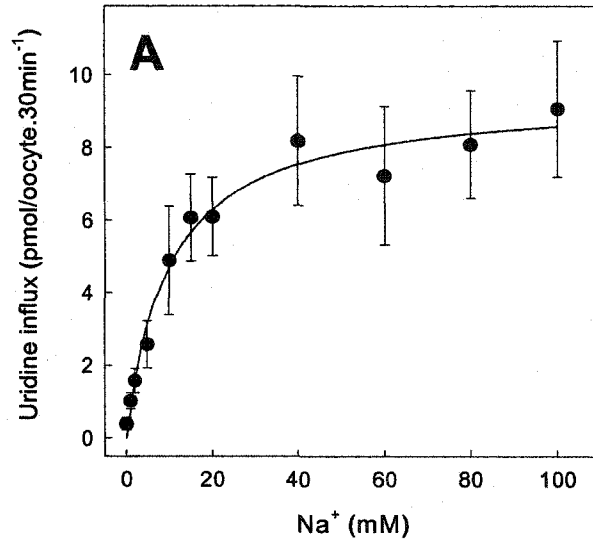


Figure 5-10. Uptake of nucleosides and anti-viral nucleoside drugs by hFCNT/hCNT1 chimera HF/H. Nucleoside and antiviral nucleoside drug uptake (10 μ M, 20°C, 30 min) was measured in transport medium containing 100 mM NaCl in oocytes injected with RNA transcript (*hatched bars*) or water alone (*open bars*). Each value is the mean \pm S.E. of 10-12 oocytes.

Figure 5-11. Sodium-dependence of uridine, thymidine, and cytidine influx by hfcNT/hCNT1 chimera HF/H. Initial rates of transporter-mediated influx of uridine (*A*), thymidine (*B*) or cytidine (*C*) (10 μ M, 20°C, 30 min) were measured in transport media containing 0-100 mM NaCl, using choline chloride to maintain isomolarity. Mediated uptake was calculated as uptake in hfcNT-producing oocytes minus uptake in control water-injected oocytes. Each value is the mean \pm S.E. of 10-12 oocytes, and error bars are not shown where S.E. values were smaller than that represented by the symbols.



Bibliography

- Baldwin SA, Mackey JR, Cass CE, and Young JD** (1999) Nucleoside transporters: molecular biology and implications for therapeutic development. *Mol Med Today* 5: 216-224.
- Bardack D** (1991) First fossil hagfish (Myxinoidea): a record from the Pennsylvanian of Illinois. *Science* 254: 701-703.
- Botfield MC, Wilson DM, and Wilson TH** (1990) The melibiose carrier of *Escherichia coli*. *Res Microbiol* 141: 328-331.
- Cass CE** (1995) Nucleoside transport. In *Drug Transport in antimicrobial and anticancer chemotherapy*. (Georgopapadakou NH, ed) pp. 404-451, Marcel Dekker, New York.
- Che M, Ortiz DF, and Arias IM** (1995) Primary structure and functional expression of a cDNA encoding the bile canalicular, purine-specific Na⁺-nucleoside cotransporters. *J Biol Chem* 270: 13596-13599.
- Cheeseman CI, Mackey JR, Cass CE, Baldwin SA, and Young JD** (2000) Molecular mechanism of nucleoside and nucleoside drug transport. In *Gastrointestinal Transport*. (Barrett KE and Donowitz M, eds.) pp. 330-379, Academic Press, San Diego.
- Chen XZ, Shayakul C, Berger UV, Tian W, and Hediger MA** (1998) Characterization of a rat Na⁺-dicarboxylate cotransporters. *J Biol Chem* 273: 20972-20981.
- Crawford CR, Patel DH, Naeve C, and Belt JA** (1998) Cloning of a human equilibrative, nitrobenzylmercaptapurine riboside (NBMPR)-insensitive nucleoside transporter *ei* by functional expression in a transport-deficient cell line. *J Biol Chem* 273: 5288-5293.
- Diez-Sampedro A, Eskandari S, Wright EM, and Hirayama BA** (2001) Na⁺-to-sugar stoichiometry of SGLT3. *Am J Physiol* 49: F278-F282.
- Dunwiddie TV, and Masino SA** (2001) The role and regulation of adenosine in the central nervous system. *Annu Rev Neurosci* 24: 31-55.
- Ellory JC, and Wolowyk MW** (1991) Evidence for bumetanide-sensitive, Na⁺-dependent, partial Na-K-Cl co-transport in red blood cells of a primitive fish. *Can J Physiol Pharmacol* 69: 588-591.
- Felsenstein J.** (1989) Phylip-Phylogeny inference package (version 3.2). *Cladistics* 5: 164-166.
- Fincham DA, Wolowyk MW, and Young JD** (1991) Nucleoside uptake by red blood cells from a primitive vertebrate, the Pacific hagfish (*Eptatretus stouti*), is mediated by a nitrobenzylthioinosine-insensitive transport system. *Biochim Biophys Acta* 1069: 123-126.
- Forey PL, and Janvier P** (1993) Agnathans and the origin of jawed vertebrates. *Nature* 361: 129-134.

- Griffith DA, and Jarvis SM** (1996) Nucleoside and nucleobase transport systems of mammalian cells. *Biochim Biophys Acta* 1286: 153-181.
- Griffiths M, Beaumont N, Yao SYM, Sundaram M, Bouman CE, Davies A, Kwong FYP, Coe IR, Cass CE, Young JD, and Baldwin SA** (1997a) Cloning of a human nucleoside transporter implicated in the cellular uptake of adenosine and chemotherapeutic drugs. *Nat Med* 3: 89-93.
- Griffiths M, Yao SYM, Abidi F, Phillips SEV, Cass CE, Young JD, and Baldwin SA** (1997b) Molecular cloning and characterization of a nitrobenzylthioinosine-insensitive (*et*) equilibrative nucleoside transporter from human placenta. *Biochem J* 328: 739-743.
- Gunshin H, MacKenzie B, Berger UV, Gunshin Y, Romero MF, Boron WF, Nussberger S, Gollan JL, and Hediger MA** (1997) Cloning and characterization of a mammalian proton-coupled metal-ion transporter. *Nature* 388: 482-488.
- Halestrap AP, and Price NT** (1999) The proton-linked monocarboxylate transporter (MCT) family: structure, function and regulation. *Biochem J* 343: 281-299.
- Hama H, and Wilson TH** (1992) Primary structure and characteristics of the melibiose carrier of *Klebsiella pneumoniae*. *J Biol Chem* 267: 18371-18376.
- Hama H, and Wilson TH** (1994) Replacement of alanine-58 by asparagines enables the melibiose carrier of *Klebsiella pneumoniae* to couple sugar transport to Na⁺. *J Biol Chem* 269: 1063-1067.
- Hamilton SR, Yao SYM, Ingram JC, Hadden DA, Ritzel MWL, Gallagher MP, Henderson PJ, Cass CE, Young JD, and Baldwin SA** (2001) Subcellular distribution and membrane topology of the mammalian concentrative Na⁺-nucleoside cotransporters rCNT1. *J Biol Chem* 276: 27981-27988.
- Hediger MA** (1994) Structure, function and evolution of solute transporters in prokaryotes and eukaryotes. *J Exp Biol* 196: 15-49.
- Hong M, Schlichter L, and Bendayan R** (2000) A novel zidovudine uptake system in microglia. *J Pharmacol Exp Ther* 292: 366-374.
- Horton RM, Hunt HD, Ho SN, Pullen JK, and Pease LR** (1989) Engineering hybrid genes without the use of restriction enzymes: gene splicing by overlap extension. *Gene* 77: 51-59.
- Huang QQ, Yao SYM, Ritzel MWL, Paterson ARP, Cass CE, and Young JD** (1994) Cloning and functional expression of a complementary DNA encoding a mammalian nucleoside transport protein. *J Biol Chem* 269: 17757-17760.
- Janvier P.** Tree of life: Hyperotreti [*online*]. University of Arizona. <http://phylogeny.arizona.edu/tree/eukaryotes/animals/chordata/hyperotreti/hyperotreti.html>, [2001, Sept. 19th].
- Kaback HR, Satin-Tóth M, and Weinglass AB** (2001) The Kamikaze approach to membrane transport. *Nat Rev Mol Cell Biol* 2: 610-620.

- Liman ER, Tytgat J, and Hess P** (1992) Subunit stoichiometry of a mammalian K⁺ channel determined by construction of multimeric cDNAs. *Neuron* 9: 861-871.
- Loewen SK, Ng AM, Yao SY, Cass CE, Baldwin SA, and Young JD** (1999) Identification of amino acid residues responsible for the pyrimidine and purine nucleoside specificities of human concentrative Na⁺ nucleoside cotransporters hCNT1 and hCNT2. *J Biol Chem* 274: 24475-24484.
- Mackey JR, Baldwin SA, Young JD, and Cass CE** (1998) Nucleoside transport and its significance for anticancer drug resistance. *Drug Resistance Updates* 1: 310-324.
- Meredith D, and Boyd CA** (2000) Structure and function of eukaryotic peptide transporters. *Cell Mol Life Sci* 57: 754-778.
- Ono-Koyanagi, K., Suga, H., Katoh, K, and Miyata, T** (2000) Protein tyrosine phosphatases from amphioxus, hagfish, and ray: divergence of tissue-specific isoform genes in the early evolution of vertebrates. *J Mol Evol* 50: 302-311.
- Pajor AM, and Wright EM** (1992) Cloning and functional expression of a mammalian Na⁺-nucleoside cotransporters. A member of the SGLT family. *J Biol Chem* 267: 3557-3560.
- Ritzel MWL, Yao SYM, Huang MY, Elliot JF, Cass CE, and Young JD** (1997) Molecular cloning and functional expression of cDNAs encoding a human Na⁺-nucleoside cotransporters (hCNT1). *Am J Physiol* 272, C707-C714.
- Ritzel MWL, Yao SYM, Ng AML, Mackey JR, Cass CE, and Young JD** (1998) Molecular cloning, functional expression and chromosomal localization of a cDNA encoding a human Na⁺ nucleoside cotransporters (hCNT2) selective for purine nucleosides and uridine. *Mol Membr Biol* 15: 203-211.
- Ritzel MWL, Ng AML, Yao SYM, Graham K, Loewen SK, Smith KM, Ritzel RG, Mowles DA, Carpenter P, Chen X-Z, Karpinski E, Hyde RJ, Baldwin SA, Cass CE, and Young JD** (2001) Molecular identification and characterization of novel human and mouse concentrative Na⁺-nucleoside cotransporters proteins (hCNT3 and mCNT3) broadly selective for purine and pyrimidine nucleosides (system *cib*). *J Biol Chem* 276: 2914-2927.
- Shryock JC, and Belardinelli L** (1997) Adenosine and adenosine receptors in the cardiovascular system: biochemistry, physiology and pharmacology. *Am J Cardiol* 79: 2-10.
- Shu D-G, Luo H-L, Conway Morris S, Zhang X-L, Hu S-X, Chen L, Han J, Zhu M, Li Y, and Chen L-Z.** (1999) Lower Cambrian vertebrates from south China. *Nature* 402, 42-46.
- Sundaram M, Yao SYM, Ingram JC, Bery ZA, Adidi F, Cass CE, Baldwin SA, and Young JD** (2001) Topology of a human equilibrative, nitrobenzylthioinosine (NBMPR)-sensitive nucleoside transporter (hENT1) implicated in the cellular uptake of adenosine and anti-cancer drugs. *J Biol Chem* 276: 4520-45275.
- Tiihonen K, Yao SYM, Nikinmaa M, and Young JD** (2000) Sodium-dependent transport of pyruvate in erythrocytes of the Pacific hagfish (*Eptatretus stouti*). *Can J Zool* 78: 2019-2026.

- Thompson JD, Gibson TJ, Plewniak F, Jeanmougin F, and Higgins DG (1997)** The CLUSTAL_X windows interface: flexible strategies for multiple sequence alignment aided by quality analysis tools. *Nucleic Acids Res* 25: 4876-4882.
- Uldry M, Ibberson M, Horisberger JD, Chatton JY, Riederer BM, and Thorens B (2001)** Identification of a mammalian H⁺-myo-inositol symporter expresses predominantly in the brain. *EMBO J* 20: 4467-4477.
- Wang J, Su SF, Dresser MJ, Schaner ME, Washington CB, and Giacomini KM (1997)** Na⁺-dependent purine nucleoside transporter from human kidney: cloning and functional characterization. *Am J Physiol* 273: F1058-F1065.
- Wu X, Yuan G, Brett CM, Hui AC, and Giacomini KM (1992)** Sodium-dependent nucleoside transport in choroid plexus from rabbit. Evidence for a single transporter for purine and pyrimidine nucleosides. *J Biol Chem* 267: 8813-8818.
- Xiao GQ, Wang J, Tangen T, and Giacomini KM (2001)** A novel proton-dependent nucleoside transporter, CeCNT3, from *Caenorhabditis elegans*. *Mol Pharmacol* 59: 339-348.
- Yao SYM, Ng AML, Ritzel MWL, Gati WP, Cass CE, and Young JD (1996)** Transport of adenosine by recombinant purine- and pyrimidine-selective sodium/nucleoside cotransporters from rat jejunum expressed in *Xenopus laevis* oocytes. *Mol Pharmacol* 50: 1529-1535.
- Yao SYM, Ng AML, Muzyka WR, Griffiths M, Cass CE, Baldwin SA, and Young JD (1997)** Molecular cloning and functional characterization of nitrobenzylthioinosine (NBMPR)-sensitive (*es*) and NBMPR-insensitive (*et*) equilibrative nucleoside transporter proteins (rENT1 and rENT2) from rat tissues. *J Biol Chem* 272: 28423-28430.
- Yao SYM, Cass CE, and Young JD (2000)** The *Xenopus* oocyte expression system for the cDNA cloning and characterization of plasma membrane transport proteins. In *Membrane Transport. A Practical Approach*. pp. 47-78, Oxford University Press, Oxford.
- Yao SYM, Ng AML, Sundaram M, Cass CE, Baldwin SA and Young JD (2001)** Transport of antiviral 3'-deoxy-nucleoside drugs by recombinant human and rat equilibrative, NBMPR-insensitive (ENT2) nucleoside transporter proteins produced in *Xenopus* oocytes. *Mol Membr Biol* 18: 161-167.
- Yao SYM, Ng AML, Sundaram M, Cass CE, Baldwin SA, and Young JD (2002)** Functional and molecular characterization of nucleobase transport by recombinant human and rat ENT1 and ENT2 equilibrative nucleoside transport proteins: chimeric constructs reveal a role for the ENT2 helix 5-6 region in nucleobase translocation. *J Biol Chem* (in press).
- Young JD, Ellory JC, and Wolowyk MW (1987)** Hagfish (*Eptatretus stouti*) erythrocytes show minimal chloride transport activity. *J Exp Biol* 129: 377-383.
- Young JD, Fincham DA, and Harvey CM (1991)** Cation and harmaline interactions with Na⁺-independent dibasic amino acid transport system y⁺ in human erythrocytes and in erythrocytes from a primitive vertebrate the pacific hagfish (*Eptatretus stouti*). *Biochim Biophys Acta* 1071: 111-118.

Young JD, Yao SYM, Tse CM, Davies A, and Baldwin SA (1994) Functional and molecular characteristics of a primitive vertebrate glucose transporter: studies of glucose transport by erythrocytes from the pacific hagfish (*Eptatretus stouti*). *J Exp Biol* 186: 23-41.

CHAPTER VI:*

Transport of antiviral and antineoplastic nucleoside drug by recombinant *Escherichia coli* H⁺/nucleoside cotransporter (NupC) produced in *Xenopus laevis* oocytes.**

*A version of this chapter has been submitted for publication.

Loewen SK, Yao SYM, Turner RJ, Mackey JR, Weiner JH, Gallagher MP, Henderson PJF, Baldwin SA, Cass CE, and Young JD (2002) *Mol Pharmacol* (submitted).

**Dr. Sylvia Yao provided that initial NupC cDNA, which I subcloned into pGEM-HE and undertook its functional characterization.

Introduction

The capacity for nucleoside uptake mediated by specialized plasma membrane nucleoside transporter (NT) proteins is widespread amongst bacteria (Kubitschek, 1968; Kirchman *et al.*, 1982), and is required for nucleic acid synthesis and energy metabolism in mammalian cell types that lack *de novo* pathways for nucleotide biosynthesis (Cheeseman *et al.*, 2000). NTs also provide the cellular uptake route for many cytotoxic nucleoside derivatives used in the treatment of viral and neoplastic diseases (Baldwin *et al.*, 1999). Such drugs may exert more than one therapeutic action. AZT, for example, is used as an antiviral drug to combat HIV infection in AIDS, but also provides an important ancillary benefit by suppressing bacterial infections in these immunocompromised individuals (Monno *et al.*, 1997). Conversely, nucleoside drugs may perturb the natural balance of healthy intestinal microflora, thereby increasing patient susceptibility to infections by nucleoside drug-resistant opportunistic organisms. Infectious complications, for instance, are also common in cancer patients (Sanders *et al.*, 1992; Robak, 2001). Enteric *Escherichia coli* cells compete directly with host transport systems and are proficient scavengers of nucleosides and other nutrients.

In human and other mammalian cells, uptake of nucleosides is brought about by members of the ENT (equilibrative, Na⁺-independent) and CNT (concentrative, Na⁺-dependent) NT families (Baldwin *et al.*, 1999). ENTs are widely distributed in eukaryotes, but so far appear to be absent from prokaryotes, while CNTs are present in both. Three CNT isoforms have been identified in humans and rodents (Huang *et al.*, 1994; Che *et al.*, 1995, Wang *et al.*, 1997; Ritzel *et al.*, 1997, 1998, 2001). Human (h) and rat (r) CNT1 and CNT2 both transport uridine (and adenosine), but are otherwise selective for pyrimidine (hCNT1 and rCNT1) and purine (hCNT2 and rCNT2) nucleosides. hCNT3 and its mouse (m) ortholog mCNT3 transport both pyrimidine and purine nucleosides. The relationships of these proteins to transport processes defined by functional studies are: CNT1 (*cit*), CNT2 (*cif*) and CNT3 (*cib*). Other CNTs that have been characterized functionally include hfCNT from an ancient marine pre-vertebrate, the Pacific hagfish (Yao *et al.*, 2002), CaCNT from *Candida albicans* (as described in Chapter VII) and CeCNT3 from *Caenorhabditis elegans* (Xiao *et al.*, 2001).

At least three NT proteins (NupC, NupG, and XapB) have been identified in the *E. coli* inner membrane (Westh Hansen *et al.*, 1987; Craig *et al.*, 1994; Seeger *et al.*, 1995). All are concentrative, but only one (NupC) shows sequence similarity to mammalian CNTs. *E. coli* also possesses two NupC homologs (YeiJ and YeiM) of undetermined function. In addition, the outer membrane of *E. coli* and other Gram-negative bacteria contains the passive nucleoside-specific channel-forming protein Tsx (Nieweg and Bremer, 1997). Tsx has a porin β -barrel membrane topology and is structurally unrelated to the CNT and ENT protein families.

Transport and growth studies with *E. coli* suggest that the NupC and NupG mediated processes accept a broad range of nucleosides as permeants, and can be distinguished from each other by the poor ability of NupC to transport guanosine and deoxyguanosine, and by different sensitivities to inhibition by showdomycin (Komatsu and Tanaka, 1972). XapB, previously considered to be xanthosine-specific, overlaps in permeant selectivity with NupC (Norholm and Dandanell, 2001), although the recently established close proximity of the *xapB* and *nupC* genes on the *E. coli* chromosome (54.34' and 54.13', respectively) and their similar inability to transport guanosine raises the possibility that earlier NupC studies may have grouped both activities as a single transport system (Karp *et al.*, 2002). Interpretation of *E. coli* NT transport studies in *E. coli* is further complicated by the reported presence of a low affinity, purine nucleoside-selective process of unknown molecular identity (Norholm and Dandanell, 2001). In this report, we have overcome these technical limitations by the use of heterologous expression in *Xenopus* oocytes to study nucleoside and nucleoside drug transport by recombinant *E. coli* NupC in an NT-deficient background and in the same membrane environment used previously to study recombinant mammalian CNTs.

Materials and Methods

Molecular Cloning of NupC DNA – PCR was performed on *E. coli* HB101 chromosomal DNA using Q1 (5'-ATATCTAGAAAGGAGAAATAATATGGACCGCGTCCTTC-3') as the sense primer and Q2 (5'-ATATAAAGCTTTTACAGCACCAGTGCTG-3') as the antisense primer. Q1 and Q2 corresponded to positions (underlined) 267-282 (Q1) and 1453-1469 (Q2) of the *nupC* gene (Craig *et al.*, 1994) and incorporated 5' *Xba*I (Q1) and *Hind*III (Q2) restriction sites (underlined and double-underlined, respectively). The reaction mixture (100 μ l) contained

10 mM Tris-HCl (pH 8.0), 50 mM KCl, 1.5 mM MgCl₂, 0.01% (w/v) gelatin, 1 µg HB101 chromosomal DNA, 100 pmol of each primer and 2.5 units of *Taq* polymerase. Amplification was accomplished by incubation at 94°C for 1 min, 47°C for 1.5 min and 72°C for 1.5 min (RoboCycler™40 temperature cycler, Stratagene). After 25 cycles, the reaction mixture was separated on a 1% (w/v) non-denaturing agarose gel (Gibco/BRL) containing 0.25 µg/ml ethidium bromide. The resulting 1203 bp product was ligated into pGEM-3Z (Promega) and subcloned into the enhanced *Xenopus* expression vector pGEM-HE (pNUPC-HE) (Liman *et al.*, 1992). By providing additional 5'- and 3'- untranslated regions from a *Xenopus* β-globin gene, the pGEM-HE construct gave 20-fold greater functional activity than pGEM-3Z and was used in subsequent transport characterization of NupC. The 1203 bp insert of pNUPC-HE was sequenced in both directions by *Taq* DyeDeoxyterminator cycle sequencing using an automated model 373A DNA Sequencer (Applied Biosystems).

Functional Production of Recombinant NupC in *Xenopus* Oocytes – NupC plasmid DNA was digested with *Nhe*I and transcribed with the T7 RNA polymerase in the presence of 5' m⁷GpppG cap using the mMessage mMachine™ (Ambion) *in vitro* transcription system (Ambion). Healthy defolliculated stage VI *Xenopus* oocytes were microinjected with 40 nl of NupC RNA transcript (1 ng/nl) or 40 nl of water alone and incubated at 18°C in modified Barth's medium at 18°C for 5 days prior to the assay of nucleoside and nucleoside drug transport activity. A 5-day incubation period was used instead of the usual 3-day period (Huang *et al.*, 1994) because preliminary studies had established greater activity at 5 days.

NupC Radioisotope Flux Studies – Transport was traced using the appropriate ³H-labeled nucleoside or nucleoside drug (Moravek Biochemicals, Brea, CA or Amersham Pharmacia Biotech) at a concentration of 2 mCi/ml. [³H]Gemcitabine (2'-deoxy-2',2'-difluorocytidine) was a gift from Eli Lilly Inc. (Indianapolis, IN). Flux measurements were performed at room temperature (20 °C) as described previously (Huang *et al.*, 1994; Ritzel *et al.*, 1997) on groups of 12 oocytes in 200 µl of transport medium containing either 100 mM NaCl or 100 mM choline chloride and 2 mM KCl, 1 mM CaCl₂, 1 mM MgCl₂, and 10 mM HEPES (pH 5.5, 6.5, 7.5 or 8.5). Unless otherwise specified, the permeant concentration was 1 µM. To maximize potential transmembrane H⁺-gradients, cells were first washed into pH 7.5 NaCl or

choline chloride transport buffer and only exposed to either high (pH 8.5) or low pH medium (pH 5.5 or 6.5) immediately prior to the assay of transport activity. In competition experiments, nonradioactive nucleosides (200 μ M) were added to oocytes simultaneously with [3 H]uridine. At the end of the incubation, extracellular radioactivity was removed by six rapid washes in the appropriate ice-cold transport buffer. Individual oocytes were dissolved in 0.5 ml of 5% (w/v) sodium dodecyl sulphate for quantitation of oocyte-associated 3 H by liquid scintillation counting (LS 6000IC, Beckman Canada Inc.). The flux values shown are the means \pm S.E. of 10-12 oocytes from one representative experiment. Significant differences in mean flux values were determined by Student's t-test ($P = 0.05$). Each experiment was performed at least twice on different batches of cells. Kinetic (K_m and V_{max}) parameters \pm S.E. were determined using ENZFITTER software (Elsevier-Biosoft, Cambridge, UK). We have established previously that oocytes lack endogenous nucleoside transport processes (Huang *et al.*, 1994).

Results

Cloning of the *nupC* Gene – When primers were designed to encompass the whole open reading frame of *E. coli nupC* (Craig *et al.*, 1994) were used for PCR amplification of *E. coli* HB101 chromosomal DNA, a product of the correct size (1203 bp) was obtained. Subcloning of this PCR product into the plasmid expression vector pGEM-HE yielded a cDNA (plasmid pNUPC-HE) whose nucleotide and deduced amino acid sequences were identical to *nupC* GenBankTM/EBI Data Bank accession number NC000913. NupC (43.5 kDa) contained 400 amino acid residues in comparison to >600 residues of the mammalian CNTs and was 26% identical (37% similar) to hCNT1, 22% identical (33% similar) to hCNT2, and 25% identical (37% similar) to hCNT3 (Fig. 6-1). The smaller NupC protein did not contain the large intracellular amino-terminus and large exofacial carboxyl-terminus characteristic of human and other mammalian CNTs. In mammalian CNTs, the latter domain contains multiple sites of N-linked glycosylation (Hamilton *et al.*, 2001). NupC also lacked the first three transmembrane helices (TMs) of the mammalian proteins, and its ten predicted TMs correspond, therefore, to TMs 4-13 of CNT1-3 (Hamilton *et al.*, 2001). Truncated constructs of human and rat CNT1 with TMs 1-3 removed have confirmed the importance of TMs 4-13 as the important core structure of the mammalian transporters (Hamilton *et al.*, 2001). NupC showed greatest sequence similarity to the carboxyl-terminal half of hCNT1-3, particularly in TMs 10-12 .

including the exofacial loop between TMs 11 and 12 (Fig 6-1). These regions may therefore have particular functional and/or structural significance.

Functional Production and Cation-specificity of NupC in *Xenopus* Oocytes – Fig. 6-2A (*insert*) presents a representative transport experiment in NaCl medium at pH 5.5 that compares time courses of uptake of 1 μM [^3H]uridine by NupC-producing oocytes and control (water-injected) oocytes. In both, uptake was linear for at least 30 min. After 10 min, the uptake interval selected for subsequent initial rate measurements, influx in NupC-producing oocytes was 49-fold higher than in control oocytes. Consistent with NupC being a H^+ -dependent transporter, influx was pH-dependent. As shown in Fig. 6-2A, values for NupC-mediated uridine influx (uptake in RNA-injected oocytes *minus* uptake in water-injected oocytes) increased 6-fold between pH 8.5 and 5.5, while basal influx in water-injected oocytes remained unchanged. For comparison, uridine influx (10 μM) mediated by Na^+ -dependent rCNT1 was independent of external pH (Fig. 6-2B). A small (<5%) slippage component of rCNT1 uridine influx seen when Na^+ in the transport medium is replaced by equimolar choline $^+$ (Huang *et al.*, 1994) was also unaffected by changes in external pH (data not shown). In contrast, NupC retained full functional activity in the absence of Na^+ and, in a representative experiment, NupC-mediated uridine influx (1 μM) was 0.84 ± 0.19 and 0.97 ± 0.08 pmol/oocyte.10 min $^{-1}$ in NaCl and choline chloride transport medium, respectively, at pH 5.5, and 0.14 ± 0.03 and 0.16 ± 0.03 pmol/oocyte.10 min $^{-1}$, respectively, at pH 8.5.

Substrate Selectivity of Recombinant NupC – Fig. 6-3A compares uridine influx (1 μM , pH 5.5, 10min flux) with transport of a panel of other radiolabeled nucleosides and nucleobases. Similar to the *cit*-type functional activity of hCNT1 and rCNT1 (Huang *et al.*, 1994; Ritzel *et al.*, 1997), uridine, cytidine and thymidine gave similar NupC-mediated fluxes, while guanosine was not transported. Unlike rCNT1 and hCNT1, however, there was also modest transport of inosine. This was verified in the insert to Fig. 6-3A, which shows time courses of inosine uptake by control and NupC-producing oocytes. Discrimination between inosine and guanosine was also observed in competition experiments: inosine inhibited NupC-mediated uridine influx (1 μM) with an IC_{50} value of 287 ± 8 μM , whereas 1 mM guanosine was without effect (data not shown). Fig. 6-3A also shows that NupC transported adenosine at a rate similar to uridine. For hCNT1 and rCNT1, in contrast, fluxes of adenosine are 1-2 orders

of magnitude lower than for uridine (Yao *et al.*, 1996a; Ritzel *et al.*, 1997). There was no significant mediated uptake of uracil or hypoxanthine, establishing NupC as a nucleoside-specific transporter.

Nucleoside Drug Transport by Recombinant NupC – Previously, we have used *Xenopus* expression to establish that human and rodent CNTs, in common with the hagfish CNT3 ortholog hfCNT, accept antiviral dideoxynucleosides as permeants (Huang *et al.*, 1995, Yao *et al.*, 1996b; Ritzel *et al.*, 1997, 1998, 2001; Yao *et al.*, 2002). hcCNT1 transports AZT and ddC (but not ddI), hcCNT2 transports only ddI, and hcCNT3 transports AZT, ddC and ddI. Similarly, the clinically important anticancer deoxycytidine analog, gemcitabine, is a permeant of hcCNT1 and hcCNT3, but not of hcCNT2 (Mackey *et al.*, 1999). As shown in the radiolabeled drug uptake studies presented in Fig. 6-3B, NupC also accepted pyrimidine nucleoside analogs as permeants. The magnitudes of fluxes for 1 μ M AZT and ddC were smaller than that for uridine, but similar to those found previously for human CNTs. NupC-mediated uptake of gemcitabine was intermediate between uridine and AZT/ddC. Consistent with the modest inosine transport by NupC cross-inhibition studies (Fig. 6-3A), ddI also showed significantly greater influx in NupC-producing oocytes than in control water-injected oocytes (0.014 ± 0.001 versus 0.004 ± 0.001 pmol/oocyte.10 min⁻¹ in Fig. 6-3B), suggesting a small amount of NupC-mediated ddI transport.

Kinetic properties – Fig. 6-4 shows representative concentration dependence curves for NupC-mediated transport of uridine, adenosine, AZT, ddC and gemcitabine. Kinetic parameters derived from the data are summarized in Table 6-1, together with corresponding apparent K_m and V_{max} values for recombinant hcCNT1 and rCNT1. To facilitate comparisons between transporters, V_{max} values are presented as pmol/oocyte.min⁻¹. NupC apparent K_m values varied between 1.6 and 130 μ M (adenosine, uridine, gemcitabine \ll AZT, ddC) and, for physiological nucleosides, were in the same range as values for total uridine and cytidine transport measured in *E. coli* containing multiple NT activities (Mygrind and Munch-Petersen, 1975; Munch-Petersen and Mygrind, 1983). In general, NupC apparent K_m values were lower than for hcCNT1 and rCNT1, the bacterial and mammalian proteins showing similar relative apparent affinities for the different substrates tested. Apparent V_{max} values for the different NupC permeants differed by a maximum of 3.6-fold, while $V_{max}:K_m$ ratios, a measure of

transport efficiency, were greatest for adenosine and uridine, intermediate for gemcitabine, and lowest for AZT and ddC (Table 6-1). While the level of transporter protein produced at the cell surface is unknown, corresponding $V_{\max}:K_m$ ratios for hCNT1 and rCNT1 were uridine > gemcitabine > AZT, ddC > adenosine, reflecting the relatively low V_{\max} of adenosine transport by the mammalian proteins.

Discussion

Nucleoside drugs are an integral part of chemotherapeutic strategies in the treatment of patients with viral or neoplastic diseases, where infection from bacteria in immunocompromised individuals is a major concern. Published studies of the antibacterial actions of antiviral and anticancer nucleoside drugs include the finding that AZT and other anti-HIV nucleoside drugs induce DNA repair responses in *E. coli* (Mamber *et al.*, 1990), and the demonstration that AZT has antibacterial activity against members of the Enterobacteriaceae family (Monno *et al.*, 1997). 5-Azacytidine used in the treatment of myelogenous leukaemia also has antibiotic activity (Friedman, 1982). Central to the antibacterial efficacy of such compounds is transportability across the bacterial plasma (inner) membrane.

Previous investigations of nucleoside transport in bacteria have focused primarily on *E. coli*. At least three concentrative nucleoside transport systems have been identified, mediated by the NT proteins NupC, NupG, and XapB (Komatsu and Tanaka, 1972; Munch-Petersen and Mygrind, 1983; Norholm and Dandanell, 2001). Only NupC has homologs in humans and other mammals. The functional characteristics of these bacterial transport proteins are uncertain, and little is known about their transport of antiviral and antineoplastic nucleoside drugs. BLAST searches of bacterial genome databases using *E. coli* NupC sequence as the search template reveal ~ 40 putative NupC and NupC-related CNT family members in bacteria. Most are found in Gram-negative bacteria, but examples also occur in Gram-positive species (*e.g. Bacillus* spp. and *Staphylococcus* spp.) species. This prevalence of CNT gene sequences in bacteria suggests that they fulfil important physiological functions and provides a potential route of cellular uptake for nucleoside drugs in a wide variety of different bacterial organisms. In *E. coli*, microarray data suggest that NupC and NupG are the predominant NTs expressed under both anaerobic and aerobic conditions (unpublished data).

The goal of the present study was to investigate nucleoside and nucleoside drug transport by *E. coli* NupC. Recombinant NupC was produced in *Xenopus* oocytes to avoid the problems inherent in studying native NupC against a background of other endogenous *E. coli* nucleoside transport activities, and to permit functional comparisons with recombinant human and other mammalian CNT proteins produced in the same membrane environment. Using the *Xenopus* plasmid expression vector pGEM-HE incorporating 5'- and 3'-untranslated sequence from a *Xenopus* β -globin gene, our study represents the first successful production of a functional bacterial membrane transport protein in *Xenopus* oocytes. Bacterial channel proteins that have been expressed in *Xenopus* oocytes include the LctB K⁺ channel from *Bacillus stearothermophilus* (Wolters *et al.*, 1999), the UreI H⁺-gated urea channel from *Helicobacter pylori* (Weeks *et al.*, 2000), and members of the MIP (major intrinsic protein) membrane channel family (Hohmann *et al.*, 2000).

E. coli NupC and human and rat CNT1 reportedly differ in their cation preference (H⁺ for NupC, Na⁺ for CNT1). The Na⁺-dependence of recombinant hCNT1 and rCNT1 was established by radioisotope (Huang *et al.*, 1999, Ritzel *et al.*, 1997) and electrophysiological studies (Mackey *et al.*, 1999; Dresser *et al.*, 2000; Lostao *et al.*, 2000; Yao *et al.*, 2000) in *Xenopus* oocytes. The apparent H⁺-dependence of NupC is based upon *E. coli* membrane vesicle studies in Na⁺-free medium using an artificial electron donor (phenazine methosulphate + ascorbate) (Munch-Petersen *et al.*, 1979). Although mammalian CNTs function as Na⁺-coupled nucleoside transporters, recent radioisotope and electrophysiological studies in *Xenopus* oocytes have found that H⁺ and Li⁺ can substitute for Na⁺ in CNT3, but not for CNT1, CNT2 or hagfish hfCNT (Yao *et al.*, 2002; as described in *Chapter V*). In contrast, Na⁺ replacement and pH dependence radioisotope flux experiments suggest that *C. albicans* CaCNT and *C. elegans* CeCNT3 (Xiao *et al.*, 2001) are exclusively H⁺-dependent. In the case of CaCNT, this has been confirmed by electrophysiology (as described in *Chapter VII*). The experiments reported here suggest that NupC is also exclusively H⁺-dependent.

By producing recombinant NupC in *Xenopus* oocytes, we were also able to investigate NupC permeant specificity and demonstrate, for the first time, that NupC transports clinically important antiviral and anticancer nucleoside drugs. Previously, we have identified two adjacent pairs of residues (Ser³¹⁹/Gln³²⁰ and Ser³⁵³/Leu³⁵⁴) in the TM 7-9 region of hCNT1 that, when

mutated together to the corresponding residues in hCNT2 (Gly³¹³/Met³¹⁴ and Thr³⁴⁷/Val³⁴⁸), converted hCNT1 (*cit*-type) into a transporter with *cif*-type functional characteristics (Loewen *et al.*, 1999). An intermediate broad specificity *cib*-like transport activity was produced by mutation of the two TM 7 residues alone. The amino acid residues of NupC at these four positions are Gly¹⁴⁶/Gln¹⁴⁷ in TM 4 and Ser¹⁸⁰/Ile¹⁸¹ in TM 5 (equivalent to TMs 7 and 8 of mammalian CNTs) and predict a substrate specificity intermediate between hCNT1 and hCNT2. While NupC is largely pyrimidine nucleoside-selective, our experiments demonstrate that NupC efficiently transports adenosine. Also, NupC transported inosine at a rate ~ 10% that of uridine, an interaction not observed with hCNT1 or rCNT1 (Huang *et al.*, 1994; Ritzel *et al.*, 1998). The finding that inosine is a modest NupC permeant is supported by experiments showing that *E. coli* transformed with multiple copies of *nupC*-containing plasmid grow on restricted media containing inosine, whereas control cells, which carry only a single copy of *nupC*, do not (Norholm and Dandanell, 2001). Relative to CNT1, therefore, NupC has an enhanced capability to transport adenosine and inosine. However, the weak amino acid sequence conservation between TMs 4 and 5 of NupC and TMs 7 and 8 of hCNT1/2 (19% average sequence identity between NupC and hCNT1/2 *vs.* 76% average sequence identity between hCNT1 and hCNT2) suggests that additional as yet unidentified pore-lining residues are likely to contribute to NupC nucleoside translocation and/or permeant recognition and binding.

In parallel with the selectivity of NupC for physiological pyrimidine nucleosides, adenosine and, to a lesser extent, inosine, recombinant NupC effectively transported gemcitabine, a pyrimidine nucleoside drug widely used in the therapy of solid tumors. NupC also exhibited the capacity to transport antiviral dideoxynucleoside drugs (AZT, ddC > ddI). Like mammalian CNTs, therefore, NupC is relatively tolerant of substitutions at the 2' and 3' positions of the nucleoside sugar moiety. For both physiological nucleosides and antiviral and antineoplastic nucleoside drugs, NupC exhibited greater apparent substrate affinities than human or rat CNT1. This kinetic difference also applies to other mammalian CNT (and ENT) proteins, providing the bacterial protein with a physiological advantage, but pharmacological disadvantage, when competing for nutrients and drugs with host nucleoside transport processes. Quantifying the level of nucleoside transporters will be important in this regard. In

oocytes, for example, calculated V_{\max} values would favour uptake via CNTs, although the same may not be true in their native environments. In the intestinal tract, where enteric bacteria such as *E. coli* normally reside, competition for nucleosides and nucleoside drugs will occur with CNTs present in the intestinal epithelium brush border membrane (Cheeseman *et al.*, 2000). Antiviral dideoxynucleoside drugs are administered orally and will achieve luminal concentrations in excess of the apparent K_m values reported here for NupC-mediated transport of AZT and ddC. This would imply that enteric microorganisms are likely to influence the effectiveness of nucleoside drug therapy of host cells, especially intestinal targets, via sequestration of the available drug but also, that nucleoside analogs are likely to have a disruptive influence on the native intestinal microflora of the host.

Conclusions – The contents of this chapter describe the first expression of a bacterial transport protein in *Xenopus* oocytes, and establishes the utility of the NupC-pGEM-HE/oocyte system as a tool to further our understanding of the physiological and pharmacological roles of concentrative NTs in bacteria. I have also demonstrated NupC-mediated transport of antiviral and antineoplastic nucleoside drugs. By facilitating the intracellular accumulation of cytotoxic nucleoside drugs, NupC may contribute to the antibacterial actions of these compounds.

Table 6-1 – Kinetic Parameters of Uridine, Adenosine, AZT, ddC, and Gemcitabine Influx Mediated by *E. coli* NupC and Mammalian CNT1 Transport Proteins.

Nucleoside Transporter	Substrate	Apparent K_m (μM)	V_{max} ($pmol/oocyte.min^{-1}$)	Ratio, $V_{max}:K_m$	Reference
NupC ^a	Uridine	3.6 ± 0.5	0.61 ± 0.03 ^b	0.18	
hCNT1		45 ± 16	26 ± 2	0.58	Ritzel <i>et al.</i> , 1997
rCNT1		37 ± 7	21 ± 1	0.57	Huang <i>et al.</i> , 1994
NupC ^a	Adenosine	1.6 ± 0.2	0.31 ± 0.01 ^b	0.19	
rCNT1		26 ± 7	0.07 ± 0.01 ^b	0.0027	Yao <i>et al.</i> , 1996a
NupC ^a	AZT	112 ± 15	0.43 ± 0.02 ^b	0.0038	
rCNT1		549 ± 98	26 ± 7	0.048	Yao <i>et al.</i> , 1996b
NupC ^a	ddC	130 ± 13	0.17 ± 0.01 ^b	0.0013	
rCNT1		503 ± 35	20 ± 5	0.039	Yao <i>et al.</i> , 1996b
NupC ^a	Gemcitabine	6.3 ± 1.1	0.43 ± 0.02 ^b	0.068	
hCNT1		24 ± 12	5.8 ± 0.4	0.24	Mackey <i>et al.</i> , 1999

^a, from Fig. 6-4; ^b, corrected to $pmol/oocyte.min^{-1}$

Figure 6-1. NupC is a member of the CNT family of nucleoside transport proteins. Alignment of the predicted amino acid sequences of NupC (from plasmid NupC-HE), hCNT1 (GenBank™ accession number U62967), hCNT2 (GenBank™ accession number AF036109), and hCNT3 (GenBank™ accession number AF305210) was performed using the GCG PILEUP program. Potential membrane spanning α -helices are *numbered* using the membrane topology of mammalian CNTs (Hamilton *et al.*, 2001). Putative glycosylation sites in predicted extracellular domains of hCNT1, hCNT2, and hCNT3 are shown in *lowercase (n)*, and their positions highlighted by an *asterisk* above the aligned sequences. Residues identical in NupC and one or more of the other proteins are indicated by *black boxes*.

NupC
hCNT1 -----MENDPSRRRESISLTPVAK---GLENMGADFLLESLEEGLPRSDLSPAEIRSSWS
hCNT2 -----MEKASGR--QSIALSTVET---GTVNPGLELME--KEVEPEGSKRTDAGGHS LGD
hCNT3 MELRSTAAAPRAEGYSNVGFQNEENFLENENTS GNNSIRSRRAVQSREHTNTKQDEEQVTV E

Helix 1

NupC
hCNT1 EAAPKPFPSRWRNLQPALRR-----SFCREHMQLFRWIGTGLLCTGLSAFLLVA
hCNT2 GLGPSTYQR-RSRWPFASKAR-----SFCCKTHASLFFKKILLGLLCLAYAAAYLLAA
hCNT3 QDSPRNREHMEDDDEEMQOKGCLERRRYDTVC GFCRKHKTTLRHI I IWGILLAGYLVMVISA

Helix 2

NupC
hCNT1 CLLDFQRALALFVLT CVVLTFLGHRLLKRL LGPKLRRFLKPOGHPRLLLWFKRGLALAAAF
hCNT2 CILNFQRALALFVITCLVIFVLVHSFLKRL LGKKLTRCLKPPFENSRLRLWTKWVFAVLSL
hCNT3 CVLNFHRALPLFVITVA AIFVVDHLM AKYEHRIDEMLSPGRRLLNSHWFWLKWVWISS

Helix 3

NupC
hCNT1 LGLVLWLSLDT SQR--PEQLV SFGAGICVFIALLLFACSKKHHC AVSWWRAVVSWGGLGLQFVFG
hCNT2 VGLILWLALD TAQR--PEQLIPFAGICMFLILFACSKKHHS AVSWWRAVVSWGGLGLQFVFG
hCNT3 LVLA VIFWLA FDTAKLGQQQLV SFGGLIMYIVL LFLFSKYPTRVYWWRFV LWGIGLQFVFG

Helix 4

NupC
hCNT1 WFFENS DVS LGFVKGFS EMFEKLLGFANE C TN FVFGS NDQGLAE F FFLKVLCP IIVFISAL
hCNT1 LLVIRTEP GFIAFEWLG EQIRIFLLSYTKA C S S S FVFG EALVKD--VFAFQVLP IIVFISCV
hCNT2 ILVIRTDL GYTFVFWLGS QVQIFLLNYTVA C S S S FVFG DTLVKD--VFAFQVLP IIVFISCV
hCNT3 LLIRTD DPCFI AFDWLG RQVQTF LEYTDAGAS FVFG EKYKD H--VFAFQVLP IIVFISCV

Helix 5

NupC
hCNT1 GFLQHIRVLPV LIRAI GFLLSKVN C MGK L E S F N A V S S L I L G Q S E N F I A Y K D I L G K I S R N
hCNT1 EVHV VMTGGYAT IAGSLLGAYISFGIDAT S L I A A S V M A A P C A L A L S K L V Y P E V E E S K F R R
hCNT2 V S L L Y Y L G L V Q W V V O K V A W F Q I T M G T T A T E T L A V A G N I F V S M T E A P L L I R P Y I G D M T L S
hCNT3 M S M L Y Y L G L M Q W L I R K V W I M L V T T G S S P I E S V V A S G N I F V S Q T E S P L L V R P Y L P Y I T K S

Helix 6

NupC
hCNT1 RMYTMAATAM S F V S M S I V G A Y M T M L E P K - Y V V A A L V L N M F S T F I V L S L V I N F Y R V D A S E E N
hCNT1 EVHV VMTGGYAT IAGSLLGAYISFGIDAT S L I A A S V M A A P C A L A L S K L V Y P E V E E S K F R R
hCNT2 E I H A V M T G G F A T I S G T V L S A P I A F G V D A S S L I S A S V M A A P C A L A S S K L A Y P P P E V E E S K F K S
hCNT3 E L H A I M T A G F S T I A G S V L G A Y I S F G V P S S H L L T A S V M S A P A S L A A A K L F W P P E T E K P K I T L

Helix 7

NupC
hCNT1 I Q M S N L H E G - - D S F F E M L G E Y I L A G F K V A I I V A A M L I G E I A T I A A L N A L F A T V T G W F G Y -
hCNT1 E E G V K L T Y G D A C S L I E A A S T G A A I S V K V A N I A A N L I A E L A V L D F I N A A L S W L G D M V D I Q
hCNT2 E E G V K L P R G K E R N V L E A A S N G A V D A I G L A T N V A A N L I A E L A V L A F I N A A L S W L G E L V D I Q
hCNT3 K N A M K M E S G D S G N L L E A A T Q G A S S S I S L V A N I A V N L I A E L A L L S F M S A L S W F G N M F D Y P

Helix 8

NupC
hCNT1 S I S F Q G F L G Y I F Y P I A W V M G V P S S E A L Q V G S I M A T K L V S N E F V A M M P L Q K I A S T - - - -
hCNT1 G L S F Q L I C S Y L R F V A F L M G V A W E D C P V V A E L L G I K I F L N E F V A Y Q D L S K Y K Q R R L A G A E
hCNT2 G L T F Q V I C S Y L L R P M V F M M G V E W T D C P M V A E M V G I K E F I N E F V A Y Q Q L S O Y K N K R L S G M E
hCNT3 Q L S F E L I C S Y L R F M P F S F M G V E W Q D S F M V A R L I G Y E T F F N E F V A Y E H S K W I H L R K E G G P

Helix 9

NupC
hCNT1 -----L S P R A E G I I S V F L V S F A N F S S I G I I A G A V K G L N E E Q G N V V S R F G L K L V Y G S
hCNT1 E W V G R K Q W I S V R A E V L T T F A L C G F A N F S S I G I M L G L T S M V P Q R K S D F S Q I V L R A L F T G
hCNT2 E W I E G K Q W I S V R A B I T T F S L C G F A N D S S I G I T L G L T S I V P H R K S D L S K V V R A L F T G
hCNT3 K F V N G V Q Q Y I S I R S E I L A T Y A L C G F A N I G S L G I V I G L T S M A P S R R K R D I A S G A V R A L I A G

Helix 10

NupC
hCNT1 M L V S V L S A S I A A L V L * * *
hCNT1 A C V S L V N A C M A G I L Y - - M P R G A E V D C M S L L h T T L S S S S F E I Y Q C C R E A F Q S - - - - V N P
hCNT2 A C V S L I S A C M A G I L Y - - V P R G A E A D C V S F P n t S F I n R T Y E T Y M C C R G L F Q S T S L n G T N P
hCNT3 T V A C F M T A C T A G I L S S T P V D I N C H H V L E N A F n S T F P G n T T K V I A C C Q S L S S T V A K G P G E

Helix 11

NupC
hCNT1 -----E F S P E A L D N C C R F Y n H T I C A Q -----
hCNT2 P S F S G P W E D K E F S A M A L T N C C G F Y n R T V C A -----
hCNT3 V I P G G - - - - n H S L Y S L K G C C T L L n P S T F N C N G I S N T F

Helix 12

NupC
hCNT1 -----E F S P E A L D N C C R F Y n H T I C A Q -----
hCNT2 P S F S G P W E D K E F S A M A L T N C C G F Y n R T V C A -----
hCNT3 V I P G G - - - - n H S L Y S L K G C C T L L n P S T F N C N G I S N T F

Helix 13

NupC
hCNT1 -----E F S P E A L D N C C R F Y n H T I C A Q -----
hCNT2 P S F S G P W E D K E F S A M A L T N C C G F Y n R T V C A -----
hCNT3 V I P G G - - - - n H S L Y S L K G C C T L L n P S T F N C N G I S N T F

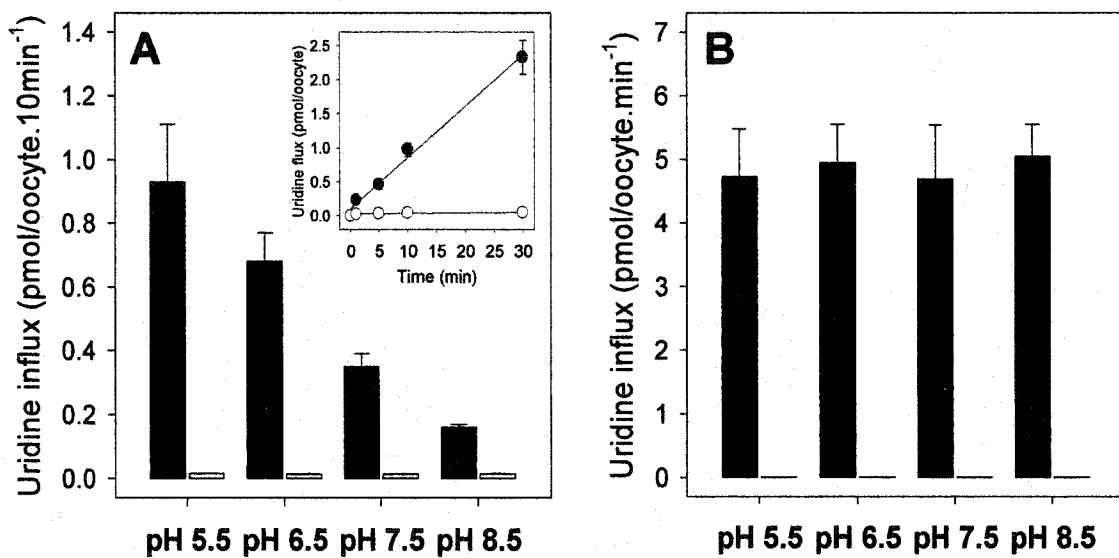


Figure 6-2. Effect of external pH on NUPC- and rCNT1-mediated uridine influx. Uptake of [³H]uridine in oocytes injected with NupC (*panel A*) or rCNT1 (*panel B*) RNA transcripts (*solid bars*) or water alone (*open bars*) was measured in transport medium containing 100 mM NaCl at pH 5.5, 6.5, 7.5 or 8.5 and uridine concentrations of 1 μ M (20°C, 10 min flux) and 10 μ M (20°C, 1 min flux) for NupC and rCNT1, respectively. *Insert*, time course of uridine uptake (1 μ M, 20°C) in NaCl transport medium at pH 5.5 by oocytes were injected with NupC RNA transcript (*solid circles*) or water (*open circles*) and incubated for 5 days at 18°C in MBM. Each value represents the mean \pm S.E. of 10-12 oocytes.

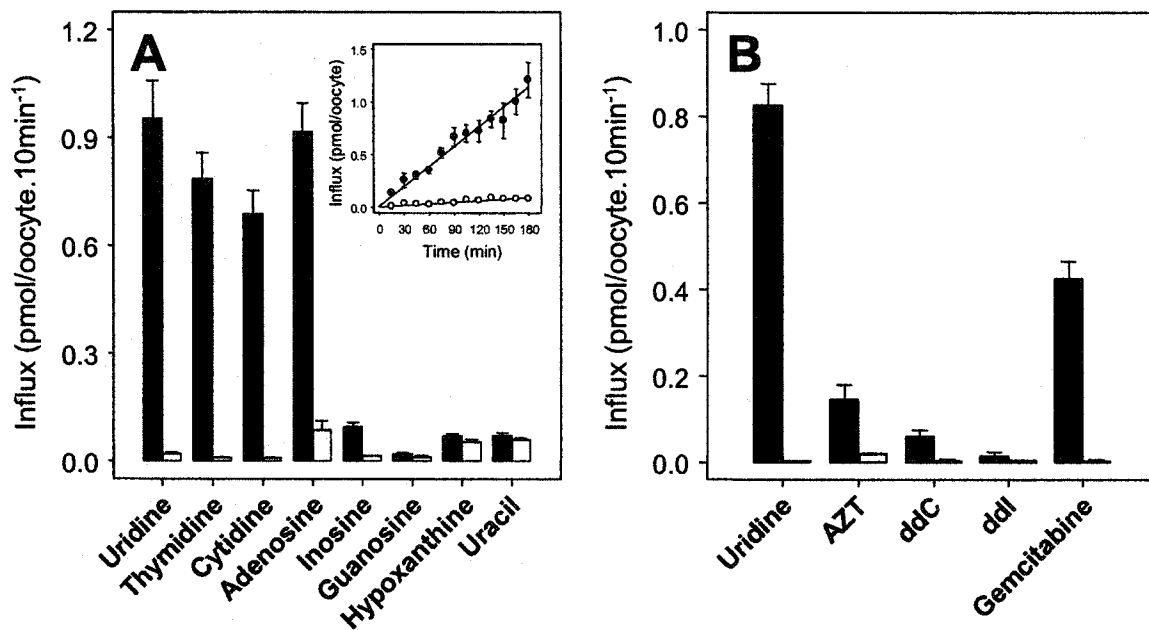
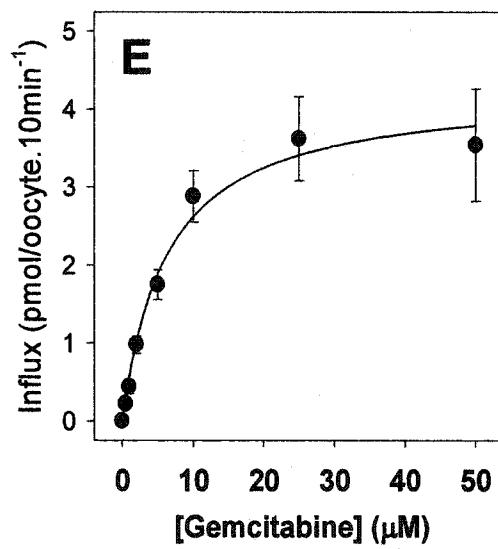
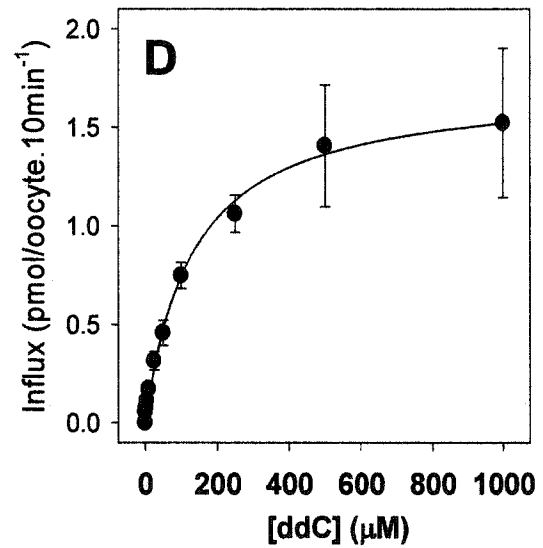
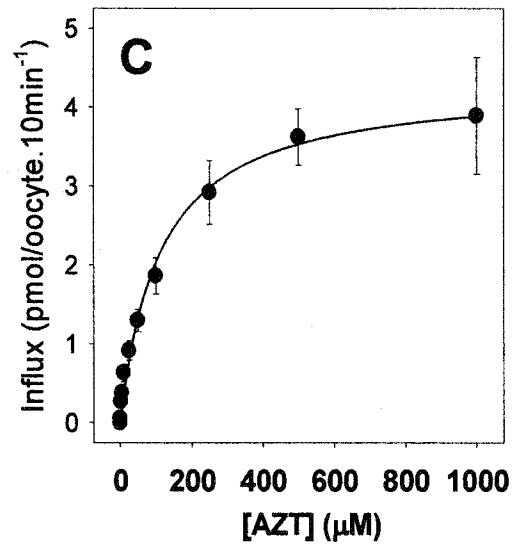
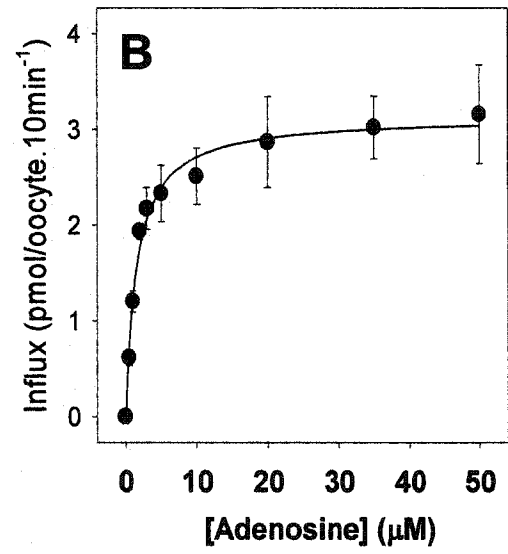
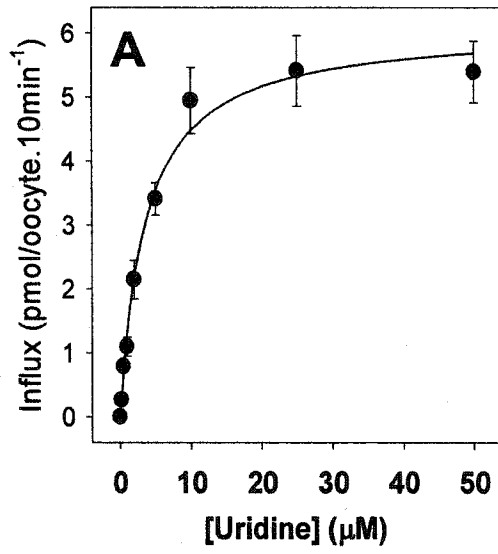


Figure 6-3. Substrate selectivity and drug transport by NupC. *A*, Influx of physiological nucleosides and nucleobases (1 μ M, 20°C, 10-min) was measured in NaCl transport medium at pH 5.5 in oocytes previously injected with NupC RNA transcripts (*solid bars*) or water alone (*open bars*). Insert, time courses of uridine uptake (1 μ M, 20°C) in NaCl transport medium at pH 5.5 by oocytes injected with NupC RNA transcripts (*solid circles*) or water (*open circles*). *B*, Fluxes of uridine and nucleoside drugs (AZT, ddC, ddI, gemcitabine) (1 μ M, 20°C, 10-min) were measured in NaCl transport medium at pH 5.5 in oocytes injected with NupC RNA transcripts (*solid bars*) or water alone (*open bars*). Each value represents the mean \pm S.E. of results obtained with 10-12 oocytes.

Figure 6-4. Kinetic properties of recombinant NupC. *A-E*, initial rates of nucleoside uptake (10-min fluxes, 20°C) in oocytes injected with NupC RNA transcript or water alone and were measured in transport medium containing 100 mM NaCl at pH 5.5. Values represent influx of NupC-injected oocytes minus the corresponding influx in water-injected cells. Kinetic parameters from these data are presented in *Table 6-1*.



Bibliography

- Baldwin SA, Mackey JR, Cass CE, and Young JD** (1999) Nucleoside transporters: molecular biology and implications for therapeutic development. *Mol Med Today* 5: 216-224.
- Che M, Ortiz DF, and Arias IM** (1995) Primary structure and function expression of a cDNA encoding the bile canalicular, purine-specific Na⁺-nucleoside cotransporter. *J Biol Chem* 270: 13596-13599.
- Cheeseman CI, Mackey JR, Cass CE, Baldwin SA, and Young JD** (2000) Molecular mechanism of nucleoside and nucleoside drug transport. In *Gastrointestinal Transport*. (Barrett KE and Donowitz M, eds.) pp. 330-379, Academic Press, San Diego.
- Craig JE, Zhang Y, and Gallagher MP** (1994) Cloning of the *nupC* gene of *Escherichia coli* encoding a nucleoside transport system, and identification of an adjacent insertion element, IS 186. *Mol Microbiol* 11: 1159-1168.
- Dresser MJ, Gerstin KM, Gray AT, Loo DD, and Giacomini KM** (2000) Electrophysiological analysis of the substrate selectivity of a sodium-coupled nucleoside transporter (rCNT1) expressed in *Xenopus laevis* oocytes. *Drug Metab Dispos* 28: 1135-1140.
- Friedman S** (1982) Bactericidal effect of 5-azacytidine on *Escherichia coli* carrying *EcoRII* restriction-modification enzymes. *J Microbiol* 151: 262-268.
- Hamilton SR, Yao SY, Ingram JC, Hadden DA, Ritzel MW, Gallagher MP, Henderson PJ, Cass CE, Young JD, and Baldwin SA** (2001) Subcellular distribution and membrane topology of the mammalian concentrative Na⁺-nucleoside cotransporter rCNT1. *J Biol Chem* 276: 27981-27988.
- Hohmann I, Bill RM, Kayingo I, and Prior BA** (2000) Microbial MIP channels. *Trends Microbiol* 8: 33-38.
- Huang QQ, Yao SY, Ritzel MW, Paterson ARP, Cass CE, and Young JD** (1994) Cloning and functional expression of a complementary DNA encoding a mammalian nucleoside transport protein. *J Biol Chem* 269: 17757-17760.
- Karp PD, Riley M, Saier M, Paulsen IT, Paley S, and Pellegrini-Toole A** (2002) The EcoCyc Database. *Nucleic Acids Res* 30: 56-58.
- Kirchman D, Ducklow H, and Mitchell R** (1982) Estimates of bacterial growth from changes in uptake rates and biomass. *Appl Environ Microbiol* 44: 1296-1307.
- Komatsu Y, and Tanaka K** (1972) A showdomycin-resistant mutant of *Escherichia coli* K-12 with altered nucleoside transport character. *Biochim Biophys Acta* 34: 891-899.
- Kubitschek HE** (1968) Constancy of uptake during the cell cycle in *Escherichia coli*. *Biophys J* 8: 1401-1412.

- Liman ER, Tytgat J, and Hess P** (1992) Subunit stoichiometry of a mammalian K⁺ channel determined by construction of multimeric cDNAs. *Neuron* 9: 861-871.
- Loewen SK, Ng AM, Yao SY, Cass CE, Baldwin SA, and Young JD** (1999) Identification of amino acid residues responsible for the pyrimidine and purine nucleoside specificities of human concentrative Na⁺ nucleoside cotransporters hCNT1 and hCNT2. *J Biol Chem* 274: 24475-24484.
- Lostao MP, Mata JF, Larrayoz IM, Inzillo SM, Casado FJ, and Pastor-Anglada M** (2000) Electrogenic uptake of nucleosides and nucleoside-derived drugs by the human nucleoside transporter 1 (hCNT1) expressed in *Xenopus laevis* oocytes. *FEBS Lett* 481: 137-140.
- Mackey JR, Yao SYM, Smith KM, Karpinski E, Cass CE, and Young JD** (1999) Gemcitabine transport in *Xenopus* oocytes expressing recombinant plasma membrane mammalian nucleoside transporters. *J Natl Cancer Inst* 21: 1876-1881.
- Mamber SW, Brookshire KW, and Forenza S** (1990) Induction of the SOS response in *Escherichia coli* by azidothymidine and dideoxynucleosides. *Antimicrob Agents Chemother* 34:1 237-1243.
- Monno R, Marcuccio L, Valenza MA, Leone E, Bitetto C, Larocca A, Maggi P, and Quarto M** (1997) *In vitro* antimicrobial properties of azidothymidine (AZT). *Acta Microbiol Immunol Hung* 44: 165-171.
- Munch-Petersen A, Mygrind B, Nicolaisen A, and Pihl NJ** (1979) Nucleoside transport in cells and membrane vesicles from *Escherichia coli* K12. *J Biol Chem* 254: 3730-3737.
- Munch-Petersen A, and Mygrind B** (1983) Transport of nucleic acid precursors. In *Metabolism of Nucleotides, Nucleosides, Nucleobases in Microorganisms*. Munch-Petersen A (ed.), pp. 259-305, Academic Press, London.
- Mygrind B, and Munch-Petersen A** (1975) Transport of pyrimidine nucleosides in cells of *Escherichia coli* K12. *Eur J Biochem* 59: 365-372.
- Norholm MH, and Dandanell G** (2001) Specificity and topology of the *Escherichia coli* xanthosine permease, a representative of the NHS subfamily of the major facilitator superfamily. *J Bacteriol* 183: 4900-4904.
- Nieweg A, and Bremer E** (1997) The nucleoside-specific Tsx channel from the outer membrane of *Salmonella typhimurium*, *Klebsiella pneumoniae* and *Enterobacter aerogenes*: functional characterization and DNA sequence analysis of the *tsx* genes. *Microbiology* 143: 603-15.
- Ritzel MWL, Yao SYM, Huang MY, Elliot JF, Cass CE, and Young JD** (1997) Molecular cloning and functional expression of cDNAs encoding a human Na⁺-nucleoside cotransporters hCNT1. *Am J Physiol* 272: C707-C714.
- Ritzel MWL, Yao SYM, Ng AML, Mackey, JR, Cass CE, and Young JD** (1998) Molecular cloning and functional expression and chromosomal localization of a cDNA encoding a human Na⁺ nucleoside cotransporter (hCNT2) selective for purine nucleosides and uridine. *Mol Membr Biol* 15: 203-211.

- Ritzel MWL, Ng AML, Yao SYM, Graham K, Loewen SK, Smith KM, Ritzel RG, Mowles DA, Carpenter P, Chen X-Z, Karpinski E, Hyde RJ, Baldwin SA, Cass CE, and Young JD (2000)** Molecular identification and characterization of novel human and mouse concentrative Na⁺-nucleoside cotransporters proteins (hCNT3 and mCNT3) broadly selective for purine and pyrimidine nucleosides. *J Biol Chem* 276: 2914-2927.
- Robak T (2001)** Cladribine in the treatment of chronic lymphocytic leukemia. *Leuk Lymphoma* 40: 551-564.
- Sanders C, Perez EA, and Lawrence HJ (1992)** Opportunistic infections in patients with chronic lymphocytic leukemia following treatment with fludarabine. *Am J Hematol* 39: 314-315.
- Seeger C, Poulsen C, and Dandanell G (1995)** Identification and characterization of genes (*xapA*, *xapB*, and *xapR*) involved in xanthosine catabolism in *Escherichia coli*. *Bacteriol* 177: 5506-5516.
- Stuhmer W (1998)** Electrophysiologic recordings from *Xenopus* oocytes. *Methods Enzymol* 293: 280-300.
- Wang J, Su SF, Dresser MJ, Schaner ME, Washington CB, and Giacomini KM (1997)** Na⁺-dependent purine nucleoside transporter from human kidney: cloning and functional characterization. *Am J Physiol* 273: F1058-F1065.
- Weeks D, Eskandari S, Scott DR, and Sachs G (2000)** A H⁺-gated urea channel: the link between *Helicobacter pylori* urease and gastric colonization. *Science* 287: 482-485.
- Westh Hansen SE, Jensen N, and Munch-Petersen A (1987)** Studies on the sequence and structure of the *Escherichia coli* K-12 *nupG* gene, encoding a nucleoside-transport system. *Eur J Biochem* 168: 385-391.
- Wolters M, Madeja M, Farrell AM, and Pongs O (1999)** *Bacillus stearothermophilus* LctB gene gives rise to functional K⁺ channels in *Escherichia coli* and in *Xenopus* oocytes. *Receptors Channels* 6: 477-491.
- Xiao G, Wang J, Tangen T, and Giacomini KM (2001)** A novel proton-dependent nucleoside transporter, CeCNT3, from *Caenorhabditis elegans*. *Mol Pharmacol* 59: 339-348.
- Yao SYM, Ng, AML, Ritzel, MWL, Gati, WP, Cass CE, and Young JD (1996a)** Transport of adenosine by recombinant purine- and pyrimidine-selective sodium/nucleoside cotransporters from rat jejunum expressed in *Xenopus laevis* oocytes. *Mol Pharmacol* 50: 1529-1535.
- Yao SYM, Cass CE, and Young JD (1996b)** Transport of antiviral nucleoside analogs 3'-azido-3'-deoxythymidine and 2',3'-dideoxycytidine by a recombinant nucleoside transporter (rCNT1) expressed in *Xenopus* oocytes. *Mol Pharmacol* 50: 388-393.
- Yao SYM, Cass CE, and Young JD (2000)** The *Xenopus* oocyte expression system for the cDNA cloning and characterization of plasma membrane transport proteins. In *Membrane Transport. A Practical Approach*. (Baldwin SA, ed.) pp 47-78, Oxford University Press, Oxford.

Yao SYM, Ng AML, Loewen SK, Cass CE, Baldwin SA, and Young JD (2002) An ancient marine pre-vertebrate Na⁺/nucleoside cotransporter (hfcNT) from the Pacific hagfish (*Eptatretus stouti*). *Am J Physiol* 283: C155-C168.

CHAPTER VII: *

Functional characterization of a H⁺/nucleoside cotransporter (CaCNT) from *Candida albicans*, a fungal member of the concentrative nucleoside transporter (CNT) family of membrane proteins. **

* *A version of this chapter has been submitted for publication.*

Loewen SK, Ng AML, Mohabir NN, Baldwin SA, Cass CE, and Young JD (2002) *Mol Microbiol* (submitted).

** All of the contents of this chapter are my own work.

Introduction

Nucleoside transporters (NTs) are specialized integral membrane proteins that mediate cellular uptake and release of nucleosides and nucleoside analog drugs (Griffith and Jarvis, 1996; Mackey *et al.*, 1998). In higher organisms (humans and rodents), nucleoside transport is mediated by members of the ENT (equilibrative, Na⁺-independent) and CNT (concentrative, Na⁺-dependent) protein families (Baldwin *et al.*, 1999; Cheeseman *et al.*, 2000; Hyde *et al.*, 2001). Two ENT and three CNT functional isoforms have been identified. Human (h) and rat (r) ENT1 and ENT2 transport pyrimidine and purine nucleosides and are distinguished functionally by differences in sensitivity to inhibition by nitrobenzylthioinosine (NBMPR) and vasoactive drugs, and by the ability of hENT2 and rENT2 to also transport nucleobases (Griffiths *et al.*, 1997a, 1997b; Yao *et al.*, 1997; Crawford *et al.*, 1998; Yao *et al.*, 2002a). CNT1 and CNT2 both transport uridine and adenosine, but are otherwise selective for pyrimidine (hCNT1 and rCNT1) and purine (hCNT2 and rCNT2) nucleosides (Huang *et al.*, 1994; Che *et al.*, 1995, Yao *et al.*, 1996a; Wang *et al.*, 1997; Ritzel *et al.*, 1997, 1998). hCNT3, its mouse (m) ortholog mCNT3 and a close relative from *Eptatretus stouti*, an ancient marine pre-vertebrate, transport both pyrimidine and purine nucleosides (Ritzel *et al.*, 2001; Yao *et al.*, 2002b). The relationships of these proteins to transport processes defined by functional studies are: ENT1 (*es*), ENT2 (*ei*), CNT1 (*ci*), CNT2 (*cif*) and CNT3 (*cib*).

Although ENTs are widely distributed in lower eukaryotes, they appear to be absent from prokaryotes. A number of ENT family members have recently been identified and functionally characterized from parasitic protozoa, including TgAT from *Toxoplasma gondii* (Chiang *et al.*, 1999), the P1- and P2-type transporters TbNT2 and TbAT1 from *Trypanosoma brucei* (Maser *et al.*, 1999; Sanchez *et al.*, 1999), LdNT1.1 from *Leishmania donovani* (Vasudevan *et al.*, 1998) and PfENT1 from *Plasmodium falciparum* (Carter *et al.*, 2000; Parker *et al.*, 2000). In contrast to their mammalian counterparts, at least some of the protozoan ENT family members appear to function as active transporters, catalyzing the symport of nucleosides with protons (de Koning and Diallinas, 2000; Carter *et al.*, 2000). PfENT1, like human and rat ENT2 also functions as a nucleobase transporter (Parker *et al.*, 2000). Unlike ENTs, CNTs are present in both eukaryotes and prokaryotes. CNTs from lower eukaryotes and prokaryotes that have been characterized

functionally include CeCNT3 from *Caenorhabditis elegans* (Xiao *et al.*, 2001) and NupC from *Escherichia coli* (Craig *et al.*, 1994; Loewen *et al.*, 2002). Both use protons as the coupling cation.

In yeast, most functional studies of nucleoside transport have focused on *Saccharomyces cerevisiae*, and little information is available on pathogenic species such as *Candida albicans* (Horák, 1997). At the molecular level, two different *S. cerevisiae* NTs have been identified and characterized (Vickers *et al.*, 2000). FUI1, a member of the uracil/allantoin permease family of transporters, exhibits high selectivity for uracil-containing ribonucleosides and imports uridine across cell-surface membranes. FUN26, a member of the ENT protein family, has a broad nucleoside selectivity and most probably functions to transport nucleosides across intracellular vacuolar membranes. FUN26 mRNA is most abundant during M phase of the cell cycle (Spellman *et al.*, 1998), suggesting a possible role in vacuolar release of nucleosides for nucleic acid synthesis during cell division. As is also the case in parasitic protozoa, no CNTs are present in the *S. cerevisiae* genome.

In *C. albicans*, nucleoside transport is complex. Although only one *C. albicans* NT (NUP), a member of the NUP protein family (Detke, 1998), has been characterized so far, BLAST searches of the Stanford *C. albicans* genome sequence databank revealed at least four more putative NT proteins of which one of these (derived from Contig6-1709 and Contig6-2474) shows sequence similarity to the CNTs. In this report, we describe the molecular cloning of the cDNA encoding this *C. albicans* CNT, designated CaCNT, and its heterologous expression in oocytes of *Xenopus laevis*. In addition, CaCNT was shown to mediate H⁺-coupled influx of physiological purine nucleosides and uridine, as well as various cytotoxic nucleoside analogs, including cordycepin, which has potent antifungal activity in preclinical model systems when used in combination with an inhibitor of adenosine deaminase (Sugar and McCaffrey, 1998).

Materials and Methods

Molecular Cloning of CaCNT – BLAST searches of the *C. albicans* genome database (Stanford Genome Technology Center) found an 1827-bp sequence from Contig6-1709 with 33% and 26% identity to hCNT1 and *E. coli* NupC, respectively. PCR was performed on *C. albicans* cDNA obtained from stationary and logarithmic growth phases (Library-in-a-Tube™, BIO 101) using oligonucleotides flanking the open reading frame of the *C. albicans* genomic

CNT sequence: 5'-ATGGTTTCTCCGTCACAGATAAAGC-3' (sense primer; corresponding to nucleotide positions 1427-1452 of Contig6-1709); and 5'-CTAGTTAATGTGGAAAGTGTTTAAATC-3' (antisense; primer corresponding to nucleotide positions 3227-3253 of Contig6-1709). PCR-ready tubes containing *C. albicans* single-stranded cDNA (prepared from 0.2 µg of total RNA) were used according to the manufacturer specifications, except that the PCR-ready mixture (0.2 ml) was diluted 5-fold before PCR amplification. The reaction mixture (30 µl) contained 10 mM Tris-HCl (pH 8.0), 50 mM KCl, 1.5 mM MgCl₂, 0.01 % (w/v) gelatin, 1 µl diluted *C. albicans* cDNA, 50 pmol of each primer and 0.5 units of *Taq*/Deep Vent DNA polymerase (100:1) and was pipetted into a 0.5 ml centrifuge tube and layered with 30 µl of mineral oil to prevent evaporation. Amplification for 1 cycle at 95°C for 10 min, 56°C for 1 min and 72°C for 1 min 50 sec, 35 cycles at 95°C for 1 min, 57°C for 1 min and 72°C for 1 min 50 sec, and 72°C for 10 min (RoboCycler™96 temperature cycler, Stratagene) produced a ~1.8 kb product of the predicted size from logarithmically growing cells that was ligated into the PCR vector pGEM-T (Promega), then subcloned into the enhanced *Xenopus* expression vector pGEM-HE (pCaCNT-HE) (Liman *et al.*, 1992). By providing additional 5'- and 3'- untranslated regions from a *Xenopus* β-globin gene flanking the multiple cloning site, the pGEM-HE construct gave greater functional activity than the pGEM-T construct and was used in the subsequent transport characterization of the yeast protein. The 1827 bp pCaCNT-HE insert was sequenced in both directions by *Taq* DyeDeoxyterminator cycle sequencing using an automated model 373A DNA Sequencer (Applied Biosystems). In PCR experiments under identical conditions with two separate preparations of *C. albicans* cDNA from stationary growth phase cells, no product was obtained.

Functional Production of CaCNT in *Xenopus* Oocytes – Plasmid pCaCNT was digested with *NbeI* and transcribed with T7 RNA polymerase mMMESSAGE MACHINE™ *in vitro* transcription system (Ambion). Healthy stage VI *Xenopus* oocytes were injected (Inject+Matic System) with 20 nl of CaCNT RNA transcript (1 ng/nl) or 20 nl of water alone and incubated at 18°C in MBM for 3 days with a daily change of medium before the assay of transport activity (Huang *et al.*, 1994; Ritzel *et al.*, 1997; Yao *et al.*, 2000).

CaCNT Radioisotope Flux Studies – Transport was traced using the appropriate $^3\text{H}/^{14}\text{C}$ -labeled nucleoside or nucleoside drug (Moravek Biochemicals, Brea, CA or Amersham Pharmacia Biotech) at a concentration of 1 mCi/ml or 2 mCi/ml for ^{14}C - and ^3H -labeled compounds, respectively. Flux measurements were performed at room temperature (20 °C) as described previously (Huang *et al.*, 1994; Ritzel *et al.*, 1997; Yao *et al.*, 2000) on groups of 12 oocytes in 200 μl of transport medium containing either 100 mM NaCl or 100 mM choline chloride and 2 mM KCl, 1 mM CaCl_2 , 1 mM MgCl_2 , and 10 mM HEPES (pH 5.5, 6.5, 7.5 or 8.5). Unless otherwise indicated, the permeant concentration was 20 μM . Transport medium for adenosine uptake experiments contained 1 μM deoxycoformycin to inhibit adenosine deaminase activity. To maximize potential transmembrane H^+ -gradients, cells were first washed into pH 7.5 NaCl or choline chloride transport medium and only exposed to either high (pH 8.5) or low (pH 5.5 or 6.5) pH medium immediately prior to the assay of transport activity. At the end of the incubation, extracellular radioactivity was removed by six rapid washes in the appropriate ice-cold transport medium. Individual oocytes were dissolved in 0.5 ml of 1% (w/v) sodium dodecyl sulphate (SDS) for quantitation of oocyte-associated ^3H or ^{14}C by liquid scintillation counting (LS 6000IC, Beckman Canada Inc.). The flux values shown are the means \pm S.E. of 10-12 oocytes from one representative experiment. Significant differences in mean flux values were determined by Student's t-test ($P = 0.05$). Each experiment was performed at least twice on different batches of cells. Kinetic (K_m and V_{\max}) parameters \pm S.E. were determined using ENZFITTER software (Elsevier-Biosoft, Cambridge, UK). We have previously established that oocytes lack endogenous nucleoside transport activity (Yao *et al.*, 2000).

Measurements of CaCNT-induced H^+ Currents – Membrane currents were measured at room temperature using the whole-cell, two-electrode voltage clamp technique (CA-1B oocyte clamp, Dagan Corp.). The microelectrodes were filled with 3 M KCl and had resistances that ranged from 0.5 to 1.5 M Ω . The CA-1B was interfaced to a dedicated computer via a Digidata 1200B A/D converter and controlled by Axoscope software (Axon Instruments). Current signals were filtered at 20 Hz (four-pole Bessel filter) at a sampling interval of 50 msec. For data presentation, the signals were further filtered at 10 Hz by use of pCLAMP software (Axon Instruments). Following microelectrode penetration, resting

membrane potential was measured over a 15 min period prior to the start of the experiment. Oocytes exhibiting an unstable membrane potential or a low membrane potential of less than -30 mV were discarded. Individual oocytes exhibiting good resting membrane potentials were clamped at -50 mV and current measurements were sampled in transport media of the same composition used in the radiolabeled isotope transport assays. During the course of data collection, the permeant-free transport medium perfusing the oocyte was changed to one containing nucleoside at a concentration of 100 μ M. After ~ 60 s, this was exchanged with fresh medium lacking the test nucleoside substrate.

H⁺:Nucleoside Coupling Ratios – CaCNT H⁺:nucleoside stoichiometry was determined by radiotracer transport-induced current measurements under voltage-clamp conditions in transport medium containing [³H]-labeled uridine (200 μ M, 2 mCi/ml). Individual oocytes were placed in a perfusion chamber and voltage-clamped at a holding potential of -50 mV in permeant-free choline chloride transport medium at pH 5.5 for a 10 min period to monitor baseline currents. The transport medium was then exchanged with medium of the same composition containing radiolabeled uridine and current was measured for 3 min followed immediately by reperfusion with permeant-free transport medium until current returned to baseline. The oocyte was recovered from the chamber and solubilized with 1% SDS for liquid scintillation counting. The total movement of charge across the plasma membrane was calculated from the current-time integral and correlated with the measured radiolabeled flux for each oocyte to calculate the charge:flux ratio. [³H]-Labeled uridine uptake in control water-injected oocytes was used to correct for basal uptake of uridine over the same incubation period. The coupling ratios (\pm S.E.) presented were determined from 10 individual oocytes.

Results and Discussion

Yeast exhibit marked differences in nucleoside transport capability. For example, *S. cerevisiae* transports only uridine (Horák, 1997), whereas the opportunistic pathogen *C. albicans* is permeable to both pyrimidine and purine nucleosides (Rao *et al.*, 1983; Fasoli and Kerridge, 1990). Two NT proteins, FUI1 and FUN26, have been identified in *S. cerevisiae* (Vickers *et al.*, 2000) and characterized functionally by reintroduction into NT-deficient *S. cerevisiae* (FUI1) or production in oocytes of *Xenopus laevis* (FUN26). FUI1 corresponds to the uridine-specific NT

present in the *S. cerevisiae* plasma membrane and is a member of the uracil/allantoin permease family of transporters. FUN26 is a homolog of mammalian ENTs and resides mostly in intracellular membranes of *S. cerevisiae*. In *Xenopus* oocytes, sufficient recombinant FUN26 reached the plasma membrane to demonstrate that it functions as a broadly selective transporter for pyrimidine and purine nucleosides (Vickers *et al.*, 2000). Based upon functional studies of native transporters in intact yeast (Losson *et al.*, 1978), FUI1 may be H⁺-coupled, although this has not been demonstrated for the recombinant protein. Recombinant FUN26 is not H⁺-dependent (Vickers *et al.*, 2000). The one NT protein characterized so far in *C. albicans*, NUP, is unrelated to FUI1 or FUN26 and is a member of the NUP transporter family (Detke, 1998). Characterized functionally in transformed *S. cerevisiae*, NUP transports purine nucleosides and, perhaps, thymidine, but not uridine (Detke, 1998). There is no information available on cation coupling for NUP.

I undertook BLAST searches of the *C. albicans* genomic database to search for other putative NT proteins. The analysis revealed *C. albicans* orthologs of FUI1 and FUN26, as well as a protein of 378 amino acid residues with 56% sequence identity to NUP. A fourth putative NT (derived from Contig6-1709 and Contig6-2474) showed sequence similarity to mammalian CNT proteins. Here, we describe the molecular and transport properties of this new *C. albicans* CNT.

***C. albicans* contains a Mammalian/Bacterial CNT Homolog** – The sense and antisense oligonucleotide primers described in *Materials and Methods* were designed to encompass the open reading frame of the full-length CNT gene in *C. albicans* Contig6-1709 (Stanford *C. albicans* genome sequence database). While no PCR product was obtained from cells from stationary cultures, PCR amplification of *C. albicans* cDNA from logarithmically growing cells generated a cDNA of the correct size (1827 bp). This product was subcloned into the enhanced *Xenopus* expression vector pGEM-HE and sequenced. The encoded 608-amino acid residue protein, designated CaCNT (Fig. 7-1), contained 13 predicted transmembrane helices (TMs) and had a putative molecular weight of 67.7 kDa. CaCNT was 33% identical (44% similar) to hCNT1, 34% identical (46% similar) to hCNT2, 38% identical (49% similar) to hCNT3, and 26% identical (37% similar) to the bacterial H⁺/nucleoside transporter NupC, the latter protein having only 10 predicted TMs (corresponding to TMs 4-13 of the other CNTs)

(Hamilton *et al.*, 2001; Yao *et al.*, 2002a). The 13 TM membrane architecture of CaCNT is also predicted for *C. elegans* CeCNT3 (Hamilton *et al.*, 2001) and suggests that this membrane topology may be common to all eukaryotic CNTs.

The nucleotide and deduced amino acid sequences of CaCNT were nearly identical to those of the open reading frame of Contig6-1709 and to an incomplete CaCNT open reading frame corresponding to CaCNT amino acid residues 120-608 in Contig6-2474. Multiple sequence alignments revealed 10 single nucleotide differences between CaCNT and either Contig6-1709 or Contig6-2474, resulting in five single residue differences in predicted amino acid sequence at residues 328, 416, 418, 483 and 506 (Fig. 7-2). At each of the five positions, CaCNT was identical to one or other of the two Contigs. One of the five positions, residue 328 in CaCNT, corresponds to a critical amino acid residue in TM 7 of mammalian CNTs, identified by chimeric and mutagenesis studies to be involved in the selectivity of human CNT1/2 for pyrimidine and purine nucleosides (Loewen *et al.*, 1999). The presence of Gly at residue 328 in CaCNT compared to Ser in hCNT1 and Gly in hCNT2 is predictive of purine nucleoside selectivity (Loewen *et al.*, 1999). The codon of CaCNT residue 417 contained the only nucleoside sequence difference unique to CaCNT and not found in either contig (codon GAG in CaCNT *versus* codon GAA in Contig6-1709 and Contig6-2474). Both codons code for Glu. The most recent Stanford reconstruction of the *C. albicans* diploid genome (Assembly 19, May 2002) identifies the Contig6-1709/2474 sequence differences in Fig. 1B as polymorphic in origin. Corresponding differences between these contigs and the nucleotide and deduced amino acid sequences of our protein provides further evidence of allelic heterozygosity within the CaCNT gene.

CaCNT lacked the lengthy carboxyl-terminal tail containing multiple consensus sites for *N*-linked glycosylation found in its human counterparts. The extracellular location of the carboxyl-terminus has been confirmed by mutagenesis of rCNT1, which is glycosylated at Asn⁶⁰⁵ and Asn⁶⁴³ (Hamilton *et al.*, 2001). Despite its extracellular location, the carboxyl-terminal tail of hCNT1-3 contains multiple conserved Cys residues, suggesting possible involvement in intramolecular or intermolecular disulfide linkages. The absence of this carboxyl-terminal domain from CaCNT and NupC (Hamilton *et al.*, 2001) indicates that such linkages, if they occur, are not required for CNT functional activity. Sequence similarity between CaCNT and

human CNTs was most pronounced in TMs 4-9 and in TMs 11-12, with an average sequence identity of 52% (61% similar) within these transmembrane helices. In contrast, N-terminal domains, including TMs 1-3, were markedly more divergent. Truncated constructs of human and rat CNT1 with TMs 1-3 removed have been shown to maintain functionality, identifying the TM 4-13 region (TMs 1-10 in NupC) as the core functional unit of the CNT family of proteins (Hamilton *et al.*, 2001).

Since we first identified rCNT1 from rat jejunum by expression cloning in *Xenopus* oocytes (Huang *et al.*, 1994), more than 80 members of the CNT protein family have been identified by cDNA cloning and genome sequencing projects. At present, 14 CNT proteins have been characterized functionally, and their phylogenetic relationships are illustrated in Fig. 7-3. CaCNT is positioned on a separate branch distinct from *E. coli* NupC, *C. elegans* CeCNT3, *E. stouti* hfCNT and the CNT members from mammals. Sequence homology searches of incomplete fungi genome databases with CaCNT identified one other putative CNT nucleoside transport protein in *Aspergillus fumigatus* (derived from TIGR_5085, GenBank™ database). The predicted open reading frame of the *A. fumigatus* CNT exhibited 54% sequence identity (65% similarity) with CaCNT. In comparison, CaCNT shares only 32% sequence identity with CeCNT3, suggesting that yeast CNT members may comprise a separate CNT subfamily from CNTs from prokaryotes and other eukaryotes.

Functional Production of CaCNT in *Xenopus* Oocytes – A representative time course of [¹⁴C]uridine uptake (20 μM, 20°C) measured in acidified NaCl transport medium at pH 5.5 in oocytes injected with CaCNT RNA transcripts or water alone is shown in Fig. 7-4. Uptake in CaCNT-producing oocytes was linear with time for 60 min. After 30 min, the uridine flux was 45 ± 6 pmol/oocyte, which was 50-fold higher than that of control water-injected oocytes (0.9 ± 0.2 pmol/oocyte). The latter value was similar to that observed in choline chloride transport medium at pH 5.5, consistent with CaCNT functioning as a H⁺/nucleoside symporter (data not shown). Subsequent kinetic experiments to determine apparent K_m and V_{max} values for different CaCNT permeants used a 5-min uptake interval to measure initial rates of nucleoside uptake (influx). In some experiments, radioisotope studies of CaCNT nucleoside and nucleoside drug specificity were performed using a 30-min uptake interval to maximize detection of weakly transported CaCNT permeants.

Permeant Selectivity of Recombinant CaCNT – Fig. 7-5A shows a representative transport experiment in *Xenopus* oocytes that measured CaCNT-mediated uptake of a panel of radiolabeled pyrimidine and purine nucleosides (20 μM , 20°C) in NaCl medium at pH 5.5. CaCNT-mediated transport was calculated as uptake in RNA transcript-injected oocytes minus uptake in control water-injected oocytes. CaCNT-producing oocytes transported all purine nucleosides tested (adenosine, inosine, guanosine). Although uridine was also a good CaCNT permeant, no significant transport was detected for other pyrimidine nucleosides (cytidine, thymidine), suggesting a *cif*-like transport profile similar to that of hCNT2 and rCNT2 (Che *et al.*, 1995, Yao *et al.*, 1996a; Wang *et al.*, 1997; Ritzel *et al.*, 1998). The purine nucleobase hypoxanthine was also not transported, suggesting that CaCNT functions exclusively as a nucleoside transport protein. Lowering the extracellular H^+ concentration by increasing the transport medium pH from 5.5 to 8.5 reduced the uridine uptake by 79% (Fig. 7-5A).

Kinetic Properties – Fig. 7-6 shows representative concentration dependence curves in NaCl medium at pH 5.5 for uridine, adenosine, guanosine, and inosine influx in CaCNT-producing oocytes, compared to corresponding control fluxes in water-injected oocytes. Kinetic parameters (apparent K_m and V_{max}) derived from the CaCNT-mediated transport data, which were consistent with simple Michaelis-Menten kinetics, are presented in Table 7-1. Apparent K_m values varied between 16 and 64 μM (adenosine < uridine < inosine, guanosine) and were in the same range as values obtained previously for recombinant mammalian CNT proteins (Huang *et al.*, 1994; Che *et al.*, 1995; Yao *et al.*, 1996a; Ritzel *et al.*, 1997; Wang *et al.*, 1997; Ritzel *et al.*, 1998, 2001). V_{max} values varied between 9.6 and 43.3 pmol/oocyte.5min⁻¹ (adenosine < uridine, inosine, guanosine), giving calculated $V_{max}:K_m$ ratios, a measure of transport efficiency, of 1.31 (uridine), 0.61 (adenosine), 0.58 (guanosine) and 0.69 (inosine). Therefore, at low permeant concentrations below the apparent K_m values, the different physiological CaCNT permeants, including adenosine, were transported at similar rates. The lower apparent K_m value for adenosine transport (15.7 μM) *versus* other nucleosides (33.0 - 64.3 μM) was consistent with adenosine having the smallest mediated flux in Fig. 7-5A (measured at a concentration of 20 μM). Since NUP is also purine nucleoside selective (Detke, 1998), *C. albicans* has at least two pathways for adenosine influx. Adenosine is a biologically important molecule in *C. albicans* and, through cyclic AMP and other adenosine-related metabolites, has

the potential to influence the dimorphic yeast-mycelium transition in *C. albicans* (Sabie and Gadd, 1992).

In contrast to the saturable nature of CaCNT-mediated transport of adenosine and the other nucleosides tested in Fig. 7-6, basal nucleoside influx in water-injected oocytes exhibited a linear concentration dependence, consistent with simple diffusion across the oocyte plasma membrane.

Nucleoside Drug Transport by Recombinant CaCNT – *Candida albicans* infections can be successfully treated with polyene antibiotics, azole derivatives, or 5-fluorocytosine, but continued emergence of drug-resistant strains of pathogenic yeast has prompted the search for new drug targets in the design of novel antifungal agents (St Georgiev, 2000). Nucleoside-based therapeutics offer one such alternative. Cordycepin (3'-deoxyadenosine), for example, when combined with adenosine deaminase inhibitors (coformycin or deoxycoformycin), has potent antifungal activity against invasive candidiasis from normal and fluconazole-resistant *Candida* isolates in mice (Sugar and McCaffrey, 1998). Because most nucleoside analog drugs cannot easily cross cell membranes by simple diffusion, transportability by NT-mediated processes is a potential determinant of cytotoxic efficacy of such compounds.

Previously, we have used *Xenopus* oocyte expression to establish that the mammalian CNT1/2/3 proteins transport a broad spectrum of antiviral and anticancer nucleoside analogs (Huang *et al.*, 1995, Yao *et al.*, 1996b; Ritzel *et al.*, 1997, 1998, 2001; Mackey *et al.*, 1999). hCNT1 and rCNT1, for instance, transport the antiviral drugs 3'-azido-3'-deoxythymidine (AZT) and 2',3'-dideoxycytidine (ddC), but not 2',3'-dideoxyinosine (ddI). hCNT2 transports only ddI, while hCNT3 and mCNT3 transport all three analogs. Purine (cladribine, fludarabine) and pyrimidine (5-fluorouridine, 5-fluoro-2'-deoxyuridine, zebularine, gemcitabine) nucleoside drugs, some of which are used in anticancer therapy, have also been shown to be CNT permeants. We therefore undertook experiments in *Xenopus* oocytes to measure CaCNT-mediated uptake of a panel of radiolabeled pyrimidine and purine nucleoside analog drugs. Uptake (20 μ M, 20°C) was measured in NaCl medium at pH 5.5 and compared with fluxes of uridine and inosine in the same batch of CaCNT-producing oocytes. As shown in Fig. 7-5B, CaCNT accepted purine nucleosides (cordycepin, ddI, fludarabine, cladribine) and uridine

analog drugs (5-fluorouridine, 5-fluoro-2'-deoxyuridine, zebularine) as permeants. Fluxes were lowest for cordycepin, fludarabine and cladribine, and highest for 5-fluorouridine and 5-fluoro-2'-deoxyuridine.

With the exception of 5-fluorouridine, the measured fluxes were smaller than those for uridine and inosine, and similar to those reported previously for hCNT2-mediated transport of ddI, 5-fluorouridine, fludarabine and cladribine in oocytes and transfected mammalian cells (Ritzel *et al.*, 1998; Lang *et al.*, 2001). CaCNT was, therefore, relatively tolerant of substitutions at the 2' (5-fluoro-2'-deoxyuridine, cladribine, fludarabine) and 3' (cordycepin, ddI) positions of the sugar, with significant import at micromolar concentrations. Substitution of the 5-H group (5-fluorouridine and 5-fluoro-2'-deoxyuridine) of the pyrimidine nucleobase moiety did not significantly affect uptake, although lack of the 4-OH group (zebularine) or the presence of halogens at the 2-position (cladribine, fludarabine) of the purine nucleobase moiety may have contributed to reduced transport activity. The demonstration that cordycepin is a low-level CaCNT permeant suggests that CaCNT may play a role in cytotoxic action of this compound against *C. albicans*. As with the parent nucleoside adenosine and some other nucleoside drugs such as AZT (Yao *et al.*, 1996a, 1996b), there was also substantial diffusive entry of cordycepin into oocytes. In the experiment shown in Fig. 3B, the control (non-mediated) flux in water-injected oocytes was 1.7 ± 0.2 pmol/oocyte.30min⁻¹ compared with 3.6 ± 0.7 pmol/oocyte.30min⁻¹ in RNA transcript-injected oocytes, giving a mediated flux of 1.9 ± 0.8 pmol/oocyte.30min⁻¹. The extent of the mediated uptake of cordycepin in *C. albicans* will depend on: (i) the level of the cell-surface abundance of CaCNT, and (ii) contributions from other *C. albicans* NTs.

CaCNT H⁺:Nucleoside Cotransport – *C. albicans* are dimorphic fungi that can exist in either yeast or hyphal forms, with the latter implicated in the virulence of systemic yeast infections (Odds, 1994). A number of environmental factors, including ambient pH, play a part in the transition between the two forms (Odds, 1985; Gow, 1997). Alkaline pH, for instance, promotes germ tube formation whereas acidic pH encourages yeast growth (Buchan and Gow, 1991). In yeast, protons are likely to be the preferred coupling ion for nutrient transport since a H⁺ electrochemical gradient is maintained by plasma membrane H⁺/ATPase (Monk *et al.*, 1991). In *C. albicans*, proton-pump inhibitors have been shown to inhibit germ tube formation,

favouring instead a period of extended yeast growth (Biswas *et al.*, 2001), presumably by reducing the alkalization of intracellular pH that normally precedes the yeast-hyphal transition (Kaur *et al.*, 1988; Kaur and Mishra, 1991a). More extensive blockage of H⁺/ATPase activity leads to cell death (Manavathu *et al.*, 1999). The presence of either native or environmental inwardly-directed H⁺ gradients are required to drive the H⁺-coupled nutrient transport systems that, in part, are necessary to support the accelerated growth and replication rates of *C. albicans* in its yeast form.

As shown in Fig. 7-7A, external application of pyrimidine and purine nucleosides (100 μM, Na⁺-containing medium, pH 5.5) to CaCNT-producing oocytes generated inward currents of 7-26 nA for adenosine, guanosine, inosine, and uridine, but not for thymidine or cytidine, consistent with the nucleoside selectivity profile presented in Fig 7-5A. No currents were seen in water-injected oocytes in transport medium of the same composition. In addition, there were no differences between uridine-induced currents measured in Na⁺-containing or Na⁺-free choline chloride media over the pH range 5.5-8.5 (Fig. 7-7B). Similarly, there was no effect when Li⁺ was substituted for Na⁺ (data not shown). Inward currents increased markedly as pH was lowered from 8.5 to 5.5, mirroring the pH-dependence of [¹⁴C]uridine uptake seen in Fig. 7-5A. Together, these findings established that CaCNT functions as a Na⁺-independent electrogenic H⁺/nucleoside symporter. The results of the Na⁺ replacement and pH-dependence experiments with *C. elegans* CeCNT3 (Xiao *et al.*, 2001) and *E. coli* NupC (Loewen *et al.*, 2002) suggest that these transporters are also strictly H⁺-dependent, which may represent a common characteristic of CNT proteins found in prokaryotes, as well as in yeast and other lower eukaryotes. In contrast, mammalian CNTs function predominantly as Na⁺-coupled nucleoside transporters, although recent electrophysiological studies in *Xenopus* oocytes have found that H⁺ and Li⁺ can substitute for Na⁺ for CNT3, but not for CNT1 or CNT2 (unpublished observation). Therefore, the CNT family includes members that are H⁺-dependent (CaCNT, CeCNT3, NupC), Na⁺-dependent (CNT1, CNT2), and Na⁺/H⁺ (and Li⁺)-dependent (CNT3). It is not uncommon for cation preference to vary within a single gene transporter family (Reizer *et al.*, 1994). For example, the melibiose transporter (MelB) of *E. coli* mediates uphill transport of melibiose coupled to Na⁺ or H⁺ (Botfield *et al.*, 1990), while that of *Klebsiella pneumoniae* couples sugar transport to H⁺ and Li⁺ (Hama *et al.*, 1992). Similarly,

mammalian SGLT1 and SGLT3 can utilize H⁺ or Li⁺ in addition to Na⁺ as the driving force for sugar transport, whereas SGLT2 is Na⁺-specific (Wright, 2001).

A Na⁺/nucleoside coupling ratio of 2:1 has been reported for system *cib* in choroid plexus and microglia (Wu *et al.*, 1992; Hong *et al.*, 2000), whereas coupling ratios of 1:1 have been described for various *cit* and *cif* transport activities in different mammalian cells and tissues (reviewed in Cass 1995). Similarly, Hill coefficients for Na⁺-activation of radiolabeled adenosine and uridine transport by recombinant CNTs in *Xenopus* oocytes were 2 for hCNT3 and mCNT3, and 1 for rCNT1 (Yao *et al.*, 1996b, Ritzel *et al.*, 2001). In the present study, we directly determined the H⁺/nucleoside coupling ratio of CaCNT by simultaneous measurement of H⁺ currents and [¹⁴C]uridine influx under voltage clamp conditions, as described previously for the SDCT1 rat kidney dicarboxylate transporter (Chen *et al.*, 1998). The results of the experiments presented in Fig. 7-8 demonstrated that CaCNT has a H⁺/nucleoside coupling ratio of 1:1 (the slope of the regression line \pm S.E. is 1.03 ± 0.02). Using the same technique, Na⁺/nucleoside coupling ratios of 2:1 and 1:1 have been confirmed for hCNT3 and hCNT1, respectively (unpublished data).

Conclusions – BLAST searches suggested that the *C. albicans* genome encodes putative NTs from at least four different protein families: (i) CaCNT from the CNT family, the topic of the present study, (ii) a homolog of *S. cerevisiae* FUN26 from the ENT family, (iii) a homolog of *S. cerevisiae* FUI1 from the uracil/allantoin transporter family, and (iv) NUP and an additional NUP-related protein from the NUP transporter family. The *S. cerevisiae* genome, which was fully sequenced in 1996 (Goffeau *et al.*, 1996), does not contain CNT or NUP representatives.

I obtained a PCR-amplified product corresponding to CaCNT from *C. albicans* logarithmically growing, but not stationary phase cells, suggesting that expression of the CaCNT gene may be differentially regulated in the two fungal forms. The characteristics of glucose transport (Cho *et al.*, 1994) and neutral and cationic amino acid transport (Kaur and Mishra, 1991b) also differ between the two fungal forms. Certain growth media may also contribute to differential in levels of transporter activity in the plasma membrane (Horak, 1997). Unlike intracellular *S. cerevisiae* FUN26, which displayed weak (~ 3-fold above background)

nucleoside transport activity in *Xenopus* oocytes, recombinant CaCNT mediated large fluxes, consistent with its function as a plasma membrane nucleoside transporter.

Recombinant CaCNT produced in oocytes was electrogenic, H⁺-dependent, and Na⁺- and Li⁺-independent. The H⁺/nucleoside coupling stoichiometry was demonstrated to be 1:1. None of the other identified fungal NTs (NUP, FUI1 and FUN26) have been demonstrated to be cation-coupled, making CaCNT the first described secondary-active nucleoside transporter of fungi. Although CNT proteins are widely distributed in eukaryotes (mammals, fish, insects and nematodes) and prokaryotes (Gram-negative and Gram-positive bacteria), CaCNT is the first CNT family member to be identified in fungi. CaCNT mediated high affinity transport of purine nucleosides and, unlike *C. albicans* NUP, also transported uridine. The transport profile of CaCNT is therefore similar to the *cif*-type (CNT2) transport processes characteristic of mammalian cells. The present experiments demonstrate the utility of the *Xenopus* oocyte heterologous expression system for functional comparisons between mammalian and fungal members of the CNT gene family expressed in the same membrane environment.

Like mammalian CNTs, CaCNT also transported nucleoside analog drugs with antiviral and anticancer activities. The present studies also demonstrated low but significant uptake of the antifungal nucleoside analog cordycepin. While the level of drug transport was low, the results demonstrated the potential involvement of CaCNT in antifungal nucleoside drug uptake. Future structure-function studies of recombinant CaCNT produced in *Xenopus laevis* oocytes therefore have the potential to identify new compounds with greater transportability and hence greater activity as antifungal agents. Since CaCNT is expected to be present in the replicative form of *C. albicans*, CaCNT represents a potential drug target for new antifungal pharmacologic therapies, either by development of CaCNT inhibitors that might impact growth or, as illustrated by cordycepin, by its utilization as a cellular uptake mechanism for antifungal nucleoside drugs. Infectious complications due to *Candida* species are frequent in the clinical care of a variety of immunocompromised individuals such as organ transplant recipients, AIDS and cancer patients, and the elderly (Walsh and Groll, 1999; Garber, 2001). Some human antineoplastic and antiviral nucleoside drugs have ancillary benefits as antibacterial agents (Friedman, 1982; Keith *et al.*, 1989; Monno *et al.*, 1997), and the same may also be possible in the case of fungal infections.

Table 7-1 – Kinetic Parameters of CaCNT-mediated Nucleoside Influx.

Substrate	Apparent K_m^a (μM)	V_{max}^a ($pmol/oocyte.5min^{-1}$)	Ratio, $V_{max}:K_m$
Adenosine	16 ± 3	9.6 ± 0.6	0.61
Uridine	33 ± 5	43.3 ± 2.7	1.31
Inosine	57 ± 8	39.7 ± 2.3	0.69
Guanosine	64 ± 6	37.8 ± 1.5	0.58

^a, from Fig. 7-4.

CaCNT - - - - - M V S P S T D K A P S I V E L T P E T Y Q Q D V S S D I D L E S G T K K L Q N E S A W Q S H E Y T T N I D
hCNT1 - - - - - M E N D P S R R R E S I S L T P V A K - - - - - G L E N M G A D F L E S L E E G G L P R S D I S P A E I R S S W S
hCNT2 - - - - - M E K A S G R - - - - - Q S I A L S T V E T - - - - - G T V N P G L E L M E - - - - - K E V E P E G S K R T D A G C H S L C D
hCNT3 M E L R S T A A P R A E G Y S N V G F Q N E E N F L E N E N T S G N N S I R S R A V Q S R E H T N T K Q D E E Q V T V E
NupC

Helix 1

CaCNT E T S S S N T A S K L T Y I Q K L K I R - - - - - F P Y Y R L A I D I F I G C C F F T A W W L S I V I Q
hCNT1 E A A P K P F P S R W R N L Q P A L R R A R - - - - - S F C R E H M Q L F R K W I I G T C L L L C T G L S A F L L V A
hCNT2 G L G F S T Y Q R - R S R W P F S K A R - - - - - S F C K T H A S L F K K I I L L G L L C L A Y A A Y L L A A
hCNT3 Q D S F R N R E H M E D D D E E M Q Q K G C L E R R Y D T V C G F C R K H K T T L R H I I W G I L L A G Y L V M V I S A
NupC

Helix 2

CaCNT P K H R H C W L I P T V I W G M I M V R L I T W H I K I L P W L L N K V K I V W D F F T G Y V Y K V L S K K Y Q R L I T
hCNT1 C L L D F C R A L A L F V L T C V V L T F L G H R L L K R - - - - - L L G P F L R R F L K P Q G H P - - - - - R L L L W F K R G L
hCNT2 C I L N F Q R A L A L F V I T C L V I F V L V H S F L K K - - - - - L L G K K L T R C L K P F E N S - - - - - R L R L W T K W V F
hCNT3 C V L N F H R A L D L F V I T V A A I F F V V W D H L M A - - - - - K Y E H R I D E M L S P G R R L L N S H W F W L K W V I
NupC

Helix 3

CaCNT G A V I T V G V I L L G T F V P S E T E Y S K R K D R A T S E F G C I V A I F I L F V T S K A F S K I N N N A V V G G M
hCNT1 A L A A F L G L V L W L S L D T S Q - - - - - R P E Q L V S E A G I C V F I A L L F A C S K H H C A V S W R A V S W G L
hCNT2 A G V S L V G L I L L W L A L D T A Q - - - - - R P E Q L T S E A G I C M F I L L F A C S K H H S A V S W R T V F S G L
hCNT3 W S S L V L A V I F W L A F D T A K L - - - - - G Q Q Q L V S E G G L I M Y I V L L F L F S K Y F T R V Y W R P V L W G I
NupC

Helix 4

Helix 5

CaCNT L M Q F I I A L F V L R T K C G Y D V F N F I S T L A R E L L G F A K D G V A F L T N K D V S Q L G - M F F F T V L F S
hCNT1 G L Q F V L G L L V I R T D P E P C F I A F E F W L G E Q I R I F L S Y T K A G S S F V F G E A L V K D - - - - - V F A P Q V L P I
hCNT2 G L Q F V F G I L V I R T D L G C F I A F D W L G R O V Q I E L N Y T V A G S S F V F G D T L V K D - - - - - V F A P Q A L P I
hCNT3 G L Q F L L G L L I L R T D P C F I A F D W L G R O V Q T E L E Y T D A S A S E - - - - - V F G E K Y K D H - - - - - V F A P K V L P I
NupC V I E V L L A W F F L N S D V C L G F V K G F S E M F E K L L G F A N E G T N E V F G S M N D Q G L A F F F L K V L C P

Helix 6

CaCNT V A F F V A F I H I W Y F G V I Q W A I R K F A Y E F F W T L R V S G A E A I T A A A S P F I C I G E S A T L I L R P D L
hCNT1 I V F F C V I S V L Y H V G L M Q W V I K I A W L M Q V T M G T T A T E T L S V A G N I F V S Q T E A P I L L I R P Y
hCNT2 I I F F C V V S L Y L G L M Q W V I R K V A W F L Q I T M G T T A T E T L A V A G N I F V C M T E A P L L I R P Y
hCNT3 V V F F S T V M S M L Y L G L M Q W I T R K V G W I M L V T T G S S P I E S V V S G N I F V C Q T E A S P L L V R P Y
NupC I V F I S A L I G H L Q H I R V L P V I T E A I G F L L S K V N G M G K L E S F N A V S S L I L G Q S E N F H A Y R D I

Helix 7

Helix 8

CaCNT M P Y L T F A E L H Q F M T S G F S T I S G A V I V G Y I G L G L N P Q A L V S S C V M S I F A S L A V S K L R Y P E L
hCNT1 L A D M T L S E V H V V M T G G Y A T I A G S L L G A V I S F G I D A T S L I A A S V M A A P C A L A L S K L V Y P E V
hCNT2 L G D N T L S E I H A V M T G G F A T I S G T V L G A F I A P G V D A S S L I S A S V M A A P C A L A S S K L A Y P E V
hCNT3 L P Y I T K S E L H A I M T A G F S T I A G S V L G A V I S F G V P S S H L L T A S V M S A P A S L A A A K L F W P E T
NupC L G K I S R N R M Y T M A A T A M S T V S M S I V G A Y M T M L E P K - Y V V A A L V L N M P S T F I V L S L I N P Y R

Helix 9

Helix 10

CaCNT E N E I S S G T V M I P K V E D S E A A R E K S K D E P Q N V L Q A F S N G A T L G L R I A G T M M I Q C M C I I G L V
hCNT1 E E S K F R R E E G V K L T Y G D A Q S L I E A A S T G A A I S V K V V A N I A A N L I A F L A V L D F I N A A A L S W L
hCNT2 E E S K F K S E E G V K L P R G K E R N V L E A A S N G A V D A I G L A T N V A A N L I A F L A V L A F I N A A L S W L
hCNT3 E K K I T L K N A M K M E S G D S G N L L E A A T Q G A S S I S L V A N I A V N L I A F L A L L S F M N S A L S W F
NupC V D A S E E N I Q M S N L H E G - - - - - Q S F F E M L G E Y I L A G F K V A I I V A A M L I G F I A L I A A L N A L F A T V

Helix 11

CaCNT A L C N G I L T W F G N Y W N I D H L T L E L I L S Y I F Y P I G F L L G T E R N E I L L V N K L L A Y K F I Q N E Y V
hCNT1 G D M V D I Q - - - - - G L S F Q L I C S Y I L R P V A F L M G V A W E D C P V V A E L L G I K L F L N E F V
hCNT2 G E L V D I Q - - - - - G L F Q V I C S Y I L R P M V F M M C V E W T D C P M V A E M V G I K F F I N E F V
hCNT3 G N M F D Y P - - - - - Q L S F E L I C S Y I F M S F S F M M G V E W Q D S F M V A R L G Y K T F F N E F V
NupC T G W F G Y - - - - - S I S F Q G I L G Y I F Y P I A W V M G V E S E A L Q V G S I M A T K L V S N E F V

Helix 12

CaCNT A Y N L E T N E A P Y N E - - - - - M S K R G T L I A T Y A C C G F A N L G S L G I T L G V E N T L T N
hCNT1 A Y Q D L S K Y K Q R R L A G A B E W V G N R K Q W I S V R A E V L T T F A L C G F A N F S S I G I M L G G L T S M V P
hCNT2 A Y Q Q L S Q Y K N K R L S G M E E W I E G E K Q W I S V R A E I I T T F S L C G F A N L S S I G I T L G G L T S I V P
hCNT3 A Y E H L S K W I H L R K E G G P K F V N G V Q Y I S I R S E I I A T Y A L C G F A N I G S L G I V I G G L T S M A P
NupC A N M D L Q K I A S T - - - - - L S P R A E G I I S V F L V S F A N F S S I G I I A C A V K G L N E

Helix 13

CaCNT N S R A K D I S S I I S A L F C G A I A T M L S A A I A G M V M H D L N T F H I N - - - - - * * *
hCNT1 Q R K S D F S Q I V L R A L F T G A C V S L V N A C M A G I L Y - - - - - M P R G A E V D C M S L L N T T L S S S S F E I Y
hCNT2 H R K S D L S K V V V R A L F T G A C V S L I S A C M A G I L Y - - - - - V P R G A E A D C V S F P N T S F T N R T Y E Y
hCNT3 S R K R I A S G A V R A L I A G T V A C F M T A C I A G I L S S T P V D I N C H H V L E N A F N S T F P G N T T K V I
NupC E Q G N V V S R F G L K L V Y G S T L V S V L S A S I A L V L - - - - -

CaCNT - - - - - * - - - - - * - - - - - *
hCNT1 Q C C R E A F Q S - - - - - V N P - - - - - E F S P E A L D N C C R F Y N H T I C A Q - - - - -
hCNT2 M C C R G L F Q S T S L N G T N P P S F S G P W E D K E F S A M A L T N C C G F Y N T V C A - - - - -
hCNT3 A C C Q S L L S S T V A K G P G E V I P G G - - - - - n H S L Y S L K G C C T L L n P S T F N C N G I S N T F
NupC

	<i>Residue number</i>								
	188	283	328	416	417	418	441	483	506
pCaCNT-HE	A (GCT)	T (TTT)	G (GGT)	S (TCT)	E (GAG)	A (GCA)	G(GGA)	I (ATA)	N (AAT)
Contig6-1709	A (GCT)	T (TTT)	S (AGT)	S (TCT)	E (GAA)	A (GCA)	G(GGA)	I (ATA)	N (AAT)
Contig6-2474	A (GCC)	T (TTC)	G (GGT)	P (CCT)	E (GAA)	E (GAA)	G(GGG)	M (ATG)	S (AGT)

Figure 7-2. Differences in deduced amino acid sequences of CaCNT and those derived from Contig6-1704 and Contig6-2474 (Stanford Genome Technology Center database). Nucleotide sequences encoding each amino acid residue are provided in *parentheses*. Amino acid residues and nucleotides common to CaCNT and one or both contigs are highlighted in *bold*. A possible strain difference or PCR-induced mutation is *boxed*.

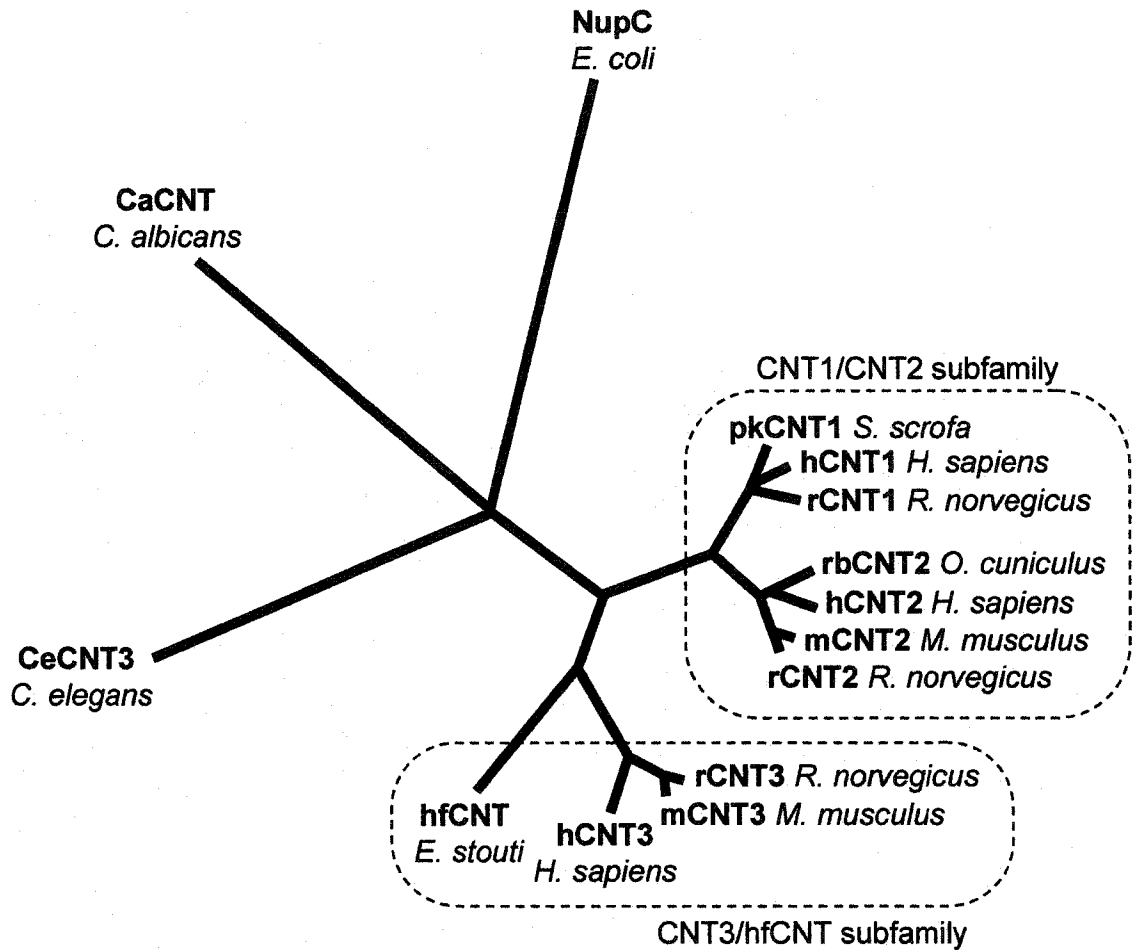


Figure 7-3. Phylogenetic tree showing relationships between CaCNT and other functionally characterized members of the CNT transporter family. In addition to those listed in *Figure 7-1A*, these are: rCNT1 (rat CNT1, GenBank™ accession number U10279); pkCNT1 (pig kidney CNT1, GenBank™ accession number AF009673); rCNT2 (rat CNT2, GenBank™ accession number U25055); mCNT2 (mouse CNT2, GenBank™ accession number AF079853); rbCNT2 (rabbit CNT2, GenBank™ accession number AF161716); hfCNT (hagfish CNT, GenBank™ accession number AF036109), mCNT3 (mouse CNT3, GenBank™ accession number AF305211) and rCNT3 (rat CNT3, GenBank™ accession number AY059414); and CeCNT3 (also known as F27E11.2, *Caenorhabditis elegans*, GenBank™ accession number AF016413). The phylogenetic tree was constructed from a multiple alignment of the 14 CNT sequences using ClustalX version 1.81 for Windows (Thompson *et al.*, 1997) and KITSCH, PHYLIP version 3.57c software (Felsenstein, 1989).

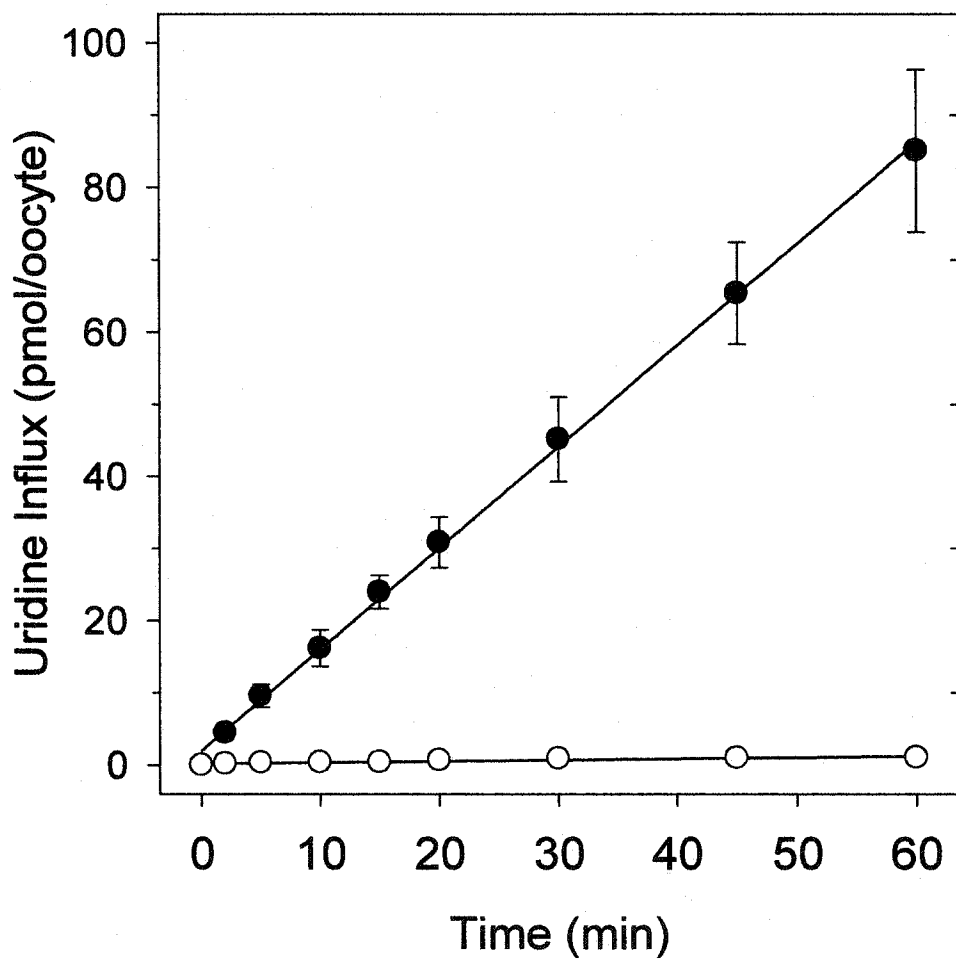


Figure 7-4. Time course of uridine uptake by recombinant CaCNT produced in *Xenopus* oocytes. Oocytes injected with 20 nl of water containing 20 ng of CaCNT RNA transcript were incubated for 3 days at 18°C in MBM (modified Barth's medium). Uptake of uridine (20 μ M, 20°C) was then measured in transport medium containing 100 mM NaCl, pH 5.5 (*solid circles*) and compared with uptake in NaCl medium by control oocytes injected with 20 nl of water alone (*open circles*). Each value is the mean \pm S.E. of 10-12 oocytes. Error bars are not shown where S.E. values were smaller than that represented by the symbols.

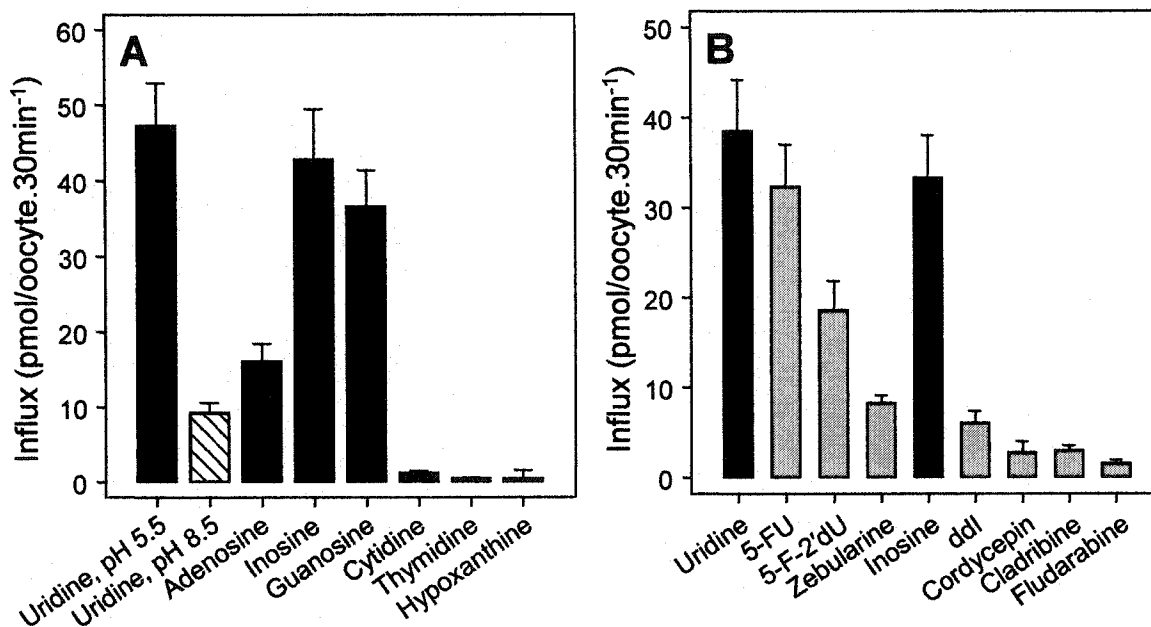


Figure 7-5. Substrate selectivity and drug transport by CaCNT. *A*, CaCNT-mediated nucleoside (uridine, adenosine, inosine, guanosine, cytidine and thymidine) and nucleobase (hypoxanthine) influx (20 μ M, 20°C, 30 min) was measured in transport buffer containing 100 mM NaCl, pH 5.5 (*solid bars*) or 100 mM NaCl, pH 8.5 (*batched bars*). *B*, CaCNT-mediated fluxes of nucleosides (uridine, inosine) (*solid bars*) and nucleoside drugs (5-FU, 5-fluorouridine; 5-F-2'dU, 5-fluoro-2'-deoxyuridine; zebularine, ddl, cordycepin, fludarabine, and cladribine) (*shaded bars*) (20 μ M, 20°C, 30 min) were measured in the transport medium containing 100 mM NaCl at pH 5.5. Mediated transport in *panels A* and *B* was calculated as uptake in RNA-injected oocytes minus uptake in oocytes injected with water alone. Each value represents mean \pm S.E. of 10-12 oocytes.

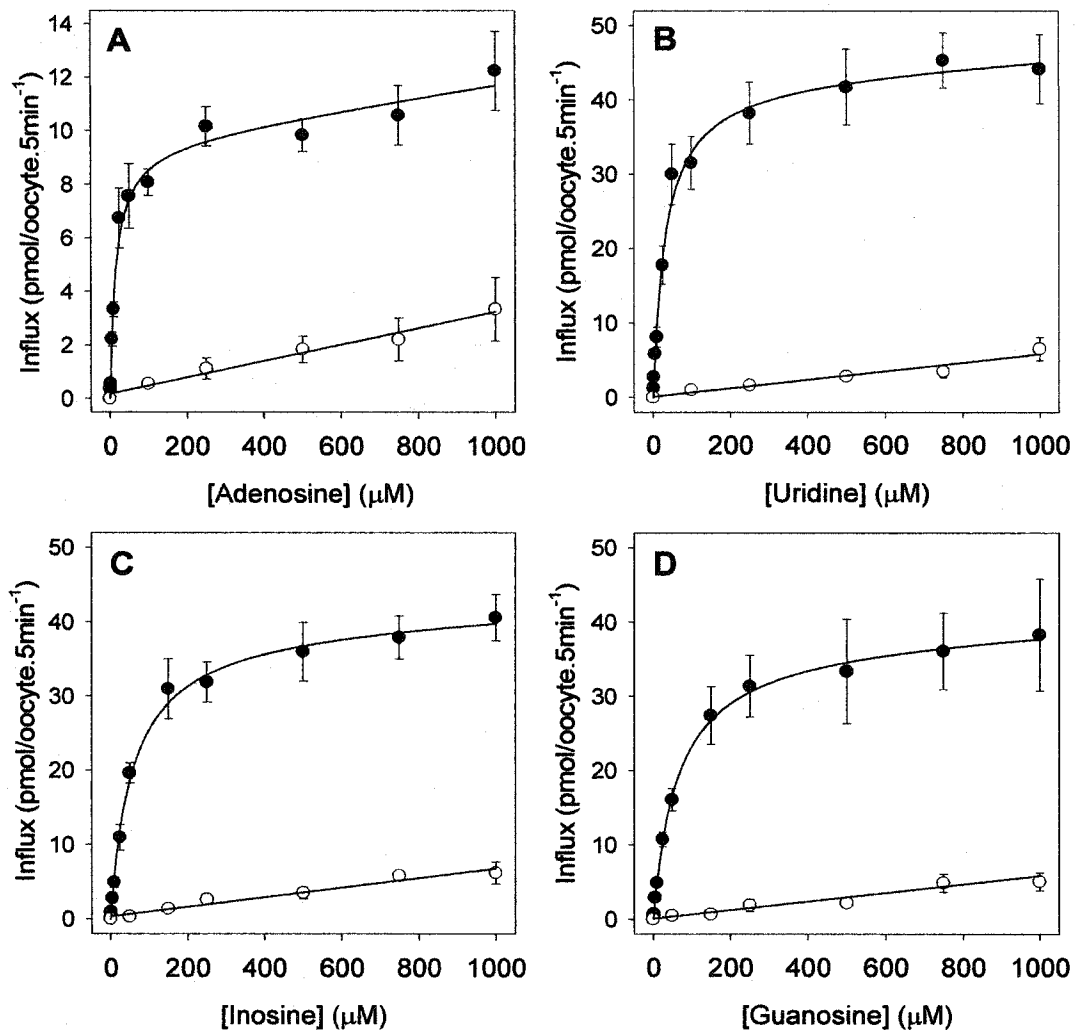
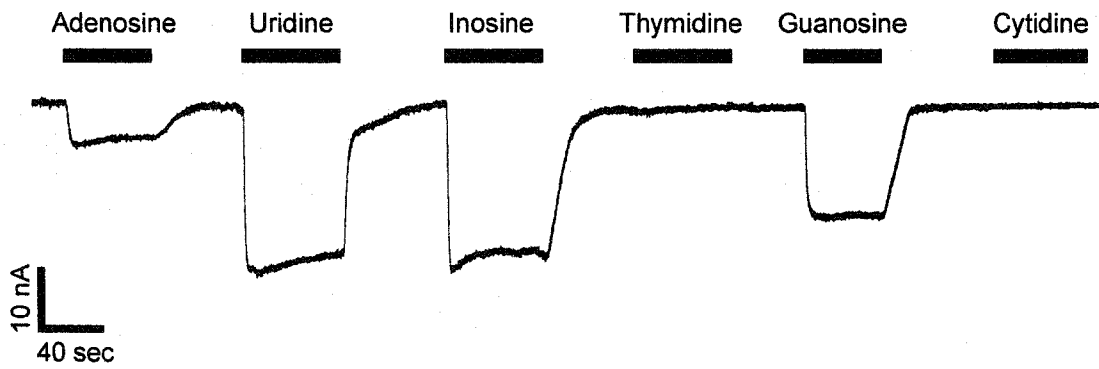
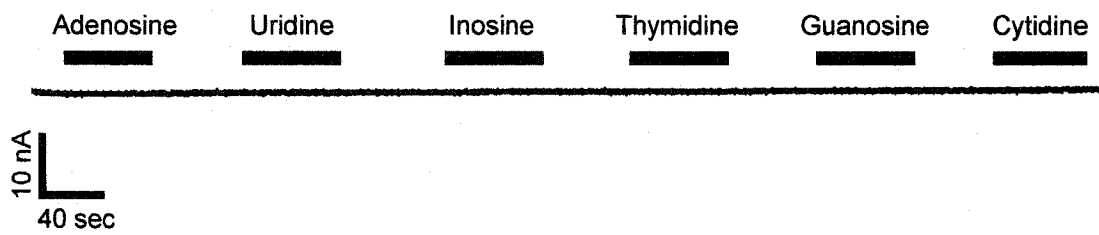
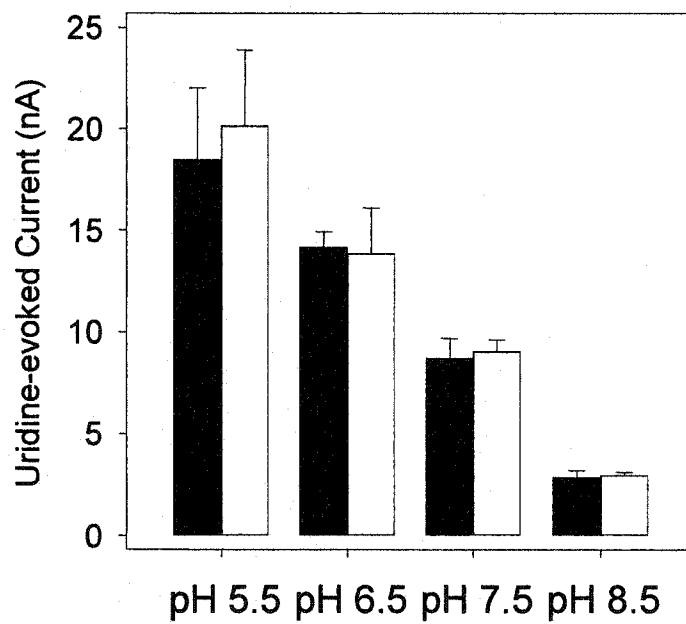


Figure 7-6. Kinetic properties of CaCNT. Initial rates of adenosine (A), uridine (B), inosine (C) and guanosine uptake (D) (5 min fluxes, 20°C) in oocytes injected with RNA transcript (solid circles) or water alone (open circles) were measured in transport medium containing 100 mM NaCl at pH 5.5. Kinetic parameters calculated from the mediated component of transport (uptake in RNA-injected oocytes *minus* uptake in oocytes injected with water alone) are presented in Table 7-1. Each value is the mean \pm S.E. of 10-12 oocytes. Error bars are not shown where S.E. values were smaller than that represented by the symbols.

Figure 7-7. Proton currents induced by exposure of recombinant CaCNT to nucleoside permeants. *A*, Current traces of a representative voltage-clamped CaCNT-producing oocyte (*upper panel*) or water-injected oocyte (*lower panel*) perfused at room temperature with NaCl transport medium at pH 5.5 containing different pyrimidine and purine nucleosides (100 μ M). A downward deflection of the current trace signifies an inward movement of positively-charged molecules. Nucleosides remain uncharged at pH 5.5. *B*, Uridine-evoked maximal currents generated by CaCNT-producing oocytes in transport medium containing either 100 mM NaCl (*black bars*) or 100 mM choline chloride (*open bars*) at pH 5.5, 6.5, 7.5 or 8.5. Each value is the mean \pm S.E. of 6 data sets produced from 6 individual oocytes tested in both Na⁺-containing and Na⁺-restricted media over the pH range 5.5-8.5.

A**CaCNT-producing oocytes****H2O-injected oocytes****B**

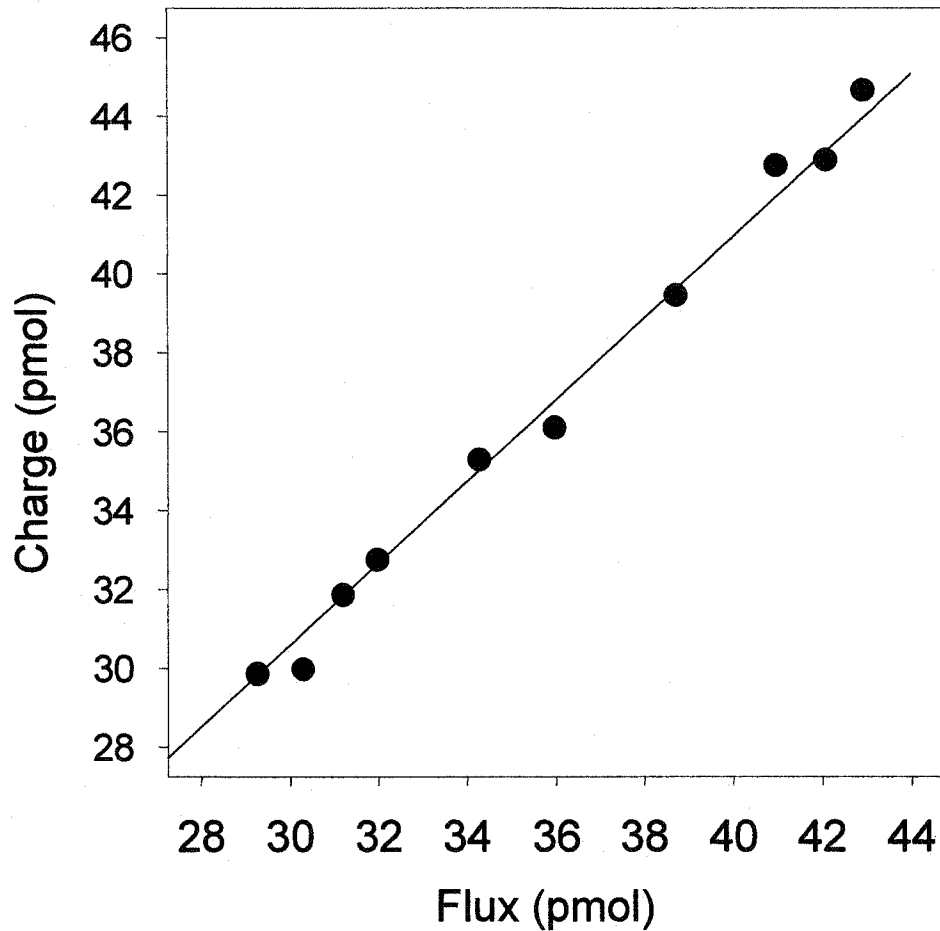


Figure 7-8. Stoichiometry of H⁺/uridine cotransport by recombinant CaCNT. Uridine-dependent charge and [³H]-uridine uptake were simultaneously determined at $V_m = -50$ mV in the presence of a proton gradient for 3 min. Integration of the uridine-evoked inward current with time was used to calculate the net cation influx by converting picocoulombs to picomoles using the Faraday constant. Mediated [³H]-uridine uptake was calculated as uptake in CaCNT-producing oocytes *minus* uptake in water-injected oocytes. Each data point represents a single oocyte.

Bibliography

- Baldwin, SA, Mackey, JR, Cass CE, and Young JD** (1999) Nucleoside transporters: molecular biology and implications for therapeutic development. *Mol Med Today* 5: 216-224.
- Biswas SK, Yokoyama K, Kamei K, Nishimura K, and Miyaji M** (2001) Inhibition of hyphal growth of *Candida albicans* by activated lansoprazole, a novel benzimidazole proton pump inhibitor. *Med Mycol* 39: 283-285.
- Botfield MC, Wilson DM, and Wilson TH** (1990) The melibiose carrier of *Escherichia coli*. *Res Microbiol* 141: 328-331.
- Buchan AD, and Gow NA** (1991) Rates of germ tube formation from growing and non-growing yeast cells of *Candida albicans*. *FEMS Microbiol Lett* 65: 15-18.
- Carter NS, Ben Mamoun C, Liu W, Silva EO, Landfear SM, Goldberg DE, and Ullman B** (2000) Isolation and functional characterization of the PfNT1 nucleoside transporter gene from *Plasmodium falciparum*. *J Biol Chem* 275: 10683-10691.
- Cass CE** (1995) Nucleoside transport. In *Drug Transport in Antimicrobial and Anticancer Chemotherapy*. (Georgopapadakou NH, ed.), pp. 404-451, Marcel Dekker, New York.
- Che M, Ortiz DF, and Arias IM** (1995) Primary structure and function expression of a cDNA encoding the bile canalicular, purine-specific Na⁺-nucleoside cotransporter. *J Biol Chem* 270: 13596-13599.
- Chen X-Z, Shayakul C, Berger UV, Tian W, and Hediger MA** (1998) Characterization of a rat Na⁺-dicarboxylate cotransporters. *J Biol Chem* 273: 20972-20981.
- Cheeseman CI, Mackey JR, Cass CE, Baldwin SA, and Young JD** (2000) Molecular mechanism of nucleoside and nucleoside drug transport. In *Gastrointestinal Transport*. (Barrett KE and Donowitz M, eds.) pp. 330-379, Academic Press, San Diego.
- Chiang CW, Carter N, Sullivan WJ Jr, Donald RG, Roos DS, Naguib FN, el Kouni MH, Ullman B, and Wilson CM** (1999) The adenosine transporter of *Toxoplasma gondii*. Identification by insertional mutagenesis, cloning, and recombinant expression. *J Biol Chem* 274: 35255-35261.
- Cho T, Hagihara Y, Kaminishi H, and Watanabe K** (1994) The relationship between the glucose uptake system and growth cessation in *Candida albicans*. *J Med Vet Mycol* 32: 461-466.
- Craig JE, Zhang Y, and Gallagher MP** (1994) Cloning of the *nupC* gene of *Escherichia coli* encoding a nucleoside transport system, and identification of an adjacent insertion element, IS 186. *Mol Microbiol* 11: 1159-1168.
- Crawford CR, Patel DH, Naeve C, and Belt JA** (1998) Cloning of a human equilibrative, nitrobenzylmercaptapurine riboside (NBMPR)-insensitive nucleoside transporter *ei* by functional expression in a transport-deficient cell line. *J Biol Chem* 273: 5288-5293.

- de Koning H, and Dhalluin G** (2000) Nucleobase transporters (review). *Mol Membr Biol* 17: 75-94.
- Detke S** (1998) Cloning of the *Candida albicans* nucleoside transporter by complementation of nucleoside transport-deficient *Saccharomyces*. *Yeast* 14: 1257-1265.
- Fasoli MO, and Kerridge D** (1990) Uptake of pyrimidines and their derivatives into *Candida glabrata* and *Candida albicans*. *J Gen Microbiol* 136: 1475-1481.
- Felsenstein J** (1989) Phylip-Phylogeny inference package (version 3.2). *Cladistics* 5: 164-166.
- Friedman S** (1982) Bactericidal effect of 5-azacytidine on *Escherichia coli* carrying *EcoRII* restriction-modification enzymes. *J Microbiol* 151: 262-268.
- Garber G** (2001) An overview of fungal infections. *Drugs* 61 Suppl 1: 1-12.
- Goffeau A, Barrell BG, Bussey H, Davis RW, Dujon B, Feldmann H, et al.** (1996) Life with 6000 genes. *Science* 274: 546, 563-567.
- Gow NA** (1997) Germ tube growth of *Candida albicans*. *Curr Top Med Mycol* 8: 43-55.
- Griffith DA, and Jarvis SM** (1996) Nucleoside and nucleobase transport systems of mammalian cells. *Biochim Biophys Acta* 1286: 153-181.
- Griffiths M, Beaumont N, Yao, SYM, Sundaram M, Bouman CE, Davies A, Kwong FYP, Coe IR, Cass CE, Young JD, and Baldwin SA** (1997a) Cloning of a human nucleoside transporter implicated in the cellular uptake of adenosine and chemotherapeutic drugs. *Nat Med* 3: 89-93.
- Griffiths M, Yao SYM, Abidi F, Phillips SEV, Cass CE, Young JD, and Baldwin SA** (1997b) Molecular cloning and characterization of a nitrobenzylthioinosine-insensitive (*et*) equilibrative nucleoside transporter from human placenta. *Biochem J* 328: 739-743.
- Hama H, and Wilson TH** (1992) Primary structure and characteristics of the melibiose carrier of *Klebsiella pneumoniae*. *J Biol Chem* 267: 18371-18376.
- Hamilton SR, Yao SYM, Ingram JC, Hadden DA, Ritzel MWL, Gallagher MP, Henderson PJF, Cass CE, Young JD, and Baldwin SA** (2001) Subcellular distribution and membrane topology of the mammalian concentrative Na⁺-nucleoside cotransporter rCNT1. *J Biol Chem* 276: 27981-27988.
- Hong M, Schlichter L, and Bendayan R** (2000) A novel zidovudine uptake system in microglia. *J Pharmacol Exp Ther* 292: 366-374.
- Horak J** (1997) Yeast Nutrient Transporters. *Biochim Biophys Acta* 1331: 41-79.
- Huang QQ, Yao SYM, Ritzel MWL, Paterson ARP, Cass CE, and Young JD** (1994) Cloning and functional expression of a complementary DNA encoding a mammalian nucleoside transport protein. *J. Biol. Chem.* 269: 17757-17760.

- Kaur S, Mishra P, and Prasad R** (1988) Dimorphism-associated changes in intracellular pH of *Candida albicans*. *Biochim Biophys Acta* 972: 277-282.
- Kaur S, and Mishra P** (1991a) Dimorphism-associated changes in plasma membrane H⁺-ATPase activity of *Candida albicans*. *Arch Microbiol* 156: 412-415.
- Kaur S, and Mishra P** (1991b) Amino acid uptake as a function of differentiation in *Candida albicans*: studies of a non-germinative variant. *FEMS Microbiol Lett* 66: 341-344.
- Keith BR, White G, and Wilson HR** (1989) In vivo efficacy of zidovudine (3'-azido-3'-deoxythymidine) in experimental gram-negative-bacterial infections. *Antimicrob Agents Chemother* 33: 479-483.
- Lang TT, Selner M, Young JD, and Cass CE** (2001) Acquisition of human concentrative nucleoside transporter 2 (hCNT2) activity by gene transfer confers sensitivity to fluoropyrimidine nucleosides in drug-resistant leukemia cells. *Mol Pharmacol* 60: 1143-1152.
- Loewen SK, Ng AML, Yao SYM, Cass CE, Baldwin SA, Young JD** (1999) Identification of amino acid residues responsible for the pyrimidine and purine nucleoside specificities of human concentrative Na⁺ nucleoside cotransporters hCNT1 and hCNT2. *J Biol Chem* 274: 24475-24484.
- Loewen SK, Yao SYM, Turner RJ, Weiner JH, Gallagher MP, Henderson PJF, Baldwin SA, Cass CE, and Young JD** (2002) Antiviral and antineoplastic nucleoside drug transport by recombinant *Escherichia coli* H⁺/nucleoside cotransporter (NupC) expressed in *Xenopus laevis* oocytes. *Mol Pharmacol* (submitted).
- Losson R, Jund R, and Chevallier MR** (1978) Properties of three distinct pyrimidine transport systems in yeast. Evidence for distinct energy coupling. *Biochim Biophys Acta* 513: 296-300.
- Mackey JR, Baldwin SA, Young JD, and Cass CE** (1998) Nucleoside transport and its significance for anticancer drug resistance. *Drug Resistance Updates* 1: 310-324.
- Mackey JR, Yao SYM, Smith KM, Karpinski E, Baldwin SA, Cass CE, and Young JD** (1999) Gemcitabine transport in *Xenopus* oocytes expressing recombinant plasma membrane mammalian nucleoside transporters. *J Natl Cancer Inst* 91: 1876-1881.
- Manavathu EK, Dimmock JR, Vashishtha SC, and Chandrasekar PH** (1999) Proton-pumping-ATPase-targeted antifungal activity of a novel conjugated styryl ketone. *Antimicrob Agents Chemother* 43: 2950-2959.
- Maser P, Sutterlin C, Kralli A, and Kaminsky R** (1999) A nucleoside transporter from *Trypanosoma brucei* involved in drug resistance. *Science* 285: 242-244.
- Monk BC, Kurtz MB, Marrinan JA, and Perlin DS** (1991) Cloning and characterization of the plasma membrane H⁺-ATPase from *Candida albicans*. *J Bacteriol* 173: 6826-6836.

- Monno R, Marcuccio L, Valenza MA, Leone E, Bitetto C, Larocca A, Maggi P, and Quarto M** (1997) *In vitro* antimicrobial properties of azidothymidine (AZT). *Acta Microbiol Immunol Hung* 44: 165-171.
- Odds FC** (1985) Morphogenesis in *Candida albicans*. *Crit Rev Microbiol* 12: 45-93.
- Odds FC** (1994) Pathogenesis of *Candida* infections. *J Am Acad Dermatol* 31: S2-5.
- Parker MD, Hyde RJ, Yao SYM, McRobert L, Cass CE, Young JD, McConkey GA, and Baldwin SA** (2000) Identification of a nucleoside/nucleobase transporter from *Plasmodium falciparum*, a novel target for anti-malarial chemotherapy. *Biochem J* 349: 67-75.
- Rao TV, Verma RS, and Prasad R** (1983) Transport of purine, pyrimidine bases and nucleosides in *Candida albicans*, a pathogenic yeast. *Biochem Int* 6: 409-417.
- Reizer J, Reizer A, and Saier MH Jr** (1994) A functional superfamily of sodium/solute symporters. *Biochim Biophys Acta* 1197:133-166.
- Ritzel MWL, Yao SYM, Huang MY, Elliot JF, Cass CE, and Young JD** (1997) Molecular cloning and functional expression of cDNAs encoding a human Na⁺-nucleoside cotransporters hCNT1. *Am J Physiol* 272: C707-C714.
- Ritzel MWL, Yao SYM, Ng AML, Mackey JR, Cass CE, and Young JD** (1998) Molecular cloning and functional expression and chromosomal localization of a cDNA encoding a human Na⁺ nucleoside cotransporter (hCNT2) selective for purine nucleosides and uridine. *Mol Membr Biol* 15: 203-211.
- Ritzel MWL, Ng AML, Yao SYM, Graham K, Loewen SK, Smith KM, Ritzel RG, Mowles DA, Carpenter P, Chen X-Z, Karpinski E, Hyde RJ, Baldwin SA, Cass CE, and Young JD** (2001) Molecular identification and characterization of novel human and mouse concentrative Na⁺-nucleoside cotransporters proteins (hCNT3 and mCNT3) broadly selective for purine and pyrimidine nucleosides (system *cit*). *J Biol Chem* 276: 2914-2927.
- Sabie FT, and Gadd GM** (1992) Effect of nucleosides and nucleotides and the relationship between cellular adenosine 3':5'-cyclic monophosphate (cyclic AMP) and germ tube formation in *Candida albicans*. *Mycopathologia* 119: 147-156.
- Sanchez MA, Ullman B, Landfear SM, and Carter NS** (1999) Cloning and functional expression of a gene encoding a P1 type nucleoside transporter from *Trypanosoma brucei*. *J Biol Chem* 274: 30244-30249.
- Spellman PT, Sherlock G, Zhang MQ, Iyer VR, Anders K, Eisen MB, Brown PO, Botstein D, and Futcher B** (1998) Comprehensive identification of cell cycle-regulated genes of the yeast *Saccharomyces cerevisiae* by microarray hybridization. *Mol Biol Cell* 9: 3273-3297.
- St Georgiev V** (2000) Membrane transporters and antifungal drug resistance. *Curr Drug Targets* 1: 261-284.

- Sugar AM, and McCaffrey RP (1998)** Antifungal activity of 3'-deoxyadenosine (cordycepin). *Antimicrob Agents Chemother* 42: 1424-1427.
- Thompson JD, Gibson TJ, Plewniak F, Jeanmougin F, and Higgins DG (1997)** The CLUSTAL_X windows interface: flexible strategies for multiple sequence alignment aided by quality analysis tools. *Nucleic Acids Res* 25: 4876-4882.
- Yao SYM, Ng AML, Ritzel MWL, Gati WP, Cass CE, and Young JD (1996a)** Transport of adenosine by recombinant purine- and pyrimidine-selective sodium/nucleoside cotransporters from rat jejunum expressed in *Xenopus laevis* oocytes. *Mol Pharmacol* 50: 1529-1535.
- Yao SYM, Cass CE, and Young JD (1996b)** Transport of antiviral nucleoside analogs 3'-azido-3'-deoxythymidine and 2',3'-dideoxycytidine by a recombinant nucleoside transporter (rCNT1) expressed in *Xenopus* oocytes. *Mol Pharmacol* 50: 388-393.
- Yao SYM, Ng AML, Muzyka WR, Griffiths M, Cass CE, Baldwin SA, and Young JD (1997)** Molecular cloning and functional characterization of nitrobenzylthioinosine (NBMPR)-sensitive (*es*) and NBMPR-insensitive (*ei*) equilibrative nucleoside transporter proteins (rENT1 and rENT2) from rat tissues. *J Biol Chem* 272: 28423-28430.
- Yao SYM, Cass CE, and Young JD (2000)** The *Xenopus* oocyte expression system for the cDNA cloning and characterization of plasma membrane transport proteins. In *Membrane Transport. A Practical Approach*. (Baldwin SA, ed.) pp. 47-78, Oxford, Oxford University Press.
- Yao SYM, Ng AML, Loewen SK, Cass CE, Baldwin SA, and Young JD (2002a)** An ancient marine pre-vertebrate Na⁺/nucleoside cotransporter (hfCNT) from the Pacific hagfish (*Eptatretus stouti*). *Am J Physiol* 283: C155-C168.
- Yao SYM, Ng AML, Sundaram M, Cass CE, Baldwin SA, and Young JD (2002b)** Functional and molecular characterization of nucleobase transport by recombinant human and rat ENT1 and ENT2 equilibrative nucleoside transport proteins: chimeric constructs reveal a role for the ENT2 helix 5-6 region in nucleobase translocation. *J Biol Chem* (in press).
- Vasudevan G, Carter NS, Drew ME, Beverley SM, Sanchez MA, Seyfang A, Ullman B, and Landfear SM (1998)** Cloning of Leishmania nucleoside transporter genes by rescue of a transport-deficient mutant. *Proc Natl Acad Sci U S A* 95: 9873-9878.
- Vickers MF, Yao SYM, Baldwin SA, Young JD, and Cass CE (2000)** Nucleoside transporter proteins of *Saccharomyces cerevisiae*. Demonstration of a transporter (FUI1) with high uridine selectivity in plasma membranes and a transporter (FUN26) with broad nucleoside selectivity in intracellular membranes. *J Biol Chem* 275: 25931-25938.
- Walsh TJ, and Groll AH (1999)** Emerging fungal pathogens: evolving challenges to immunocompromised patients for the twenty-first century. *Transpl Infect Dis* 1: 247-261.
- Wang J, Su SF, Dresser MJ, Schaner ME, Washington CB, and Giacomini KM (1997)** Na⁺-dependent purine nucleoside transporter from human kidney: cloning and functional characterization. *Am J Physiol* 273: F1058-F1065.

Wright EM (2001) Renal Na⁺-glucose cotransporters. *Am J Physiol Renal Physiol* 280: F10-F18.

Wu X, Yuan G, Brett CM, Hui AC, and Giacomini KM (1992) Sodium-dependent nucleoside transport in choroid plexus from rabbit. Evidence for a single transporter for purine and pyrimidine nucleosides. *J Biol Chem* 267: 8813-8818.

Xiao G, Wang J, Tangen T, and Giacomini KM (2001) A novel proton-dependent nucleoside transporter, CeCNT3, from *Caenorhabditis elegans*. *Mol Pharmacol* 59: 339-348.

CHAPTER IX:

General Discussion

The first objective of my research presented in this thesis was to use recombinant DNA technology in combination with heterologous expression in *Xenopus* oocytes to identify and characterize new members of the CNT protein family. As described in *Chapter IV*, I participated in the cDNA cloning and characterization of the human and mouse proteins responsible for *cib*-type nucleoside transport activity. This new protein, designated CNT3, and the previously identified CNT1 (system *cit*) and CNT2 (system *cif*) isoforms represent the three major concentrative transport processes found in human and other mammalian cells and tissues. In oocytes, human and mouse CNT3 exhibited broad permeant selectivity for purine and pyrimidine nucleosides, was insensitive to inhibition by NBMPR and dipyrindamole, and had a Na⁺:uridine coupling ratio of 2:1, consistent with *cib*-type activity reported by earlier cell and tissue uptake studies (Lee *et al.*, 1991; Wu *et al.*, 1992; Huang *et al.*, 1993; Lee *et al.*, 1994; Wu *et al.*, 1994; Washington *et al.*, 1995; Redlak *et al.*, 1996; Waclawski and Sinko, 1996; Hong *et al.*, 2000). Differences between CNT3 and the other two CNT isoforms include the narrower substrate specificities of CNT1 and CNT2 (pyrimidine nucleoside- and purine nucleoside-selective, respectively) and the 1:1 Na⁺:nucleoside stoichiometry of CNT1/2. CNT3, unlike CNT1/2, was also H⁺- (and Li⁺-) dependent. In contrast to Na⁺-coupled CNT3, H⁺-coupled CNT3 had a H⁺:uridine coupling ratio of 1:1 and did not appear to mediate transport of antiviral nucleoside drugs. In *Chapter V*, I was also part of a group effort to clone and characterize a CNT member from an ancient marine prevertebrate, the Pacific hagfish (*Eptatretus stouti*). hfCNT produced in oocytes was broadly selective for both purine and pyrimidine nucleosides, had a Na⁺:uridine coupling ratio of 2:1, and was more closely related to mammalian CNT3 proteins than to CNT1 or CNT2, thus forming a separate CNT3/hfCNT transporter subfamily (Figs. 1-7, 4-3, 5-2 and 7-3). Unlike mammalian CNT proteins, hfCNT had a much lower apparent affinity for Na⁺ (> 100 mM). Unlike the mammalian CNT3 isoform, hfCNT was not H⁺-dependent. In *Chapter VII*, I used sequence information derived from the *C. albicans* genome database (Stanford Genome Technology Center) and *Xenopus* expression to PCR clone and functionally characterize a purine nucleoside-selective transporter (CaCNT). CaCNT represents the first described cation-coupled nucleoside transporter in yeasts, and is the first member of the CNT family of proteins to be characterized from a unicellular eukaryotic organism. *Chapter VI* described the anticancer and antiviral nucleoside drug transport properties of *E. coli* NupC, a prokaryotic member of the

CNT family. These studies confirmed NupC's H⁺-dependence and preference for pyrimidine nucleosides and adenosine. They also represent the first described functional expression of a recombinant bacterial transporter in *Xenopus* oocytes.

The second objective of my research was to undertake structure/function studies of CNT proteins. In *Chapter II*, I used chimeric and site-directed mutagenesis approaches between hCNT1 and hCNT2 to identify two pairs of adjacent residues in TM 7 (Ser³¹⁹ and Gln³²⁰) and TM 8 (Ser³⁵³ and Leu³⁵⁴) of hCNT1 that, when mutated to the corresponding residues in hCNT2, changed the permeant substrate specificity from *cit* to *cif*. In these studies, sequence comparisons between human and rat CNT1/2 and hCNT (with its broad substrate selectivity for both pyrimidine and purine nucleosides) played an important role in identifying potential amino acid residues for mutagenesis. Initial mutation of the two hCNT1 TM 7 residues to the corresponding amino acids in hCNT2 (Gly and Met, respectively) converted the transporter from *cit* to *cib*, the mutant (hCNT1/S319G/Q320M) transporting both pyrimidine and purine nucleosides. Additional mutation of Ser³⁵³ in TM 8 to Thr changed the substrate selectivity of hCNT1/S319G/Q320M from *cib* to *cif*, producing a transporter selective for purine nucleosides and uridine, but with relatively low transport activity for adenosine. Substitution of the adjacent TM 8 residue Leu³⁵⁴ to Val enhanced the adenosine transport capability of the hCNT1/S319G/Q320M/S353T, producing a full *cif*-type phenotype. In an extension of these studies described in *Chapter III*, single or combination mutations in TM 8 alone produced novel recombinant proteins with uridine-preferring transport characteristics (hCNT1/S353T and hCNT1/S353T/L354V) and/or partially uncoupled transport properties (hCNT1/S353T/L354V and hCNT1/L354V). Chimeric studies using hCNT3 and hCNT in combination with hCNT1 (described in *Chapters IV* and *V*, respectively) identified regions of the proteins (TMs 7-13) involved in cation coupling.

System *cib* belongs to the CNT Family

In 1992, a rabbit protein, SNST1, from the sodium/solute symporter (SSS) family (formerly the Na⁺/glucose cotransporter (SGLT) family) was reported to possess low-level *cib*-type transport activity when expressed in *Xenopus* oocytes (Pajor and Wright, 1992). This protein, however, is now recognized as a rabbit ortholog of human SGLT2 and has been

reclassified as rbSGLT2 (Turk and Wright, 1997; Wright, 2001). Reported uridine fluxes for SNST1 (rbSGLT2) expressed in *Xenopus* oocytes were only marginally higher than background, suggesting that nucleosides are not physiological substrates for this transporter.

Several lines of evidence suggested, instead, that an unrecognized member of the CNT family might be responsible for *cib*-type activity in mammalian cells. First, the prevertebrate hagfish transporter (hfCNT) was shown to possess a *cib*-type nucleoside specificity, an indication that CNT proteins with broad nucleoside specificity were also possible in higher vertebrates. Second, residue mutations in TM 7 of hCNT1 changed the transporter's specificity from pyrimidine nucleoside-selective (system *cit*) to one broadly selective for both purine and pyrimidine nucleosides (system *cib*). A major breakthrough came at the end of 1999 when BLAST searches of human and mouse genomic and EST sequence databases uncovered new putative CNT protein sequences that differed from the known sequences of CNT1 and CNT2. The new sequences showed greater similarity to hfCNT than to mammalian CNT1/2. This information, in conjunction with RT-PCR and traditional PCR cloning techniques, isolated two cDNAs from human and mouse that encoded proteins (hCNT3 and mCNT3, respectively) with all of the hallmark characteristics of mammalian *cib* (Chapter IV). The rat homolog rCNT3 has also recently been cloned and shows *cib*-type functional activity when produced in *Xenopus* oocytes (unpublished data; Chapter V). CNT3 proteins also possess unique H⁺- (and Li⁺-) dependent transport characteristics that have not previously been reported in studies of cells containing *cib*-type functional activity. There are some circumstances, as in the gastrointestinal tract, where protons may augment CNT3-mediated nucleoside transport. The finding that H⁺-activated hCNT3 failed to transport antiviral dideoxynucleoside drugs suggests that the Na⁺-coupled and H⁺-coupled forms of the transporter are not directly equivalent. Future work with CNT3 will include mutagenesis studies to identify the residues responsible for this H⁺-driven activity. Chimeric studies with between hCNT1 and hCNT3 suggest that this activity resides in the C-terminal half of the protein.

From a physiological and evolutionary perspective, it is interesting, as discussed in Chapter V, that hfCNT may be the only concentrative nucleoside transporter present in hagfish, which diverged from the main line of vertebrate evolution ~ 550 million years ago.

Application of CaCNT in Biochemical and Biophysical Studies of CNT Proteins

One of the most important forthcoming goals in CNT transport biology is the harvesting sufficient purified protein for biochemical and biophysical studies. Yeast and bacterial expression systems are the most likely to be useful in this regard. Unfortunately, expression levels of mammalian CNT proteins in yeast are not yet sufficient for structural investigation (Vickers *et al.*, 2001). Over-production of the yeast transporter, CaCNT, may, however, be more successful.

Similar studies are in progress with our UK collaborators, Professors Stephen Baldwin and Peter Henderson (University of Leeds) and Dr. Maurice Gallagher (University of Edinburgh), to over-express NupC, in *E. coli*. Levels of expression equivalent to approximately 25% of the total membrane protein have been achieved. The protein has been purified to homogeneity in functional form as a maltose-binding protein fusion on a large scale (tens of mg), setting the stage for future 2-D and 3-D crystallization trials and other biophysical and biochemical determinations. NupC, however, lacks structural elements found in eukaryotic CNTs (large intracellular N-terminus, TMs 1-3, and large extracellular C-terminus) (Fig. 8-1). Therefore, even though NupC represents the catalytic core of CNTs, parallel biochemical and biophysical studies of eukaryotic CNTs, such as CaCNT, will still be important.

Development of a Single Unified Transport Model for the CNT Family

In *Chapter III*, a model was proposed that incorporates a slippage pathway for uncoupled (or equilibrative) transport of nucleosides, while still maintaining an overall cation-coupled, concentrative transport mechanism (Fig. 3-8). It was shown in this thesis, that hCNT3 and hfCNT have 2:1 Na⁺:uridine coupling ratios, compared to the 1:1 stoichiometry proposed for CNT1/2. Several of the CNTs studied in this thesis are Na⁺-dependent (hCNT1, hCNT2 and hfCNT), H⁺-dependent (NupC and CaCNT), or both Na⁺- and H⁺-dependent (hCNT3 and mCNT3). Although the molecular mechanisms for these diverse transport properties are still unknown, their activities can be readily incorporated into the model proposed in Fig. 3-8. For example, the difference in the number of Na⁺ ions needed for transport activation can be explained by the equilibrium governing the T_o'A ↔ T_o"A states, requiring either 1 or 2 Na⁺ ions to “unlock” or open the nucleoside binding site. Other cations may also be able to substitute

for Na^+ , which would serve as a different transport activator (“A” in Fig. 3-8), and potentially result in a different conformation of the nucleoside binding pocket upon cation-activation. This would explain, for example, why H^+ -coupled CNT3 does not seem to transport antiviral nucleoside drugs such as AZT and ddC. A goal of future biochemical studies (see below) will be to determine the structural basis of the different modes of cation coupling seen in CNT-mediated nucleoside transport.

Helix Modeling of the CNT Permeation Pathway through Mutagenesis Studies

While 2-D and 3-D crystal structures of CNTs remain important goals for future research, mutagenesis studies presented in this thesis have identified TMs 7 and 8 of hCNT1 as part of nucleoside permeation pathway (*Chapter II*). Thus, residues in both helices have important complementary roles in determining pyrimidine/purine nucleoside specificity. TM 8 mutants also showed uncoupled transport characteristics (*Chapter III*). Although the latter phenotype most likely results from altered helix-helix packing, the results of these experiments are nevertheless consistent with a common nucleoside/cation translocation channel. Similarly, the hCNT3/hCNT1 and hfCNT/hCNT1 chimeric studies described in *Chapters V* and *VI* suggest that the structural determinants of cation coupling reside within in the C-terminal halves of the proteins. This situation contrasts with the Na^+ -dependent glucose transporter SGLT1, where there is evidence that the sugar and cation translocation pathways are in separate halves of the protein (Panayotova-Heiermann *et al.*, 1996, 1997, 1999).

Helical wheel analyses in combination with multiple CNT sequence alignments and our mutagenesis studies of hCNT1/2 substrate specificity have allowed us to perform initial helix modeling of the TM 7-9 region of hCNT1 (*Chapter II*). A goal of future research will be to undertake parallel mutagenesis studies of cation coupling in the different CNT family members described in this thesis. It will also be informative to incorporate these newly characterized CNTs into investigations of the molecular basis of nucleoside substrate specificity, using both physiological nucleosides and nucleoside analogs to probe the structural determinants of nucleoside recognition and translocation. Molecular information derived from these studies will refine our model of the translocation pore, including the identification of additional pore-lining TMs. Systematic cysteine-scanning mutagenesis of critical TMs will

also be informative. Although mammalian CNTs have extensive numbers of Cys residues (hCNT1, for example, has 20), *E. coli* NupC has only one, and a Cys-less version of the transporter with good functional activity in *Xenopus* oocytes has been produced as a template Cys-based mutagenesis and biochemical studies (unpublished observation).

Examples of nucleoside analogs that will have utility as probes for continued studies of the molecular basis of nucleoside binding and translocation include the uridine analogs used to study TM 8 mutants of hCNT1 (*Chapter II*), and AZT and ddC, which discriminate between Na⁺-coupled and H⁺-coupled hCNT3 forms (*Chapter V*). In experiments not included in this thesis, I have also found that the adenosine analog tubercidin (7-deazaadenosine) exhibits distinct transporter-specific interactions with hCNT1, hCNT2, hCNT3 and hCNT.

The Role of CNT Proteins in Future Therapeutic Drug Delivery and Chemoprotective Strategies

An emphasis of this thesis is the ability of CNT proteins to mediate transport of chemotherapeutic nucleoside analog drugs used in the treatment of cancer and viral diseases as well as bacterial and fungal infections. Advances in our understanding of the structures and functions of these proteins are increasing at an accelerating rate, in part due to already completed and on-going genomic sequencing projects. Immunologic and molecular probes are rapidly becoming available to define the numbers and identities of nucleoside transporters present in normal and diseased tissue. Soon it will be feasible to tailor nucleoside chemotherapy to match the nucleoside transporter profile of target cells. Given the diversity in nucleoside and nucleoside drug selectivity exhibited by CNT proteins in nature, however, it may also be possible in the future to engineer CNT proteins with tailored cytotoxic nucleoside drug transport capabilities and to target the recombinant transporters to a particular tissue location. A “designer” CNT for fludarabine, for example, could be useful in current gene-directed enzyme prodrug therapy (GDEPT) approaches to combat hepatocellular carcinoma. These employ an *E. coli* purine nucleoside phosphorylase (PNP)/fludarabine suicide gene system introduced by an adenovirus targeting vector and are highly dependent upon entry of fludarabine into the cell (Mohr *et al.*, 2000; Krohne *et al.*, 2001).

Likewise, it may be possible to develop a CNT protein that can substitute another cation, such as K^+ in place of Na^+ or H^+ , thereby creating a nucleoside efflux pump by coupling the protein to the outwardly-directed K^+ electrochemical gradient. CNT proteins coupled to K^+ may already exist in nature. For example, a K^+ -dependent amino acid transporter (KAAT1) related to the mammalian Na^+ -Cl⁻-coupled transporter family has been cloned from Lepidopteran insect larval midgut, which lacks Na^+/K^+ ATPase activity and has a high K^+ and a low Na^+ content within the intestinal lumen (Castagna *et al.*, 1998). Targeted expression of a recombinant K^+ -coupled CNT would have the potential to protect important chemotherapeutic-sensitive cells, such as bone marrow and hematopoietic stem cells, thereby decreasing side effects associated with drug administration. A similar efflux chemoprotective strategy using the drug efflux pump, P-glycoprotein (MDR1), introduced by retroviral transduction into hematopoietic stem cells, has resulted in cell protection from the toxicity of anticancer chemotherapy agents (Licht *et al.*, 1995). Recently characterized members of the OAT and OCT protein families that have been reported to function as nucleoside drug efflux mechanisms (*Chapter I*) may also have utility in this regard. Endogenous OATs and OCTs also represent a potential mechanism of drug resistance.

While gene therapy initiatives will not be possible without advances in gene delivery systems, the development of engineered transporters with enhanced drug transport capabilities is also required. For CNTs, this requires an intimate understanding of the molecular basis of both substrate and cation recognition and translocation. The contents of this thesis represent a significant step in that direction.

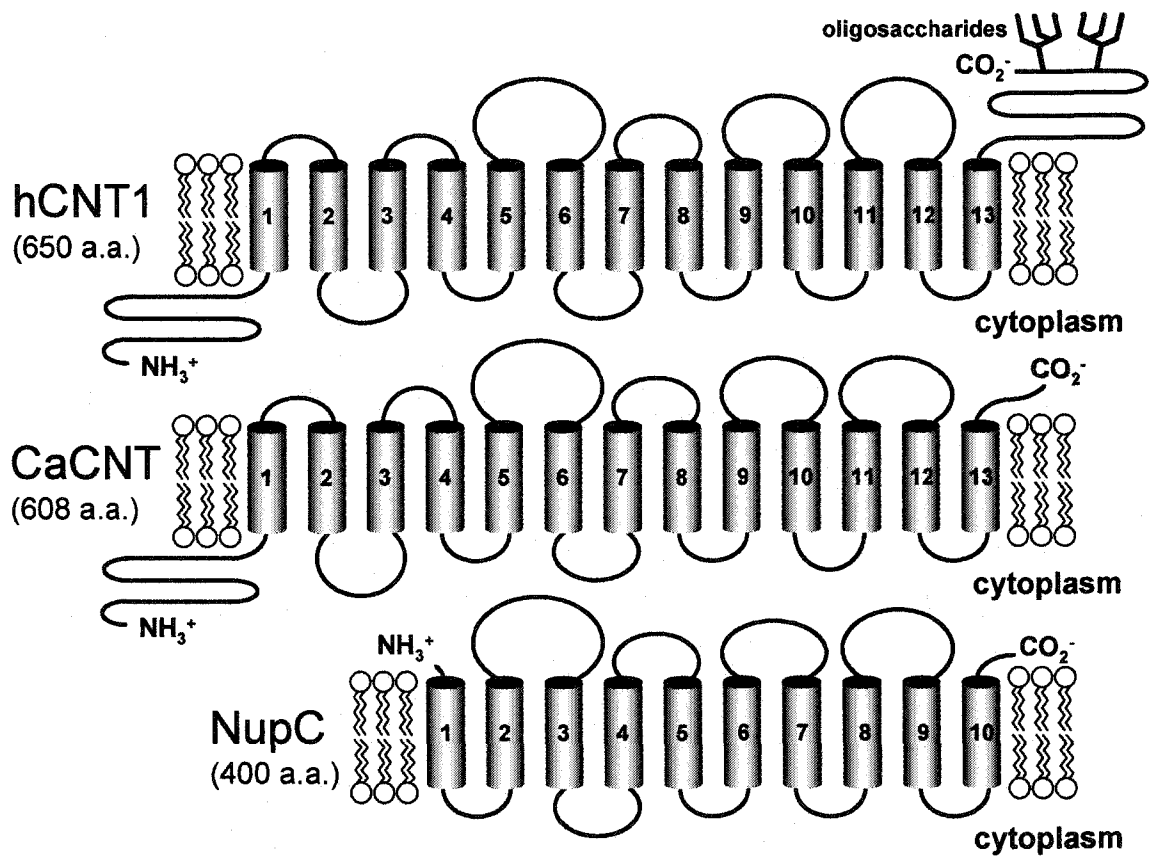


Figure 8-1. Topologies of hCNT1, CaCNT and NupC. Potential membrane-spanning α -helices are *numbered*, and putative glycosylation sites in predicted extracellular domains in hCNT1 are indicated and labeled accordingly.

Bibliography

- Castagna M, Shayakul C, Trotti D, Sacchi VF, Harvey WR, and Hediger MA** (1998) Cloning and characterization of a potassium-coupled amino acid transporter. *Proc Natl Acad Sci U S A* 95: 5395-5400.
- Hong M, Schlichter L, and Bendayan R** (2000) A Na⁺-dependent nucleoside transporter in microglia. *J Pharmacol Exp Ther* 292: 366-374.
- Huang QQ, Harvey CM, Paterson AR, Cass CE, and Young JD** (1993) Functional expression of Na⁺-dependent nucleoside transport systems of rat intestine in isolated oocytes of *Xenopus laevis*. Demonstration that rat jejunum expresses the purine-selective system N1 (cif) and a second, novel system N3 having broad specificity for purine and pyrimidine nucleosides. *J Biol Chem* 268: 20613-20619.
- Krohne TU, Shankara S, Geissler M, Roberts BL, Wands JR, Blum HE, and Mohr L** (2001) Mechanisms of cell death induced by suicide genes encoding purine nucleoside phosphorylase and thymidine kinase in human hepatocellular carcinoma cells *in vitro*. *Hepatology* 34: 511-518.
- Lee CW, Sokoloski JA, Sartorelli AC, and Handschumacher RE** (1991) Induction of the differentiation of HL-60 cells by phorbol 12-myristate 13-acetate activates a Na⁺-dependent uridine-transport system. Involvement of protein kinase C. *Biochem J* 274: 85-90.
- Lee CW, Sokoloski JA, Sartorelli AC, and Handschumacher RE** (1994) Differentiation of HL-60 cells by dimethylsulfoxide activates a Na⁺-dependent nucleoside transport system. *In Vivo* 8: 795-801.
- Licht T, Gottesman MM, and Pastan I** (1995) Transfer of the MDR1 (multidrug resistance) gene: protection of hematopoietic cells from cytotoxic chemotherapy, and selection of transduced cells *in vivo*. *Cytokines Mol Ther* 1: 11-20.
- Mohr L, Shankara S, Yoon SK, Krohne TU, Geissler M, Roberts B, Blum HE, and Wands JR** (2000) Gene therapy of hepatocellular carcinoma *in vitro* and *in vivo* in nude mice by adenoviral transfer of the Escherichia coli purine nucleoside phosphorylase gene. *Hepatology* 31: 606-614.
- Pajor AM, and Wright EM** (1992) Cloning and functional expression of a mammalian Na⁺/nucleoside cotransporter. A member of the SGLT family. *J Biol Chem* 267: 3557-3560.
- Panayotova-Heiermann M, Loo DD, Kong CT, Lever JE, and Wright EM** (1996) Sugar binding to Na⁺/glucose cotransporters is determined by the carboxyl-terminal half of the protein. *J Biol Chem* 271: 10029-10034.
- Panayotova-Heiermann M, Eskandari S, Turk E, Zampighi GA, and Wright EM** (1997) Five transmembrane helices form the sugar pathway through the Na⁺/glucose cotransporter. *J Biol Chem* 272: 20324-20327.

- Panayotova-Heiermann M, Leung DW, Hirayama BA, and Wright EM** (1999) Purification and functional reconstitution of a truncated human Na⁺/glucose cotransporter (SGLT1) expressed in *E. coli*. *FEBS Lett* 459: 386-390.
- Redlak MJ, Zehner ZE, and Betcher SL** (1996) Expression of rabbit ileal N3 Na⁺/nucleoside cotransport activity in *Xenopus laevis* oocytes. *Biochem Biophys Res Commun* 225: 106-111.
- Turk E, and Wright EM** (1997) Membrane topology motifs in the SGLT cotransporter family. *J Membr Biol* 159: 1-20.
- Vickers MF, Young JD, Baldwin SA, Ellison MJ and Cass CE** (2001) Functional production of mammalian concentrative nucleoside transporters in *Saccharomyces cerevisiae*. *Mol Membr Biol* 18: 73-79.
- Waclawski AP, and Sinko PJ** (1996) Oral absorption of anti-acquired immune deficiency syndrome nucleoside analogues. 2. Carrier-mediated intestinal transport of stavudine in rat and rabbit preparations. *J Pharm Sci* 85: 478-485.
- Washington CB, Brett CM, Wu X, and Giacomini KM** (1995) The effect of N-ethylmaleimide on the Na⁺-dependent nucleoside transporter (N3) in rabbit choroid plexus. *J Pharmacol Exp Ther* 274: 110-114.
- Wright EM** (2001) Renal Na⁺-glucose cotransporters. *Am J Physiol Renal Physiol* 280: F10-F18.
- Wu X, Yuan G, Brett CM, Hui AC, and Giacomini KM** (1992) Sodium-dependent nucleoside transport in choroid plexus from rabbit. Evidence for a single transporter for purine and pyrimidine nucleosides. *J Biol Chem* 267: 8813-8818.
- Wu X, Gutierrez MM, and Giacomini KM** (1994) Further characterization of the sodium-dependent nucleoside transporter (N3) in choroid plexus from rabbit. *Biochim Biophys Acta* 1191: 190-196.